PEETER JOOT

CONDENSED MATTER PHYSICS

CONDENSED MATTER PHYSICS

PEETER JOOT

Notes and problems from UofT PHY487H1F 2013

August 2023 – version V0.1.12-3

Peeter Joot: *Condensed Matter Physics,* Notes and problems from UofT PHY487H1F 2013, © August 2023

COPYRIGHT

DOCUMENT VERSION

Version V0.1.12-3

Sources for this notes compilation can be found in the github repository

https://github.com/peeterjoot/phy487-qmsolids

The last commit (Aug/25/2023), associated with this pdf was 79c89955f301567318d427a0769028f517cf500b

Should you wish to actively contribute typo fixes (or even more significant changes) to this book, you can do so by contacting me, or by forking your own copy of the associated git repositories and building the book pdf from source, and submitting a subsequent merge request.

```
#!/bin/bash

git clone git@github.com:peeterjoot/latex-notes-compilations.
    git peeterjoot
cd peeterjoot

submods="figures/phy487-qmsolids phy487-qmsolids mathematica
    latex"
for i in $submods ; do
   git submodule update --init $i
   (cd $i && git checkout master)
done

export PATH=‘pwd‘/latex/bin:$PATH

cd phy487-qmsolids
make
```

I reserve the right to impose dictatorial control over any editing and content decisions, and may not accept merge requests as-is, or at all. That said, I will probably not refuse reasonable suggestions or merge requests.

Dedicated to:
Aurora and Lance, my awesome kids, and
Sofia, who not only tolerates and encourages my studies, but is also awesome enough to think that math is sexy.

PREFACE

This book contains my lecture notes for the Winter 2013, University of Toronto Condensed Matter Physics course (PHY487H1F), taught by Prof. Stephen Julian.

Official course description: "Introduction to the concepts used in the modern treatment of solids. The student is assumed to be familiar with elementary quantum mechanics. Topics include: bonding in solids, crystal structures, lattice vibrations, free electron model of metals, band structure, thermal properties, magnetism and superconductivity (time permitting)"

We worked from the text [10]. I personally found [1] not only helpful, but superior in almost every aspect, containing better diagrams, clearer descriptions, more complete and clearer mathematics, and no typos (that I spotted).

This book contains:

- Plain old lecture notes. These mirror what was covered in class, possibly augmented with additional details.
- Personal notes exploring details that were not clear to me from the lectures, or from the texts associated with the lecture material.
- Some worked problems attempted as course prep, for fun, or for test preparation, or post test reflection.
- Links to Mathematica workbooks associated with this course.

My thanks go to Professor Julian for teaching this course.

Peeter Joot peeterjoot@pm.me

CONTENTS

LIST OF FIGURES

1 BONDING.

1.1 CHEMICAL BONDING IN SOLIDS.

Reading: §1.1, §1.2 [10], [1] ch. 19.

- Different types of chemical bonds explain many of the differences between solids.
- Differences in solids: hard/soft. Example: Lithium, so soft that a pure sample will flow if set on a desk ; metal vs insulating, melting points

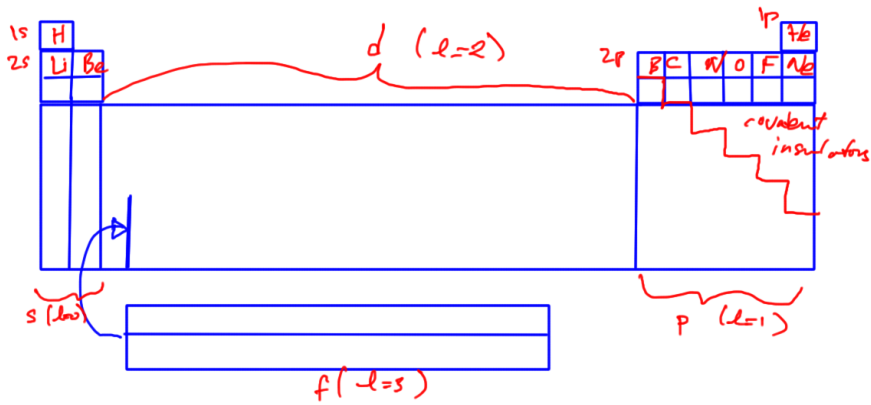

Figure 1.1: Periodic table annotated with orbital filling notes.

Elements in the periodic table are classified according to which type of orbital is being filled. This is roughly sketched in fig. 1.1, with much better figures are everywhere (such as figure 7.28 of [3].)

Hydrogen, or other super ionized material (example: iron with all but one electron observed in supernova spectra) fig. 1.2.

Recall that we have the following ranges for our states

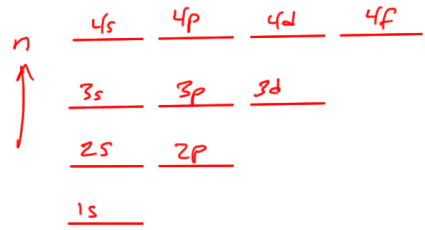

Figure 1.2: Hydrogenic atom (only one electron).

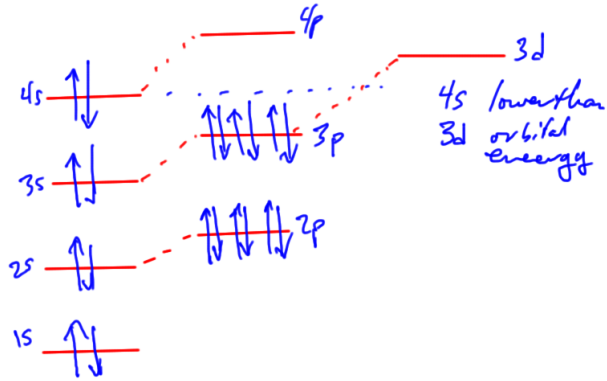

Figure 1.3: Two electron atom. eg: Ti_{22}.

- $l \in n-1, n-2, \cdots 0$ (n)
- $m \in l, l-1, \cdots, -l$ $(2l+1)$
- $S \in \pm$ (2)
- upper right hand of periodic table: covalent bonding
- lower left hand of periodic table: metallic bonding
- mixed left hand with right hand of periodic table: ionic bonding

1.2 COVALENT BONDING.

Consider a pair of hydrogen nuclei sharing one electron. §1.2 [10] has a mathematical description (not examinable)

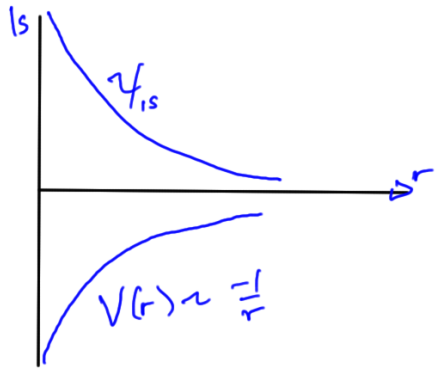

Figure 1.4: Potential and radial distribution for 1*s* state.

In fig. 1.9, observe that only partially filled orbitals can participate in covalent bonding.

Reading: §10.6 [3]. Figures 10.23, 10.24 for example.

Covalent bonding involves electrons shared between materials, forming between partially filled orbitals on small atoms. Example H_2.

Only half filled orbitals (eg. $2p_z^1$) form covalent bonds. Two shared electrons in bonding orbitals. We need small, directional

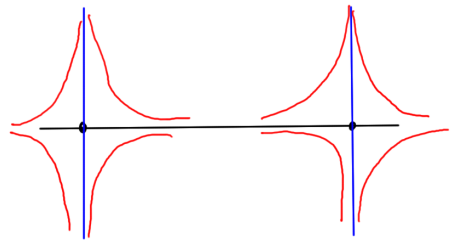

Figure 1.5: Far apart.

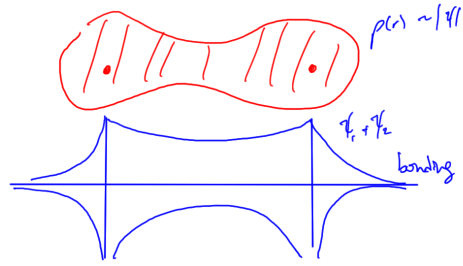

Figure 1.6: Close together.

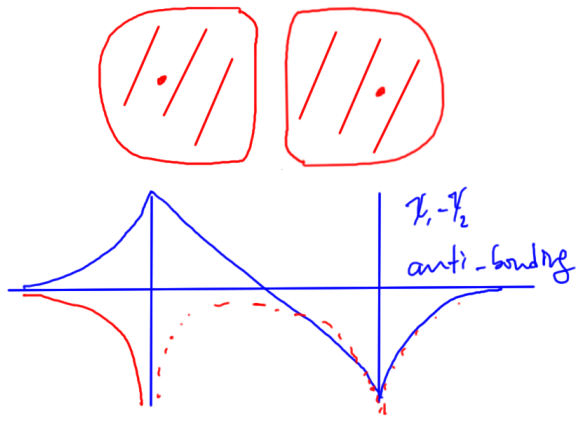

Figure 1.7: Close together, bonding.

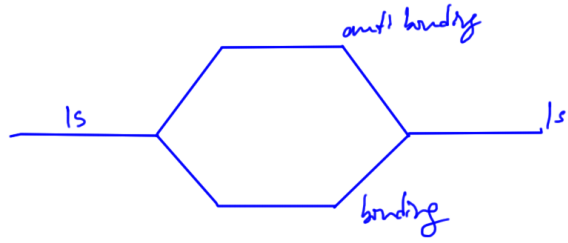

Figure 1.8: Chemistry diagram.

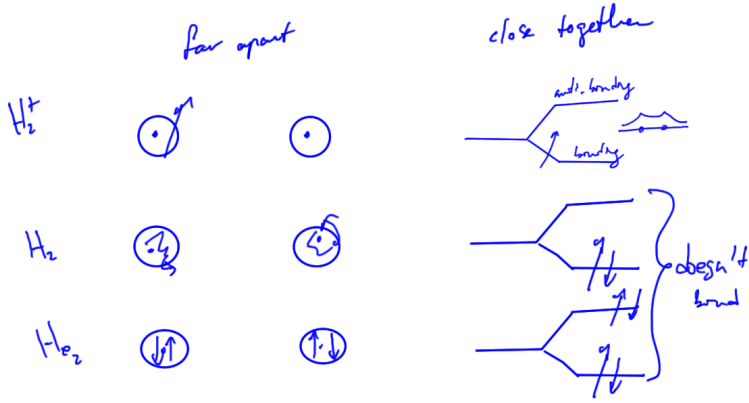

Figure 1.9: Adding more electrons.

orbitals. We find this sort of bonding in the upper triangular segment of the periodic table as in fig. 1.10.

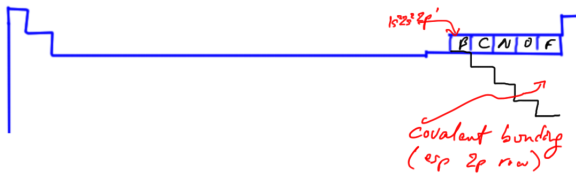

Figure 1.10: Covalent bonding region.

An example of such a covalent bond is that of two $2p_z^1$ orbitals of Fluoride F ($1s^2 2s^2 2p_x^2 2p_y^2 2p_z$), as in fig. 1.11.

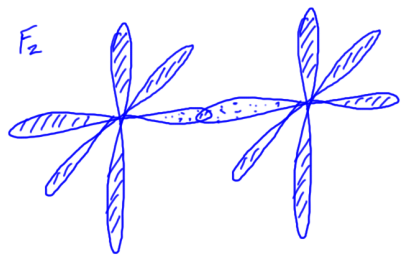

Figure 1.11: Fluorine gas molecule.

With Fluorine we cannot make a covalently bonded solid, since there are no orbitals left over for bonding with anything else.

Fluorine solid? Can we get a Fluorine solid with promotion of two $2p$ states to $3s^2$, then have three orbitals left for bonding?

Probably, but the energy cost of doing so may be exorbitant, and could require high pressures. This is more likely with Bromine since the difference between the $4s$ and $5p$ states is less.

First important cases, C, Si, Ge Looks like two bonds form. Normally carbon is 3 or 4 fold coordinated. Two such mechanisms for carbon bonding are promotion and hybridization

See: [10] ch. 1

For carbon ($1s^2 2s^2 2p_x^1 2p_y^1 2p_z^0$), promotion possibilities are illustrated in fig. 1.12.

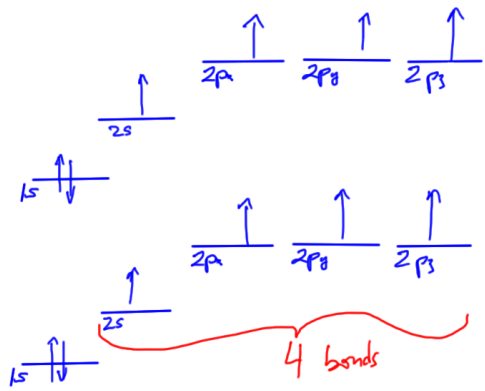

Figure 1.12: 2*s* promotion in carbon allowing for 4 way bonding.

It turns out that

$$E_{4\text{ bonds}} + E_{\text{promotion}} < E_{2\text{ bonds}}. \tag{1.1}$$

This allows for linear combinations of $2s + 2p$ orbitals that have highly directional compact orbitals, perfect for covalent bonding.

1. sp_1 hybrid. $2s + 2p_x$

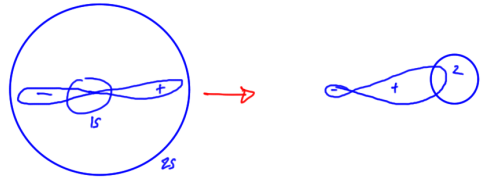

Figure 1.13: sp_1 hybrid.

2. sp_2 hybrid (like graphene.) Discussion left to problem set 1.
3. sp_3 hybrid orbitals.

   Covalent bonds are some of the strongest. In diamond, where each C has 4 nn (nearest neighbors) we have a melting point

   $$T_m \sim 4000K. \tag{1.2}$$

   and has the highest hardness of any material.

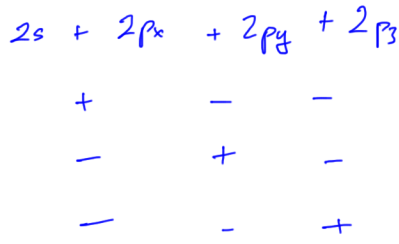

Figure 1.14: sp_3 hybrid sign configurations.

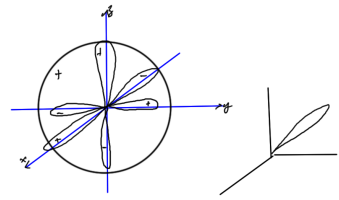

Figure 1.15: sp_3 hybrid

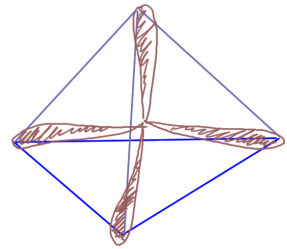

Figure 1.16: Lobes point to the 4 vertexes of a tetrahedron.

1.3 IONIC BONDING.

Reading: [1] ch. 20.

Here we are combining different atoms, especially the left and right hand sides of the period table.

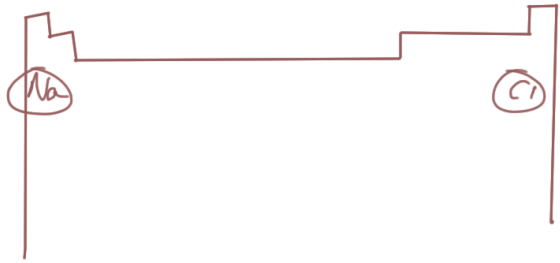

Figure 1.17: *NaCl* periodic table locations.

Examples: NaCl, KF, CsCl, Li_2O, CaO

NaCl Na has 1 weakly bound 3s electron. Cl has one vacancy in its $3p$ shell.

Energetics The energy transitions for ionization are illustrated in fig. 1.18.

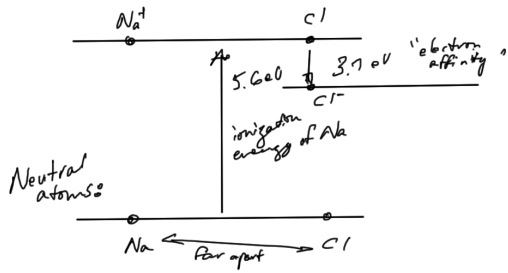

Figure 1.18: Energy ionization transitions for *NaCl* atoms (far apart).

The energy released moving the ions together is illustrated in fig. 1.19.

Relative to fig. 1.18 we have a $-3.1eV$ energy change in the transition to this final state.

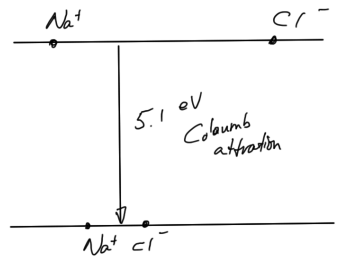

Figure 1.19: Energy transitions for Coulomb interaction of ionized *NaCl* atoms.

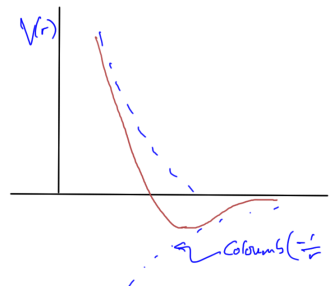

Figure 1.20: Potential well.

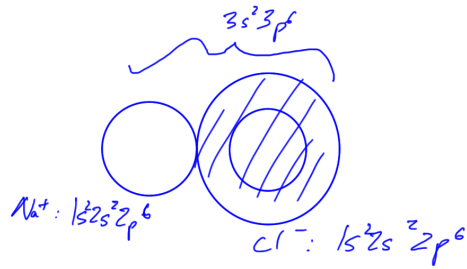

Figure 1.21: Final state for pair of ions.

Observe that the final state is not obviously predictable from the initial states. The hybrid state can probably be derived from first principles, but this determination may be easier with spectroscopy.

Solid NaCl (See: 02_lecture.pdf, and [10] fig 1.6)

Have 2 interpenetrating free lattices. Each Na^+Cl^- has 6 nn (nearest neighbor) Cl^-Na^+. Binding energy 7.95 eV/pair.

CsCl The CsCl structure. Cl on corners. Cs in center of cube. 8 nn. Better than NaCl structure. But, Na^+ is small, so in the CsCl (where Cs is big compared to Na) structure, the next nn (nnn) Cl^- would touch. There's a strong Coulomb repulsion.

We introduce the Madelung constant A for the potential energy of the solid configuration

$$\begin{aligned}\Phi_{tot} &= \sum_i \phi_i = \frac{1}{2}\sum_{i\neq j}\phi_{ij} \\ &= \frac{1}{2}N\Big(-\frac{e^2}{4\pi\epsilon_\circ r}\underbrace{\sum_{i\neq j}\frac{(\pm 1)}{p_{ij}}}_{A} + \frac{B}{r^n}\sum_{i\neq j}\frac{1}{p_{ij}^n}\Big),\end{aligned} \tag{1.3}$$

where N is the number of ions in the solid, r is the nn separation (center to center), and $r_{ij} = p_{ij}r$, as illustrated in fig. 1.22.

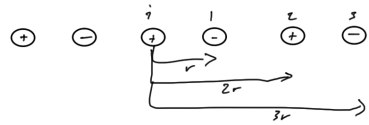

Figure 1.22: Madelung separation.

As an additional illustration, we have the NaCl configuration in fig. 1.23.

Examination hint: Eminently examinable material (since it can be calculated).

Examples

- NaCl structure $A = 1.748$

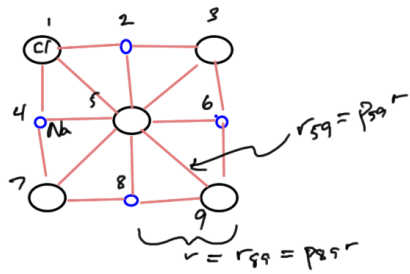

Figure 1.23: NaCl lattice separation.

- CsCl structure $A = 1.763$

Ionic bonds are weaker than covalent, non-directional. One indicator of this is the melting points

$$T_m = 1074K \quad \text{NaCl} \tag{1.4a}$$

$$T_m = 918K \quad \text{CsCl.} \tag{1.4b}$$

1.4 METALLIC BONDING.

We now focus on the regions of the periodic table illustrated in fig. 1.24.

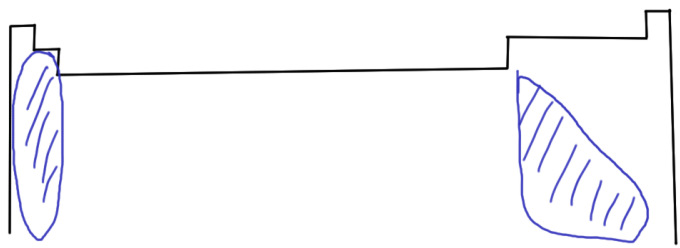

Figure 1.24: Metallic bonding regions in the periodic table.

Curiously, the name is somewhat misleading. Just because something is a metal doesn't mean it is metallic bonded.

- s-orbitals from $2s$ to $5s$,

- p-orbitals from $n = 4, 5, 6, 7$.

These are big orbitals that extend beyond the nn, as illustrated in fig. 1.25.

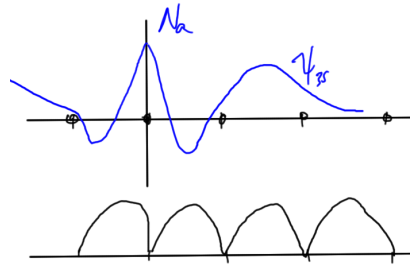

Figure 1.25: Extensive wave function.

Weakly bound electrons overlap many nearby potential wells. This lowers the Coulomb energy. This is like a non-directional covalent bond. This non-directionality results in malleability.

Pure metallic bonds are weak. Melting points are correspondingly low, where for column 1 elements T_m ranges from room temperature to 200° C.

1.5 TRANSITION METALS.

Here we have both metallically bonded s-orbitals and covalent d-orbitals fig. 1.26.

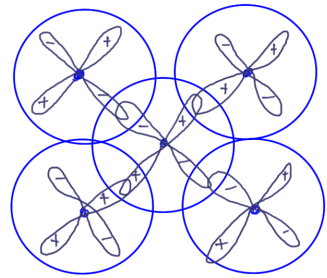

Figure 1.26: Overlapping s and p orbitals.

$$T_m \gtrsim 2000^\circ C. \tag{1.5}$$

On sign conventions. The $+, -$'s assume real representation of wave functions. Here bonding is matching signs (constructive interference), and antibonding is when the signs are in opposition (destructive interference).

Reading: §1.5, 1.6 [10].

1.6 PROBLEMS.

Exercise 1.1 Orbitals and bonding. (*2013 ps1 p1*)

(*The reading assignments covered sections 1, 1.1, 1.5 and 1.6 of Ibach and Luth.*)

a. Explain $5s$ $4d$ orbital filling ordering. In a hydrogenic atom (nuclear charge Ze, only one electron) the $4d$ levels have a lower energy than the $5s$ levels. According to the periodic table, however, the $5s$ levels become occupied before the $4d$ levels do. Explain why.

b. Explain power of Van der Waals potential. Briefly explain why the Van der Waals potential has a $1/r^6$ dependence.

Answer for Exercise 1.1

Part a. The $4d$ levels has a lower energy than the $5s$ level in a single electron system. In a multiple electron system completely filled (and perhaps partially filled) orbitals have the effect of shielding additional electrons from a subset of the nuclear charge, reducing the effective total charge of the system with respect to that additional electron. This shifts the d, p, f orbitals up in the staircase like fashion illustrated in class, and puts $5s$ below $4d$ in such multiple electron systems.

Grading remark: Re: "Why should the screening have less of an effect on the $5s$ orbital than the $4d$ orbital?" The posted solutions explain that the underlying reason for this difference is not screening, but because the s orbitals have zero angular momentum (i.e. s orbital corresponds to the angular momentum quantum number $l = 0$). This is then used to argue that the electron distribution

closer to the nucleus for such orbitals and lowers the energy required to fill these states. FIXME: followup on this argument with some calculations to remove the handwaving from this argument. This simple shielding description breaks down in a number of cases, as there are multi-body interactions at play here too. This results in a number of exceptions in the ordering of the $5s$, $4d$ filling. For example Pd in its ground state has the $4d$ orbitals completely filled ($4d^{10}$) with no $5s$ state electrons. We see the resumption of the $5s$ orbital filling in the subsequent Ag and Cd atoms retaining the completely filled $4d^{10}$ orbitals that we see first in Pd. This can be loosely described by stating it is more stable (lower energy) to have a single set of completely filled $4d^{10}$ orbitals, than a have a pair of partially filled orbitals in both states like $4d^9 5s^1$.

Part b. Our text [10] §1.6 does a loose and fast description of the $1/r^6$ Van der Waals dependence, indicating that it is due to oscillation of a dipole field that has a $1/r^3$ dependence. When the neighboring atom has a polarizability α its stated that there is a secondary dipole induced in this neighbor that also has a $1/r^3$ dependence, but proportional to both the initiating field and the new dipole.

To translate from this descriptive rationalization of the $1/r^6$ dependence, I found it helpful to remind myself of the specific form of this dipole dependence. In [11] §9.2 it is argued that a charge oscillation (i.e. charge and current density changes of the form $\rho(\mathbf{x})e^{-i\omega t}$) lead to an electric field of the form

$$\mathbf{p} = \int \mathbf{x}' \rho(\mathbf{x}') d^3x' \tag{1.6a}$$

$$\mathbf{E} = k^2 (\mathbf{n} \times \mathbf{p}) \times \mathbf{n} \frac{e^{ikr}}{r} + (3\mathbf{n}(\mathbf{n} \cdot \mathbf{p}) - \mathbf{p}) \left(\frac{1}{r^3} - \frac{ik}{r^2} \right) e^{ikr}. \tag{1.6b}$$

In particular observe that the near field ($r \sim 0$) is dominated by

$$\mathbf{E} = (3\mathbf{n}(\mathbf{n} \cdot \mathbf{p}) - \mathbf{p}) \frac{1}{r^3}. \tag{1.7}$$

Referring to [6] for a definition of polarizability, we find that polarizability is a dipole electric-field proportionality

$$\mathbf{p} = \alpha \mathbf{E}. \tag{1.8}$$

So if the second atom has polarizability α, the dipole field due to its internal dipole moment (say $\mathbf{p}' = \alpha\mathbf{E}$, with respect to normal $\mathbf{n}'$), then the electric field from this second atom (directed back towards the original oscillating atomic dipole and others) is, in the near field approximation

$$\begin{aligned}\mathbf{E}' &= \left(3\mathbf{n}'(\mathbf{n}'\cdot\mathbf{E}) - \mathbf{E}\right)\frac{\alpha}{r^3} \\ &= \left(3\mathbf{n}'(\mathbf{n}'\cdot\mathbf{n})(\mathbf{n}\cdot\mathbf{p}) - 3\mathbf{n}'(\mathbf{n}'\cdot\mathbf{p}) - \mathbf{n}(\mathbf{n}\cdot\mathbf{p}) + \mathbf{p}\right)\frac{3\alpha}{r^6}.\end{aligned} \tag{1.9}$$

Here we see explicitly the $1/r^6$ dependence of the field due to both the oscillation of the dipole $\mathbf{p}$ of the atom itself, as well the polarizability α of its neighbor.

Exercise 1.2 sp^2 hybrid orbitals. (*2013 ps1 p2*)

The $2s$ and $2p$ orbitals of a hydrogenic atom (i.e. one electron, nuclear charge Ze) are:

$$\begin{aligned}\phi_{2s}(\rho) &= \mathcal{N}\,\mathrm{e}^{-\rho}(1-\rho) \\ \phi_{2p_z}(\rho) &= \mathcal{N}\,\mathrm{e}^{-\rho}\rho\cos\theta \\ \phi_{2p_x}(\rho) &= \mathcal{N}\,\mathrm{e}^{-\rho}\rho\sin\theta\,\cos\phi \\ \phi_{2p_y}(\rho) &= \mathcal{N}\,\mathrm{e}^{-\rho}\rho\sin\theta\,\sin\phi\end{aligned}$$

where $\rho = Zr/2a_\circ$, $a_\circ$ is the Bohr radius, r is the radial distance from the nucleus, and θ and ϕ are the polar and azimuthal angles. $\mathcal{N} = (Z/2a_\circ)^{3/2}/\sqrt{\pi}$ is the normalization constant.

Four sp^2 hybrid orbitals are constructed from these orbitals as follows:

$$\begin{aligned}\psi_1 &= \frac{1}{\sqrt{3}}\phi_{2s} + \sqrt{\frac{2}{3}}\phi_{2p_x} \\ \psi_2 &= \frac{1}{\sqrt{3}}\phi_{2s} - \frac{1}{\sqrt{6}}\phi_{2p_x} + \frac{1}{\sqrt{2}}\phi_{2p_y} \\ \psi_3 &= \frac{1}{\sqrt{3}}\phi_{2s} - \frac{1}{\sqrt{6}}\phi_{2p_x} - \frac{1}{\sqrt{2}}\phi_{2p_y} \\ \psi_4 &= \phi_{2p_z}\end{aligned}$$

a. Orthonormality. Assuming that the ϕ_{2s} and ϕ_{2p} orbitals are orthogonal and normalized (i.e. you don't need to show this), show that the sp^2 hybrid orbitals are also orthonormal.

b. Coordinates for maximum probability density. Find the ϕ and θ values for which the probability density of the ψ_1 hybrid orbital is maximized (i.e. find the direction in which this orbital is pointing).

c. Contour plots. Using whatever plotting package you wish (e.g. gnuplot, Matlab, or using the 'contour' or 'contourf' functions in SciPy; and please see me if you don't know how to approach this question), make two-dimensional contour plots for the ψ_1 and ψ_2 hybrid orbital wave-functions, and their moduli, in the $x - y$ plane (that is for $\theta = \pi/2$). Hand in the code you used to generate the contour plots, as well as a printout of the plots (plots can be submitted by email if you want to submit a colour contour plot and you don't have a colour printer).
(I have put some hints for how do this using python with the Problem Set 1 questions on the blackboard site.)

d. Sigma bonding.
Bonus (for fun, will not be marked): Modify your program so that two adjacent atoms have sp^2 hybrid orbitals directed towards each other to form a σ bond, and plot contours of the wave-function in the $x - y$ plane. Once you know how to do this you can do quite a lot. It is easy for example to put atoms on a honeycomb lattice, with the in-plane sp^2 hybrid orbitals forming covalent bonds, and the resulting contour plot is a map of the wave function in the plane of the carbon atoms in graphene. Or you can put two $2p_z$ orbitals on adjacent atoms on the x-axis and map out the wave-function of a π orbital. (In addition to the in-plane sp^2 hybrid orbitals graphene has π bonds between the $2p_z$ orbitals on adjacent atoms.) Or, you can look at the electron density in anti-bonding orbitals. etc. If you don't feel like doing this yourself, a bit of hacking around on the internet will turn up many nice examples, but it's also nice to see how easy it is to do it yourself.

Answer for Exercise 1.2

Part a. Verification of orthonormality of the $2s$ and $2p$ orbital basis functions is easily computed in software.

For the superposition orthonormality, let's rewrite the sp^2 hybrid wave functions as

$$\begin{aligned}
\psi_1 &= \frac{1}{\sqrt{6}}\left(\sqrt{2}\phi_{2s} + 2\phi_{2p_x}\right) \\
\psi_2 &= \frac{1}{\sqrt{6}}\left(\sqrt{2}\phi_{2s} - \phi_{2p_x} + \sqrt{3}\phi_{2p_y}\right) \\
\psi_3 &= \frac{1}{\sqrt{6}}\left(\phi_{2s} - \phi_{2p_x} - \sqrt{3}\phi_{2p_y}\right) \\
\psi_4 &= \phi_{2p_z}.
\end{aligned}$$

Now, let's verify the normalization of these wave functions

$$\begin{aligned}
\langle\psi_1|\psi_1\rangle &= \frac{1}{6}\left\langle \sqrt{2}\phi_{2s} + 2\phi_{2p_x} \middle| \sqrt{2}\phi_{2s} + 2\phi_{2p_x} \right\rangle \\
&= \frac{1}{6}\left(\sqrt{2}^2 + 2^2\right) \\
&= \frac{1}{6}(2+4) \\
&= 1
\end{aligned} \tag{1.10a}$$

$$\begin{aligned}
\langle\psi_2|\psi_2\rangle &= \frac{1}{6}\left\langle \sqrt{2}\phi_{2s} - \phi_{2p_x} + \sqrt{3}\phi_{2p_y} \middle| \sqrt{2}\phi_{2s} - \phi_{2p_x} + \sqrt{3}\phi_{2p_y} \right\rangle \\
&= \frac{1}{6}(2+1+3) \\
&= 1
\end{aligned} \tag{1.10b}$$

$$\begin{aligned}
\langle\psi_3|\psi_3\rangle &= \frac{1}{6}\left\langle \sqrt{2}\phi_{2s} - \phi_{2p_x} - \sqrt{3}\phi_{2p_y} \middle| \sqrt{2}\phi_{2s} - \phi_{2p_x} - \sqrt{3}\phi_{2p_y} \right\rangle \\
&= \frac{1}{6}(2+1+3) \\
&= 1
\end{aligned} \tag{1.10c}$$

$$\begin{aligned}\langle\psi_4|\psi_4\rangle &= \langle\phi_{2p_z}|\phi_{2p_z}\rangle \\ &= 1.\end{aligned} \tag{1.10d}$$

That verifies that these hybrid orbitals are all normalized. Checking all the inner products pairwise zeros will complete the verification of orthonormality. It's clear that ψ_4 is normal to all others since only ψ_4 has a ϕ_{2p_z} component. For the rest we have

$$\begin{aligned}\langle\psi_1|\psi_2\rangle &= \frac{1}{6}\left\langle \sqrt{2}\phi_{2s} + 2\phi_{2p_x} \middle| \sqrt{2}\phi_{2s} - \phi_{2p_x} + \sqrt{3}\phi_{2p_y} \right\rangle \\ &= \frac{1}{6}(2-2) \\ &= 0\end{aligned} \tag{1.11a}$$

$$\begin{aligned}\langle\psi_1|\psi_3\rangle &= \frac{1}{6}\left\langle \sqrt{2}\phi_{2s} + 2\phi_{2p_x} \middle| \sqrt{2}\phi_{2s} - \phi_{2p_x} - \sqrt{3}\phi_{2p_y} \right\rangle \\ &= \frac{1}{6}(2-2) \\ &= 0\end{aligned} \tag{1.11b}$$

$$\begin{aligned}\langle\psi_2|\psi_3\rangle &= \frac{1}{6}\left\langle \sqrt{2}\phi_{2s} - \phi_{2p_x} + \sqrt{3}\phi_{2p_y} \middle| \sqrt{2}\phi_{2s} - \phi_{2p_x} - \sqrt{3}\phi_{2p_y} \right\rangle \\ &= \frac{1}{6}(2+1-3) \\ &= 0.\end{aligned} \tag{1.11c}$$

Part b. The probability density for ψ_1 has the form

$$\begin{aligned}|\psi_1|^2 &= \frac{1}{3}\left(\phi_{2s} + \sqrt{2}\phi_{2p_x}\right)^*\left(\phi_{2s} + \sqrt{2}\phi_{2p_x}\right) \\ &= \frac{1}{3}\left(|\phi_{2s}|^2 + 2\left|\phi_{2p_x}\right|^2 + 2\sqrt{2}\phi_{2s}\phi_{2p_x}\right) \\ &= \frac{\mathcal{N}^2}{3}e^{-2\rho}\Bigg((1-\rho)^2 + 2\rho^2\sin^2\theta\cos^2\phi \\ &\qquad + 2\sqrt{2}\rho(1-\rho)\sin\theta\cos\phi\Bigg).\end{aligned} \tag{1.12}$$

Integrating this to find the fraction of the probability density along each radial ray, we find

$$\begin{aligned}
&\frac{\mathcal{N}^2}{3}\int_0^\infty r^2 dr e^{-2\rho}\left((1-\rho)^2+2\rho^2\sin^2\theta\cos^2\phi+2\sqrt{2}\rho(1-\rho)\sin\theta\cos\phi\right)\\
&=\frac{\mathcal{N}^2}{3}\left(\frac{2a_\circ}{Z}\right)^3\\
&\quad\int_0^\infty \rho^2 d\rho e^{-2\rho}\left((1-\rho)^2+2\rho^2\sin^2\theta\cos^2\phi+2\sqrt{2}\rho(1-\rho)\sin\theta\cos\phi\right)\\
&=\frac{1}{3\pi}\int_0^\infty \frac{1}{8}x^2 dx e^{-x}\times\\
&\qquad\left(\left(1-\frac{x}{2}\right)^2+2\left(\frac{x}{2}\right)^2\sin^2\theta\cos^2\phi+2\sqrt{2}\frac{x}{2}\left(1-\frac{x}{2}\right)\sin\theta\cos\phi\right)\\
&=\frac{1}{24\pi}\left(\text{const}+\frac{1}{2}4!\sin^2\theta\cos^2\phi+\sqrt{2}\sin\theta\cos\phi\left(3!-\frac{4!}{2}\right)\right).
\end{aligned} \tag{1.13}$$

Setting θ and ϕ partials equal to zero respectively we have

$$12\times 2\sin\theta\cos\theta\cos^2\phi+\sqrt{2}\cos\theta\cos\phi(-6)=0 \tag{1.14a}$$

$$-12\times 2\sin^2\theta\cos\phi\sin\phi+\sqrt{2}\sin\theta\sin\phi(-6)=0, \tag{1.14b}$$

or

$$\left(4\sin\theta\cos\phi-\sqrt{2}\right)\cos\theta\cos\phi=0 \tag{1.15a}$$

$$\left(4\sin\theta\cos\phi-\sqrt{2}\right)\sin\theta\sin\phi=0. \tag{1.15b}$$

Neglecting the first common factor, some experimentation yields

Grading remark: Marked wrong. Review this.

the solution $\phi=\pi/2$, $\theta\in\{0,\pi\}$. The probability density is maximized along the z,y plane pointing towards either of the poles.

Part c.

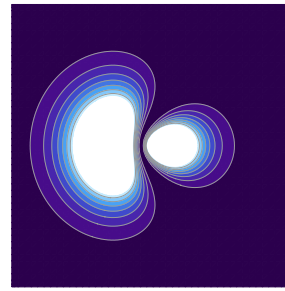

Figure 1.27: $|\psi_1|^2$, contour plot in $x - y$ plane.

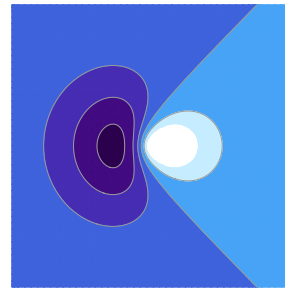

Figure 1.28: ψ_1, contour plot in $x - y$ plane.

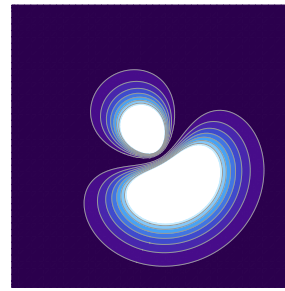

Figure 1.29: $|\psi_2|^2$, contour plot in $x - y$ plane.

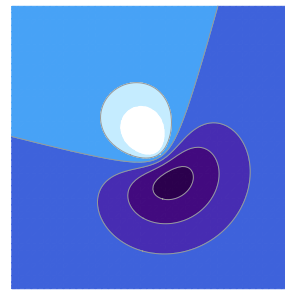

Figure 1.30: ψ_2, contour plot in $x - y$ plane.

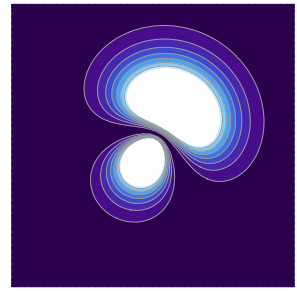

Figure 1.31: $|\psi_3|^2$, contour plot in $x - y$ plane.

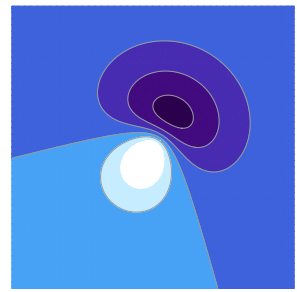

Figure 1.32: ψ_3, contour plot in $x - y$ plane.

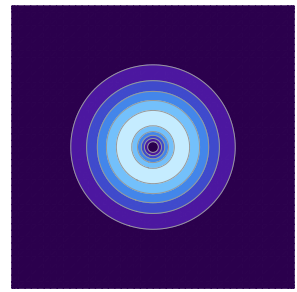

Figure 1.33: $|\psi_4|^2$, contour plot in $x - y$ plane.

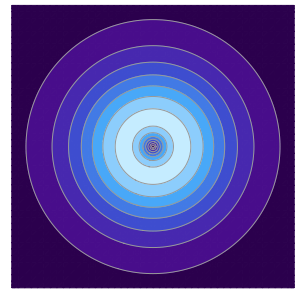

Figure 1.34: ψ_4, contour plot in $x - y$ plane.

Part d.

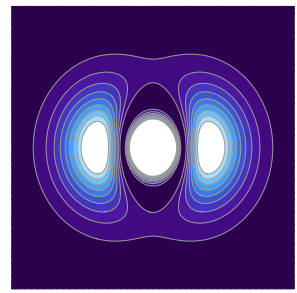

Figure 1.35: $|\psi_5|^2$, contour plot in $x - y$ plane.

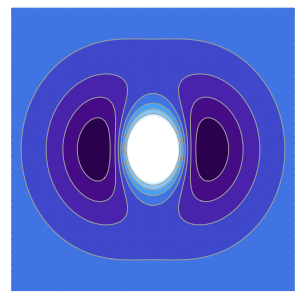

Figure 1.36: ψ_5, contour plot in $x - y$ plane.

Exercise 1.3 The Madelung constant. (*2013 ps1 p3*)

From: (Ibach and Luth, Q1, Chapter 1).

a. Calculate the Madelung constant A for a linear ionic chain.

b. Approximate numerical calculations for the NaCl lattice. Make approximate numerical calculations (on a computer) for the NaCl lattice. First use a cubic geometry in which $2ma$ is the cube side-length, with a the separation of nearest neighbors, and second a spherical geometry where ma is the radius of the sphere. Carry out the calculation for m values of 97, 98 and 99, and compare the results. Please submit your code for this question, as well as a discussion of why calculations in the two geometries behave so differently.

Answer for Exercise 1.3

Part a. Consider an ionic arrangement as illustrated in fig. 1.37.

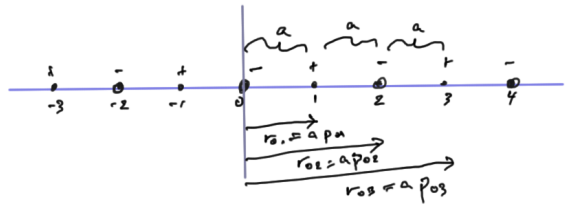

Figure 1.37: Linear ionic solid configuration.

With $r_{ij} = ap_{ij}$, with p_{ij} the difference in the enumeration indices, our Madelung constant for the ion at position zero is

$$\begin{aligned} A_0 &= \sum_{i\neq 0} \frac{z_i}{|r_{0i}/a|} \\ &= \sum_{i\neq 0, i \text{ odd}} \frac{1}{i} - \sum_{i\neq 0, i \text{ odd}} \frac{1}{i} \\ &= 2\sum_{j=0}^{\infty} \frac{1}{2j+1} - 2\sum_{j=0}^{\infty} \frac{1}{2j+2} \\ &= 2\left(\frac{1}{1} - \frac{1}{2} + \frac{1}{3} - \frac{1}{4} + \cdots\right) \\ &= 2\ln(1+1) \\ &\approx 1.39. \end{aligned} \tag{1.16}$$

Part b. Positioning the Cl^- ion in the center, we want to sum

$$A = \sum_{i,j,k\in[-m,m],\{i,j,k\}\neq\{0,0,0\}} \frac{(-1)^{i+j+k+1}}{\sqrt{i^2+j^2+k^2}}. \tag{1.17}$$

For the spherical geometry this sum will be limited by an additional constraint on the sum of

$$i^2 + j^2 + k^2 \leq m^2. \tag{1.18}$$

For the calculations see qmSolidsPs1P3b.nb

The sum over the cubic configuration appears to converge on a value in the range $(1.741, 1.753)$. On the other hand for $m = 97, 98, 99$ we have $A = 15.405, -4.513, 3.570$ respectively. This spherical summation is wildly divergent for small values of m, oscillating between positive and negative values with no apparent regularity. Given the symmetry of the cubic structure with respect to additional shells of charge it is not surprising that this sum is better behaved for low values of m. With a rough estimate of 10^{18} atoms in a grain of salt, we'd still have m of the order $10^8 \gg 99$ for a crystal structure of decent extent. A sum with $m = 99$ is still very small. This is apparently small enough that we can't expect any sort of convergence for a spherical summation that has no inherent symmetry as new spherical "shells" are added.

Grading remarks: Lost marks for the underlined text above, with comment "Explain specifically and in physical terms what this means." The posted solutions included a nice table that shows how the number of positive vs number of negative atoms in the lattice as m increases, and how that difference in the total charge difference oscillates wildly when we increase the spherical volume but very little when increasing the volume of the cube.

Exercise 1.4 Bonding, structure, melting points. (*2013 ps2 p1*)

Explain how trends in melting points in the periodic table might be explained in terms of the relationship between the type of bonding and the character of the valence electrons.

For the melting points see the periodic table handed out in the first lecture, which can also be found at:

http://www.sciencegeek.net/tables/lbltable.pdf

Specifically discuss melting points of (a) the alkali metals (the first column of the periodic table not including hydrogen); (b) the noble gases (the last column of the periodic table); (c) boron and carbon; (d) oxygen and nitrogen; and (e) the transition metals.

You should write around 300 words (or more).

Answer for Exercise 1.4

Starting with the group 1A, the alkali metals , we see in fig. 1.38 a clear trend of decreasing melting points as the atomic number increases, starting with Li melting at 453 K, down to Cs melting at the hot summer temperature of 302 K. Elemental solids for these elements are held together by metallic bonding . It's likely that the single "available" ns^1 orbital electrons are most involved in this metallic bonding. Because these orbitals increase in size with the atomic radius, we have a delocalization of the electrons involved in this metallic bonding, and it makes sense that there is an associated decrease in melting point with Z since the electrons involved in the bonding of the corresponding solids are proportionally spread spatially.

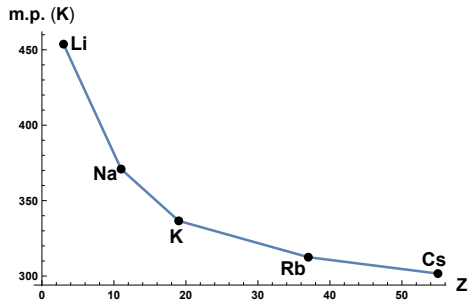

Figure 1.38: alkali metal melting points.

Moving to group 8, the noble gases , we see in fig. 1.39 that the melting points are all extremely low. Unlike the alkali metals, the melting points increase with Z. With these elements all having completely filled orbitals (ns^2np^6) we expect the melting points to be low, since the bonding in the solid state is going to be dominated by Van der Waals bonding. We have an increase of atomic radii with Z as we go down the column. It seems plausible that energy supplied to these elements in solid form would tend to disrupt stable dipole configurations, especially as the radii increases for larger Z elements. That is consistent with an inhibition of Van

der Waals bonding, accounting for the increase in melting points with Z that we see in the periodic table data.

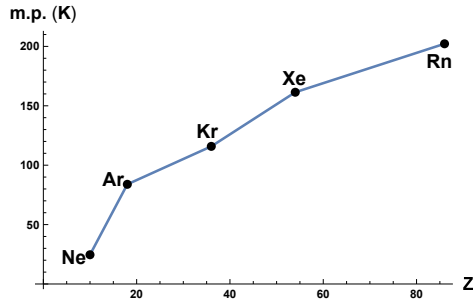

Figure 1.39: noble gas melting points.

The melting points of B ($1s^2 2s^2 p^1$) and C ($1s^2 2s^2 p^2$), as plotted in fig. 1.40 are very large compared to the alkali metals and noble gases. Bonding in these elements is covalent, and high energies will be required to break these bonds. Solid boron is found as B_{12} [16]. With each boron atom in such a crystal we have enough $1p$ orbital electrons to populate the equivalent of two covalent $1p^6$ bonds. The melting points of both the tetrahedral diamond solid structure and the planar graphite structure are similar, with graphite melting 2-47 K higher than diamond. We can have strong

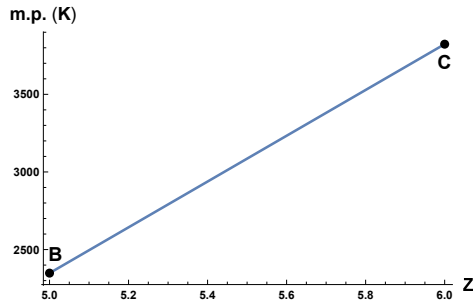

Figure 1.40: boron and carbon melting points.

Moving along the $1p$ period to N we have a remarkable drop in melting point, down to 63 K from 4100 for C. Observe that N with state $1s^2 2s^2 1p^3$ has half filled orbitals and thus has an inherent stability even in isolation. We see similar drops in melting points at other points where we have half or completely filled orbitals, such

as Mn ($[Ar]3d^5 4s^2$ fig. 1.42), Tc ($[Kr]4d^5 5s^2$ fig. 1.43), Eu and Yb ($[Xe]4f^7 6s^2$, $[Xe]4f^{14} 6s^2$ fig. 1.44), and also in the noble gases with np^6 states. We will still have covalent bonding for N and O but this can occur in the smaller geometric configurations N_2 and O_2 which is consistent with lower melting points. The lower melting point of O compared to N is somewhat of an oddity and not accounted for by the drop and rise of melting point that we see in the periodic table when transitioning into and from half filled orbital states. However, we've noted that we can have sp hybridization in O. It seems reasonable that a difference in stability for this hybrid bonding compared to the purely $1p$ covalent bonding of solid N accounts for the lower melting point of solid O compared to solid N.

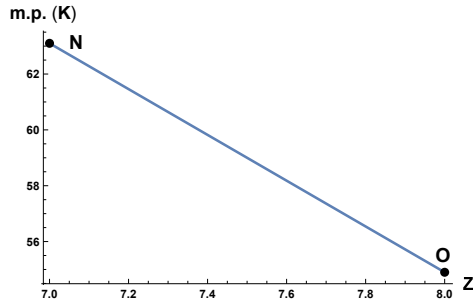

Figure 1.41: oxygen and nitrogen melting points.

The transition metals are those elements characterized by incomplete filled d and f orbitals in their ground state (although some of these may also have incomplete s orbitals as the filling sequence is not necessarily uniform). These elements, plotted in fig. 1.42, fig. 1.43, and fig. 1.44 form metallic bonds due to these delocalized d, and f-orbital electrons. The melting point dips at Mn, Tc, as noted above, are the elements for which we have exactly half filled orbitals. The maximum melting points are found in the neighborhood of these half filled orbital states, and decrease towards the completely filled orbital states on either side (or the column 1 elements which are fairly close to completely filled) as one progresses up or down the period. We've seen with the noble gases with their completely filled p orbitals have the lowest melting points, but we have local minimums just past the transition metals at Zn, Cd, Hg ($[Ar]3d^1 04s^2$, $[Kr]4d^1 05s^2$, $[Xe]4f^1 45d^1 06s^2$

) just before the p block. This last element mercury is very familiar as the oddball metal that is liquid at room temperature. We see this is a consequence of the stability of its completely filled orbitals. With the higher melting points in the central regions of the transition metal periods is appears that more delocalized (but incompletely filled) orbitals allows for stronger bonding, requiring more energy to break the metallic bonds and melt the metal.

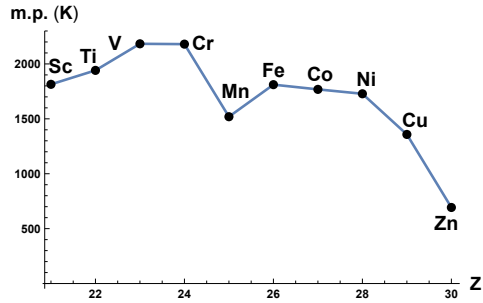

Figure 1.42: period 4 transition metal melting points.

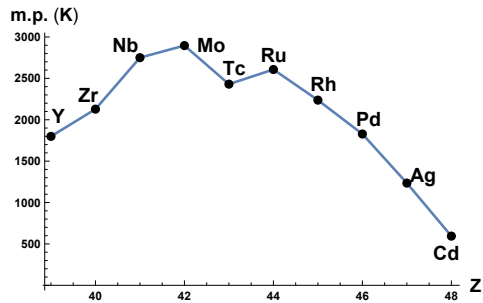

Figure 1.43: period 5 transition metal melting points.

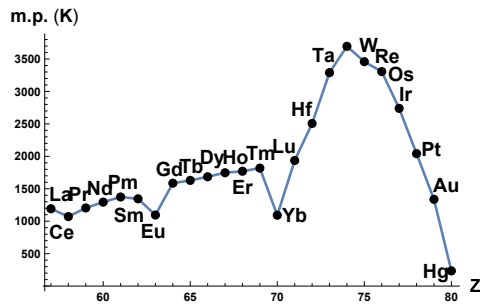

Figure 1.44: period 6 transition metal melting points.

2 LATTICE STRUCTURE AND DIFFRACTION.

2.1 PERIODICITY.

Reading: §2.0 [10]. Also very helpful is [14].

Most solids prefer a periodic arrangement of their atoms. This is due to directional bonding, and is easy to see in some cases, as in our diamond tetrahedral pattern of fig. 2.1.

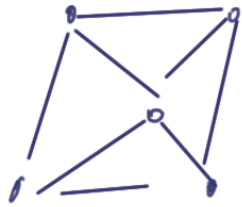

Figure 2.1: Diamond tetrahedron.

Unproven theorem of no name: lowest energy configuration of atoms in a solid is periodic.

Minimum Coulomb energy for integer ratios of atoms Na_1Cl_1, Fe_2O_3, Fe_3O_4, $PrOs_4Sb_{12}$, $YbCO_2Zn_{20}$.

There's a lot of info on "amorphous/glassy" materials are not periodic. We won't consider these.

Mathematical description of periodicity Starting with a 2D lattice as in fig. 2.2. Two vectors can generate a lattice (or 2 lengths and 1 angle)

We'll assign each atomic center a vector

$$\mathbf{r_n} = n_1\mathbf{a} + n_2\mathbf{b}. \tag{2.1}$$

Only five cases (in 2D) that are symmetrically distinct that leave no spaces

FIXME: No figure – too fast with the eraser. $a \neq b$, $\gamma = \pi/2$?

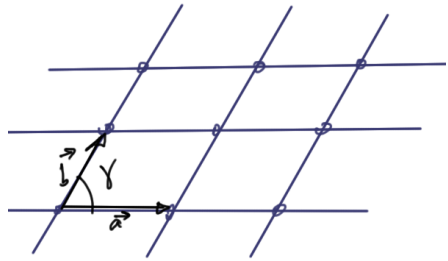

Figure 2.2: 2D lattice.

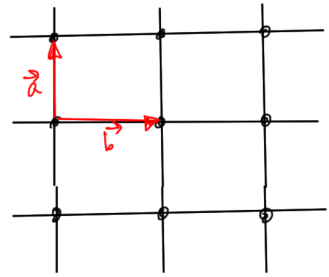

Figure 2.3: square lattice. $a = b$, $\gamma = \pi/2$.

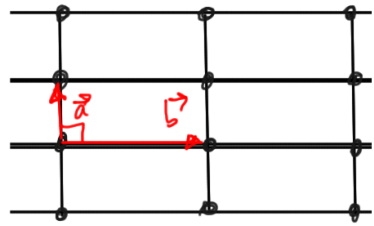

Figure 2.4: Rectangular. $a \neq b$, $\gamma = \pi/2$.

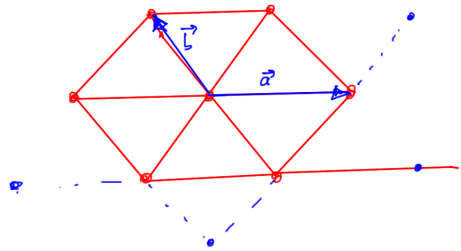

Figure 2.5: Hexagonal close packed.

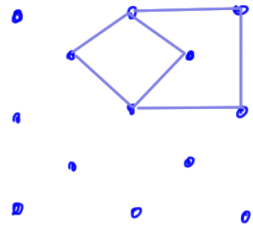

Figure 2.6: Rhombic, or centered rectangular. $a = b$, $\gamma \neq \pi/2, \pi/3$.

2.2 CRYSTAL STRUCTURES.

Reading: pp. 23-24 [10]. Handout: Bravais lattices in three dimensions [17].

We have seven possibilities that fill space (see handout). We need 3 vectors or three lengths angle pairs to describe the geometries, as in fig. 2.7.

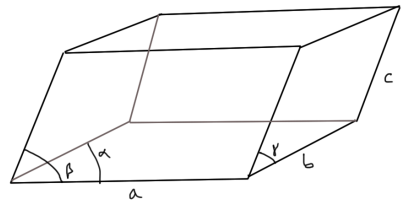

Figure 2.7: Lattice geometry.

Lots of study of hexagonal structures since there appears to be a preference for that in many superconducting materials.

2.3 POINT GROUP SYMMETRY.

Reading: §2.2 [10].

One way to distinguish crystal structures is according to the symmetries that they have. Each crystal structure has symmetry operations that map the crystal onto itself.

To illustrate fig. 2.8 (also on the slide)

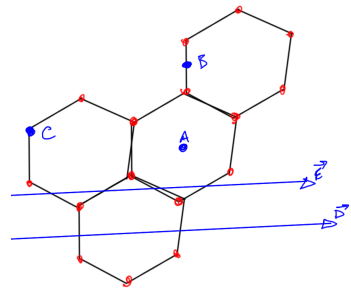

Figure 2.8: Symmetries of a graphene lattice.

- A is a 6 fold rotation axis.
- B is a 2 fold rotation axis.
- C is a 3 fold rotation axis.
- D is a 2 fold rotation axis.

A and B are inversion centers, so that ($\mathbf{r} \rightarrow -\mathbf{r}$) maps any lattice point onto an existing lattice point.

The plane perpendicular to the page, containing **D**, is a mirror plane.

C is a 6-fold rotation-inversion axis, so that under rotation then inversion, each point maps onto an existing lattice point.

Have other symmetries. For example, the glide plane **E** has a symmetry operation under inversion followed by translation.

Symmetry operations tell you about degeneracies of energy eigenstates, and the number of independent elastic constants, ...

Group theory ideas of symmetries described too briefly in §2.3, 2.4 [10], read if desired.

2.4 SIMPLE CRYSTAL STRUCTURES.

Reading: [1] ch. 4

Assume one atom per lattice point. This is called a 1 atom basis.

Simple cubic Very rare: only Po, which is very toxic. This is in fact the toxic substance that was used as in the assassination by injection in the UK of Alexander Litvinenko, the former KGB and FSB agent turned undesirable reporter for Chechenia [18].

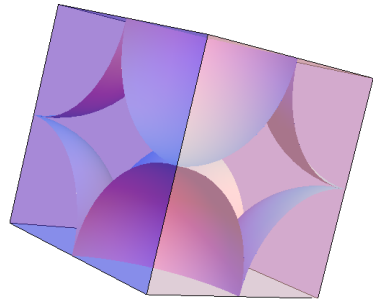

Figure 2.9: Simple cubic.

Face centered cubic (FCC) (Cu, Ni, Au, Pd)
This one is very common

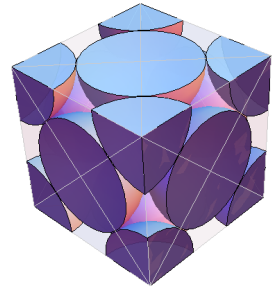

Figure 2.10: Element of a face centered cubic.

Fig 2.8 in the text.
This is a conventional unit cell.
Total 4 atoms per conventional unit cell

$$8 \text{ corners} \times \tfrac{1}{8} = 1 \text{ atoms} \tag{2.2a}$$

$$6 \times \tfrac{1}{2} \text{ faces} = 3 \text{ atoms.} \tag{2.2b}$$

The primitive lattice vectors are

$$\mathbf{a} = \left(\frac{1}{\sqrt{2}}, \frac{1}{\sqrt{2}}, 0\right) a \tag{2.3a}$$

$$\mathbf{b} = \left(\frac{1}{\sqrt{2}}, 0, \frac{1}{\sqrt{2}}\right) a \tag{2.3b}$$

$$\mathbf{c} = \left(0, \frac{1}{\sqrt{2}}, \frac{1}{\sqrt{2}}\right) a. \tag{2.3c}$$

Describing this Bravais lattice as

$$\mathbf{r}_n = n_1\mathbf{a} + n_2\mathbf{b} + n_3\mathbf{c}. \tag{2.4}$$

The primitive unit cell contains 1 lattice point. In [1] ch. 4 a distinction is made between a Bravais lattice structure, and a Bravais lattice basis eq. (2.4). The Bravais lattice is the smallest cell that can be repeated to recover the periodic structure. This does not necessarily contain just a single atom. Two Bravais lattice structure choices are illustrated for a 2D cubic centered lattice in fig. 2.11. These are both two point lattice structures, with one containing two whole atoms, and the other containing one whole atom and four quarter atoms.

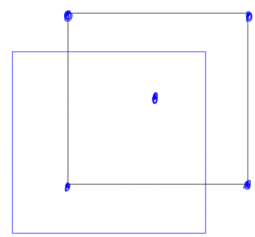

Figure 2.11: Two Bravais lattice choices for 2D cubic centered.

A, B, C are 4-fold axes.

Cube diagonal is a 3-fold axis.

Face centered cubic (FCC) is actually a stack of 2-d hexagonal close packed (HCP fig. 2.12) planes (fig: see slides 04_handout.pdf).

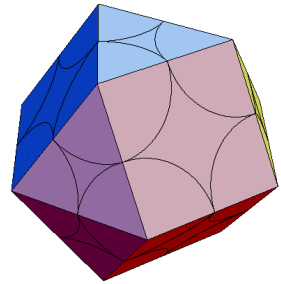

Figure 2.12: Hex close packing.

A common form of dislocation in crystal structures is a mix of face centered and hexagonal close packed. Not over layer 1 => FCC. Both lattices have filling factor 0.7406.

Transition metals often like FCC because of covalent d bonding, as roughly illustrated in fig. 2.13.

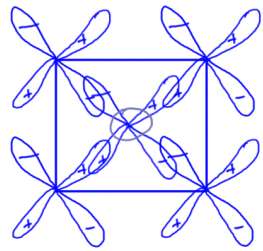

Figure 2.13: D orbital bonding in a plane.

But, for example Co has an HCP phase due to s, p, d hybrid orbitals.

In the p-block:

- sp_2 hybrids $\rightarrow$ hexagonal.
- sp_3 hybrids $\rightarrow$ diamond.

Body centered cubic (BCC)
Total 3 atoms per conventional unit cell

$$8 \text{ corners} \times \frac{1}{8} = 1 \text{ atoms} \tag{2.5a}$$

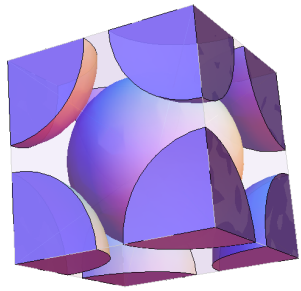

Figure 2.14: Element of a body centered cubic.

1 center = 1 atom. (2.5b)

BCC has 8 nn, FCC has 12.

FCC is more common, but column 1 of the periodic table are all body centered cubic.

Because n s orbitals are huge

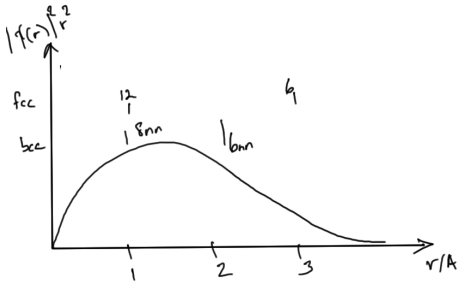

Figure 2.15: Large extent of *ns* orbitals.

Diamond lattice

See: 04_lecture

This is an FCC + 4 tetrahedral holes that are filled due to sp_3 hybridization.

Reading: pp. 35, 36 [10]. Skip phase diagrams.

2.5 GENERAL THEORY OF DIFFRACTION.

Our diffraction geometry is illustrated in fig. 2.16.

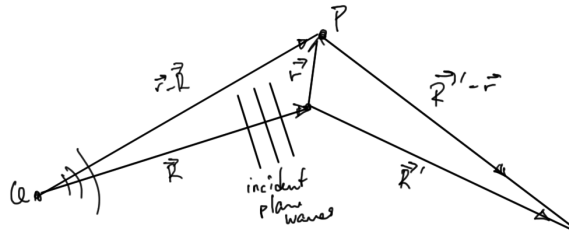

Figure 2.16: Diffraction in crystal by x-rays, neutrons, ...

In the crystal we can imagine light and atom interaction as illustrated in fig. 2.17.

Figure 2.17: Diffraction interaction in the crystal.

The incident beam makes electrons vibrate at frequency $\omega_\circ$, and re-radiate at $\omega_\circ$.

The diffraction pattern is the constructive interference of the re-radiated x-rays (or neutrons)

At P, primary beam has amplitude

$$A_p(\mathbf{r}, t) = A_\circ \exp\left(i\left(k_\circ \cdot (\mathbf{R} + \mathbf{r}) - \omega_\circ t\right)\right). \tag{2.6}$$

Here $A_\circ$ is constant everywhere and $k_\circ = 2\pi/\lambda_\circ$.

Scattered wave at P has amplitude

$$\rho(\mathbf{r}) A_p(\mathbf{r}, t). \tag{2.7}$$

where

$$\rho(\mathbf{r}) = \text{“scattering density”}. \tag{2.8}$$

For neutrons we've got interactions with the nuclei, and things get messier, but for x-rays

$$\rho(\mathbf{r}) \sim \text{electron density.} \tag{2.9}$$

This density is largest near the nucleus, at least for large Z (heavy) atoms like La, and Ac. Large Z atoms are easier to see.

Amplitude at B, due to $\mathbf{r}$

$$\begin{aligned} A_B(\mathbf{r}) &= A_p(\mathbf{r})\rho(\mathbf{r})\frac{e^{i\mathbf{k}\cdot(\mathbf{R}'-\mathbf{r})}}{|\mathbf{R}'-\mathbf{r}|} \\ &\approx A_p(\mathbf{r},t)\rho(\mathbf{r})\frac{e^{i\mathbf{k}\cdot(\mathbf{R}'-\mathbf{r})}}{|\mathbf{R}'|}. \end{aligned} \tag{2.10}$$

time independent part of $\rho(\mathbf{r})$ => secondary beam has frequency $\omega_\circ$, or

$$|\mathbf{k}| = |\mathbf{k}_\circ| = \frac{\omega_\circ}{c}. \tag{2.11}$$

This is the elastic scattering. We ignore inelastic scattering.

The vector $\mathbf{R}'$ determines the direction of $\mathbf{k}$.

If $R' \gg r$, $\mathbf{k}$ is close to the same for all $\mathbf{r}$. Then eq. (2.10) is approximately

independent of $\mathbf{r}$ dependent of $\mathbf{r}$

$$A_B(\mathbf{r}) \approx \frac{A_\circ}{R'}e^{i(\mathbf{k}_\circ\cdot\mathbf{R}+\mathbf{k}\cdot\mathbf{R}')}\,\rho(\mathbf{r})e^{i(\mathbf{k}_\circ-\mathbf{k})\cdot\mathbf{r}}e^{-i\omega_\circ t}. \tag{2.12}$$

Total amplitude at B

$$\equiv -\mathbf{K}$$

$$A_B \propto e^{-i\omega_\circ t}\int \rho(\mathbf{r})e^{i\overbrace{(\mathbf{k}_\circ-\mathbf{k})}\cdot\mathbf{r}}d\mathbf{r}. \tag{2.13}$$

So that the intensity is

$$I_\mathbf{B} \propto |A_B|^2 \propto \left|\int \rho(\mathbf{r})e^{-i\mathbf{K}\cdot\mathbf{r}}d\mathbf{r}\right|^2. \tag{2.14}$$

This is the Fourier transform of the scattering density.

2.6 RECIPROCAL LATTICE.

Reading: [1] ch. 5.

- 1D crystal. Illustrated in fig. 2.18.

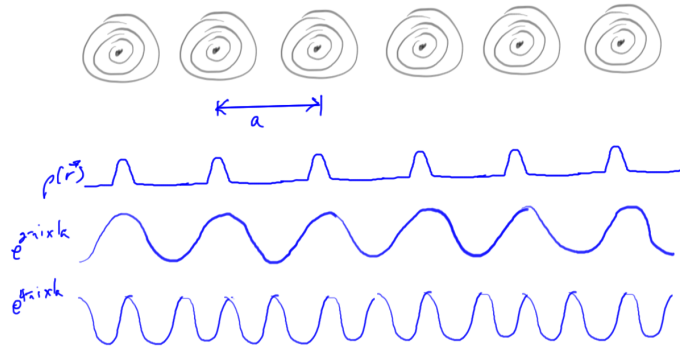

Figure 2.18: 1D crystal diffraction electron density.

$$\rho(x) = \sum_n p_n e^{in2\pi x/a}. \tag{2.15}$$

Show that

$$\rho(x + ma) = \rho(x). \tag{2.16}$$

- 3D lattice

$$\rho(\mathbf{r}) = \sum_{\mathbf{G}} \rho_{\mathbf{G}} e^{i\mathbf{G}\cdot\mathbf{r}}. \tag{2.17}$$

With

$$\mathbf{r}_n = n_1\mathbf{a}_1 + n_2\mathbf{a}_2 + n_3\mathbf{a}_3, \tag{2.18}$$

find the $\mathbf{G}$'s, such that

$$\rho(\mathbf{r} + \mathbf{r}_n) = \rho(\mathbf{r}). \tag{2.19}$$

$$e^{i\mathbf{G}\cdot\mathbf{r}_n} = 1, \tag{2.20}$$

or

$$\mathbf{G}\cdot\mathbf{r}_n = 2\pi m, \tag{2.21}$$

where m is an integer.

Try

$$\mathbf{G} = h\mathbf{g}_1 + k\mathbf{g}_2 + l\mathbf{g}_3, \tag{2.22}$$

where h, k, l are integers.

The $\mathbf{G}$'s are wave vectors of waves with the periodicity of the lattice.

Example 2.1: 2D periodic lattice.

An example of reciprocal projection is illustrated in fig. 2.19.

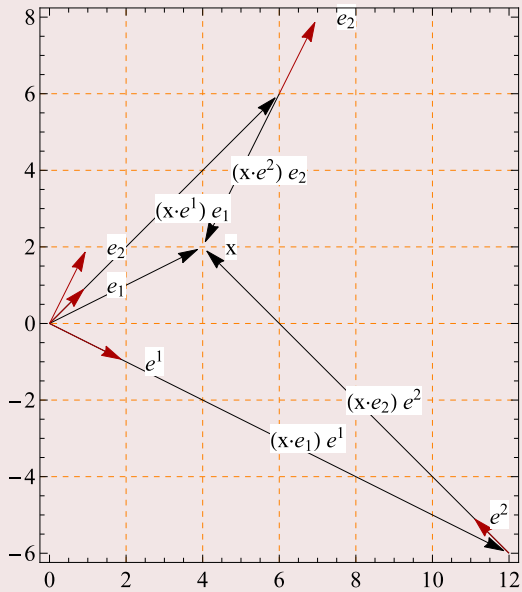

Figure 2.19: reciprocal projection.

Here $e^i \cdot e_j = \delta^i_j$, not using the 2π scaling factor that we are using in this diffraction context.

FIXME: Our prof used the following to illustrate (which I did a brute force cut and paste of from the prof's notes: 05 lecture.pdf). Re-draw once I figure out what he was illustrating.

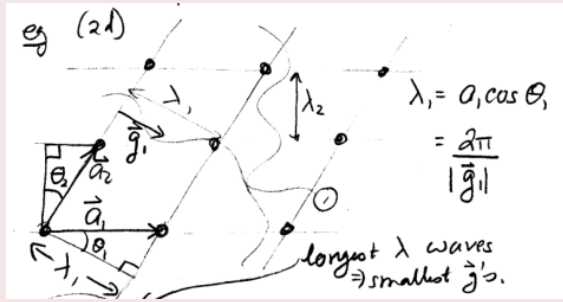

Figure 2.20: 2d periodic lattice.

Wave 1 :

$$\mathbf{g}_1 \cdot \mathbf{a}_1 = g_1 a_1 \cos\theta_1 = 2\pi \tag{2.23a}$$

$$\mathbf{g}_1 \cdot \mathbf{a}_2 = 0. \tag{2.23b}$$

Wave 2 : $\mathbf{g}_2 \cdot \mathbf{a}_1 = 0$,

$$\mathbf{g}_2 \cdot \mathbf{a}_1 = 0 \tag{2.24a}$$

$$\mathbf{g}_2 \cdot \mathbf{a}_2 = g_2 a_2 \cos\theta_2 = 2\pi. \tag{2.24b}$$

We can read off relations between the wavelengths from these

$$\begin{aligned} \lambda_1 &= a_1 \cos\theta_1 \\ \lambda_2 &= a_2 \cos\theta_2. \end{aligned} \tag{2.25}$$

We introduce reciprocal vectors defined by

$$\mathbf{g}_i \cdot \mathbf{a}_j = 2\pi\delta_{ij}. \tag{2.26}$$

The general formula in 3D is

$$\mathbf{g}_1 = 2\pi \frac{\mathbf{a}_2 \times \mathbf{a}_3}{\mathbf{a}_1 \cdot (\mathbf{a}_2 \times \mathbf{a}_3)} \tag{2.27a}$$

$$\mathbf{g}_2 = 2\pi \frac{\mathbf{a}_3 \times \mathbf{a}_2}{\mathbf{a}_2 \cdot (\mathbf{a}_3 \times \mathbf{a}_1)} \tag{2.27b}$$

$$\mathbf{g}_3 = 2\pi \frac{\mathbf{a}_1 \times \mathbf{a}_3}{\mathbf{a}_3 \cdot (\mathbf{a}_1 \times \mathbf{a}_2)}. \tag{2.27c}$$

The numerator cross product ensures that $\mathbf{g}_1$ is perpendicular to $\mathbf{a}_2$ and $\mathbf{a}_3$. The one in the denominator "cancels" the $\mathbf{a}_2 \times \mathbf{a}_3$ in the numerator.

2.7 CONSTRUCTIVE INTERFERENCE.

Constructive interference is diffraction peaks (spots). In general the intensity is

$$I(\mathbf{K}) = \frac{|A_\circ|^2}{R'^2} \left| \int \rho(\mathbf{r}) e^{-i\mathbf{K}\cdot\mathbf{r}} d\mathbf{r} \right|^2, \tag{2.28}$$

so that after a periodic decomposition we have

$$I(\mathbf{K}) = \frac{|A_\circ|^2}{R'^2} \left| \sum_{\mathbf{G}} \rho_{\mathbf{G}} \int e^{i(\mathbf{G}-\mathbf{K})\cdot\mathbf{r}} d\mathbf{r} \right|^2. \tag{2.29}$$

When

$$\mathbf{K} = \mathbf{k} - \mathbf{k}_\circ = \mathbf{G}. \tag{2.30}$$

the integrand is unity (so the integral is the area of the diffraction aperture), whereas if

$$\mathbf{K} \neq \mathbf{G}. \tag{2.31}$$

integrand oscillates, and the integral ~ 0.

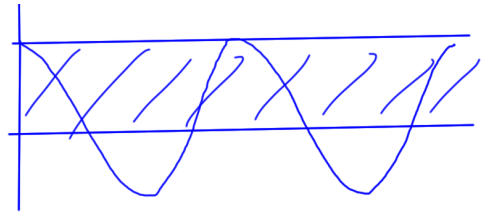

Figure 2.21: Cancellation.

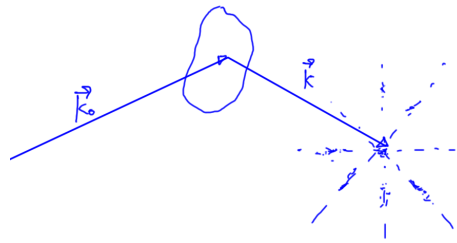

Figure 2.22: Diffraction.

This is effectively a $\delta_{\mathbf{K},\mathbf{G}}$ condition, defining the Laue condition for constructive interference.

$$\boxed{\mathbf{K} = \mathbf{G}.} \tag{2.32}$$

In particular

$$I(\mathbf{K} = \mathbf{G}) = \frac{|A_\circ|^2}{R'^2}|\rho_{\mathbf{G}}|^2 V^2, \tag{2.33}$$

where V is the scattering volume. This is discussed further in [10] §3.3.

2.8 EWALD SPHERE.

Reading: [1] ch. 6.

As mentioned elastic scattering is characterized by $|\mathbf{k}| = |\mathbf{k}_\circ|$. This allows for a geometric (in reciprocal space) interpretation of the Laue condition. The procedure is

1. Draw reciprocal lattice (r.l.)
2. draw $\mathbf{k}_\circ$ with the head at a r.l. point
3. draw sphere of radius $\mathbf{k}_\circ$ around the tail
4. if there sphere intersects other r.l. points we have diffraction.

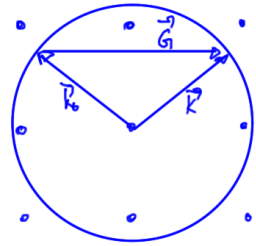

Figure 2.23: Ewald sphere.

2.9 SCATTERING IN TERMS OF LATTICE POINTS.

A lattice has an infinite number of sets of parallel planes that contain all lattice points.

A given set of planes is labeled by Miller indices.

1. start at the origin
2. With m, n, o all integers,
   - go $m\mathbf{a}_1$ to next plane.
   - go $n\mathbf{a}_2$ to next plane.
   - go $o\mathbf{a}_3$ to next plane.
3. Find $\left(\frac{p}{m}, \frac{p}{n}, \frac{p}{o}\right)$. These triplets are called the Miller indices.

Example 2.2: Simple cubic.

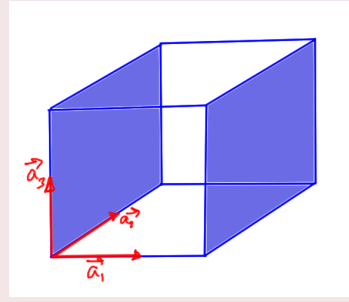

Figure 2.24: Cubic Miller planes.

$$(1 \times \mathbf{a}_1, \infty \times \mathbf{a}_2, \infty \times \mathbf{a}_3). \tag{2.34}$$

$$\left(\frac{p}{1}, \frac{p}{\infty}, \frac{p}{\infty}\right). \tag{2.35}$$

with $p = 1$ this gives Miller indices of

$$(1, 0, 0). \tag{2.36}$$

As another example, consider an fcc configuration, as in fig. 2.25. Here two possible Miller planes are indicated. We use

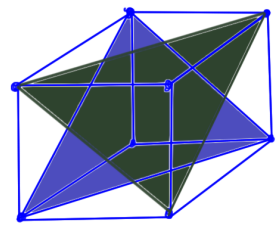

Figure 2.25: fcc Miller planes.

$$\mathbf{G}_{hkl} = j\mathbf{g}_1 + k\mathbf{g}_2 + l\mathbf{g}_3, \tag{2.37}$$

with this perpendicular to a plane that we can identify as the (h, k, l) plane.

Example 2.3: Miller index demonstration.

FIXME: figure stolen from Prof's notes. Was hard to draw in class.

Here we illustrate two pairs of arbitrary planes each passing through two lattice points.

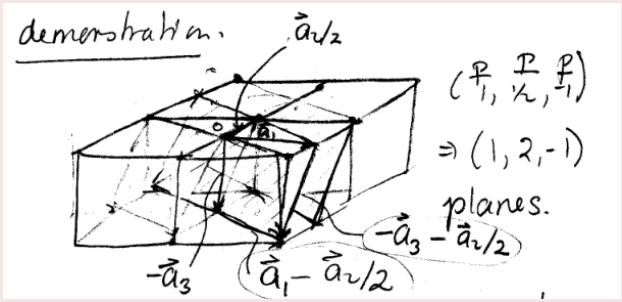

Figure 2.26: Miller index demonstration.

$$\left(1 \times \mathbf{a}_1, \frac{1}{2} \times \mathbf{a}_2, -\mathbf{a}_3\right) \implies \left(\frac{p}{1}, \frac{p}{\frac{1}{2}}, -\frac{p}{1}\right) \implies (1, 2, -1)\,. \tag{2.38}$$

To find the perpendicular, define 2 non-parallel vectors in a plane: $\mathbf{a}_1 - \mathbf{a}_2/2$, $-\mathbf{a}_3 - \mathbf{a}_2/2$.

Perpendicular vector is

$$\begin{aligned} &\propto (\mathbf{a}_1 - \mathbf{a}_2/2) \times (-\mathbf{a}_3 - \mathbf{a}_2/2) \\ &= \frac{1}{2}\mathbf{a}_2 \times \mathbf{a}_3 + \mathbf{a}_3 \times \mathbf{a}_1 - \frac{1}{2}\mathbf{a}_1 \times \mathbf{a}_2 \\ &\propto \mathbf{g}_1 + 2\mathbf{g}_2 - \mathbf{g}_3 = \mathbf{G}_{1,2,-1}. \end{aligned} \tag{2.39}$$

A more general treatment can be found in [10] §3.4. That section of the text introduces a variety of indices that are worth enumerating

- (m, n, o). These provide the scaling $\mathbf{r}_n = m\mathbf{a}_1 + n\mathbf{a}_2 + o\mathbf{a}_3$ for each of the lattice points in position space.
- $(h', k', l') = (1/m, 1/n, 1/o)$. These are non integral reciprocal indices, that are to be scaled by a integral constant p.
- $(h, k, l) = p(h', k', l')$. After scaling with an appropriate constant p (for example, $p = mno$), these are integer valued constants that are reciprocal to the (m, n, o) position space indices.

The text uses $(m, n, o) = (1, 2, 2)$ as an example. It is redrawn here with just two planes in fig. 2.27.

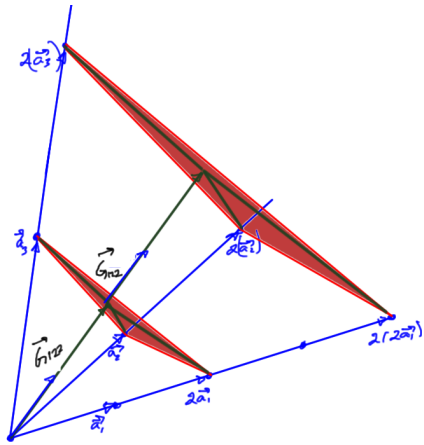

Figure 2.27: Lattice planes example.

Identification of $\mathbf{G}_{hkl}$ with the lattice plane for mno We can factor $\mathbf{G}_{hkl}$ as the cross products of two vectors in the plane

$$\begin{aligned}
&\frac{2\pi p}{mno\mathbf{a}_1 \cdot (\mathbf{a}_2 \times \mathbf{a}_3)} (m\mathbf{a}_1 - n\mathbf{a}_2) \times (n\mathbf{a}_2 - o\mathbf{a}_3) \\
&= \frac{2\pi p}{mno\mathbf{a}_1 \cdot (\mathbf{a}_2 \times \mathbf{a}_3)} (mn\mathbf{a}_1 \times \mathbf{a}_2 + no\mathbf{a}_2 \times \mathbf{a}_3 + om\mathbf{a}_3 \times \mathbf{a}_1) \\
&= \frac{2\pi p}{\mathbf{a}_1 \cdot (\mathbf{a}_2 \times \mathbf{a}_3)} \left(\frac{1}{o}\mathbf{a}_1 \times \mathbf{a}_2 + \frac{1}{m}\mathbf{a}_2 \times \mathbf{a}_3 + \frac{1}{n}\mathbf{a}_3 \times \mathbf{a}_1 \right) \\
&= \frac{2\pi p}{\mathbf{a}_1 \cdot (\mathbf{a}_2 \times \mathbf{a}_3)} (h'\mathbf{a}_2 \times \mathbf{a}_3 + k'\mathbf{a}_3 \times \mathbf{a}_1 l'\mathbf{a}_1 \times \mathbf{a}_2) \\
&= \frac{2\pi}{\mathbf{a}_1 \cdot (\mathbf{a}_2 \times \mathbf{a}_3)} (h\mathbf{a}_2 \times \mathbf{a}_3 + k\mathbf{a}_3 \times \mathbf{a}_1 + l\mathbf{a}_1 \times \mathbf{a}_2) \\
&= h\mathbf{g}_1 + k\mathbf{g}_2 + l\mathbf{g}_3 \\
&= \mathbf{G}_{hkl}.
\end{aligned} \tag{2.40}$$

Observe that this geometrical identification shows that the *hkl* indices of $\mathbf{G}_{hkl}$ are the reciprocal lattice indices in momentum (dual) space, not the original *mno* indices of the position space lattice.

Distance between lattice planes Looking back to fig. 2.27 we see that the distance between integer multiples of the same lattice points can be calculated by projecting any one of the $m\mathbf{a}_1, n\mathbf{a}_2, o\mathbf{a}_3$ vectors onto the direction of the corresponding $\hat{\mathbf{G}}_{hkl}$

The text calls the distance from the origin to the first lattice plane

$$\begin{aligned} d'_{hkl} &= m\mathbf{a}_1 \cdot \hat{\mathbf{G}}_{hkl} \\ &= m\mathbf{a}_1 \cdot \frac{\mathbf{G}_{hkl}}{G_{hkl}} \\ &= m\frac{2\pi h}{G_{hkl}} \\ &= \frac{2\pi p}{G_{hkl}}. \end{aligned} \tag{2.41}$$

and then scales this as

$$d_{hkl} = \frac{d'_{hkl}}{p} = \frac{2\pi}{G_{hkl}}, \tag{2.42}$$

calling this the distance to the "nearest" lattice plane. It initially seemed to me that d'_{hkl} ought to be described as the distance to the nearest lattice plane, since the distance from the origin appeared like it was the separation of the two closest planes. A classmate James explained what I had failed to understand. The entire lattice that the sample primitive lattice cell would generate is not just replicated for integer multiples of $2\mathbf{a}_1$, but all the multiples of $\mathbf{a}_1$ (there are many possible lattice planes and we have to allow for all integer multiples $\mathbf{r}_n = m\mathbf{a}_1 + n\mathbf{a}_2 + o\mathbf{a}_3$). This is illustrated in fig. 2.28.

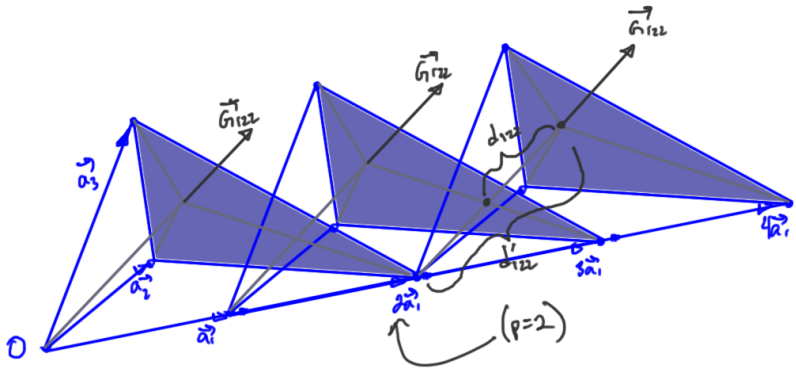

Figure 2.28: Primitive cell replication and all the Miller 122 planes.

Observe how there ends up being a plane between the origin and plane for which $2\mathbf{a}_1$ was a lattice point. This is why we need to divide this value by two (in this $p = 2$ case), and more generally introduce the scaling $d_{hkl} = d'_{hkl}/p$.

2.10 BRAGG CONDITION.

Reading: [1] ch. 6.

In fig. 2.29, is a geometric depiction of $\mathbf{G}$ in reciprocal space, with the hkl plane perpendicular to the page.

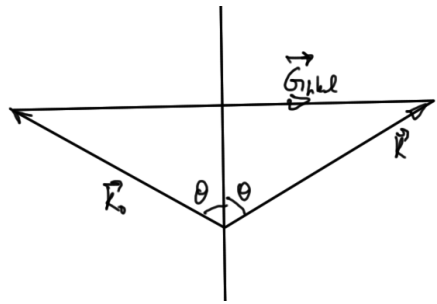

Figure 2.29: Diffraction geometry.

Observe that

$$\mathbf{G}_{hkl} \cdot \hat{\mathbf{k}}_\circ = k_\circ \sin\theta = \frac{G_{hkl}}{2}. \tag{2.43}$$

With G_{hkl} from eq. (2.42), we have

$$\frac{2\pi}{d_{hkl}} = 2k_\circ \sin\theta = 2\frac{2\pi}{\lambda_\circ}\sin\theta, \tag{2.44}$$

or

$$\boxed{\lambda_\circ = 2d_{hkl}\sin\theta.} \tag{2.45}$$

This is the Bragg condition, which we showed is equivalent to the Laue condition, and illustrated in fig. 2.30. Path difference is $2d\sin\theta = n\lambda$ for constructive interference.

2.11 STRUCTURE FACTOR.

Reading: [1] ch. 6, ch. 9 (§in monatomic lattices).

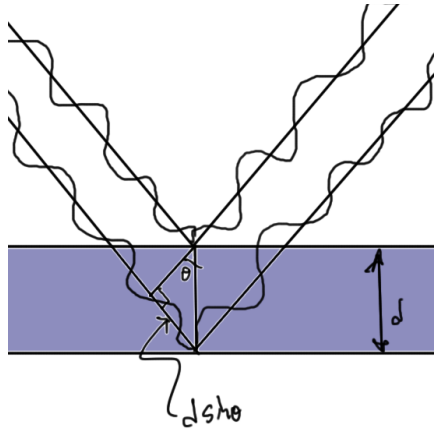

Figure 2.30: Bragg condition.

It is useful to quantify the interference between waves scattered from a unit cell. To do so the structure factor is introduced, and the ideas are outlined here. See [10] §3.6, and [1] ch. 6, for more complete treatments.

Recall that the aperture function for a period lattice was defined by

$$\rho(\mathbf{r}) = \sum_{hkl} \rho_{hkl} e^{i\mathbf{G}_{hkl}\cdot\mathbf{r}}. \tag{2.46}$$

The Fourier coefficient ρ_{hkl} can be recovered by integrating over a unit cell as depicted in fig. 2.31

$$\rho_{hkl} = \frac{1}{V_{\text{cell}}} \int_{\text{cell}} \rho(\mathbf{r}) e^{-i\mathbf{G}_{hkl}\cdot\mathbf{r}} d\mathbf{r}. \tag{2.47}$$

Note that $\rho(\mathbf{r})$ is large close to each nucleus. Using the change of variables to atom centered bases, we find

$$\rho_{hkl} \sim \frac{1}{V_{\text{cell}}} \sum_{\alpha} e^{i\mathbf{G}_{hkl}\cdot\mathbf{r}_\alpha} \int \rho_\alpha(\mathbf{r}') e^{-i\mathbf{G}_{hkl}\cdot\mathbf{r}} d\mathbf{r}', \tag{2.48}$$

where the index α is used to sum over all atoms in a primitive unit cell. The integral portion is the atomic scattering factor (which can be tabulated), and is designated

$$f_\alpha = \int \rho_\alpha(\mathbf{r}') e^{-i\mathbf{G}_{hkl}\cdot\mathbf{r}} d\mathbf{r}'. \tag{2.49}$$

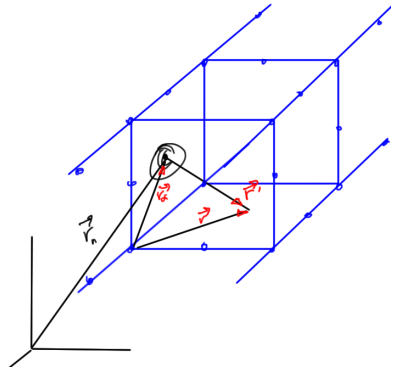

Figure 2.31: Cell relative vector positions.

In terms of the scattering factor, eq. (2.48) is

$$\rho_{hkl} \sim \frac{1}{V_{\text{cell}}} \underbrace{\sum_{\alpha} f_{\alpha} e^{-i\mathbf{G}_{hkl}\cdot\mathbf{r}_{\alpha}}}_{S_{hkl},\ \text{the structure factor}}. \tag{2.50}$$

Recall from eq. (2.33) that the intensity at $\mathbf{K} = \mathbf{G}$ is proportional to $|\rho_{\mathbf{G}}|^2$. Because of this and eq. (2.50), we can utilize the structure factor as a measure of intensity at a reciprocal lattice point

$$I(\mathbf{K} = \mathbf{G}_{hkl}) \propto |S_{hkl}|^2. \tag{2.51}$$

Example 2.4: BCC lattice as simple cubic and 2 atom basis.

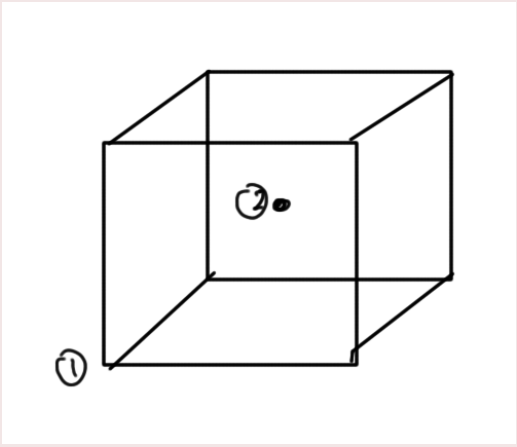

Figure 2.32: Bcc.

$$\mathbf{r}_1 = \begin{bmatrix} 0 \\ 0 \\ 0 \end{bmatrix} \tag{2.52a}$$

$$\mathbf{r}_2 = \frac{a}{2} \begin{bmatrix} 1 \\ 1 \\ 1 \end{bmatrix} \tag{2.52b}$$

$$\mathbf{G}_{hkl} \cdot \mathbf{r}_n = 2\pi m. \tag{2.53}$$

$$S_{hkl} = f(\underbrace{1}_{\text{corner}} + e^{-i \overbrace{\pi(h+k+l)}^{\text{body center}}}). \tag{2.54}$$

A bcc lattice has same diffraction pattern as simple cubic, except all $h + k + l$ = odd spots are missing.

Reading: [10] §3.7

2.12 BRILLOUIN ZONES.

We can define a special primitive unit cell, by bisecting the (reciprocal) lattice vectors with a plane. In 2D consider fig. 2.33

All points inside the first Brillouin zone are closer to $(0, 0)$ than to any other lattice point.

Example: 07 lecture.pdf

Fcc lattice has a bcc reciprocal lattice.

Some 3D figures from [15] were shown in slides.

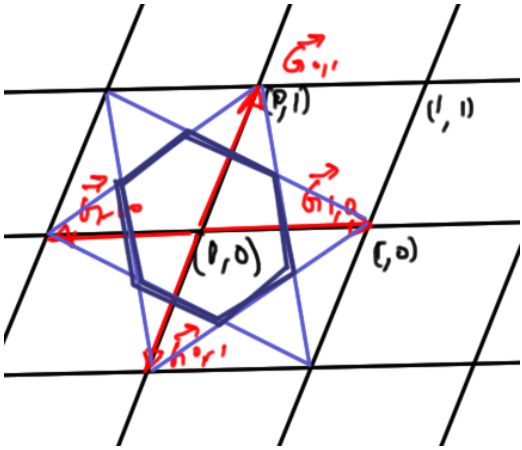

Figure 2.33: First Brillouin zone.

Examination hint: A frequent exam question will be to draw a primitive unit cell for a lattice: follow this procedure.

2.13 PROBLEMS.

Exercise 2.1 Packing of spheres on lattices. (*2013 ps2 p2*)

(based on question 2.7 of Ibach and Luth) Supposing the atoms to be rigid spheres in contact, calculate the fraction of space that is filled by atoms in

a. the fcc lattice.
b. the primitive cubic lattice.
c. the hcp lattice.

Answer for Exercise 2.1

Part a. For fcc we refer to fig. 2.10 to see that if the cube width is a the radius of any of the spherical pieces is $\sqrt{2}a/4$, and the volume occupied is

$$\begin{aligned}\frac{4}{3}\pi\left(\sqrt{2}\frac{a}{4}\right)^3\left(\frac{1}{2}\times 6+\frac{1}{8}\times 8\right) &= \frac{\cancel{4}}{3}\pi a^3\frac{2\sqrt{2}}{\cancel{4}\cancel{4}\cancel{4}}(\cancel{3+1}) \\ &= \pi a^3\frac{\sqrt{2}}{6},\end{aligned} \tag{2.55}$$

so that the occupied fraction for fcc is

$$\boxed{\rho_{fcc} = \frac{\sqrt{2}\pi}{6} \approx 0.740.} \tag{2.56}$$

Part b. For bcc we refer to fig. 2.14.

For the bcc element twice our diameter is the diagonal cross length of $\sqrt{3a^2}$, so our filling fraction is

$$\frac{4}{3}\pi \left(\frac{\sqrt{3}}{4}\right)^3 \left(1 + \frac{1}{8} \times 8\right). \tag{2.57}$$

This simplifies to

$$\boxed{\rho_{bcc} \frac{\sqrt{3}\pi}{8} \approx 0.680.} \tag{2.58}$$

Grading remark: "simple cubic?". Oops. I calculated bcc instead of simple cubic. For simple cubic fig. 2.9 the occupied volume is

$$8 \times \frac{1}{8}\frac{4}{3}\pi a^3, \tag{2.59}$$

so that the occupied fraction is this divided by $(2a)^3$, or

$$\rho_{\text{simple cubic}} = \frac{\pi}{6} \approx 0.5236. \tag{2.60}$$

Part c. From http://youtu.be/GAd18wfbXfY I frame grabbed an hcp hexagonal unit cell diagram fig. 2.34 to calculate from.

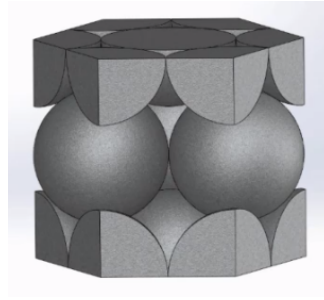

Figure 2.34: Hex Close Packed unit cell.

Some authors appear to call this structure the unit cell for hcp, since it is clearly possible to construct a periodic structure using it. However, others divide it into three parts and call each of those parts the primitive unit cell for hcp as in fig. 2.35.

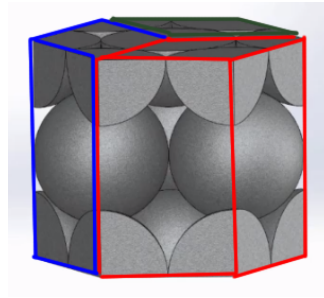

Figure 2.35: hcp primitive unit cell.

It is apparently possible to use repetition of this structure (likely after various transformations) to do the 3D hcp tiling, but that's not obvious when viewing a 2D diagram of such a unit cell. We can do the packing density calculation using the hexagonal structure instead.

An attempt to actually construct this structure shows that the representation of fig. 2.34 is actually deceptive, since it make it appear that the three interior spheres are tidily constrained by the walls of the hexagonal prism. We find instead that there is portions of those three interior spheres are sheared off by the unit cell walls, but those sheared portions can be fit back in. This is illustrated in fig. 2.36 (note that I glued in the relocated piece slightly incorrectly, and it should be shifted up as illustrated).

Finally, the key to the density calculation is the observation that we have three tetrahedrons formed between the bottom and middle layers of the unit cell. Two of these three tetrahedrons are marked in fig. 2.37.

Moving on the calculation, first consider the base of the tetrahedron, which has the form illustrated in fig. 2.38.

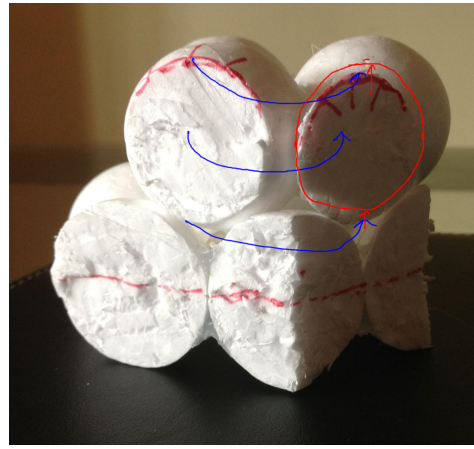

Figure 2.36: Second layer overlap packing in hcp.

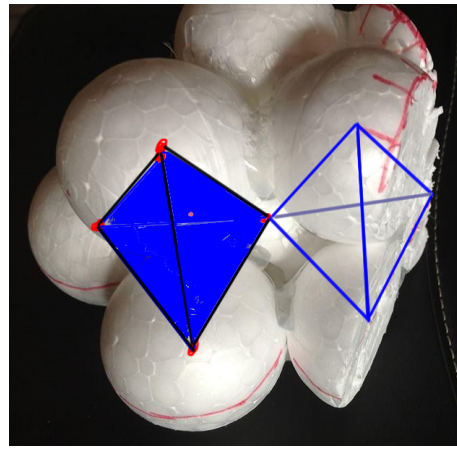

Figure 2.37: Tetrahedral packing of two hcp layers.

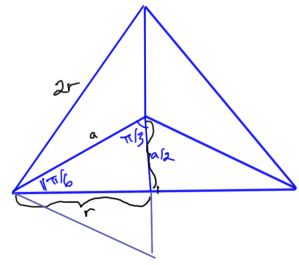

Figure 2.38: Tetrahedral base.

We want the interior distance a on the base, which we find from

$$\begin{aligned} r^2 &= a^2 - \left(\frac{a}{2}\right)^2 \\ &= a^2\left(1 - \frac{1}{4}\right), \end{aligned} \tag{2.61}$$

or

$$a = \frac{2\sqrt{3}r}{3}. \tag{2.62}$$

Next we calculate the height of the tetrahedron, referring to fig. 2.39.

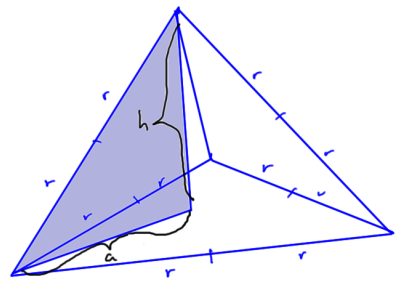

Figure 2.39: Tetrahedral height.

The height of the tetrahedron is

$$\begin{aligned} h^2 &= (2r)^2 - a^2 \\ &= \left(4 - \frac{4}{3}\right) r^2 \\ &= \frac{8}{3} r^2, \end{aligned} \tag{2.63}$$

so we have, for the height of half the hexagonal cell

$$h = \sqrt{\frac{8}{3}} r. \tag{2.64}$$

The base of the hexagonal structure is depicted in fig. 2.40

We calculate that area to be

$$A = 12 \times \sqrt{3} r^2, \tag{2.65}$$

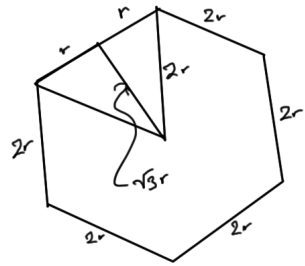

Figure 2.40: Hex cell base area calculation.

so that the total volume is

$$\begin{aligned} V &= 12\sqrt{3}\sqrt{\frac{8}{3}}r^3 \\ &= 24\sqrt{2}r^3. \end{aligned} \tag{2.66}$$

We can now compute the density

$$\frac{\frac{4}{3}\pi r^3\left(6\times\frac{1}{6}+6\times\frac{1}{6}+3+2\times\frac{1}{2}\right)}{24\sqrt{2}r^3} = \frac{\frac{4}{3}\pi 6}{24\sqrt{2}}, \tag{2.67}$$

or

$$\boxed{\rho_{hcp} = \frac{\sqrt{2}\pi}{6} \approx 0.740.} \tag{2.68}$$

This is the same packing density as we had in the fcc configuration, both more dense than the simple cubic lattice.

Exercise 2.2 Lattice vectors and unit cell. (*2013 ps2 p3*)

A crystal has a basis of one atom per lattice point and a set of primitive translation vectors is

$$\mathbf{a} = 3\hat{\mathbf{x}} \qquad \mathbf{b} = 3\hat{\mathbf{y}} \qquad \mathbf{c} = 1.5(\hat{\mathbf{x}}+\hat{\mathbf{y}}+\hat{\mathbf{z}}),$$

where $\hat{\mathbf{x}}$, $\hat{\mathbf{y}}$ and $\hat{\mathbf{z}}$ are the unit vectors in the x,y and z directions.

Assume that the dimensions are Angstroms, Å.

What is the lattice type of this crystal, what is the volume of the primitive unit cell, and what is the volume of the conventional unit cell?

Answer for Exercise 2.2

First observe that the integer multiple span of vectors **a** and **b** cover all the grid points separated by 3 units (Å). Also observe that the combination

$$2\mathbf{c} - \mathbf{a} - \mathbf{b} = 3\hat{\mathbf{z}}, \tag{2.69}$$

means that we have coverage of all cubic grid points separated by 3 units, and will have the same grid coverage from any plane that we can reach. Finally, note that moving **c** from the origin takes us to the center of the width three cubic lattice in the first quadrant. This means that we have cubic coverage with all centers filled.

This is a bcc lattice, and is plotted in fig. 2.41.

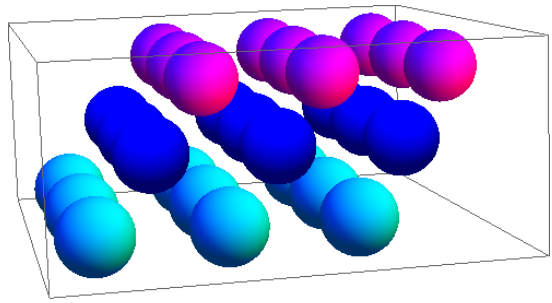

Figure 2.41: Bcc lattice.

The primitive unit cell volume is that of the parallelepiped formed by the vectors **a**, **b**, **c**, which is

$$\begin{aligned} V_{\text{primitive}} &= 3 \times 3 \times \frac{3}{2} \begin{vmatrix} 1 & 0 & 0 \\ 0 & 1 & 0 \\ 1 & 1 & 1 \end{vmatrix} \text{Å}^3 \\ &= \frac{27}{2} \text{Å}^3. \end{aligned} \tag{2.70}$$

The conventional unit cell is depicted in fig. 2.14, and has volume

$$V_{\text{conventional}} = 27 \text{Å}^3, \tag{2.71}$$

which is twice the primitive cell volume in this case.

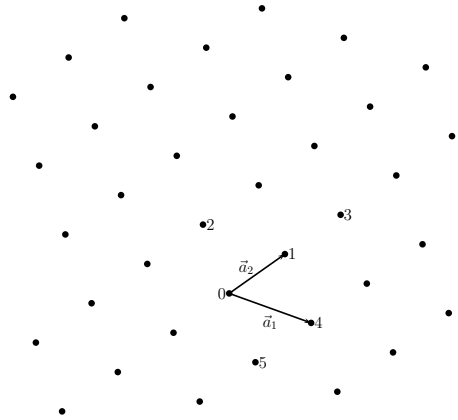

Figure 2.42: A sample lattice.

Exercise 2.3 Geometry of reciprocal lattice. (*2013 ps3 p1*)

Figure 2.42. shows a two-dimensional lattice together with two vectors.

a. Demonstrate that $\mathbf{a}_1$ and $\mathbf{a}_2$ are basis vectors by showing that you can reach the sites numbered 1 through 5 by a combination of $\mathbf{a}_1$ and $\mathbf{a}_2$. (e.g. to reach site 1 use $0 * \mathbf{a}_1 + 1 * \mathbf{a}_2$, etc..)

b. On the page and using a ruler and/or protractor and/or any other drafting tools you may require, draw the two basis vectors $\mathbf{g}_1$ and $\mathbf{g}_2$ of the corresponding reciprocal lattice. Draw $\mathbf{g}_1$ and $\mathbf{g}_2$ to scale (so they have the correct length relative to each other).

c. Consider three waves, with wave-vectors $\mathbf{k}_a = \mathbf{g}_1$, $\mathbf{k}_b = \mathbf{g}_2$ and $\mathbf{k}_c = \mathbf{g}_1 + 2\mathbf{g}_2$, draw lines on the diagram to indicate the positions of the wave-crests, assuming that one of the crests passes through the point “o". If these lines correspond to “planes" in the two-dimensional crystal, give the Miller indices of the planes.

Answer for Exercise 2.3

Part a. Our linear combinations are

1. $\mathbf{a}_2$

2. $\mathbf{a}_2 - \mathbf{a}_1$
3. $2\mathbf{a}_2$
4. $\mathbf{a}_1$
5. $\mathbf{a}_1 - \mathbf{a}_2$

Part b. With the x-axis measured along $\mathbf{a}_1$ in cm, I measure

$$\begin{aligned}\mathbf{a}_1 &= (2, 0) \pm 0.05 \\ \mathbf{a}_2 &= ((1.75, 2.6) \pm 0.05)\end{aligned} \tag{2.72}$$

Computing the reciprocal frame by inversion, we have

$$\begin{aligned}\begin{bmatrix}\mathbf{g}_1 & \mathbf{g}_2\end{bmatrix} &= 2\pi \begin{bmatrix}\mathbf{a}_1^T \\ \mathbf{a}_2^T\end{bmatrix} \\ &= \begin{bmatrix}3.14159 & 0. \\ -2.11453 & 4.83322\end{bmatrix}\end{aligned} \tag{2.73}$$

These are drawn out on the fig. 2.43.

Part c. Referring again to fig. 2.43.

- The wave crests for $\mathbf{k}_a = \mathbf{g}_1$ are shown in blue. For this wave we have $\mathbf{k}_a \cdot \mathbf{a}_1 = g_1 a_1 \cos\theta = 2\pi$, or a wave length of $2\pi/|\mathbf{g}_1|$. The Miller indices for this wave are $1, 0, 0$.
- The wave crests for $\mathbf{k}_b = \mathbf{g}_2$ are shown in red. For this wave we have $\mathbf{k}_b \cdot \mathbf{a}_2 = g_2 a_2 \cos\theta = 2\pi$, or a wave length of $2\pi/|\mathbf{g}_2|$. The Miller indices for this wave are $0, 1, 0$.
- The wave crests for $\mathbf{k}_c = \mathbf{g}_1 + 2\mathbf{g}_2$ are shown in pink and green.

  For the pink wave we have $\mathbf{k}_c \cdot \mathbf{a}_1 = k_c a_1 \cos\theta = g_1 a_1 = 2\pi$, or a wave length of $2\pi/|\mathbf{k}_c|$. The angle between $\mathbf{k}_c$ and $\mathbf{a}_1$ is $\cos\theta = 1/\sqrt{5}$, or $\theta \sim 63°$.

  For the green wave we have $\mathbf{k}_c \cdot \mathbf{a}_2 = k_c a_2 \cos\theta = 2g_2 a_2 = 4\pi$, or a wave length of $4\pi/|\mathbf{k}_c|$. The angle between $\mathbf{k}_c$ and $\mathbf{a}_2$ is $\cos\theta = 2/\sqrt{5}$, or $\theta \sim 26°$.

  The Miller indices for this wave are $1, 2, 0$.

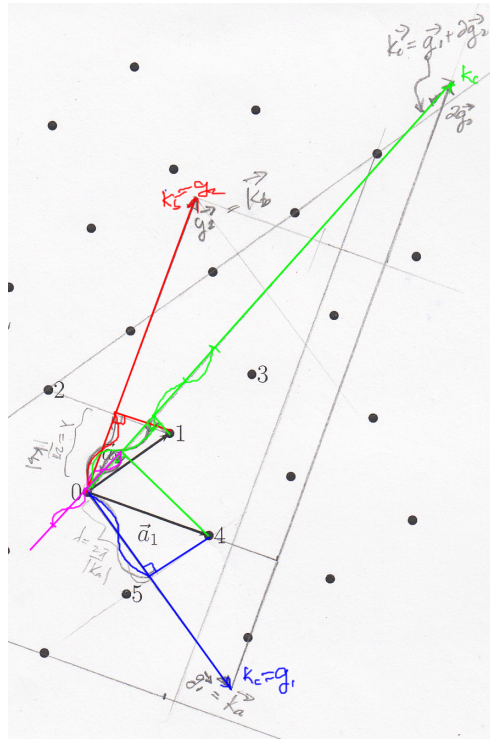

Figure 2.43: reciprocal vectors and sample wave trains.

Exercise 2.4 FCC reciprocal lattice. (*2013 ps3 p2*)

Now for a face-centered cubic lattice with conventional unit cell of side length a:

a. Draw the conventional unit cell and number all of the corner and face-centered atoms, and demonstrate that the vectors $\mathbf{a}_1 = \frac{a}{2}(1,1,0)$, $\mathbf{a}_2 = \frac{a}{2}(1,0,1)$ and $\mathbf{a}_3 = \frac{a}{2}(0,1,1)$, are primitive lattice vectors in the sense that you can get to every lattice point in the unit cell using these vectors.

b. Using the formula from the lectures show that the volume of the primitive unit cell is $1/4$ of the volume of the conventional unit cell.

c. Using the formula from the lectures, find the basis vectors of the corresponding reciprocal lattice, and show that these basis vectors generate a body-centered-cubic lattice in reciprocal space.

Answer for Exercise 2.4

Part a. The lattice and the primitive lattice vectors are sketched in fig. 2.44.

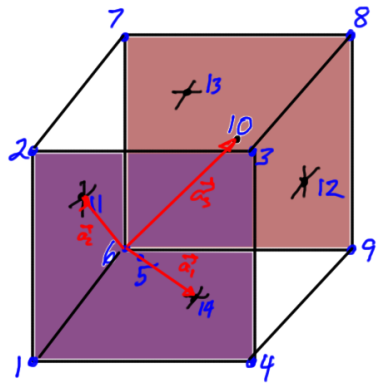

Figure 2.44: Fcc lattice and primitive lattice vectors.

To demonstrate that we can get to each lattice point, we first invert a matrix of the lattice vectors

$$\begin{bmatrix} 1 & 1 & 0 \\ 1 & 0 & 1 \\ 0 & 1 & 0 \end{bmatrix}^{-1} = \frac{1}{2}\begin{bmatrix} 1 & 1 & -1 \\ 1 & -1 & 1 \\ -1 & 1 & 1 \end{bmatrix}. \tag{2.74}$$

This allows us to read off the corners of the cube in terms of the primitive lattice vectors (which perhaps could have been done by inspection)

$$\mathbf{a}_1 + \mathbf{a}_2 - \mathbf{a}_3 = \begin{bmatrix} a \\ 0 \\ 0 \end{bmatrix} \tag{2.75a}$$

$$\mathbf{a}_1 + \mathbf{a}_3 - \mathbf{a}_2 = \begin{bmatrix} 0 \\ a \\ 0 \end{bmatrix} \tag{2.75b}$$

$$\mathbf{a}_2 + \mathbf{a}_3 - \mathbf{a}_1 = \begin{bmatrix} 0 \\ 0 \\ a \end{bmatrix}. \tag{2.75c}$$

Our lattice points, in terms of the primitive vectors are

1. $\mathbf{a}_1 + \mathbf{a}_2 - \mathbf{a}_3$
2. $2\mathbf{a}_2$
3. $\mathbf{a}_1 + \mathbf{a}_2 + \mathbf{a}_3$
4. $2\mathbf{a}_1$
5. $\mathbf{a}_1 + \mathbf{a}_2$
6. o
7. $\mathbf{a}_1 + \mathbf{a}_3 + \mathbf{a}_1$
8. $2\mathbf{a}_3$

9. $\mathbf{a}_1 + \mathbf{a}_3 - \mathbf{a}_2$
10. $\mathbf{a}_3$
11. $\mathbf{a}_2$
12. $\mathbf{a}_1 + \mathbf{a}_3$
13. $\mathbf{a}_2 + \mathbf{a}_3$
14. $\mathbf{a}_1$

Part c. Computing the three sets of cross products we have

$$\mathbf{a}_2 \times \mathbf{a}_3 = \left(\frac{a}{2}\right)^2 \begin{vmatrix} \hat{\mathbf{x}} & \hat{\mathbf{y}} & \hat{\mathbf{z}} \\ 1 & 0 & 1 \\ 0 & 1 & 1 \end{vmatrix} = \left(\frac{a}{2}\right)^2 \begin{bmatrix} -1 \\ -1 \\ 1 \end{bmatrix} \tag{2.76a}$$

$$\mathbf{a}_3 \times \mathbf{a}_1 = \left(\frac{a}{2}\right)^2 \begin{vmatrix} \hat{\mathbf{x}} & \hat{\mathbf{y}} & \hat{\mathbf{z}} \\ 0 & 1 & 1 \\ 1 & 1 & 0 \end{vmatrix} = \left(\frac{a}{2}\right)^2 \begin{bmatrix} -1 \\ 1 \\ -1 \end{bmatrix} \tag{2.76b}$$

$$\mathbf{a}_1 \times \mathbf{a}_2 = \left(\frac{a}{2}\right)^2 \begin{vmatrix} \hat{\mathbf{x}} & \hat{\mathbf{y}} & \hat{\mathbf{z}} \\ 1 & 1 & 0 \\ 1 & 0 & 1 \end{vmatrix} = \left(\frac{a}{2}\right)^2 \begin{bmatrix} 1 \\ -1 \\ -1 \end{bmatrix}. \tag{2.76c}$$

Our triplet product is

$$\mathbf{a}_1 \cdot (\mathbf{a}_2 \times \mathbf{a}_3) = \left(\frac{a}{2}\right)^3 (-2). \tag{2.77}$$

Putting these together we have

$$\mathbf{g}_1 = 2\pi \frac{\mathbf{a}_2 \times \mathbf{a}_3}{\mathbf{a}_1 \cdot (\mathbf{a}_2 \times \mathbf{a}_3)} = \frac{2\pi}{a} \begin{bmatrix} 1 \\ 1 \\ -1 \end{bmatrix} \tag{2.78a}$$

$$\mathbf{g}_2 = 2\pi \frac{\mathbf{a}_3 \times \mathbf{a}_1}{\mathbf{a}_1 \cdot (\mathbf{a}_2 \times \mathbf{a}_3)} = \frac{2\pi}{a} \begin{bmatrix} 1 \\ -1 \\ 1 \end{bmatrix} \tag{2.78b}$$

$$\mathbf{g}_3 = 2\pi \frac{\mathbf{a}_3 \times \mathbf{a}_1}{\mathbf{a}_1 \cdot (\mathbf{a}_2 \times \mathbf{a}_3)} = \frac{2\pi}{a} \begin{bmatrix} -1 \\ 1 \\ 1 \end{bmatrix}. \tag{2.78c}$$

Note that we can also compute all the reciprocal basis vectors more directly by inversion

$$\begin{aligned} \begin{bmatrix} \mathbf{g}_1 & \mathbf{g}_2 & \mathbf{g}_3 \end{bmatrix} &= 2\pi \begin{bmatrix} \mathbf{a}_1^{\mathrm{T}} \\ \mathbf{a}_2^{\mathrm{T}} \\ \mathbf{a}_3^{\mathrm{T}} \end{bmatrix} \\ &= 2\pi \frac{2}{a} \begin{bmatrix} 1 & 1 & 0 \\ 1 & 0 & 1 \\ 0 & 1 & 1 \end{bmatrix}^{-1} \\ &= \frac{2\pi}{a} \begin{bmatrix} 1 & 1 & -1 \\ 1 & -1 & 1 \\ -1 & 1 & 1 \end{bmatrix}, \end{aligned} \tag{2.79}$$

consistent with the cross product calculation of eq. (2.78).

Part b. We've already computed the (signed) volume element in eq. (2.77). The absolute value of this is the volume of the primitive unit cell

$$\begin{aligned} V_{\text{primitive}} &= |\mathbf{a}_1 \cdot (\mathbf{a}_2 \times \mathbf{a}_3)| \\ &= \frac{1}{4} a^3, \end{aligned} \tag{2.80}$$

which is $1/4$ of the conventional cell volume.

FIXME: Grading remark: "BCC?" Ooops. Revisit: looks like I missed doing a portion of this question.

Exercise 2.5 Ewald construction for 2D lattice. (*2013 ps3 p3*)

Show that the reciprocal lattice of a two-dimensional lattice can be represented by rods. Discuss the Ewald construction for diffraction from a two-dimensional lattice and determine the diffracted beam for a particular orientation and magnitude of $\mathbf{k}_\circ$. (It helps

to draw a three-dimensional diagram showing the plane of the reciprocal lattice, the rods, and the Ewald sphere.)

Explain why you always see a diffraction pattern from a two-dimensional crystal, provided that the magnitude of $\mathbf{k}_\circ$ exceeds a critical value, regardless of its orientation.

Answer for Exercise 2.5

Let's consider first the reciprocal frame for a 2D surface by direct computation. In matrix form we want to solve

$$\begin{bmatrix} \mathbf{a}_1^{\mathrm{T}} \\ \mathbf{a}_2^{\mathrm{T}} \end{bmatrix} \begin{bmatrix} \mathbf{g}_1 & \mathbf{g}_2 \end{bmatrix} = 2\pi \begin{bmatrix} 1 & 0 \\ 0 & 1 \end{bmatrix}. \tag{2.81}$$

Inverting yields the reciprocal frame vectors in columnar matrix form

$$\begin{aligned} \begin{bmatrix} \mathbf{g}_1 & \mathbf{g}_2 \end{bmatrix} &= 2\pi \begin{bmatrix} a_{11} & a_{12} \\ a_{21} & a_{22} \end{bmatrix}^{-1} \\ &= \frac{2\pi}{a_{11}a_{22} - a_{12}a_{21}} \begin{bmatrix} a_{22} & -a_{12} \\ -a_{21} & a_{11} \end{bmatrix}, \end{aligned} \tag{2.82}$$

or

$$\mathbf{g}_1 = \frac{2\pi}{a_{11}a_{22} - a_{12}a_{21}} \begin{bmatrix} a_{22} \\ -a_{21} \end{bmatrix} \tag{2.83a}$$

$$\mathbf{g}_2 = \frac{2\pi}{a_{11}a_{22} - a_{12}a_{21}} \begin{bmatrix} -a_{12} \\ a_{11} \end{bmatrix}. \tag{2.83b}$$

This is considerably messier than the cross product formulation that we used in 3D. Given familiarity with the geometric algebra formalism of [4] it is clear that can be tidied up nicely. Introducing a planar pseudoscalar $I = \mathbf{e}_1 \wedge \mathbf{e}_2$, and using the distribution identity $\mathbf{a} \cdot (\mathbf{b} \wedge \mathbf{c}) = (\mathbf{a} \cdot \mathbf{b})\mathbf{c} - (\mathbf{a} \cdot \mathbf{c})\mathbf{b}$, the end result is somewhat reminiscent of the cross product result from the text and class

$$\mathbf{g}_1 = \frac{2\pi}{(\mathbf{a}_1 \wedge \mathbf{a}_2)I} \mathbf{a}_2 \cdot I \tag{2.84a}$$

$$\mathbf{g}_2 = -\frac{2\pi}{(\mathbf{a}_1 \wedge \mathbf{a}_2)I} \mathbf{a}_1 \cdot I. \tag{2.84b}$$

We have no reason to introduce a third dimension in either position or momentum space, but as with angular momentum and other quantities that are naturally planar (and thus logically expressed as bivector wedge products), we can also introduce an additional dimension so that we can work with the old familiar 3D toolbox (i.e. cross products).

Let's try such a 3D extension of the lattice space and see if the results are consistent, and what the reciprocal frame vectors are. To do so we extend the lattice to a triplet $\{\mathbf{a}_1, \mathbf{a}_2, \mathbf{a}_3\}$, where $\mathbf{a}_3 = \mathbf{e}_3$, a unit vector in a normal direction to the plane, now extended to 3D. Our reciprocal frame vectors are

$$\mathbf{g}_1 = \frac{2\pi}{\mathbf{e}_3 \cdot (\mathbf{a}_1 \times \mathbf{a}_2)} \mathbf{a}_2 \times \mathbf{e}_3 \tag{2.85a}$$

$$\mathbf{g}_2 = \frac{2\pi}{\mathbf{e}_3 \cdot (\mathbf{a}_1 \times \mathbf{a}_2)} \mathbf{e}_3 \times \mathbf{a}_1 \tag{2.85b}$$

$$\mathbf{g}_3 = \frac{2\pi}{\mathbf{e}_3 \cdot (\mathbf{a}_1 \times \mathbf{a}_2)} \mathbf{a}_1 \times \mathbf{a}_2. \tag{2.85c}$$

Observe that the triple produce is the same determinant that we found by matrix inversion for the duality calculation

$$\begin{aligned} \mathbf{e}_3 \cdot (\mathbf{a}_1 \times \mathbf{a}_2) &= \mathbf{e}_3 \cdot \left((a_{11}\mathbf{e}_1 + a_{12}\mathbf{e}_2) \times (a_{21}\mathbf{e}_1 + a_{22}\mathbf{e}_2) \right) \\ &= \mathbf{e}_3 \cdot \left(a_{11}a_{22}\mathbf{e}_3 - a_{12}a_{21}\mathbf{e}_3 \right) \\ &= a_{11}a_{22} - a_{12}a_{21}. \end{aligned} \tag{2.86}$$

Expanding out all the 3D extended reciprocal vectors we have

$$\mathbf{g}_1 = \frac{2\pi}{a_{11}a_{22} - a_{12}a_{21}} \begin{bmatrix} a_{22} \\ -a_{21} \\ 0 \end{bmatrix} \tag{2.87a}$$

$$\mathbf{g}_2 = \frac{2\pi}{a_{11}a_{22} - a_{12}a_{21}} \begin{bmatrix} -a_{12} \\ a_{11} \\ 0 \end{bmatrix} \tag{2.87b}$$

$$\mathbf{g}_3 = 2\pi \begin{bmatrix} 0 \\ 0 \\ 0 \end{bmatrix} . \tag{2.87c}$$

Observe that the first two reciprocal vectors are consistent with the planar computation of eq. (2.83).

We see that extension of our lattice frame by introducing an arbitrary set of normal lattice points, introduces an additional reciprocal vector, also normal to those of the purely planar treatment. Since the scaling of these normal reciprocal vectors are completely arbitrary, we can think of that vector as the span of possible normal lattice points. This can be characterized as a rod.

Having arrived at an algebraic meaning for "rod" in this context, let's move on to the diagram that was suggested. This is drafted in fig. 2.45.

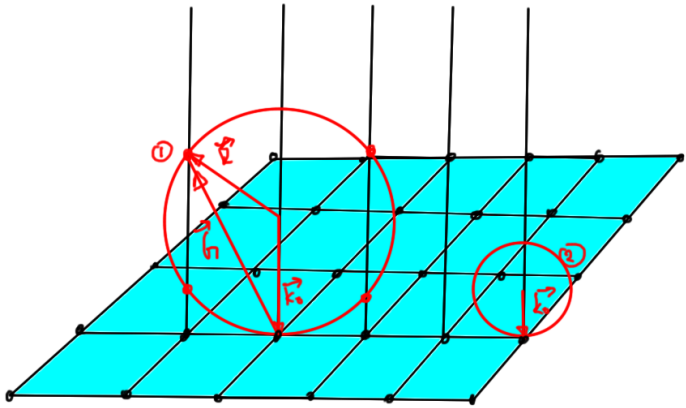

Figure 2.45: Ewald sphere for 2D lattice.

Two spheres, depicted as circles, are indicated in the figure. Both have a $\mathbf{k}_\circ$ vector directed downwards towards the plane from the center of the sphere.

The larger of these spheres (1) passes through the normal "rods" in four potential places (really eight, but the additional dimensions are not indicated in the figure). Each of those positions allows for the construction of a **G** vector in the reciprocal space, so

as indicated in the problem, there will necessarily be diffraction provided the incident wave $\mathbf{k}_\circ$ is a large enough magnitude.

The smaller sphere, marked (2), depicts an incident wave with magnitude insufficient (not past the critical threshold) to cross any of the "rods". We cannot construct a $\mathbf{G}$ that has a component normal to the reciprocal lattice frame for such an incident wave, since it is smaller than the critical value required.

Exercise 2.6 Laue vs. powder diffraction. (*2013 ps4 p1*)

This is based on assigned reading, §3.7, pp. 69-70.

You are given a single crystal of an unknown material and asked to determine the lattice constants. Should you use Laue or powder x-ray diffraction to do this? Explain why. (Note that in order to do powder diffraction you would have to crush the single crystal. Assume that you are allowed to do this.)

Answer for Exercise 2.6

We should use powder diffraction to determine the lattice constants of this unknown material.

For a material of known structure we can use Laue diffraction to determine the orientation of the lattice, for example, to prepare a hexagonal prism sample of a crystal so that the planes of the sample are oriented in a fashion that matches the internal structure. Laue diffraction employs a continuous spectrum of x-rays, allowing for observation of all the reflections with lattice points for which the Ewald sphere intersections lie within the range of $\mathbf{k}_\circ$ values of this radiation. That is sufficient to observe the symmetries associated with the orientation of the crystal.

Grading remark : "Why not lattice constants?" Reviewing the grading remarks, it appears that an explicit reference to the Bragg condition was desired here. The $\mathbf{G} = \mathbf{K}$ condition required for Laue diffraction corresponds $n\lambda = 2d_{hkl}\sin\theta$. Since Laue diffraction is using all wavelengths, when we get a spot we do not know the specific wavelength and thus cannot extract d, since that requires knowing both θ and λ. Conversely when we use powder diffraction where λ is fixed (and we measure θ) we can determine d (or integer multiples of it?) from the Bragg condition. When using a fixed wavelength source (and thus a source with fixed $k_\circ$),

we obtain diffraction only when that source is suitably oriented so that the $\mathbf{k}_\circ$ passes through lattice points on the Ewald sphere. When that specific orientation is available it should allow for accurate determination of the lattice constants associated with that orientation, allowing a subset of the lattice structure to be determined accurately. The powder diffraction method allows for that internal structure to be measured by using a sample of the crystal that has been broken into pieces small enough that all possible orientations of the crystal are present. Given that distribution of orientations, a fixed wavelength source (and thus fixed $k_\circ$) can be used to obtain reflections for all the Ewald sphere orientations passing through the reciprocal lattice points.

3 PHONONS.

3.1 PHONONS.

Reading: [1] ch. 21, 22.

Consider a 1D chain of N atoms, coupled by harmonic springs with periodic boundary conditions. We suppose that we have $N \sim 10^{23}$. This is illustrated in fig. 3.1. Vibrations of the complete structure are called phonon modes .

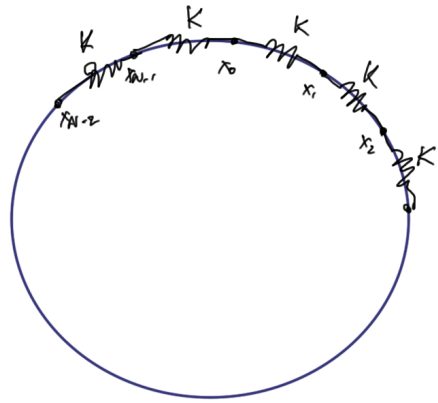

Figure 3.1: Coupled periodic oscillators.

With equilibrium positions x_j, and displacement distances from equilibrium of u_j, as in fig. 3.2.

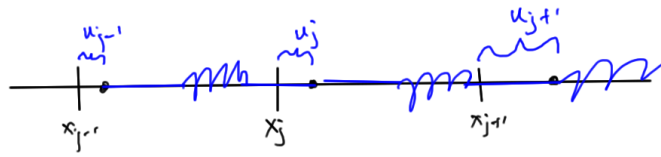

Figure 3.2: Equilibrium and displacement positions.

Our force balance is

$$m\ddot{u}_j = K\left(u_{j+1} - u_j\right) + K\left(u_{j-1} - u_j\right). \tag{3.1}$$

We have 10^{23} coupled equations.

The periodicity requirement imposes a constraint on

$$e^{iq(x_j+Na)}, \tag{3.2}$$

so that

$$q\overbrace{Na}^{L} = 2\pi n, \tag{3.3}$$

or

$$q = \frac{2\pi n}{L}. \tag{3.4}$$

In class we used trial solutions of the form

$$u_j = \frac{1}{\sqrt{m}} \sum_q u_q e^{i\left(qx_j - \omega_q t\right)}. \tag{3.5}$$

Constraint on frequency In class we plugged eq. (3.5) into eq. (3.1) and after some rushed arithmetic we arrived at a constraint on the frequency.

Because that was rushed I had a bit of trouble following, but thought I had the general idea. I found a simpler treatment in [**?**] which used single frequency trial solution

$$u_n = \epsilon e^{iqna - \omega t}. \tag{3.6}$$

Our derivatives are

$$\dot{u}_n = -i\omega\epsilon e^{iqna-\omega t} \tag{3.7a}$$

$$\ddot{u}_n = -\omega^2\epsilon e^{iqna-\omega t}, \tag{3.7b}$$

and insertion back into eq. (3.1) gives

$$\begin{aligned} 0 &= \epsilon e^{-i\omega t}\left(\frac{m}{K}\omega^2 e^{iqna} + e^{iq(n+1)a} - 2e^{iqna} + e^{iq(n-1)a}\right) \\ &= \epsilon e^{-i\omega t}e^{iqna}\left(\frac{m}{K}\omega^2 + e^{iqa} - 2 + e^{-iqa}\right) \\ &= \epsilon e^{-i\omega t}e^{iqna}\left(\frac{m}{K}\omega^2 + -2 + 2\cos qa\right) \\ &= \epsilon e^{-i\omega t}e^{iqna}\left(\frac{m}{K}\omega^2 + -4\sin^2\left(\frac{qa}{2}\right)\right). \end{aligned} \tag{3.8}$$

Requiring equality means that we must have

$$\boxed{\sqrt{\frac{m}{K}}\omega = 2\sin\left(\frac{qa}{2}\right).} \tag{3.9}$$

With superposition of frequency components Putting an index on ϵ and ω, and expressing q explicitly we have a slightly more general trial solution

$$u_n = \sum_s \epsilon_s e^{i\left(\frac{2\pi sn}{N} - \omega_s t\right)}, \tag{3.10}$$

where s is an integer. Plugging this into our EOM we have

$$\begin{aligned} 0 &= \sum_s \epsilon_s e^{-i\omega_s t}\left(\frac{m}{K}\omega_s^2 e^{i\frac{2\pi sn}{N}} + e^{i\frac{2\pi s(n+1)}{N}} - 2e^{i\frac{2\pi sn}{N}} + e^{i\frac{2\pi s(n-1)}{N}}\right) \\ &= \sum_s \epsilon_s e^{-i\omega_s t}e^{i\frac{2\pi sn}{N}}\left(\frac{m}{K}\omega_s^2 + e^{i\frac{2\pi s}{N}} - 2 + e^{-i\frac{2\pi s}{N}}\right) \\ &= \sum_s \epsilon_s e^{-i\omega_s t}e^{i\frac{2\pi sn}{N}}\left(\frac{m}{K}\omega_s^2 + 2\cos\left(\frac{2\pi s}{N}\right) - 2\right) \\ &= \sum_s \epsilon_s e^{-i\omega_s t}e^{i\frac{2\pi sn}{N}}\left(\frac{m}{K}\omega_s^2 - 4\sin^2\left(\frac{\pi s}{N}\right)\right). \end{aligned} \tag{3.11}$$

From this, we see that if

$$\frac{m}{K}\omega_s^2 = 4\sin^2\left(\frac{\pi s}{N}\right), \tag{3.12}$$

then our equation is solved. This is just the frequency constraint of eq. (3.9).

Q: In class, the equality above that resulted from us applying the trial solution was operated on by $\sum_{q'} e^{-iq'na}$ to decouple the equations. If the frequency constraint was what was desired, why did we even apply that operator? I believe that the response for this was that without doing so, it as if one assumes a-priori that the solutions are decoupled. In retrospect, I am still not sure that this resolves my confusion, since it seems to me that this summation operator is really just a statement that the exponentials form a basis (i.e. forming a resolution of identity).

normal modes Last time, considering a 1D linear harmonic chain

$$w_q = \sqrt{\frac{4k}{m}} \left| \sin \frac{qa}{2} \right| \tag{3.13a}$$

$$q = \frac{2\pi n}{L}. \tag{3.13b}$$

These were described as wave like solutions, but these are in fact the normal modes of oscillations.

These are sketched in fig. 3.3.

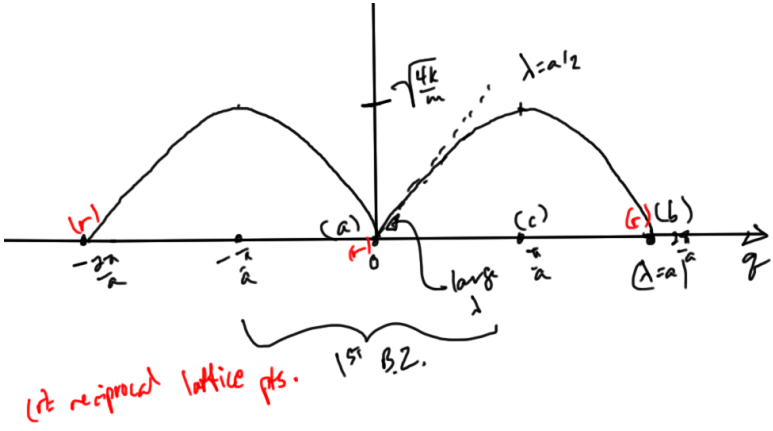

Figure 3.3: Harmonic oscillator chain normal mode frequencies.

(a) At $q = 0$, fig. 3.4, we really have uniform translation of the entire chain.

Figure 3.4: Uniform motion.

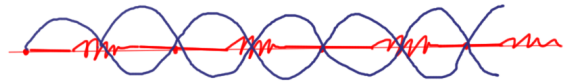

Figure 3.5: Displaced uniform motion.

(b) At $q = a$, fig. 3.5, we have displaced, but also uniform translation of the entire chain.

(c) At $q = a/2$, fig. 3.6, we have maximum oscillation.

Figure 3.6: Maximum oscillation.

3.2 3D POTENTIALS FOR REAL SOLIDS.

Reading: [10] §4.1

Our problems in 3D are mostly notational, where we have the problem of indexing all the particles and their directions of motion. Our index convention is illustrated in fig. 3.7.

$$u_{n\alpha i}. \tag{3.14}$$

for the displacement of the αth atom in the nth unit cell, in the ith ($i \in \{x, y, z\}$ direction.

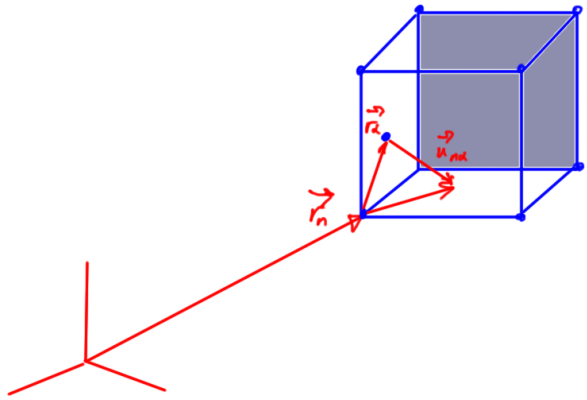

Figure 3.7: Displacement relative to primitive cell origin.

The total potential energy can be written

$$\Phi(r_{n\alpha i} + u_{n\alpha i}) = \Phi(r_{n\alpha i}) + \frac{1}{2} \sum_{n\alpha i, m\beta j} \overbrace{\frac{\partial^2 \Phi}{\partial r_{n\alpha i} \partial m\beta j}}^{\Phi^{m\beta j}_{n\alpha i}} u_{n\alpha i} u_{m\beta j}, \quad (3.15)$$

where $r_{n\alpha i}$ is the equilibrium position and $u_{n\alpha i}$ is the displacement. This can be written as

$$\Phi(r_{n\alpha i} + u_{n\alpha i}) = \Phi(r_{n\alpha i}) + \frac{1}{2} \sum_{n\alpha i, m\beta j} \Phi^{m\beta j}_{n\alpha i} u_{n\alpha i} u_{m\beta j}. \quad (3.16)$$

Example 3.1: 1D chain.

To illustrate our index convention consider fig. 3.8 for the harmonic oscillator chain we previously treated.

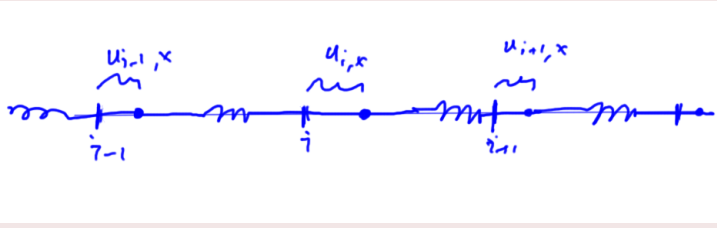

Figure 3.8: direction relative indexing example.

$$\Phi = \frac{1}{2}ku_{ix}^2 + \frac{1}{2}ku_{ix}^2 = . \tag{3.17}$$

$$I_{nx}^{nx} = 2k. \tag{3.18}$$

Equation of motion From this generalized quadratic potential, we form the Lagrangian

$$\mathcal{L} = T - U = \frac{1}{2}\sum_{n\alpha i} M_n \dot{u}_{n\alpha i}^2 - \frac{1}{2}\sum_{n\alpha i, m\beta j} \Phi_{n\alpha i}^{m\beta j} u_{n\alpha i} u_{m\beta j}, \tag{3.19}$$

The equations of motion follow from the Euler-Lagrange equations

$$\frac{d}{dt}\frac{\partial \mathcal{L}}{\partial \dot{u}_{n\alpha i}} = \frac{\partial \mathcal{L}}{\partial u_{n\alpha i}}, \tag{3.20}$$

the generalized equivalent to $\mathbf{F} = -\boldsymbol{\nabla}\Phi$. This provides the force on atom α in unit cell n, in direction i, due to displacement of atom β in cell m in direction j. That is

$$M_\alpha \ddot{u}_{n\alpha i} + \sum_{m\beta j} \Phi_{n\alpha i}^{m\beta j} u_{m\beta j} = 0. \tag{3.21}$$

For example,

$$m\ddot{u}_j = k(u_{j+1} - u_j) + k(u_{j-1} - u_j). \tag{3.22}$$

Using trial solution

$$u_{n\alpha i} = \frac{1}{\sqrt{m_\alpha}}\sum_q u_{\alpha i}(q) e^{-i(\mathbf{q}\cdot\mathbf{r}_n - \omega_q t)}. \tag{3.23}$$

This yields, after operation with $\sum_{q'} e^{i\mathbf{q}'\cdot\mathbf{r}_n}$ as before, and cancelling terms

$D_{\alpha i}^{\beta j}$, the Dynamical matrix, independent of n

$$-\omega_q^2 u_{\alpha i}(q) + \sum_{\beta j}\left[\sum_m \frac{1}{\sqrt{m_\alpha m_\beta}} \Phi_{n\alpha i}^{m\beta j} e^{-i\mathbf{q}\cdot(\mathbf{r}_m - \mathbf{r}_n)}\right] u_{\beta j}(q) = 0, \tag{3.24}$$

or

$$-\omega_q^2 u_{\alpha i}(q) + \sum_{\beta j} D_{\alpha i}^{\beta j} u_{\beta j}(q) = 0. \tag{3.25}$$

We want to solve

$$\det\left(D^{\beta j}_{\alpha i} - \omega_q^2 \mathbf{1}\right) = 0. \tag{3.26}$$

Example 3.2: Diatomic linear chain.

As a second example consider fig. 3.9 for a diatomic linear chain. This example can also be found outlined in [10] §4.3.

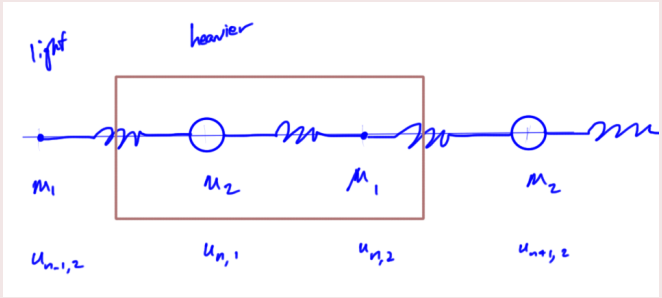

Figure 3.9: Diatomic linear chain.

Our potentials are

$$\Phi_{n,1} = \frac{f}{2}\left(u_{n,1} - u_{n-1,2}\right)^2 + \frac{f}{2}\left(u_{n,2} - u_{n,1}\right)^2 \tag{3.27a}$$

$$\Phi_{n,2} = \frac{f}{2}\left(u_{n+1,1} - u_{n,2}\right)^2 + \frac{f}{2}\left(u_{n,2} - u_{n,1}\right)^2, \tag{3.27b}$$

with partials

$$\frac{\partial \Phi_{n,1}}{\partial u_{n,1}} = f\left(2u_{n,1} - u_{n-1,2} - u_{n,2}\right) \tag{3.28a}$$

$$\frac{\partial \Phi_{n,2}}{\partial u_{n,2}} = f\left(-u_{n+1,1} + 2u_{n,2} - u_{n,1}\right). \tag{3.28b}$$

In the general notation the force equations are

$$M_1 \ddot{u}_{n,1} + \Phi^{n-1,2}_{n,1} u_{n-1,2} + \Phi^{n,1}_{n,1} u_{n,1} + \Phi^{n,2}_{n,1} u_{n,2} = 0 \tag{3.29a}$$

$$M_2\ddot{u}_{n,2} + \Phi^{n,1}_{n,2}u_{n-1,2} + \Phi^{n,2}_{n,2}u_{n,2} + \Phi^{n+1,1}_{n,2}u_{n+1,1} = 0, \quad (3.29b)$$

and from the partials and the Euler-Lagrange equations this is

$$M_1\ddot{u}_{n,1} + f\left(2u_{n,1} - u_{n-1,2} - u_{n,2}\right) = 0 \quad (3.30a)$$

$$M_2\ddot{u}_{n,2} + f\left(2u_{n,2} - u_{n,1} - u_{n+1,1}\right) = 0. \quad (3.30b)$$

We can read off the potential derivatives

$$\Phi^{n,1}_{n,1} = \Phi^{n,2}_{n,2} = 2f \quad (3.31a)$$

$$\Phi^{n,2}_{n,1} = -f. \quad (3.31b)$$

The trial substitution to use (the text calls this an ansatz) is:

$$u_{n,\alpha} = \frac{1}{M_\alpha}u_\alpha(q)e^{i(\overbrace{an}^{x_n} - \omega_q t)}. \quad (3.32)$$

Substitution into eq. (3.30) gives

$$\left(\frac{2f}{M_1} - \omega_q^2\right)u_1(q) - \frac{f}{\sqrt{M_1M_2}}\left(1 + e^{-iqa}\right)u_2(q) = 0 \quad (3.33a)$$

$$-\frac{f}{\sqrt{M_1M_2}}\left(1 + e^{iqa}\right)u_1(q) + \left(\frac{2f}{M_2} - \omega_q^2\right)u_2(q) = 0. \quad (3.33b)$$

We thus want to solve

$$\begin{vmatrix} \left(\frac{2f}{M_1} - \omega_q^2\right) & -\frac{f}{\sqrt{M_1M_2}}\left(1 + e^{-iqa}\right) \\ -\frac{f}{\sqrt{M_1M_2}}\left(1 + e^{iqa}\right) & \left(\frac{2f}{M_2} - \omega_q^2\right) \end{vmatrix} = 0, \quad (3.34)$$

We find in IbachAndLuth4_15_verify.nb that this has solution

$$\omega_q^2 = f\left(\frac{1}{M_1}+\frac{1}{M_2}\right) \pm f\sqrt{\left(\frac{1}{M_1}+\frac{1}{M_2}\right)^2 - \frac{4}{M_1 M_2}\sin^2\frac{qa}{2}}. \tag{3.35}$$

Plotting in fig. 3.10.

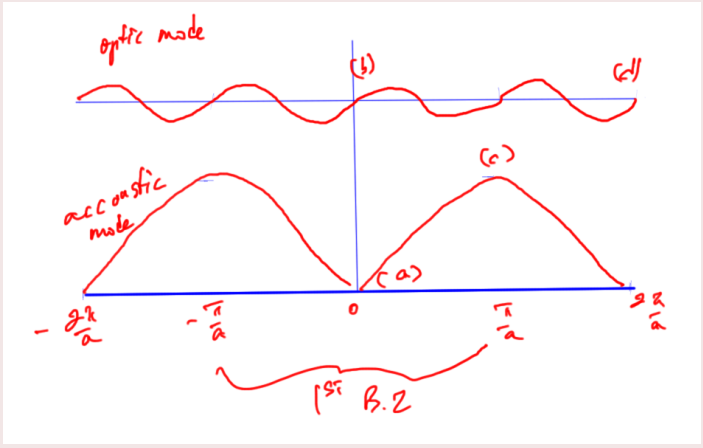

Figure 3.10: Optic and acoustic modes.

There are two solutions for $q = 0$
$\omega^2 = 0$, or $\omega^2 = 2f(1/M_1 + 1/M_2)$.
(a)

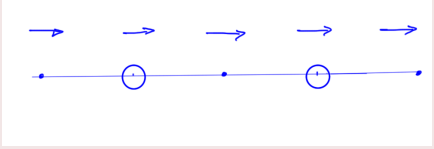

Figure 3.11: Uniform translation.

(b)

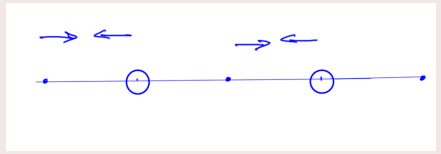

Figure 3.12: Pairwise oscillation.

(c)

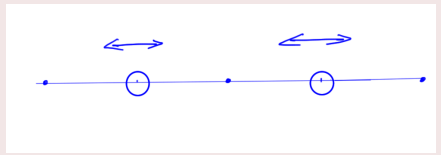

Figure 3.13: Heavier atoms oscillating.

(d)

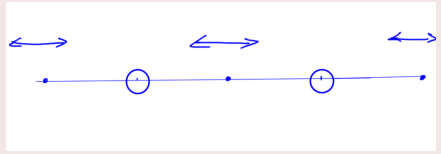

Figure 3.14: Lighter atoms oscillating.

Reading §4.3

3.3 PROBLEMS.

Exercise 3.1 1D chain, two spring constants. (*2013 ps4 p2*)

Consider the one-dimensional chain of fig. 3.15 in which all masses have the same value, m, but the spring constant alternates between k and k', as shown below. The equilibrium length of the springs is the same, and equal to $a/2$, where a is the lattice spacing.

a. Find the coupled equations of motion for $u_{n,1}$ and $u_{n,2}$, and then make the ansatz

$$u_{n,\alpha} = u_\alpha(q)e^{i(qx_n-\omega t)},$$

to obtain coupled equations for $u_1(q)$ and $u_2(q)$.

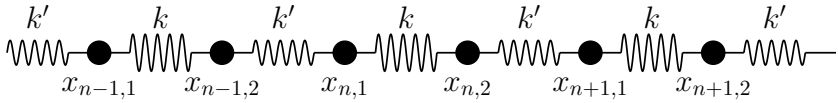

Figure 3.15: Two springs chain.

b. Solve these coupled equations, putting $k = k_\circ + \delta$ and $k' = k_\circ - \delta$, to show that the dispersion relation is:

$$\omega^2 = \frac{2k_\circ}{m}\left(1 \pm \sqrt{\cos^2\frac{qa}{2} + \frac{\delta^2}{k_\circ^2}\sin^2\frac{qa}{2}}\right).$$

c. At $q = 0$, plug the two solutions for ω back into the coupled equations for $u_1(q)$ and $u_2(q)$ to find the relative motion of masses 1 and 2 in each primitive unit cell. Explain how these relative motions of the two masses give rise to the two frequencies at $q = 0$.

d. Plot $\omega(q)$ vs. q in the range $q = 0$ to $q = 2\pi/a$, for $\delta/k_\circ = 0.9, 0.1$ and 0. Indicate the boundary of the first Brillouin zone. (I did this by programming my equation for $\omega(q)$ into a plotting package; you can also do it by hand.)

e. For $\delta/k_\circ = 0.9$ explain why the two branches of the phonon spectrum are so far apart. What happens in the limit where $\delta = k_\circ$? Explain the dispersion relation (or rather, lack thereof) of the acoustic and optical branches in this limit.

f. For $\delta = 0$, explain the form of your plot (hint: when $\delta = 0$ the two springs are identical, so think about the primitive unit cell and first Brillouin zone size in this case; also, you may recall the calculation of the structure factor in which we treated a bcc lattice as simple cubic with a two-atom basis).

Answer for Exercise 3.1

Part a. In order to avoid the mental trauma of trying to figure out all the signs for the spring constant potential coefficients, we can describe the system by the Lagrangian

$$\begin{aligned}\mathcal{L} = \sum_{n,\alpha} \frac{m}{2}\dot{u}_{n,\alpha}^2 - \frac{k'}{2}\left(u_{n,1} - u_{n-1,2}\right)^2 \\ - \frac{k}{2}\left(u_{n,2} - u_{n,1}\right)^2 - \frac{k'}{2}\left(u_{n+1,1} - u_{n,2}\right)^2 - \cdots\end{aligned} \tag{3.36}$$

The force equations then follow directly from the Euler-Lagrange equations

$$0 = \frac{d}{dt}\frac{\partial \mathcal{L}}{\partial \dot{u}_{n,\alpha}} - \frac{\partial \mathcal{L}}{\partial u_{n,\alpha}}. \tag{3.37}$$

That is

$$\begin{aligned}0 &= m\ddot{u}_{n,1} + (k+k')u_{n,1} - ku_{n,2} - k'u_{n-1,2} \\ 0 &= m\ddot{u}_{n,2} + (k+k')u_{n,2} - ku_{n,1} - k'u_{n+1,1}\end{aligned} \tag{3.38}$$

Our trial solution functions from above are

$$\begin{aligned}u_{n-1,2} &= u_2 e^{i(qa(n-1)-\omega t)} \\ u_{n,1} &= u_1 e^{i(qan-\omega t)} \\ u_{n,2} &= u_2 e^{i(qan-\omega t)} \\ u_{n+1,1} &= u_1 e^{i(qa(n+1)-\omega t)},\end{aligned} \tag{3.39}$$

which gives us

$$\begin{aligned}0 = &-m\omega^2 u_1 \cancel{e^{i(qan-\omega t)}} \\ &+ (k+k')u_1 \cancel{e^{i(qan-\omega t)}} - ku_2 \cancel{e^{i(qan-\omega t)}} - k'u_2 e^{i(qa(n-1)-\omega t)} \\ 0 = &-\omega^2 m u_2 \cancel{e^{i(qan-\omega t)}} \\ &+ (k+k')u_2 \cancel{e^{i(qan-\omega t)}} - ku_1 \cancel{e^{i(qan-\omega t)}} - k'u_1 e^{i(qa(n+1)-\omega t)},\end{aligned} \tag{3.40}$$

or

$$\begin{aligned}0 &= -m\omega^2 u_1 + 2k_\circ u_1 - (k_\circ + \delta)u_2 - (k_\circ - \delta)u_2 e^{-iqa} \\ 0 &= -m\omega^2 u_2 + 2k_\circ u_2 - (k_\circ + \delta)u_1 - (k_\circ - \delta)u_1 e^{iqa}.\end{aligned} \tag{3.41}$$

Part b. We seek ω^2 solutions to the determinant

$$
\begin{aligned}
0 &= \begin{vmatrix} -m\omega^2 + 2k_\circ & -(k_\circ + \delta) - (k_\circ - \delta)e^{-iqa} \\ -(k_\circ + \delta) - (k_\circ - \delta)e^{iqa} & -m\omega^2 + 2k_\circ \end{vmatrix} \\
&= (-m\omega^2 + 2k_\circ)^2 - \left((k_\circ + \delta) + (k_\circ - \delta)e^{-iqa}\right)\left((k_\circ + \delta) + (k_\circ - \delta)e^{iqa}\right) \\
&= (-m\omega^2 + 2k_\circ)^2 \\
&\quad - \left((k_\circ + \delta)e^{iqa/2} + (k_\circ - \delta)e^{-iqa/2}\right)e^{-iqa/2} \times \\
&\quad e^{iqa/2}\left((k_\circ + \delta)e^{-iqa/2} + (k_\circ - \delta)e^{iqa/2}\right) \\
&= (-m\omega^2 + 2k_\circ)^2 \\
&\quad - \left(2k_\circ \cos(qa/2) + 2i\delta \sin(qa/2)\right)\left(2k_\circ \cos(qa/2) - 2i\delta \sin(qa/2)\right) \\
&= (-m\omega^2 + 2k_\circ)^2 - 4\left(k_\circ^2 \cos^2(qa/2) + \delta^2 \sin^2(qa/2)\right)
\end{aligned}
\tag{3.42}
$$

or

$$
\omega^2 = \frac{2k_\circ}{m}\left(1 \pm \sqrt{\cos^2(qa/2) + \frac{\delta^2}{k_\circ}\sin^2(qa/2)}\right), \tag{3.43}
$$

as desired.

Part c. At $q = 0$ we have

$$
\omega^2 = \frac{2k_\circ}{m}(1 \pm 1), \tag{3.44}
$$

or

$$
\omega \in \{\pm 2\omega_\circ, 0\}, \tag{3.45}
$$

where the natural frequency for the average spring constant is

$$
\omega_\circ^2 = \frac{k_\circ}{m}. \tag{3.46}
$$

Zero frequency case. For the $\omega = 0, q = 0$ case, our equations of motion eq. (3.41), now take the form

$$
\begin{aligned}
2k_\circ u_1 &= \left((k_\circ + \delta) + (k_\circ - \delta)e^{-iqa}\right)u_2 \\
&= \left((k_\circ + \delta) + (k_\circ - \delta)\right)u_2 \\
&= 2k_\circ u_2.
\end{aligned}
\tag{3.47}
$$

Both the "motions" in the primitive unit cell is described by

$$\begin{aligned} u_{n,1} &= u_2 \\ u_{n,2} &= u_2, \end{aligned} \tag{3.48}$$

where $u_2 = u_2(q)$ an arbitrary undetermined function. This solution represents uniform translation.

Non-zero frequency case. For the non-constant time dependent solutions, where $\omega \neq 0, q = 0$, we have

$$\omega = \pm 2\omega_\circ, \tag{3.49}$$

so that our equations of motion eq. (3.41), now take the form

$$\begin{aligned} -m\omega_\circ^2 u_1 &= (k_\circ + \delta)u_2 + (k_\circ - \delta)u_2 \\ &= 2k_\circ u_2, \end{aligned} \tag{3.50}$$

or

$$u_1 = -u_2. \tag{3.51}$$

The equations for $u_{n,1}$ and $u_{n,2}$ are

$$\begin{aligned} u_{n,1} &= -u_2 e^{\pm 2i\omega_\circ t} \\ u_{n,2} &= u_2 e^{\pm 2i\omega_\circ t} \end{aligned} \tag{3.52}$$

where, again, $u_2 = u_2(0)$ is the initial time displacement of the $x_{n,2}$ atom. We see that when $q = 0$, the variation δ of the spring constants from their average value $k_\circ$ makes no difference to the motion of the atoms. This motion is a pairwise oscillation of the form fig. 3.16.

Part d. The frequencies $\omega(q)$ are plotted in fig. 3.17. The Brillouin zone bisects this figure vertically along the line $qa = \pi$ line.

Part e. To examine both the limiting scenario and the case $\delta/k_\circ = 0.9$, let

$$\epsilon = 1 - \left(\frac{\delta}{k_\circ}\right)^2, \tag{3.53}$$

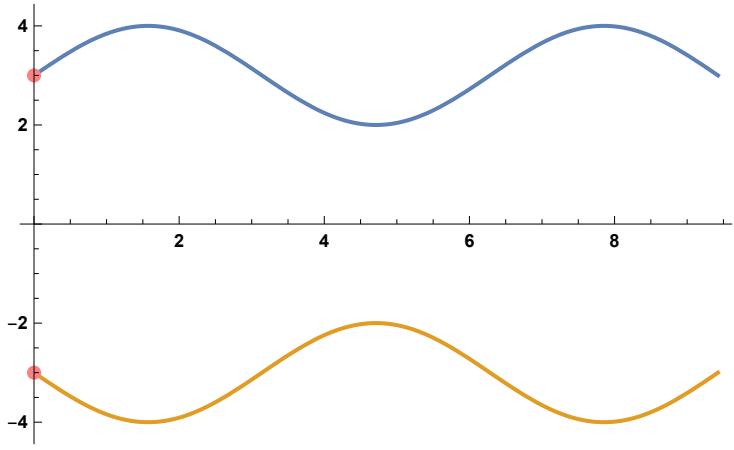

Figure 3.16: Pairwise oscillation.

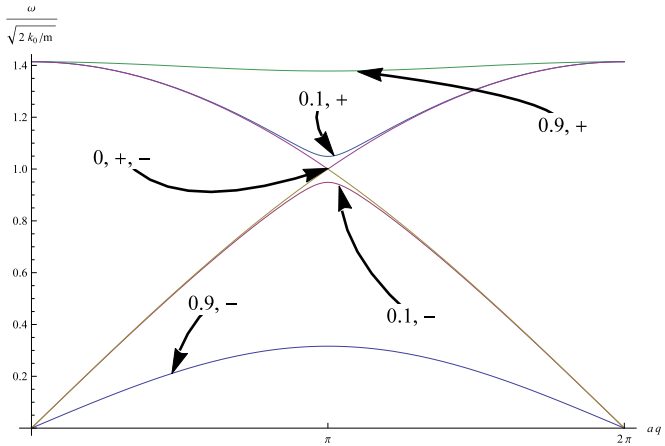

Figure 3.17: Frequencies for $\delta/k_\circ \in \{0.9, 0.1, 0\}$.

so that

$$\begin{aligned}\omega^2 &= 2\omega_\circ^2\left(1 \pm \sqrt{\cos^2\frac{qa}{2} + (1-\epsilon)\sin^2\frac{qa}{2}}\right)\\ &= 2\omega_\circ^2\left(1 \pm \sqrt{1-\epsilon\sin^2\frac{qa}{2}}\right)\\ &\approx 2\omega_\circ^2\left(1 \pm \left(1 - \frac{\epsilon}{2}\sin^2\frac{qa}{2}\right)\right)\\ &= \left\{2\omega_\circ^2\left(2 - \frac{\epsilon}{2}\sin^2\frac{qa}{2}\right), \omega_\circ^2\epsilon\sin^2\frac{qa}{2}\right\},\end{aligned} \tag{3.54}$$

where $\omega_\circ^2 = k_\circ/m$, as above. Taking roots and further approximations we have

$$\begin{aligned}\omega &\approx \left\{2\omega_\circ\sqrt{1 - \frac{\epsilon}{4}\sin^2\frac{qa}{2}}, \omega_\circ\sqrt{\epsilon}\sin\frac{qa}{2}\right\}\\ &\approx \left\{2\omega_\circ\left(1 - \frac{\epsilon}{8}\sin^2\frac{qa}{2}\right), \omega_\circ\sqrt{\epsilon}\sin\frac{qa}{2}\right\},\end{aligned} \tag{3.55}$$

In optical range, we have $\omega \approx 2\omega_\circ$, with only small deviations from that. As $\delta/k_\circ$ gets small, this will become increasingly flat. In fact, we see this close to linear even for the 0.9 case where we have

$$\omega \approx 2\omega_\circ\left(1 - 0.024\sin^2\frac{qa}{2}\right). \tag{3.56}$$

In the acoustic range we have a uniformly damped sinusoid. For this 0.9 case that is

$$\omega \approx 0.43\omega_\circ\sin\frac{qa}{2}. \tag{3.57}$$

Grading remark: "Explain physically what is going on." Examining the posted solution, what was being looked for was a characterization of the motion itself (i.e. what sort of specific motions of the springs is occurring, are they in phase or out of phase, ...)

Part f. The $\delta = 0$ values are somewhat tricky to distinguish in fig. 3.17 above. The optical case is re-plotted separately in fig. 3.18, and the acoustic in fig. 3.19.

Grading remark: "Only one mode" was marked under fig. 3.19, with an X beside the figure. Reviewing the posted solution, it appears that the correct response to this part of the problem is to

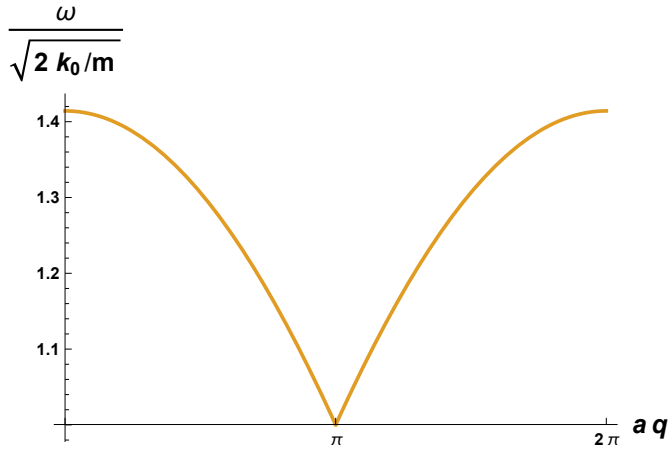

Figure 3.18: Optical dispersion at $\delta = 0$.

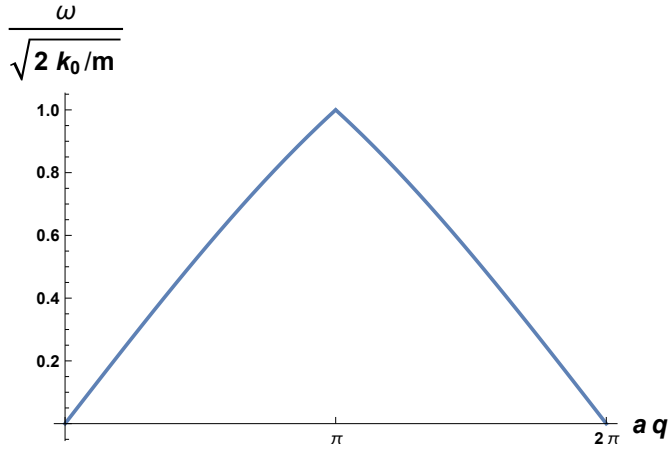

Figure 3.19: Acoustic dispersion at $\delta = 0$.

observe that treating this primitive cell as one with two masses is no longer appropriate. A correct analysis of this limit requires is that of a one atom basis, not two. To examine the nature of these curves in more detail, observe that for $\delta = 0$ we have

$$\omega^2 = 2\omega_\circ^2 \left(1 \pm \cos \frac{qa}{2}\right), \tag{3.58}$$

or

$$\omega = \sqrt{2}\omega_\circ \sqrt{1 \pm \cos \frac{qa}{2}}. \tag{3.59}$$

Noting that

$$\begin{aligned} 1 - \cos x &= 2 \sin^2 x/2 \\ 1 + \cos x &= 2 \cos^2 x/2, \end{aligned} \tag{3.60}$$

provided $qa < \pi$ we can write the optical and acoustic ranges for ω at $\delta = 0$ respectively as

$$\omega \in \left\{ 2\omega_\circ \cos \frac{qa}{4}, 2\omega_\circ \sin \frac{qa}{4} \right\}. \tag{3.61}$$

These meet at $qa = \pi$ before switching directions (the border of the Brillouin zone).

Exercise 3.2 Anharmonic 1D oscillator. ([7] pr 5.5)

How that the equation of motion for an anharmonic oscillator

$$M\ddot{u} + fu - \frac{1}{2}gu^2 = 0, \tag{3.62}$$

is solved by an approximate solution involving multiples of the harmonic frequency $\omega_\circ^2 = f/M$:

$$u = \sum_{n=1}^{\infty} a_n e^{in\omega_\circ t}. \tag{3.63}$$

Discuss the result in relation to phonon decay. What is the analogy to electrical circuits and to signal transmission in nonlinear media?

Answer for Exercise 3.2

Let's write our differential equation as

$$\ddot{u} + \omega_\circ^2 u - h u^2 = 0, \tag{3.64}$$

where $g/2M = h$. Now consider a product of the form u^2

$$\begin{aligned}
&\left(a_1 e^{ix} + a_2 e^{2ix} + a_3 e^{3ix} + \cdots\right)\left(a_1 e^{ix} + a_2 e^{2ix} + a_3 e^{3ix} + \cdots\right) \\
&= \begin{array}{llll} a_1 a_1 e^{2ix} & +a_1 a_2 e^{3ix} & +a_1 a_3 e^{4ix} & +a_1 a_4 e^{5ix} + \cdots \\ & +a_2 a_1 e^{3ix} & +a_2 a_2 e^{4ix} & +a_2 a_3 e^{5ix} + \cdots \\ & & +a_3 a_2 e^{4ix} & +a_3 a_3 e^{5ix} + \cdots \end{array} \\
&= a_1^2 e^{2ix} + a_2^2 e^{4ix} + a_3^2 e^{6ix} + \cdots + 2a_1 a_2 e^{3ix} + 2a_1 a_3 e^{4ix} + \cdots \\
&= \sum_{n=1}^{\infty} a_n^2 e^{2nix} + 2 \sum_{1 \le n < m < \infty} a_n a_m e^{(n+m)ix}.
\end{aligned} \tag{3.65}$$

Now we are set to take derivatives

$$\begin{aligned}
0 &= \ddot{u} + \omega_\circ^2 - h u^2 \\
&= \sum_{n=1}^{\infty} \omega_\circ^2 (1 - n^2) a_n e^{in\omega_\circ t} - h \sum_{n=1}^{\infty} a_n^2 e^{2ni\omega_\circ t} - 2h \sum_{1 \le n < m < \infty} a_n a_m e^{(n+m)i\omega_\circ t} \\
&= \left(-3\omega_\circ^2 a_2 - h a_1^2\right) e^{2i\omega_\circ t} \\
&+ \left(-8\omega_\circ^2 a_3 - 2h a_1 a_2\right) e^{3i\omega_\circ t} \\
&+ \left(-15\omega_\circ^2 a_4 - h a_2^2\right) e^{4i\omega_\circ t} \\
&+ \left(-24\omega_\circ^2 a_5 - 2h(a_1 a_4 + a_2 a_3)\right) e^{5i\omega_\circ t} \\
&+ \cdots
\end{aligned} \tag{3.66}$$

Setting $a_1 = 1$ we can proceed to calculate all the constants a_n.

$$a_2 = -\frac{h}{3\omega_\circ^2} \tag{3.67a}$$

$$a_3 = \frac{h^2}{12\omega_\circ^4} \tag{3.67b}$$

$$\begin{aligned}
a_4 &= -\frac{h}{15\omega_\circ^2}\left(-\frac{h}{3\omega_\circ^2}\right)^2 \\
&= -\frac{h^3}{135\omega_\circ^6}.
\end{aligned} \tag{3.67c}$$

Observe that each of these has powers of

$$\frac{h}{\omega_\circ^2} = \frac{g}{2M\omega_\circ^2} = \frac{g}{2f}. \tag{3.68}$$

The magnitude of the anharmonic perturbation "spring constant" $g/2$ compared to the actual spring constant f is assumed to be small. This means that the magnitude of each progressive term in the series is smaller than the previous.

This is enough to verify that the solution can be expressed in a series formed from powers of the harmonic frequency phasor. Looking at a specific example, with $m = f = 1$, and $g = 0.5$, we have

$$u(t) = e^{it} - 0.0833e^{2it} + 0.00521e^{3it} - 0.000116e^{4it}. \tag{3.69}$$

The Real part of this is plotted in fig. 3.20 along with separate plots of the first two terms.

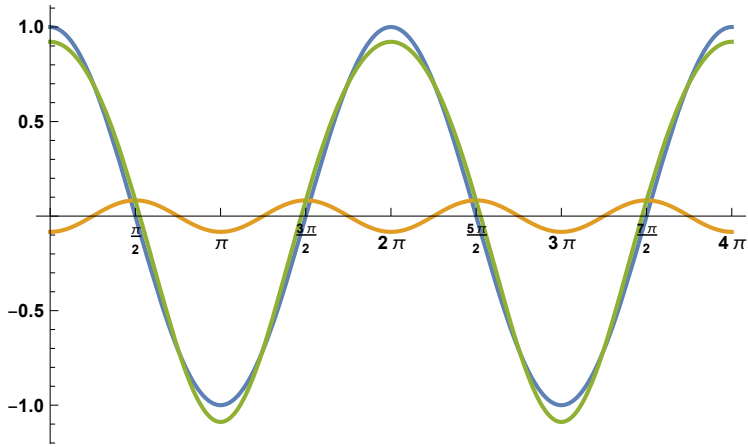

Figure 3.20: Anharmonic sum and two components.

Observe that the difference from $u(t)$ and the harmonic solution is very small. However, that difference is essentially that of superposition of the $\omega_\circ$ mode with that of the $2\omega_\circ$ mode. The non-linearity can be thought of as essentially splitting the single harmonic mode into a pair of harmonic modes, one at the fundamental frequency and another (of smaller magnitude) at twice that. We require a steady state solution of this form, so if we start

with something that is just a single frequency, there will be a perturbation process that will result in a decay into the spectrum determined above. A calculation of that impulse response (very much like initial conditions in a circuit before flipping a switch) would be interesting, but likely difficult.

Exercise 3.3 Two body harmonic oscillator in 3D.

Solve a two mass harmonically coupled system without considering any equilibrium separation.

Answer for Exercise 3.3

For the system illustrated in fig. 3.21 the Lagrangian is

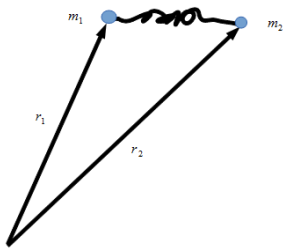

Figure 3.21: Two masses with harmonic coupling.

$$\mathcal{L} = \frac{1}{2} m_1 \left(\dot{\mathbf{r}}_1\right)^2 + \frac{1}{2} m_2 \left(\dot{\mathbf{r}}_2\right)^2 - \frac{K}{2} \left(\mathbf{r}_2 - \mathbf{r}_1\right)^2 . \tag{3.70}$$

We wish to solve the equations of motion

$$\frac{d}{dt} \boldsymbol{\nabla}_{\dot{\mathbf{r}}_i} \mathcal{L} = \boldsymbol{\nabla}_{\mathbf{r}_i} \mathcal{L}. \tag{3.71}$$

Noting that $\boldsymbol{\nabla}_{\mathbf{x}} \mathbf{a} \cdot \mathbf{x} = \mathbf{a}$, the coupled system to solve is

$$\begin{aligned} m_1 \ddot{\mathbf{r}}_1 &= -K \left(\mathbf{r}_1 - \mathbf{r}_2\right) \\ m_2 \ddot{\mathbf{r}}_2 &= -K \left(\mathbf{r}_2 - \mathbf{r}_1\right) . \end{aligned} \tag{3.72}$$

These can be decoupled using differences and sums

$$\begin{aligned} m_1 \left(m_2 \ddot{\mathbf{r}}_2\right) - m_2 \left(m_1 \ddot{\mathbf{r}}_1\right) &= -(m_1 + m_2) K \left(\mathbf{r}_2 - \mathbf{r}_1\right) \\ m_1 \ddot{\mathbf{r}}_1 + m_2 \ddot{\mathbf{r}}_2 &= 0 \end{aligned} \tag{3.73}$$

The second is the equation for the acceleration of the center of mass $\mathbf{R}_{\mathrm{CM}}(t)$. That center of mass relation is directly integrable. With $M = m_1 + m_2$, that is

$$\begin{aligned} M\mathbf{R}_{\mathrm{CM}}(t) &= m_1\mathbf{r}_1 + m_2\mathbf{r}_2 \\ &= (t - t_\circ)M\mathbf{V}_{\mathrm{CM}} + M\mathbf{R}_{\mathrm{CM}}(t_\circ). \end{aligned} \tag{3.74}$$

The first is the harmonic oscillation about the center of mass position. Introducing the reduced mass

$$\mu = \frac{m_1 m_2}{m_1 + m_2}, \tag{3.75}$$

that oscillation equation is

$$\frac{d^2}{dt^2}\left(\mathbf{r}_2 - \mathbf{r}_1\right) = -\frac{K}{\mu}\left(\mathbf{r}_2 - \mathbf{r}_1\right). \tag{3.76}$$

With angular frequency $\omega^2 = \frac{K}{\mu}$, vector difference $\Delta\mathbf{r}(t) = \mathbf{r}_2(t) - \mathbf{r}_1(t)$, and initial time values $\Delta\mathbf{r}_\circ = \Delta\mathbf{r}(t_\circ)$, and $\Delta\mathbf{v}_\circ = \Delta\mathbf{r}'(t_\circ)$ the solution for $\Delta\mathbf{r}(t)$, by inspection, is

$$\Delta\mathbf{r}(t) = \Delta\mathbf{r}_\circ \cos\left(\omega(t - t_\circ)\right) + \frac{\Delta\mathbf{v}_\circ}{\omega}\sin\left(\omega(t - t_\circ)\right). \tag{3.77}$$

The reference time can be picked to allow for solutions of arbitrary phase. For example, for cosine solutions, pick $t_\circ$ as the time for which the amplitude difference is maximized.

To find for the individual $\mathbf{r}_i$ vectors we have only to invert the matrix relation

$$\begin{bmatrix} -1 & 1 \\ m_1 & m_2 \end{bmatrix}\begin{bmatrix} \mathbf{r}_1 \\ \mathbf{r}_2 \end{bmatrix} = \begin{bmatrix} \Delta\mathbf{r}(t) \\ M\mathbf{R}_{\mathrm{CM}}(t) \end{bmatrix}, \tag{3.78}$$

or

$$\begin{bmatrix} \mathbf{r}_1 \\ \mathbf{r}_2 \end{bmatrix} = \frac{1}{m_2 + m_1}\begin{bmatrix} -m_2 & 1 \\ m_1 & 1 \end{bmatrix}\begin{bmatrix} \Delta\mathbf{r}(t) \\ M\mathbf{R}_{\mathrm{CM}}(t) \end{bmatrix} \tag{3.79}$$

The final solution is

$$\begin{aligned} \mathbf{r}_1(t) &= -\frac{\mu}{m_1}\Delta\mathbf{r}(t) + \mathbf{R}_{\mathrm{CM}}(t) \\ \mathbf{r}_2(t) &= \frac{\mu}{m_2}\Delta\mathbf{r}(t) + \mathbf{R}_{\mathrm{CM}}(t) \end{aligned} \tag{3.80}$$

Looking at this, it appears non-sensical. At the very least, it is unphysical, and allows the masses to pass through each other. This is illustrated in the animation of harmonicOscillatorTwoMasses.cdf

Our Lagrangian needs to model the equilibrium length of the spring.

Exercise 3.4 1D, non-zero equilibrium length.

In the absence of any initial angular momentum, the problem previously considered is essentially one dimensional.

Let's consider a physically realistic harmonic oscillator system, with coupling that is relative to an equilibrium length (the length of an uncompressed or unstretched spring for example). That system is illustrated in fig. 3.22.

Figure 3.22: Linear harmonic coupling with equilibrium length.

Answer for Exercise 3.4

Adjusting for a rest length $a = a_2 - a_1$ for the spring, the new system is described by

$$\mathcal{L} = \frac{1}{2} m_1 (\dot{x}_1)^2 + \frac{1}{2} m_2 (\dot{x}_2)^2 - \frac{K}{2} (x_2 - x_1 - a)^2 . \tag{3.81}$$

Now our equations of motion are

$$\begin{aligned} m_1 \ddot{x}_1 &= -K (x_1 - x_2 + a) \\ m_2 \ddot{x}_2 &= -K (x_2 - x_1 - a) . \end{aligned} \tag{3.82}$$

With $u = x_2 - x_1 - a$, this is

$$\ddot{u} = -\frac{K}{\mu} u. \tag{3.83}$$

Solving and back substituting for $\Delta x(t) = x_2(t) - x_1(t)$, we have

$$\Delta x(t) = a + (\Delta x(0) - a) \cos \omega t + \frac{\Delta v(0)}{\omega} \sin \omega t. \tag{3.84}$$

Note that this does not model collision effects, should the initial position or velocity be sufficient to bring the masses into contact.

Exercise 3.5 3D non-zero equilibrium length.

Derive the equations of motion for a 3D harmonically coupled system with a non-zero equilibrium length using a Lagrange multiplier to enforce a linear constraint.

Answer for Exercise 3.5

The geometric of a 3D harmonically coupled system with a non-zero equilibrium length is sketched in fig. 3.23.

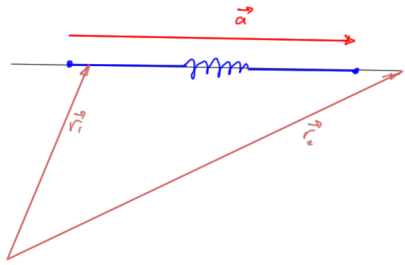

Figure 3.23: Two mass harmonic coupled system.

We can model the coupling spring as a line segment colinear with the difference vector, or

$$\begin{aligned}\mathcal{L} = &\frac{1}{2} m_1 \left(\dot{\mathbf{r}}_1\right)^2 + \frac{1}{2} m_2 \left(\dot{\mathbf{r}}_2\right)^2 - \frac{K}{2} \left(\Delta\mathbf{r} - \mathbf{a}\right)^2 \\ &+ \lambda \left(\Delta\mathbf{r} - \left(\hat{\mathbf{a}} \cdot \Delta\mathbf{r}\right) \hat{\mathbf{a}}\right)^2 .\end{aligned} \tag{3.85}$$

A Lagrange multiplier λ is used to enforce a requirement that the difference vector $\Delta\mathbf{r}$ is colinear with $\mathbf{a}$ (i.e. zero component perpendicular to the projection along $\hat{\mathbf{a}}$.)

The rejection square expands as

$$\begin{aligned}\left(\Delta\mathbf{r} - \left(\hat{\mathbf{a}} \cdot \Delta\mathbf{r}\right) \hat{\mathbf{a}}\right)^2 &= \left(\Delta\mathbf{r}\right)^2 - 2 \left(\hat{\mathbf{a}} \cdot \Delta\mathbf{r}\right)^2 + \left(\hat{\mathbf{a}} \cdot \Delta\mathbf{r}\right)^2 \\ &= \left(\Delta\mathbf{r}\right)^2 - \left(\hat{\mathbf{a}} \cdot \Delta\mathbf{r}\right)^2 .\end{aligned} \tag{3.86}$$

The Euler-Lagrange equations expand as

$$m_1 \ddot{\mathbf{r}}_1 = K \left(\Delta\mathbf{r} - \mathbf{a}\right) - 2 \left(\Delta\mathbf{r} - \left(\hat{\mathbf{a}} \cdot \Delta\mathbf{r}\right) \hat{\mathbf{a}}\right) \tag{3.87a}$$

$$m_2 \ddot{\mathbf{r}}_2 = -K \left(\Delta\mathbf{r} - \mathbf{a}\right) + 2 \left(\Delta\mathbf{r} - \left(\hat{\mathbf{a}} \cdot \Delta\mathbf{r}\right) \hat{\mathbf{a}}\right) \tag{3.87b}$$

$$0 = \left(\Delta\mathbf{r} - (\hat{\mathbf{a}} \cdot \Delta\mathbf{r})\,\hat{\mathbf{a}}\right)^2 . \tag{3.87c}$$

Equation (3.87c) indicates that the norm of the rejection is zero, so that rejection is also zero $\Delta\mathbf{r} - (\hat{\mathbf{a}} \cdot \Delta\mathbf{r})\,\hat{\mathbf{a}} = 0$. This kills off the λ terms, leaving just

$$\begin{aligned} m_1\ddot{\mathbf{r}}_1 &= K\left(\Delta\mathbf{r} - \mathbf{a}\right) \\ m_2\ddot{\mathbf{r}}_2 &= -K\left(\Delta\mathbf{r} - \mathbf{a}\right) . \end{aligned} \tag{3.88}$$

Taking differences this is

$$\Delta\ddot{\mathbf{r}} = -\frac{K}{\mu}\left(\Delta\mathbf{r} - \mathbf{a}\right) . \tag{3.89}$$

By inspection the solution for the difference is

$$\begin{aligned} \Delta\mathbf{r}(t) = \mathbf{a} &+ \left(\Delta\mathbf{r}_\circ - \mathbf{a}\right)\cos\left(\omega(t - t_\circ)\right) \\ &+ \frac{\Delta\mathbf{v}_\circ}{\omega}\sin\left(\omega(t - t_\circ)\right) . \end{aligned} \tag{3.90}$$

with the individual mass position vectors still given by eq. (3.80).

We get a strong hint here why we wish to work with displacement coordinates.

Exercise 3.6 Equilibrium position constraint.

Without the use of the somewhat forced seeming direction constraint used above, rederive the equations of motion.

Answer for Exercise 3.6

Here's a more natural way of specifying that we have an equilibrium length constraint

$$\begin{aligned} \mathcal{L} &= \frac{1}{2}m_1\left(\dot{\mathbf{r}}_1\right)^2 + \frac{1}{2}m_2\left(\dot{\mathbf{r}}_2\right)^2 - \frac{K}{2}\left(|\mathbf{r}_2 - \mathbf{r}_1| - a\right)^2 \\ &= \frac{1}{2}m_1\left(\dot{\mathbf{r}}_1\right)^2 + \frac{1}{2}m_2\left(\dot{\mathbf{r}}_2\right)^2 - \frac{K}{2}\left(\left(\mathbf{r}_2 - \mathbf{r}_1\right)^2 - 2a|\mathbf{r}_2 - \mathbf{r}_1| + a^2\right) . \end{aligned} \tag{3.91}$$

The evaluation of the absolute value gradient in the Euler-Lagrange equations can be done implicitly, computing the absolute square gradient in two different ways

$$\frac{\partial|\mathbf{x}|^2}{\partial\mathbf{x}} = \frac{\partial\mathbf{x}^2}{\partial\mathbf{x}} = 2\mathbf{x} \tag{3.92a}$$

$$\frac{\partial |\mathbf{x}|^2}{\partial \mathbf{x}} = 2|\mathbf{x}| \frac{\partial |\mathbf{x}|}{\partial \mathbf{x}}, \tag{3.92b}$$

so that

$$\frac{\partial |\mathbf{x}|}{\partial \mathbf{x}} = \frac{\mathbf{x}}{|\mathbf{x}|}. \tag{3.93}$$

This gives us

$$\begin{aligned} m_1 \ddot{\mathbf{r}}_1 &= -K \left(\mathbf{r}_1 - \mathbf{r}_2 - a \frac{\mathbf{r}_1 - \mathbf{r}_2}{|\mathbf{r}_2 - \mathbf{r}_1|} \right) \\ m_2 \ddot{\mathbf{r}}_2 &= -K \left(\mathbf{r}_2 - \mathbf{r}_1 - a \frac{\mathbf{r}_2 - \mathbf{r}_1}{|\mathbf{r}_2 - \mathbf{r}_1|} \right) \end{aligned} \tag{3.94}$$

With $\Delta\mathbf{r} = \mathbf{r}_2 - \mathbf{r}_1$ and $\hat{\Delta}_{21} = (\mathbf{r}_2 - \mathbf{r}_1)/|\mathbf{r}_2 - \mathbf{r}_1|$, this gives

$$\boxed{\mu \Delta \ddot{\mathbf{r}} = -K \left(\Delta\mathbf{r} - a\hat{\Delta}_{21} \right).} \tag{3.95}$$

In general, $\hat{\Delta}_{21}$ could rotate in space (non-zero angular momentum for the system), meaning that we'd also have a directional dependence on the LHS. A specific solution is possible if we assume that the direction is fixed, and introduce scalar displacement coordinates, relative to the center of the equilibrium position as illustrated in fig. 3.24.

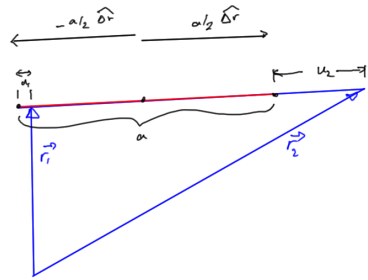

Figure 3.24: Coupling directed along difference vector.

$$\begin{aligned} \mathbf{r}_1 &= \left(-\frac{a}{2} + u_1 \right) \hat{\Delta}_{21} \\ \mathbf{r}_2 &= \left(\frac{a}{2} + u_2 \right) \hat{\Delta}_{21}. \end{aligned} \tag{3.96}$$

With $\Delta u = u_2 - u_1$, eq. (3.95) takes the form

$$\mu \Delta \ddot{u} = -K \Delta u. \tag{3.97}$$

We see exactly how natural displacement coordinates are for the two mass problem. We have also avoided the awkward requirement for a Lagrange multiplier constraint in the Lagrangian model of the system.

Exercise 3.7 Potential about equilibrium point.

Compute the linear expansion of a two mass potential, with masses located at $\mathbf{r}_1, \mathbf{r}_2$ and equilibrium positions $\mathbf{a}_1, \mathbf{a}_2$.

Answer for Exercise 3.7

$$\begin{aligned}\phi(\mathbf{r}_1, \mathbf{r}_2) &= \frac{K}{2} \left(|\mathbf{r}_2 - \mathbf{r}_1| - |\mathbf{a}_2 - \mathbf{a}_1| \right)^2 \\ &= \frac{K}{2} \left((\mathbf{r}_2 - \mathbf{r}_1)^2 - 2 |\mathbf{a}_2 - \mathbf{a}_1| |\mathbf{r}_2 - \mathbf{r}_1| + (\mathbf{a}_2 - \mathbf{a}_1)^2 \right).\end{aligned} \tag{3.98}$$

With $\Delta \mathbf{a} = \mathbf{a}_2 - \mathbf{a}_1$, and $\mathbf{r}_k = \sum_i \mathbf{e}_i r_{ki}$, this has first derivatives

$$\frac{\partial \phi}{\partial r_{1i}} = K \left((\mathbf{r}_1 - \mathbf{r}_2) \cdot \mathbf{e}_i - |\mathbf{a}_2 - \mathbf{a}_1| \frac{r_{1i} - r_{2i}}{|\mathbf{r}_2 - \mathbf{r}_1|} \right). \tag{3.99}$$

Regrouping and noting the $\mathbf{r}_2, \mathbf{r}_1$ swapping symmetry, these first derivatives are

$$\begin{aligned}\frac{\partial \phi}{\partial r_{1i}} &= K (r_{1i} - r_{2i}) \left(1 - \frac{|\mathbf{a}_2 - \mathbf{a}_1|}{|\mathbf{r}_2 - \mathbf{r}_1|} \right) \\ \frac{\partial \phi}{\partial r_{2i}} &= K (r_{2i} - r_{1i}) \left(1 - \frac{|\mathbf{a}_2 - \mathbf{a}_1|}{|\mathbf{r}_2 - \mathbf{r}_1|} \right).\end{aligned} \tag{3.100}$$

At the equilibrium positions $\mathbf{a}_1, \mathbf{a}_2$, the first order derivatives are all zero for this potential, a property used in the equilibrium potential expansion discussions of [10] and [1]. Proceeding to calculate the second derivatives

$$\begin{aligned}&\frac{\partial}{\partial r_{1j}} \frac{\partial \phi}{\partial r_{1i}} \\ &= K \delta_{ij} \left(1 - \frac{|\mathbf{a}_2 - \mathbf{a}_1|}{|\mathbf{r}_2 - \mathbf{r}_1|} \right) - K (r_{1i} - r_{2i}) |\mathbf{a}_2 - \mathbf{a}_1| \frac{\partial}{\partial r_{1j}} \left((\mathbf{r}_1 - \mathbf{r}_2)^2 \right)^{-1/2} \\ &= K \delta_{ij} \left(1 - \frac{|\mathbf{a}_2 - \mathbf{a}_1|}{|\mathbf{r}_2 - \mathbf{r}_1|} \right) + K (r_{1i} - r_{2i}) |\mathbf{a}_2 - \mathbf{a}_1| \frac{2 (r_{1j} - r_{2j})}{2 |\mathbf{r}_1 - \mathbf{r}_2|^3}.\end{aligned}$$

(3.101)

At the equilibrium positions, this is

$$\left.\frac{\partial}{\partial r_{1j}}\frac{\partial \phi}{\partial r_{1i}}\right|_{\mathbf{a}_1,\mathbf{a}_2} = +K\frac{\Delta a_i}{|\Delta \mathbf{a}|}\frac{\Delta a_j}{|\Delta \mathbf{a}|}. \tag{3.102}$$

These ratios are the direction cosines, as illustrated in fig. 3.25, where $\Delta\mathbf{a} = |\Delta\mathbf{a}|\,(\cos\theta_1, \cos\theta_2, \cos\theta_3)$. Again employing symmetries, the second derivatives for the non-mixed coordinates are

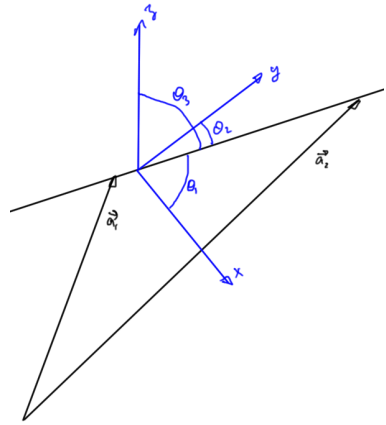

Figure 3.25: Direction cosines relative to equilibrium position difference vector.

$$\begin{aligned}\left.\frac{\partial}{\partial r_{1j}}\frac{\partial \phi}{\partial r_{1i}}\right|_{\mathbf{a}_1,\mathbf{a}_2} &= K\cos\theta_i\cos\theta_j \\ \left.\frac{\partial}{\partial r_{2j}}\frac{\partial \phi}{\partial r_{2i}}\right|_{\mathbf{a}_1,\mathbf{a}_2} &= K\cos\theta_i\cos\theta_j.\end{aligned} \tag{3.103}$$

For the mixed derivatives

$$\begin{aligned}&\frac{\partial}{\partial r_{2j}}\frac{\partial \phi}{\partial r_{1i}} \\ &= -K\delta_{ij}\left(1-\frac{|\mathbf{a}_2-\mathbf{a}_1|}{|\mathbf{r}_2-\mathbf{r}_1|}\right) - K\left(r_{1i}-r_{2i}\right)|\mathbf{a}_2-\mathbf{a}_1|\frac{\partial}{\partial r_{2j}}\left(\left(\mathbf{r}_2-\mathbf{r}_1\right)^2\right)^{-1/2} \\ &= -K\delta_{ij}\left(1-\frac{|\mathbf{a}_2-\mathbf{a}_1|}{|\mathbf{r}_2-\mathbf{r}_1|}\right) + K\left(r_{1i}-r_{2i}\right)|\mathbf{a}_2-\mathbf{a}_1|\frac{2\left(r_{2j}-r_{1j}\right)}{2|\mathbf{r}_1-\mathbf{r}_2|^3}.\end{aligned}$$

(3.104)

At the equilibrium positions, this is

$$\frac{\partial}{\partial r_{2j}}\frac{\partial \phi}{\partial r_{1i}}\bigg|_{\mathbf{a}_1,\mathbf{a}_2} = \frac{\partial}{\partial r_{1j}}\frac{\partial \phi}{\partial r_{2i}}\bigg|_{\mathbf{a}_1,\mathbf{a}_2} = -K\cos\theta_i\cos\theta_j, \tag{3.105}$$

so to second order, with displacement coordinates $\mathbf{u}_i = \mathbf{r}_i - \mathbf{a}_i$, the potential is

$$\begin{aligned}\phi(\mathbf{u}_1, \mathbf{u}_2) &\approx \phi(\mathbf{a}_1, \mathbf{a}_2) \\ &+ \frac{K}{2}\sum_{ij}\cos\theta_i\cos\theta_j\left(u_{1j}u_{1i} - u_{2j}u_{1i} - u_{1j}u_{2i} + u_{2j}u_{2i}\right),\end{aligned} \tag{3.106}$$

but since $\phi(\mathbf{a}_1, \mathbf{a}_2) = 0$, we have

$$\boxed{\phi(\mathbf{u}_1, \mathbf{u}_2) \approx \frac{K}{2}\sum_{ij}\cos\theta_i\cos\theta_j\left(u_{2i} - u_{1i}\right)\left(u_{2j} - u_{1j}\right).} \tag{3.107}$$

As a check observe that if $\Delta\mathbf{a}$ is directed along $\mathbf{e}_1$, we have to second order $\phi(\mathbf{u}_1, \mathbf{u}_2) = \frac{K}{2}\left(u_{21} - u_{11}\right)^2$, as we found previously.

The complete Lagrangian is, to second order about the equilibrium positions,

$$\begin{aligned}\mathcal{L} &= \sum_j \frac{m_i}{2}\dot{u}_{ij}^2 \\ &\quad - \frac{K}{2}\sum_{ij}\cos\theta_i\cos\theta_j\left(u_{2i} - u_{1i}\right)\left(u_{2j} - u_{1j}\right).\end{aligned} \tag{3.108}$$

Evaluating the Euler-Lagrange equations for m_2 we have

$$\frac{d}{dt}\frac{\partial \mathcal{L}}{\partial \dot{u}_{2k}} = m_2\ddot{u}_{2k}. \tag{3.109}$$

With $\hat{\Delta}_{21} = \Delta\mathbf{a}/|\Delta\mathbf{a}|$, the position derivatives are

$$\begin{aligned}\frac{\partial \mathcal{L}}{\partial u_{2k}} &= -\frac{K}{2}\sum_{ij}\cos\theta_i\cos\theta_j\left(\delta_{ik}\left(u_{2j} - u_{1j}\right) + \left(u_{2i} - u_{1i}\right)\delta_{jk}\right) \\ &= -K\sum_j\cos\theta_k\cos\theta_j\left(u_{2j} - u_{1j}\right) \\ &= -K\cos\theta_k\hat{\Delta}_{21}\cdot\Delta\mathbf{u}.\end{aligned} \tag{3.110}$$

The vector form of the Euler-Lagrange equations $d/dt(\partial\mathcal{L}/\partial\dot{\mathbf{u}}_i) = \partial\mathcal{L}/\partial\mathbf{u}_i$, is by inspection

$$\begin{aligned} m_1\ddot{\mathbf{u}}_1 &= K\hat{\Delta}_{21}\left(\hat{\Delta}_{21}\cdot\Delta\mathbf{u}\right) \\ m_2\ddot{\mathbf{u}}_2 &= -K\hat{\Delta}_{21}\left(\hat{\Delta}_{21}\cdot\Delta\mathbf{u}\right), \end{aligned} \tag{3.111}$$

or

$$\boxed{\begin{aligned} \mu\Delta\ddot{\mathbf{u}} &= -K\hat{\Delta}_{21}\left(\hat{\Delta}_{21}\cdot\Delta\mathbf{u}\right) \\ m_1\ddot{\mathbf{u}}_1 + m_2\ddot{\mathbf{u}}_2 &= 0. \end{aligned}} \tag{3.112}$$

Observe that on the RHS above we have a projection operator, so we could also write

$$\mu\Delta\ddot{\mathbf{u}} = -K\,\mathrm{Proj}_{\hat{\Delta}_{21}}\,\Delta\mathbf{u}. \tag{3.113}$$

Only the portion of the displacement difference $\Delta\mathbf{u}$ that is directed along the equilibrium line contributes to the acceleration of the displacement difference.

Exercise 3.8 Harmonically coupled masses.

Now let's consider masses at lattice points indexed by a lattice vector $\mathbf{n}$, as illustrated in fig. 3.26.

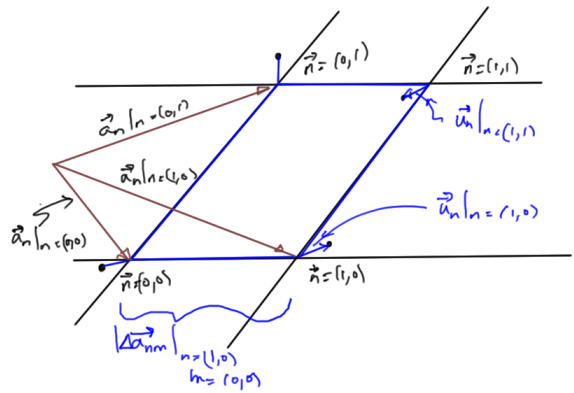

Figure 3.26: Masses harmonically coupled in a lattice.

Answer for Exercise 3.8

With a coupling constant of $K_{\mathbf{nm}}$ between lattice points indexed $\mathbf{n}$ and $\mathbf{m}$ (located at $\mathbf{a_n}$ and $\mathbf{a_m}$ respectively), and direction cosines for the equilibrium direction vector between those points given by

$$\begin{aligned}\mathbf{a_n} - \mathbf{a_m} &= \Delta \mathbf{a_{nm}} \\ &= |\Delta \mathbf{a_{nm}}|(\cos\theta_{\mathbf{nm}1}, \cos\theta_{\mathbf{nm}2}, \cos\theta_{\mathbf{nm}3}),\end{aligned} \tag{3.114}$$

the Lagrangian is

$$\begin{aligned}\mathcal{L} = &\sum_{\mathbf{n},i} \frac{m_{\mathbf{n}}}{2} \dot{u}_{\mathbf{n}i}^2 \\ &- \frac{1}{2} \sum_{\mathbf{n}\neq\mathbf{m},i,j} \frac{K_{\mathbf{nm}}}{2} \cos\theta_{\mathbf{nm}i} \cos\theta_{\mathbf{nm}j} \left(u_{\mathbf{n}i} - u_{\mathbf{m}i}\right)\left(u_{\mathbf{n}j} - u_{\mathbf{m}j}\right).\end{aligned} \tag{3.115}$$

Evaluating the Euler-Lagrange equations for the mass at index $\mathbf{n}$ we have

$$\frac{d}{dt}\frac{\partial \mathcal{L}}{\partial \dot{u}_{\mathbf{n}k}} = m_{\mathbf{n}} \ddot{u}_{\mathbf{n}k}, \tag{3.116}$$

and

$$\begin{aligned}\frac{\partial \mathcal{L}}{\partial u_{\mathbf{n}k}} &= -\sum_{\mathbf{m},i,j} \frac{K_{\mathbf{nm}}}{2} \cos\theta_{\mathbf{nm}i} \cos\theta_{\mathbf{nm}j} \left(\delta_{ik}\left(u_{\mathbf{n}j} - u_{\mathbf{m}j}\right) + \left(u_{\mathbf{n}i} - u_{\mathbf{m}i}\right)\delta_{jk}\right) \\ &= -\sum_{\mathbf{m},i} K_{\mathbf{nm}} \cos\theta_{\mathbf{nm}k} \cos\theta_{\mathbf{nm}i} \left(u_{\mathbf{n}i} - u_{\mathbf{m}i}\right) \\ &= -\sum_{\mathbf{m}} K_{\mathbf{nm}} \cos\theta_{\mathbf{nm}k} \hat{\Delta}_{\mathbf{nm}} \cdot \Delta \mathbf{u_{nm}},\end{aligned} \tag{3.117}$$

where $\Delta \mathbf{u_{nm}} = \mathbf{u_n} - \mathbf{u_m}$. Equating both, we have in vector form

$$m_{\mathbf{n}} \ddot{\mathbf{u}}_{\mathbf{n}} = -\sum_{\mathbf{m}} K_{\mathbf{nm}} \hat{\Delta}_{\mathbf{nm}} \left(\hat{\Delta}_{\mathbf{nm}} \cdot \Delta \mathbf{u_{nm}}\right), \tag{3.118}$$

or

$$\boxed{m_{\mathbf{n}} \ddot{\mathbf{u}}_{\mathbf{n}} = -\sum_{\mathbf{m}} K_{\mathbf{nm}} \operatorname{Proj}_{\hat{\Delta}_{\mathbf{nm}}} \Delta \mathbf{u_{nm}},} \tag{3.119}$$

This is an intuitively pleasing result. We have displacement and the direction of the lattice separations in the mix, but not the magnitude of the lattice separation itself. Compare that to eq. (3.95)

(the two mass result that did not use the Taylor expansion of the potential), where we had the lattice spacing explicitly along with the absolute coordinates (or rather the difference between them).

Exercise 3.9 Two atom basis, 2D diamond lattice.

As a concrete application of the previously calculated equilibrium harmonic oscillator result, find the equations of motion for a two atom basis diamond lattice where the horizontal length is a and vertical height is b.

Answer for Exercise 3.9

Indexing for the primitive unit cells is illustrated in fig. 3.27.

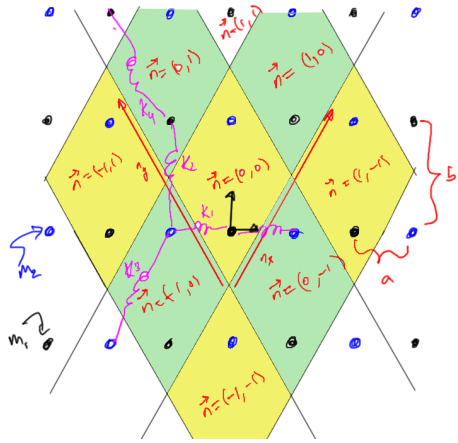

Figure 3.27: Primitive unit cells for diamond lattice.

Let's write

$$\begin{aligned}\mathbf{r} &= a(\cos\theta, \sin\theta) = a\hat{\mathbf{r}} \\ \mathbf{s} &= a(-\cos\theta, \sin\theta) = a\hat{\mathbf{s}} \\ \mathbf{n} &= (n_1, n_2) \\ \mathbf{r}_\mathbf{n} &= n_1\mathbf{r} + n_2\mathbf{s},\end{aligned} \tag{3.120}$$

For mass $m_\alpha, \alpha \in \{1, 2\}$ assume a trial solution of the form

$$\mathbf{u}_{\mathbf{n},\alpha} = \frac{\epsilon_\alpha(\mathbf{q})}{\sqrt{m_\alpha}} e^{i\mathbf{r}_n \cdot \mathbf{q} - \omega t}. \tag{3.121}$$

The equations of motion for the two particles are

$$\begin{aligned} m_1 \ddot{\mathbf{u}}_{\mathbf{n},1} = &-K_1 \operatorname{Proj}_{\hat{\mathbf{x}}} \left(\mathbf{u}_{\mathbf{n},1} - \mathbf{u}_{\mathbf{n}-(0,1),2} \right) \\ &- K_1 \operatorname{Proj}_{\hat{\mathbf{x}}} \left(\mathbf{u}_{\mathbf{n},1} - \mathbf{u}_{\mathbf{n}-(1,0),2} \right) \\ &- K_2 \operatorname{Proj}_{\hat{\mathbf{y}}} \left(\mathbf{u}_{\mathbf{n},1} - \mathbf{u}_{\mathbf{n},2} \right) \\ &- K_2 \operatorname{Proj}_{\hat{\mathbf{y}}} \left(\mathbf{u}_{\mathbf{n},1} - \mathbf{u}_{\mathbf{n}-(1,1),2} \right) \\ &- K_3 \sum_{\pm} \operatorname{Proj}_{\hat{\mathbf{r}}} \left(\mathbf{u}_{\mathbf{n},1} - \mathbf{u}_{\mathbf{n}\pm(1,0),1} \right) \\ &- K_4 \sum_{\pm} \operatorname{Proj}_{\hat{\mathbf{s}}} \left(\mathbf{u}_{\mathbf{n},1} - \mathbf{u}_{\mathbf{n}\pm(0,1),1} \right) \end{aligned} \tag{3.122a}$$

$$\begin{aligned} m_2 \ddot{\mathbf{u}}_{\mathbf{n},2} = &-K_1 \operatorname{Proj}_{\hat{\mathbf{x}}} \left(\mathbf{u}_{\mathbf{n},2} - \mathbf{u}_{\mathbf{n}+(1,0),1} \right) \\ &- K_1 \operatorname{Proj}_{\hat{\mathbf{x}}} \left(\mathbf{u}_{\mathbf{n},2} - \mathbf{u}_{\mathbf{n}+(0,1),1} \right) \\ &- K_2 \operatorname{Proj}_{\hat{\mathbf{y}}} \left(\mathbf{u}_{\mathbf{n},2} - \mathbf{u}_{\mathbf{n},1} \right) \\ &- K_2 \operatorname{Proj}_{\hat{\mathbf{y}}} \left(\mathbf{u}_{\mathbf{n},2} - \mathbf{u}_{\mathbf{n}+(1,1),1} \right) \\ &- K_3 \sum_{\pm} \operatorname{Proj}_{\hat{\mathbf{r}}} \left(\mathbf{u}_{\mathbf{n},2} - \mathbf{u}_{\mathbf{n}\pm(1,0),2} \right) \\ &- K_4 \sum_{\pm} \operatorname{Proj}_{\hat{\mathbf{s}}} \left(\mathbf{u}_{\mathbf{n},2} - \mathbf{u}_{\mathbf{n}\pm(0,1),2} \right) . \end{aligned} \tag{3.122b}$$

Insertion of the trial solution gives

$$\begin{aligned} \omega^2 \sqrt{m_1} \boldsymbol{\epsilon}_1 = &K_1 \operatorname{Proj}_{\hat{\mathbf{x}}} \left(\frac{\boldsymbol{\epsilon}_1}{\sqrt{m_1}} - \frac{\boldsymbol{\epsilon}_2}{\sqrt{m_2}} e^{-i\mathbf{s}\cdot\mathbf{q}} \right) \\ &+ K_1 \operatorname{Proj}_{\hat{\mathbf{x}}} \left(\frac{\boldsymbol{\epsilon}_1}{\sqrt{m_1}} - \frac{\boldsymbol{\epsilon}_2}{\sqrt{m_2}} e^{-i\mathbf{r}\cdot\mathbf{q}} \right) \\ &+ K_2 \operatorname{Proj}_{\hat{\mathbf{y}}} \left(\frac{\boldsymbol{\epsilon}_1}{\sqrt{m_1}} - \frac{\boldsymbol{\epsilon}_2}{\sqrt{m_2}} \right) \\ &+ K_2 \operatorname{Proj}_{\hat{\mathbf{y}}} \left(\frac{\boldsymbol{\epsilon}_1}{\sqrt{m_1}} - \frac{\boldsymbol{\epsilon}_2}{\sqrt{m_2}} e^{-i(\mathbf{r}+\mathbf{s})\cdot\mathbf{q}} \right) \\ &+ K_3 \left(\operatorname{Proj}_{\hat{\mathbf{r}}} \frac{\boldsymbol{\epsilon}_1}{\sqrt{m_1}} \right) \sum_{\pm} \left(1 - e^{\pm i\mathbf{r}\cdot\mathbf{q}} \right) \\ &+ K_4 \left(\operatorname{Proj}_{\hat{\mathbf{s}}} \frac{\boldsymbol{\epsilon}_1}{\sqrt{m_1}} \right) \sum_{\pm} \left(1 - e^{\pm i\mathbf{s}\cdot\mathbf{q}} \right) \end{aligned} \tag{3.123a}$$

$$\begin{aligned}
\omega^2\sqrt{m_2}\boldsymbol{\epsilon}_2 = {} & K_1 \operatorname{Proj}_{\hat{\mathbf{x}}}\left(\frac{\boldsymbol{\epsilon}_2}{\sqrt{m_2}} - \frac{\boldsymbol{\epsilon}_1}{\sqrt{m_1}}e^{+i\mathbf{r}\cdot\mathbf{q}}\right) \\
& + K_1 \operatorname{Proj}_{\hat{\mathbf{x}}}\left(\frac{\boldsymbol{\epsilon}_2}{\sqrt{m_2}} - \frac{\boldsymbol{\epsilon}_1}{\sqrt{m_1}}e^{+i\mathbf{s}\cdot\mathbf{q}}\right) \\
& + K_2 \operatorname{Proj}_{\hat{\mathbf{y}}}\left(\frac{\boldsymbol{\epsilon}_2}{\sqrt{m_2}} - \frac{\boldsymbol{\epsilon}_1}{\sqrt{m_1}}\right) \\
& + K_2 \operatorname{Proj}_{\hat{\mathbf{y}}}\left(\frac{\boldsymbol{\epsilon}_2}{\sqrt{m_2}} - \frac{\boldsymbol{\epsilon}_1}{\sqrt{m_1}}e^{+i(\mathbf{r}+\mathbf{s})\cdot\mathbf{q}}\right) \\
& + K_3 \left(\operatorname{Proj}_{\hat{\mathbf{r}}}\frac{\boldsymbol{\epsilon}_2}{\sqrt{m_2}}\right)\sum_{\pm}\left(1 - e^{\pm i\mathbf{r}\cdot\mathbf{q}}\right) \\
& + K_4 \left(\operatorname{Proj}_{\hat{\mathbf{s}}}\frac{\boldsymbol{\epsilon}_2}{\sqrt{m_2}}\right)\sum_{\pm}\left(1 - e^{\pm i\mathbf{s}\cdot\mathbf{q}}\right)
\end{aligned} \tag{3.123b}$$

Regrouping, and using the matrix form $\operatorname{Proj}_{\hat{\mathbf{u}}} = \hat{\mathbf{u}}\hat{\mathbf{u}}^{\mathrm{T}}$ for the projection operators, this is

$$\begin{aligned}
& \left(\omega^2 - \right. \\
& \left. \frac{2}{m_1}\left(K_1\hat{\mathbf{x}}\hat{\mathbf{x}}^T + K_2\hat{\mathbf{y}}\hat{\mathbf{y}}^T + 2K_3\hat{\mathbf{r}}\hat{\mathbf{r}}^T\sin^2(\mathbf{r}\cdot\mathbf{q}/2) + 2K_4\hat{\mathbf{s}}\hat{\mathbf{s}}^T\sin^2(\mathbf{s}\cdot\mathbf{q}/2)\right)\right)\boldsymbol{\epsilon}_1 \\
& = -\left(K_1\hat{\mathbf{r}}\hat{\mathbf{r}}^{\mathrm{T}}\left(e^{-i\mathbf{s}\cdot\mathbf{q}} + e^{-i\mathbf{r}\cdot\mathbf{q}}\right) + K_2\hat{\mathbf{s}}\hat{\mathbf{s}}^{\mathrm{T}}\left(1 + e^{-i(\mathbf{r}+\mathbf{s})\cdot\mathbf{q}}\right)\right)\frac{\boldsymbol{\epsilon}_2}{\sqrt{m_1 m_2}}
\end{aligned} \tag{3.124a}$$

$$\begin{aligned}
& \left(\omega^2 \right. \\
& \left. - \frac{2}{m_2}\left(K_1\hat{\mathbf{x}}\hat{\mathbf{x}}^T + K_2\hat{\mathbf{y}}\hat{\mathbf{y}}^T + 2K_3\hat{\mathbf{r}}\hat{\mathbf{r}}^T\sin^2(\mathbf{r}\cdot\mathbf{q}/2) + 2K_4\hat{\mathbf{s}}\hat{\mathbf{s}}^T\sin^2(\mathbf{s}\cdot\mathbf{q}/2)\right)\right)\boldsymbol{\epsilon}_2 \\
& = -\left(K_1\hat{\mathbf{r}}\hat{\mathbf{r}}^{\mathrm{T}}\left(e^{i\mathbf{s}\cdot\mathbf{q}} + e^{i\mathbf{r}\cdot\mathbf{q}}\right) + K_2\hat{\mathbf{s}}\hat{\mathbf{s}}^{\mathrm{T}}\left(1 + e^{i(\mathbf{r}+\mathbf{s})\cdot\mathbf{q}}\right)\right)\frac{\boldsymbol{\epsilon}_1}{\sqrt{m_1 m_2}}.
\end{aligned} \tag{3.124b}$$

As a single matrix equation, this is

$$A = K_1\hat{\mathbf{x}}\hat{\mathbf{x}}^T + K_2\hat{\mathbf{y}}\hat{\mathbf{y}}^T + 2K_3\hat{\mathbf{r}}\hat{\mathbf{r}}^T\sin^2(\mathbf{r}\cdot\mathbf{q}/2) + 2K_4\hat{\mathbf{s}}\hat{\mathbf{s}}^T\sin^2(\mathbf{s}\cdot\mathbf{q}/2)$$

(3.125a)

$$B = e^{i(\mathbf{r}+\mathbf{s})\cdot\mathbf{q}/2}\left(K_1\hat{\mathbf{r}}\hat{\mathbf{r}}^{\mathrm{T}}\cos\left((\mathbf{r}-\mathbf{s})\cdot\mathbf{q}/2\right)+K_2\hat{\mathbf{s}}\hat{\mathbf{s}}^{\mathrm{T}}\cos\left((\mathbf{r}+\mathbf{s})\cdot\mathbf{q}/2\right)\right) \tag{3.125b}$$

$$0 = \begin{bmatrix} \omega^2 - \frac{2A}{m_1} & \frac{B^*}{\sqrt{m_1 m_2}} \\ \frac{B}{\sqrt{m_1 m_2}} & \omega^2 - \frac{2A}{m_2} \end{bmatrix} \begin{bmatrix} \epsilon_1 \\ \epsilon_2 \end{bmatrix} \tag{3.125c}$$

Observe that this is an eigenvalue problem $E\mathbf{e} = \omega^2\mathbf{e}$ for matrix

$$E = \begin{bmatrix} \frac{2A}{m_1} & -\frac{B^*}{\sqrt{m_1 m_2}} \\ -\frac{B}{\sqrt{m_1 m_2}} & \frac{2A}{m_2} \end{bmatrix}, \tag{3.126}$$

and eigenvalues ω^2.

To be explicit lets put the A and B functions in explicit matrix form. The orthogonal projectors have a simple form

$$\mathrm{Proj}_{\hat{\mathbf{x}}} = \hat{\mathbf{x}}\hat{\mathbf{x}}^{\mathrm{T}} = \begin{bmatrix} 1 \\ 0 \end{bmatrix}\begin{bmatrix} 1 & 0 \end{bmatrix} = \begin{bmatrix} 1 & 0 \\ 0 & 0 \end{bmatrix} \tag{3.127a}$$

$$\mathrm{Proj}_{\hat{\mathbf{y}}} = \hat{\mathbf{y}}\hat{\mathbf{y}}^{\mathrm{T}} = \begin{bmatrix} 0 \\ 1 \end{bmatrix}\begin{bmatrix} 0 & 1 \end{bmatrix} = \begin{bmatrix} 0 & 0 \\ 0 & 1 \end{bmatrix} \tag{3.127b}$$

For the $\hat{\mathbf{r}}$ and $\hat{\mathbf{s}}$ projection operators, we can use half angle formulations

$$\begin{aligned} \mathrm{Proj}_{\hat{\mathbf{r}}} &= \hat{\mathbf{r}}\hat{\mathbf{r}}^{\mathrm{T}} \\ &= \begin{bmatrix} \cos\theta \\ \sin\theta \end{bmatrix}\begin{bmatrix} \cos\theta & \sin\theta \end{bmatrix} \\ &= \begin{bmatrix} \cos^2\theta & \cos\theta\sin\theta \\ \cos\theta\sin\theta & \sin^2\theta \end{bmatrix} \\ &= \frac{1}{2}\begin{bmatrix} 1+\cos(2\theta) & \sin(2\theta) \\ \sin(2\theta) & 1-\cos(2\theta) \end{bmatrix} \end{aligned} \tag{3.128a}$$

$$\begin{aligned}\text{Proj}_{\hat{\mathbf{s}}} &= \hat{\mathbf{s}}\hat{\mathbf{s}}^{\mathrm{T}} \\ &= \begin{bmatrix} -\cos\theta \\ \sin\theta \end{bmatrix} \begin{bmatrix} -\cos\theta & \sin\theta \end{bmatrix} \\ &= \begin{bmatrix} \cos^2\theta & -\cos\theta\sin\theta \\ -\cos\theta\sin\theta & \sin^2\theta \end{bmatrix} \\ &= \frac{1}{2}\begin{bmatrix} 1+\cos(2\theta) & -\sin(2\theta) \\ -\sin(2\theta) & 1-\cos(2\theta) \end{bmatrix}\end{aligned} \tag{3.128b}$$

After some manipulation, and the following helper functions

$$\begin{aligned}\alpha_\pm &= K_3 \sin^2(\mathbf{r}\cdot\mathbf{q}/2) \pm K_4 \sin^2(\mathbf{s}\cdot\mathbf{q}/2) \\ \beta_\pm &= K_1 \cos\left((\mathbf{r}-\mathbf{s})\cdot\mathbf{q}/2\right) \pm K_2 \cos\left((\mathbf{r}+\mathbf{s})\cdot\mathbf{q}/2\right),\end{aligned} \tag{3.129}$$

the block matrices of eq. (3.125) take the form

$$A = \begin{bmatrix} K_1 + \alpha_+(1+\cos(2\theta)) & \alpha_- \sin(2\theta) \\ \alpha_- \sin(2\theta) & K_2 + \alpha_+(1-\cos(2\theta)) \end{bmatrix} \tag{3.130a}$$

$$B = e^{i(\mathbf{r}+\mathbf{s})\cdot\mathbf{q}/2} \begin{bmatrix} \beta_+(1+\cos(2\theta)) & \beta_- \sin(2\theta) \\ \beta_- \sin(2\theta) & \beta_+(1-\cos(2\theta)) \end{bmatrix} \tag{3.130b}$$

A final bit of simplification for B possible, noting that $\mathbf{r}+\mathbf{s} = 2a(0,\sin\theta)$, and $\mathbf{r}-\mathbf{s} = 2a(\cos\theta, 0)$, so

$$\beta_\pm = K_1 \cos\left(a\cos\theta q_x\right) \pm K_2 \cos\left(a\sin\theta q_y\right), \tag{3.131}$$

and

$$B = e^{ia\sin\theta q_y} \begin{bmatrix} \beta_+(1+\cos(2\theta)) & \beta_- \sin(2\theta) \\ \beta_- \sin(2\theta) & \beta_+(1-\cos(2\theta)) \end{bmatrix}. \tag{3.132}$$

It isn't particularly illuminating to expand out the determinant for such a system, even though it can be done symbolically without too much programming. However, what is easy after formulating the matrix for this system, is actually solving it. This is done, and animated, in twoAtomBasisRectangularLatticeDispersionRelation.cdf

Exercise 3.10 One atom basis phonons in 2D. (*2013 final exam*)

Tackle the 2D problem of the final exam, generalizing from a square lattice to a general one atom basis in 2D. The lattice geometry to consider is illustrated in fig. 3.28.

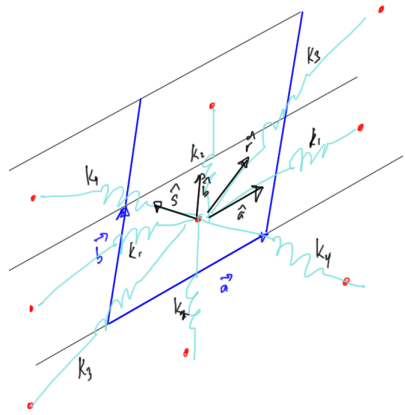

Figure 3.28: Oblique one atom basis.

Here, **a** and **b** are the vector differences between the equilibrium positions separating the masses along the K_1 and K_2 interaction directions respectively.

Answer for Exercise 3.10

The equilibrium spacing for the cross coupling harmonic forces are

$$\begin{aligned}\mathbf{r} &= (\mathbf{b} + \mathbf{a})/2 \\ \mathbf{s} &= (\mathbf{b} - \mathbf{a})/2.\end{aligned} \tag{3.133}$$

Based on previous calculations, we can write the equations of motion by inspection

$$\begin{aligned}m\ddot{\mathbf{u}}_\mathbf{n} = &- K_1 \operatorname{Proj}_{\hat{\mathbf{a}}} \sum_\pm \left(\mathbf{u}_\mathbf{n} - \mathbf{u}_{\mathbf{n}\pm(1,0)}\right)^2 \\ &- K_2 \operatorname{Proj}_{\hat{\mathbf{b}}} \sum_\pm \left(\mathbf{u}_\mathbf{n} - \mathbf{u}_{\mathbf{n}\pm(0,1)}\right)^2 \\ &- K_3 \operatorname{Proj}_{\hat{\mathbf{r}}} \sum_\pm \left(\mathbf{u}_\mathbf{n} - \mathbf{u}_{\mathbf{n}\pm(1,1)}\right)^2 \\ &- K_4 \operatorname{Proj}_{\hat{\mathbf{s}}} \sum_\pm \left(\mathbf{u}_\mathbf{n} - \mathbf{u}_{\mathbf{n}\pm(1,-1)}\right)^2.\end{aligned} \tag{3.134}$$

Inserting the trial solution

$$\mathbf{u_n} = \frac{1}{\sqrt{m}}\boldsymbol{\epsilon}(\mathbf{q})e^{i(\mathbf{r_n}\cdot\mathbf{q}-\omega t)}, \tag{3.135}$$

and using the matrix form for the projection operators, we have

$$\begin{aligned}
\omega^2\boldsymbol{\epsilon} &= \frac{K_1}{m}\hat{\mathbf{a}}\hat{\mathbf{a}}^{\mathrm{T}}\boldsymbol{\epsilon}\sum_{\pm}\left(1-e^{\pm i\mathbf{a}\cdot\mathbf{q}}\right)\\
&+ \frac{K_2}{m}\hat{\mathbf{b}}\hat{\mathbf{b}}^{\mathrm{T}}\boldsymbol{\epsilon}\sum_{\pm}\left(1-e^{\pm i\mathbf{b}\cdot\mathbf{q}}\right)\\
&+ \frac{K_3}{m}\hat{\mathbf{b}}\hat{\mathbf{b}}^{\mathrm{T}}\boldsymbol{\epsilon}\sum_{\pm}\left(1-e^{\pm i(\mathbf{b}+\mathbf{a})\cdot\mathbf{q}}\right)\\
&+ \frac{K_3}{m}\hat{\mathbf{b}}\hat{\mathbf{b}}^{\mathrm{T}}\boldsymbol{\epsilon}\sum_{\pm}\left(1-e^{\pm i(\mathbf{b}-\mathbf{a})\cdot\mathbf{q}}\right)\\
&= \frac{4K_1}{m}\hat{\mathbf{a}}\hat{\mathbf{a}}^{\mathrm{T}}\boldsymbol{\epsilon}\sin^2\left(\mathbf{a}\cdot\mathbf{q}/2\right) + \frac{4K_2}{m}\hat{\mathbf{b}}\hat{\mathbf{b}}^{\mathrm{T}}\boldsymbol{\epsilon}\sin^2\left(\mathbf{b}\cdot\mathbf{q}/2\right)\\
&+ \frac{4K_3}{m}\hat{\mathbf{r}}\hat{\mathbf{r}}^{\mathrm{T}}\boldsymbol{\epsilon}\sin^2\left((\mathbf{b}+\mathbf{a})\cdot\mathbf{q}/2\right) + \frac{4K_4}{m}\hat{\mathbf{s}}\hat{\mathbf{s}}^{\mathrm{T}}\boldsymbol{\epsilon}\sin^2\left((\mathbf{b}-\mathbf{a})\cdot\mathbf{q}/2\right).
\end{aligned} \tag{3.136}$$

This fully specifies our eigenvalue problem. Writing

$$\begin{aligned}
S_1 &= \sin^2\left(\mathbf{a}\cdot\mathbf{q}/2\right)\\
S_2 &= \sin^2\left(\mathbf{b}\cdot\mathbf{q}/2\right)\\
S_3 &= \sin^2\left((\mathbf{b}+\mathbf{a})\cdot\mathbf{q}/2\right)\\
S_4 &= \sin^2\left((\mathbf{b}-\mathbf{a})\cdot\mathbf{q}/2\right)
\end{aligned} \tag{3.137a}$$

$$\boxed{A = \frac{4}{m}\left(K_1S_1\hat{\mathbf{a}}\hat{\mathbf{a}}^{\mathrm{T}} + K_2S_2\hat{\mathbf{b}}\hat{\mathbf{b}}^{\mathrm{T}} + K_3S_3\hat{\mathbf{r}}\hat{\mathbf{r}}^{\mathrm{T}} + K_4S_4\hat{\mathbf{s}}\hat{\mathbf{s}}^{\mathrm{T}}\right),} \tag{3.137b}$$

. we wish to solve

$$A\boldsymbol{\epsilon} = \omega^2\boldsymbol{\epsilon} = \lambda\boldsymbol{\epsilon}. \tag{3.138}$$

Neglecting the specifics of the matrix at hand, consider a generic two by two matrix

$$A = \begin{bmatrix} a & b \\ c & d \end{bmatrix}, \tag{3.139}$$

for which the characteristic equation is

$$\begin{aligned} 0 &= \begin{vmatrix} \lambda - a & -b \\ -c & \lambda - d \end{vmatrix} \\ &= (\lambda - a)(\lambda - d) - bc \\ &= \lambda^2 - (a+d)\lambda + ad - bc \\ &= \lambda^2 - (TrA)\lambda + |A| \\ &= \left(\lambda - \frac{TrA}{2}\right)^2 - \left(\frac{TrA}{2}\right)^2 + |A|. \end{aligned} \tag{3.140}$$

So our angular frequencies are given by

$$\omega^2 = \frac{1}{2}\left(TrA \pm \sqrt{(TrA)^2 - 4|A|}\right). \tag{3.141}$$

The square root can be simplified slightly

$$\begin{aligned} (TrA)^2 - 4|A| &= (a+d)^2 - 4(ad - bc) \\ &= a^2 + d^2 + 2ad - 4ad + 4bc \\ &= (a-d)^2 + 4bc, \end{aligned} \tag{3.142}$$

so that, finally, the dispersion relation is

$$\boxed{\omega^2 = \frac{1}{2}\left(d + a \pm \sqrt{(d-a)^2 + 4bc}\right),} \tag{3.143}$$

Our eigenvectors will be given by

$$0 = (\lambda - a)\boldsymbol{\epsilon}_1 - b\boldsymbol{\epsilon}_2, \tag{3.144}$$

or

$$\boldsymbol{\epsilon}_1 \propto \frac{b}{\lambda - a}\boldsymbol{\epsilon}_2. \tag{3.145}$$

So, our eigenvectors, the vectoral components of our atomic displacements, are

$$\boldsymbol{\epsilon} \propto \begin{bmatrix} b \\ \omega^2 - a \end{bmatrix}, \tag{3.146}$$

or

$$\boxed{\boldsymbol{\epsilon} \propto \begin{bmatrix} 2b \\ d - a \pm \sqrt{(d-a)^2 + 4bc} \end{bmatrix}.} \tag{3.147}$$

Square lattice There is not too much to gain by expanding out the projection operators explicitly in general. However, let's do this for the specific case of a square lattice (as on the exam problem). In that case, our projection operators are

$$\hat{\mathbf{a}}\hat{\mathbf{a}}^{\mathrm{T}} = \begin{bmatrix} 1 \\ 0 \end{bmatrix} \begin{bmatrix} 1 & 0 \end{bmatrix} = \begin{bmatrix} 1 & 0 \\ 0 & 0 \end{bmatrix} \tag{3.148a}$$

$$\hat{\mathbf{b}}\hat{\mathbf{b}}^{\mathrm{T}} = \begin{bmatrix} 0 \\ 1 \end{bmatrix} \begin{bmatrix} 0 & 1 \end{bmatrix} = \begin{bmatrix} 0 & 0 \\ 0 & 1 \end{bmatrix} \tag{3.148b}$$

$$\hat{\mathbf{r}}\hat{\mathbf{r}}^{\mathrm{T}} = \frac{1}{2}\begin{bmatrix} 1 \\ 1 \end{bmatrix} \begin{bmatrix} 1 & 1 \end{bmatrix} = \frac{1}{2}\begin{bmatrix} 1 & 1 \\ 1 & 1 \end{bmatrix} \tag{3.148c}$$

$$\hat{\mathbf{s}}\hat{\mathbf{s}}^{\mathrm{T}} = \frac{1}{2}\begin{bmatrix} -1 \\ 1 \end{bmatrix} \begin{bmatrix} -1 & 1 \end{bmatrix} = \frac{1}{2}\begin{bmatrix} 1 & -1 \\ -1 & 1 \end{bmatrix} \tag{3.148d}$$

$$\begin{aligned} S_1 &= \sin^2(\mathbf{a}\cdot\mathbf{q}) \\ S_2 &= \sin^2(\mathbf{b}\cdot\mathbf{q}) \\ S_3 &= \sin^2((\mathbf{b}+\mathbf{a})\cdot\mathbf{q}) \\ S_4 &= \sin^2((\mathbf{b}-\mathbf{a})\cdot\mathbf{q}), \end{aligned} \tag{3.149}$$

Our matrix is

$$A = \frac{2}{m}\begin{bmatrix} 2K_1S_1 + K_3S_3 + K_4S_4 & K_3S_3 - K_4S_4 \\ K_3S_3 - K_4S_4 & 2K_2S_2 + K_3S_3 + K_4S_4 \end{bmatrix}, \tag{3.150}$$

where, specifically, the squared sines for this geometry are

$$S_1 = \sin^2(\mathbf{a}\cdot\mathbf{q}/2) = \sin^2(aq_x/2) \tag{3.151a}$$

$$S_2 = \sin^2(\mathbf{b}\cdot\mathbf{q}/2) = \sin^2(aq_y/2). \tag{3.151b}$$

$$S_3 = \sin^2((\mathbf{b}+\mathbf{a})\cdot\mathbf{q}/2) = \sin^2(a(q_x+q_y)/2) \tag{3.151c}$$

$$S_4 = \sin^2\left((\mathbf{b} - \mathbf{a}) \cdot \mathbf{q}/2\right) = \sin^2\left(a(q_y - q_x)/2\right). \tag{3.151d}$$

Using eq. (3.146), the dispersion relation and eigenvectors are

$$\omega^2 = \frac{2}{m}\left(\sum_i K_i S_i \pm \sqrt{(K_2 S_2 - K_1 S_1)^2 + (K_3 S_3 - K_4 S_4)^2}\right) \tag{3.152a}$$

$$\boldsymbol{\epsilon} \propto \begin{bmatrix} K_3 S_3 - K_4 S_4 \\ K_2 S_2 - K_1 S_1 \pm \sqrt{(K_2 S_2 - K_1 S_1)^2 + (K_3 S_3 - K_4 S_4)^2} \end{bmatrix}. \tag{3.152b}$$

This calculation is confirmed in oneAtomBasisPhononSquareLatticeEigensystem.nb . Mathematica calculates an alternate form (equivalent to using a zero dot product for the second row), of

$$\boldsymbol{\epsilon} \propto \begin{bmatrix} K_1 S_1 - K_2 S_2 \pm \sqrt{(K_2 S_2 - K_1 S_1)^2 + (K_3 S_3 - K_4 S_4)^2} \\ K_3 S_3 - K_4 S_4 \end{bmatrix}. \tag{3.153}$$

Either way, we see that $K_3 S_3 - K_4 S_4 = 0$ leads to only horizontal or vertical motion.

With the exam criteria In the specific case that we had on the exam where $K_1 = K_2$ and $K_3 = K_4$, these are

$$\omega^2 = \frac{2}{m}\left(K_1(S_1 + S_2) + K_3(S_3 + S_4) \pm \sqrt{K_1^2(S_2 - S_1)^2 + K_3^2(S_3 - S_4)^2}\right) \tag{3.154a}$$

$$\boldsymbol{\epsilon} \propto \begin{bmatrix} K_3\,(S_3 - S_4) \\ K_1\left((S_1 - S_2) \pm \sqrt{(S_2 - S_1)^2 + \left(\frac{K_3}{K_1}\right)^2 (S_3 - S_4)^2}\right) \end{bmatrix}. \tag{3.154b}$$

For horizontal and vertical motion we need $S_3 = S_4$, or for a $2\pi \times$ integer difference in the absolute values of the sine arguments

$$\pm(a(q_x + q_y)/2) = a(q_y - q_y)/2 + 2\pi n. \tag{3.155}$$

That is, one of

$$\begin{aligned} q_x &= \frac{2\pi}{a} n \\ q_y &= \frac{2\pi}{a} n \end{aligned} \tag{3.156}$$

In the first BZ, that is one of $q_x = 0$ or $q_y = 0$.

System in rotated coordinates On the exam, where we were asked to solve for motion along the cross directions explicitly, there was a strong hint to consider a rotated (by $\pi/4$) coordinate system. The rotated the lattice basis vectors are $\mathbf{a} = a\mathbf{e}_1, \mathbf{b} = a\mathbf{e}_2$, and the projection matrices. Writing $\hat{\mathbf{r}} = \mathbf{f}_1$ and $\hat{\mathbf{s}} = \mathbf{f}_2$, where $\mathbf{f}_1 = (\mathbf{e}_1 + \mathbf{e}_2)/\sqrt{2}, \mathbf{f}_2 = (\mathbf{e}_2 - \mathbf{e}_1)/\sqrt{2}$, or $\mathbf{e}_1 = (\mathbf{f}_1 - \mathbf{f}_2)/\sqrt{2}, \mathbf{e}_2 = (\mathbf{f}_1 + \mathbf{f}_2)/\sqrt{2}$. In the $\{\mathbf{f}_1, \mathbf{f}_2\}$ basis the projection matrices are

$$\hat{\mathbf{a}}\hat{\mathbf{a}}^{\mathrm{T}} = \frac{1}{2}\begin{bmatrix} 1 \\ -1 \end{bmatrix}\begin{bmatrix} 1 & -1 \end{bmatrix} = \frac{1}{2}\begin{bmatrix} 1 & -1 \\ -1 & 1 \end{bmatrix} \tag{3.157a}$$

$$\hat{\mathbf{b}}\hat{\mathbf{b}}^{\mathrm{T}} = \frac{1}{2}\begin{bmatrix} 1 \\ 1 \end{bmatrix}\begin{bmatrix} 1 & 1 \end{bmatrix} = \frac{1}{2}\begin{bmatrix} 1 & 1 \\ 1 & 1 \end{bmatrix} \tag{3.157b}$$

$$\hat{\mathbf{r}}\hat{\mathbf{r}}^{\mathrm{T}} = \begin{bmatrix} 1 & 0 \\ 0 & 0 \end{bmatrix} \tag{3.157c}$$

$$\hat{\mathbf{s}}\hat{\mathbf{s}}^{\mathrm{T}} = \begin{bmatrix} 0 & 0 \\ 0 & 1 \end{bmatrix} \tag{3.157d}$$

The dot products that show up in the squared sines are

$$\mathbf{a} \cdot \mathbf{q} = a\frac{1}{\sqrt{2}}(\mathbf{f}_1 - \mathbf{f}_2) \cdot (\mathbf{f}_1 k_u + \mathbf{f}_2 k_v) = \frac{a}{\sqrt{2}}(k_u - k_v) \tag{3.158a}$$

$$\mathbf{b} \cdot \mathbf{q} = a\frac{1}{\sqrt{2}}(\mathbf{f}_1 + \mathbf{f}_2) \cdot (\mathbf{f}_1 k_u + \mathbf{f}_2 k_v) = \frac{a}{\sqrt{2}}(k_u + k_v) \tag{3.158b}$$

$$(\mathbf{a}+\mathbf{b})\cdot\mathbf{q} = \sqrt{2}ak_u \tag{3.158c}$$

$$(\mathbf{b}-\mathbf{a})\cdot\mathbf{q} = \sqrt{2}ak_v. \tag{3.158d}$$

So that in this basis

$$\begin{aligned} S_1 &= \sin^2\left(\frac{a}{\sqrt{2}}(k_u - k_v)\right) \\ S_2 &= \sin^2\left(\frac{a}{\sqrt{2}}(k_u + k_v)\right) \\ S_3 &= \sin^2\left(\sqrt{2}ak_u\right) \\ S_4 &= \sin^2\left(\sqrt{2}ak_v\right) \end{aligned} \tag{3.159}$$

With the rotated projection operators eq. (3.137b) takes the form

$$A = \frac{2}{m}\begin{bmatrix} K_1S_1 + K_2S_2 + 2K_3S_3 & K_2S_2 - K_1S_1 \\ K_2S_2 - K_1S_1 & K_1S_1 + K_2S_2 + 2K_4S_4 \end{bmatrix}. \tag{3.160}$$

This clearly differs from eq. (3.150), and results in a different expression for the eigenvectors, but the same as eq. (3.152a) for the angular frequencies.

$$\boldsymbol{\epsilon} \propto \begin{bmatrix} K_2S_2 - K_1S_1 \\ K_4S_4 - K_3S_3 \mp \sqrt{(K_2S_2 - K_1S_1)^2 + (K_3S_3 - K_4S_4)^2} \end{bmatrix}, \tag{3.161}$$

or, equivalently

$$\boldsymbol{\epsilon} \propto \begin{bmatrix} K_4S_4 - K_3S_3 \mp \sqrt{(K_2S_2 - K_1S_1)^2 + (K_3S_3 - K_4S_4)^2} \\ K_1S_1 - K_2S_2 \end{bmatrix}, \tag{3.162}$$

For the $K_1 = K_2$ and $K_3 = K_4$ case of the exam, this is

$$\boldsymbol{\epsilon} \propto \begin{bmatrix} K_1(S_2 - S_1) \\ K_3\left(S_4 - S_3 \mp \sqrt{\left(\frac{K_1}{K_3}\right)^2 (S_2 - S_1)^2 + (S_3 - S_4)^2}\right) \end{bmatrix}. \tag{3.163}$$

Similar to the horizontal coordinate system, we see that we have motion along the diagonals when

$$\pm\frac{a}{\sqrt{2}}(k_u - k_v) = \frac{a}{\sqrt{2}}(k_u + k_v) + 2\pi n, \tag{3.164}$$

or one of

$$\begin{aligned} k_u &= \sqrt{2}\frac{\pi}{a}n \\ k_v &= \sqrt{2}\frac{\pi}{a}n \end{aligned} \tag{3.165}$$

Stability? The exam asked why the cross coupling is required for stability. Clearly we have more complex interaction. The constant ω surfaces will also be more complex. However, I still don't have a good intuition what exactly was sought after for that part of the question.

Numerical computations A Manipulate allowing for choice of the spring constants and lattice orientation, as shown in fig. 3.29, is available in oneAtomBasisPhonon.nb . This interface also provides a numerical calculation of the distribution relation as shown in fig. 3.30, and provides an animation of the normal modes for any given selection of $\mathbf{q}$ and $\omega(\mathbf{q})$ (not shown).

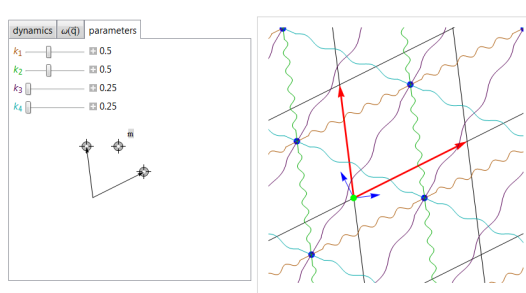

Figure 3.29: 2D Single atom basis Manipulate interface.

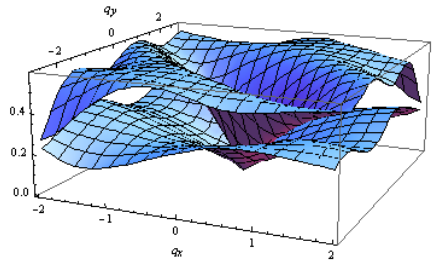

Figure 3.30: Sample distribution relation for 2D single atom basis.

4 THERMAL PROPERTIES.

4.1 THERMAL PROPERTIES.

4.2 LATTICE ENERGY.

We'll want to calculate the total energy stored in the lattice. There are a number of steps to this problem

1. Quantization. As an example, the classic SHO problem

$$m\ddot{u} = -ku, \tag{4.1}$$

results in a single frequency

$$\omega = \sqrt{\frac{k}{m}}. \tag{4.2}$$

With quantization we find only discrete frequencies, as in fig. 4.1.

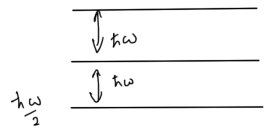

Figure 4.1: Quantized SHO energy levels.

$$\epsilon_n = \left(n + \frac{1}{2}\right)\hbar\omega. \tag{4.3}$$

For lattices we've been seeking solutions of the force equations

$$M_\alpha \ddot{u}_{n\alpha i} = -\sum_{m\beta j} \Phi^{m\beta j}_{n\alpha i} u_{m\beta j}. \tag{4.4}$$

This provided us lattice frequencies ω_q, which quantize as

$$\epsilon_{q,n} = \left(n_q + \frac{1}{2}\right)\hbar\omega_q. \tag{4.5}$$

Prof hoping that we are willing to this without proof since the proof is hard, and would take a couple days (see: [1] appendix L.)

We've apparently seen such a derivation indirectly in black-body calculations.

2. If we accept eq. (4.5), then the thermal energy is

$$U(T) = \sum_q \left(n_q + \frac{1}{2} \right) \hbar \omega_q. \tag{4.6}$$

average thermal occupancy

sum over modes

3. figuring out how to evaluate such a sum.

4.3 DENSITY OF STATES.

Reading: [10] §5.1

The density of states is the number of Phonon modes per unit energy.

- n_q depends only on energy (see below), so that we can group states by energy.
- q is quasi-continuous

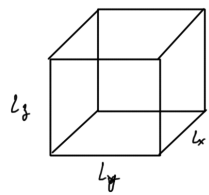

Figure 4.2: Period boundary conditions.

due to periodic boundary

$$e^{i\mathbf{q}\cdot(\mathbf{r}_n + \mathbf{L}_x)} = e^{i\mathbf{q}\cdot\mathbf{r}_n}, \tag{4.7}$$

or

$$q_x L_x = 2\pi l, \tag{4.8}$$

for integer l.

Similarly for q_y, q_z we have

$$\mathbf{q} = l\frac{2\pi}{L_x}\hat{\mathbf{x}} + m\frac{2\pi}{L_y}\hat{\mathbf{y}} + o\frac{2\pi}{L_z}\hat{\mathbf{z}}. \tag{4.9}$$

The volume per $\mathbf{q}$ point is

$$\frac{2\pi}{L_x}\frac{2\pi}{L_y}\frac{2\pi}{L_z} = \frac{(2\pi)^3}{V}. \tag{4.10}$$

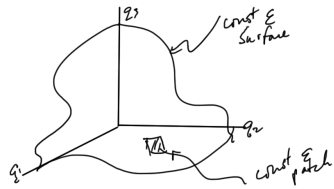

Figure 4.3: constant energy surface.

$$\begin{aligned}\sum_{\mathbf{n}} &= \sum_{n_x}\sum_{n_y}\sum_{n_z} \sim \int dn_x dn_y dn_z \\ &= \int \frac{L_x}{2\pi}dq_x \frac{L_y}{2\pi}dq_y \frac{L_z}{2\pi}dq_z \\ &= \frac{V}{(2\pi)^3}\int d^3\mathbf{q}.\end{aligned} \tag{4.11}$$

We group states of same $\hbar\omega_q$. In $d^3\mathbf{q}$ group same energy states

df_ω are constant energy area elements, so that the volume element is

$$df_\omega dq_\perp. \tag{4.12}$$

We can write

$$dq_\perp = \frac{d\omega}{\left|\boldsymbol{\nabla}_{\mathbf{q}}\omega(\mathbf{q})\right|}, \tag{4.13}$$

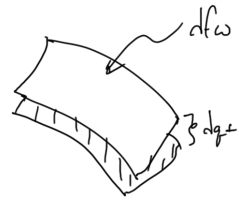

Figure 4.4: area element.

or

$$\begin{aligned}\frac{V}{(2\pi)^3}\int d^3\mathbf{q} &\to \frac{V}{(2\pi)^3}\int df_\omega dq_\perp \\ &\to \frac{V}{(2\pi)^3}\int \frac{df_\omega}{|\boldsymbol{\nabla}_\mathbf{q}\omega(\mathbf{q})|}d\omega \\ &= \int Z(\omega)d\omega.\end{aligned} \tag{4.14}$$

where $Z(\omega)$ is the density of states, the number of modes per unit energy.

Examination hint: He'll expect us to look at a phonon diagram and see where the density of states is high or low.

Example 4.1: 1D diatomic chain.

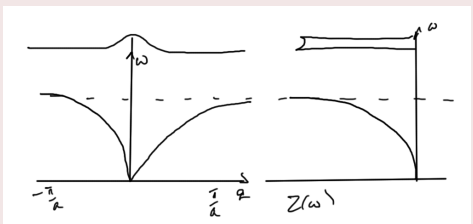

Figure 4.5: frequency distribution and density of states for diatomic chain.

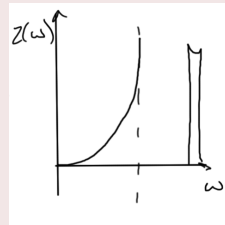

Figure 4.6: density of states.

Example 4.2: 3D solid.

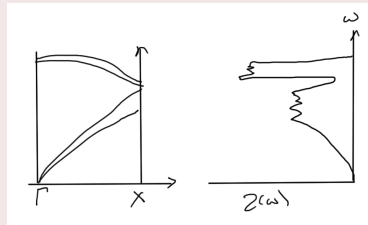

Figure 4.7: 3D solid frequency distribution and density of states.

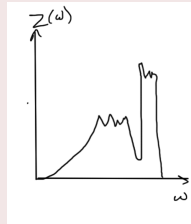

Figure 4.8: 3D solid density of states.

4.4 ISOTROPIC MODEL (DEBYE).

With a 1 atom basis (for now), we have only acoustic modes

$$\omega(\mathbf{q}) \to \omega(q). \tag{4.15}$$

same in all directions, so that the constant energy surfaces are spheres, as in fig. 4.9.

$$\boldsymbol{\nabla}_{\mathbf{q}}\omega(q) = \frac{d\omega}{dq}\hat{\mathbf{q}}, \tag{4.16}$$

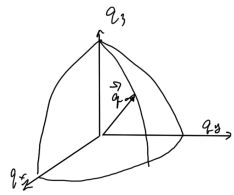

Figure 4.9: Debye surface.

at small q, the frequency for this 1 atom basis is

$$\omega = \begin{cases} C_L q & \text{longitudinal acoustic} \\ C_T q & \text{transverse acoustic (two of these)} \end{cases} \tag{4.17}$$

This gives

$$\begin{aligned} \int Z(\omega)d\omega &= \sum_{LA,TA} \frac{V}{(2\pi)^3} \int \frac{df_\omega}{\left|\boldsymbol{\nabla}_{\mathbf{q}}\omega(\mathbf{q})\right|} d\omega \\ &\qquad\qquad q \text{ space surface area element} \\ &= \frac{V}{(2\pi)^3} \int \sum_{LA,TA} \frac{df_\omega}{\frac{d\omega}{dq}} d\omega \\ &\qquad\qquad = \int df_\omega \\ &= \int \frac{V}{(2\pi)^3} \left(\frac{1}{C_L} + \frac{2}{C_T}\right) 4\pi q^2 \, d\omega \\ &= \int \frac{V}{2\pi^2} \left(\frac{q^2}{C_L} + \frac{2q^2}{C_T}\right) d\omega \\ &= \int \frac{V}{2\pi^2} \left(\frac{1}{C_L^3} + \frac{2}{C_T^3}\right) \omega^2 d\omega, \end{aligned} \tag{4.18}$$

Here we sum over the two transverse and the single longitudinal state, and refer back to eq. (4.17) introduce the C_L and C_T factors.

Because of $4\pi q^2$ phase space factor, we have

$$Z(\omega) \propto \omega^2. \tag{4.19}$$

Debye approximation Define the Debye frequency ω_D by

$$\int_0^{\omega_D} Z(\omega)d\omega = 3rN. \tag{4.20}$$

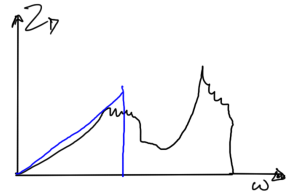

Figure 4.10: Debye approximation.

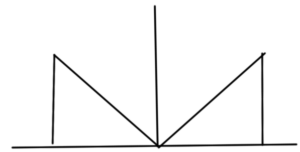

Figure 4.11: Linear Debye approximation.

and pretend we can cut off in a way that applies to all q. We get

$$\begin{aligned} 3rN &= \frac{V}{2\pi^2}\left(\frac{1}{C_L^3}+\frac{2}{C_T^3}\right)\int_0^{\omega_D}\omega^2 d\omega \\ &= \frac{V}{2\pi^2}\left(\frac{1}{C_L^3}+\frac{2}{C_T^3}\right)\frac{1}{3}\omega_D^3, \end{aligned} \tag{4.21}$$

or

$$\boxed{\frac{V}{2\pi^2}\left(\frac{1}{C_L^3}+\frac{2}{C_T^3}\right)\omega_D^3 = 9rN.} \tag{4.22}$$

4.5 THERMAL ENERGY OF A HARMONIC OSCILLATOR.

Reading: [1] ch. 23.

We talk about branches of the (LA, TA, ...) of the dispersion $\omega(\mathbf{q})$ at discrete $\mathbf{q}'s$.

The thermal occupancy is given by the Boltzman distribution

$$P_n = \frac{e^{-E_n/k_B T}}{\sum_{n=0}^{\infty} e^{-E_n/k_B T}}, \tag{4.23}$$

where the denominator

$$Z = \sum_{n=0}^{\infty} e^{-E_n/k_B T}, \tag{4.24}$$

is a normalization sum so that

$$\sum_{n=0}^{\infty} P_n = 1. \tag{4.25}$$

For the harmonic oscillator, we have

$$E_n = \left(n + \frac{1}{2}\right) \hbar\omega, \tag{4.26}$$

so that

$$\begin{aligned} Z &= \sum_{n=0}^{\infty} e^{-\left(n+\frac{1}{2}\right)\hbar\omega/k_B T} \\ &= e^{-\hbar\omega/2k_B T} \sum_{n=0}^{\infty} \left(e^{-\hbar\omega/k_B T}\right)^n \\ &= \frac{e^{-\frac{1}{2}\hbar\omega/k_B T}}{1 - e^{-\hbar\omega/k_B T}}. \end{aligned} \tag{4.27}$$

The average thermal energy

$$\begin{aligned} \mathcal{E}(\omega_q T) &= \langle E_n \rangle \\ &= \sum_n E_n P_n \\ &= \frac{\sum_n E_n e^{-E_n/k_B T}}{\sum_n e^{-E_n/k_B T}} \\ &= \frac{1}{Z}\left(-\frac{d}{d(1/k_B T)} Z\right) \\ &= -\frac{d}{d(1/k_B T)} \ln Z \\ &= -\frac{d}{d(1/k_B T)} \left(\ln\left(e^{-\frac{1}{2}\hbar\omega/k_B T}\right) - \ln\left(1 - e^{-\hbar\omega/k_B T}\right)\right) \\ &= \frac{d}{d(1/k_B T)} \left(\frac{1}{2}\hbar\omega/k_B T + \ln\left(1 - e^{-\hbar\omega/k_B T}\right)\right) \\ &= \frac{1}{2}\hbar\omega + \frac{1}{1 - e^{-\hbar\omega/k_B T}} \left(-e^{-\hbar\omega/k_B T}\right)(-\hbar\omega), \end{aligned} \tag{4.28}$$

or

$$\boxed{\mathcal{E}(\omega_q T) = \hbar\omega\left(\frac{1}{2} + \frac{1}{e^{\hbar\omega/k_B T} - 1}\right).} \tag{4.29}$$

Here

$$\frac{1}{e^{\hbar\omega/k_B T} - 1} = \langle n \rangle_T, \tag{4.30}$$

the Bose distribution. In the $k_B T \gg \hbar\omega$ we have

$$\begin{aligned}\mathcal{E}(\omega_q T) &\approx \frac{\hbar\omega}{2} + \frac{\hbar\omega}{\cancel{1} + \hbar\omega/k_B T - \cancel{1}} \\ &\approx \underbrace{\boxed{\frac{\hbar\cancel{\omega}}{\cancel{2}}}}_{\text{small}} + k_B T.\end{aligned} \tag{4.31}$$

Our $\hbar$ is "gone". This is the classical limit. This is called the equipartition where we have $\frac{1}{2}k_B T$ of kinetic energy and $\frac{1}{2}k_B T$ of potential energy.

On the other hand in the $k_B T \ll \hbar\omega$ we have

$$\mathcal{E}(\omega_q T) \approx \frac{\hbar\omega}{2} + \hbar\omega e^{-\hbar\omega/k_B T}. \tag{4.32}$$

These limits are plotted in fig. 4.12, and fig. 4.13.

4.6 LATTICE SPECIFIC HEAT CAPACITY.

Reading: [1] ch. 22,23. Define $C_V(T)$ or $C_P(T)$ as the change in the energy $U(T)$ per unit change in T.

- $C_V(T)$, is a measure at constant volume (easy to calculate).
- $C_P(T)$, is a measure at constant pressure (easy to measure).

$$C_V(T) = \left(\frac{\partial U}{\partial T}\right)_V. \tag{4.33}$$

$$U(T) = \sum_q \mathcal{E}(\omega_q, T) = \frac{1}{V}\int_0^\infty Z(\omega)\mathcal{E}(\omega_q, T)d\omega. \tag{4.34}$$

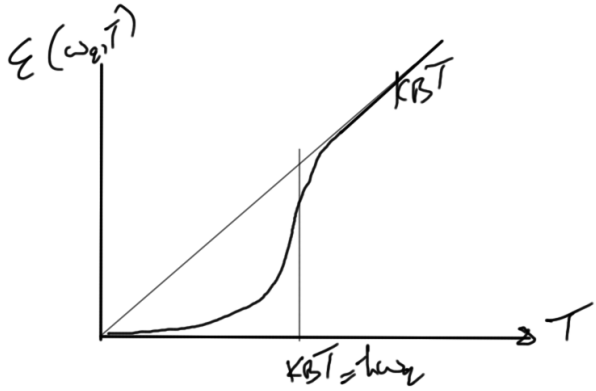

Figure 4.12: Average energy vs temperature.

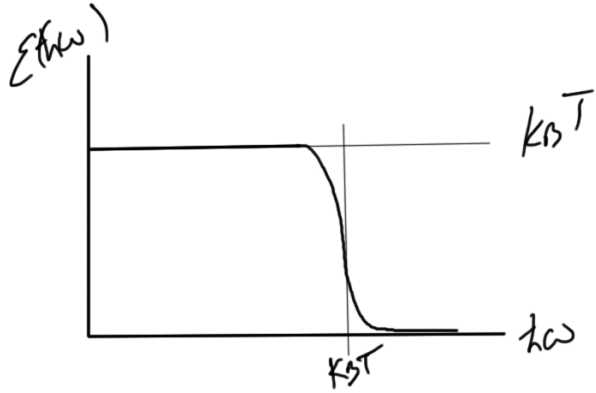

Figure 4.13: Average energy vs frequency.

In the Debye model we found in eq. (4.18) and eq. (4.22) that

$$Z(\omega)d\omega = \frac{V}{2\pi^2}\left(\frac{1}{C_{\mathrm{L}}^3}+\frac{2}{C_{\mathrm{T}}^3}\right)\omega^2 d\omega, \tag{4.35a}$$

$$\frac{V}{2\pi^2}\left(\frac{1}{C_{\mathrm{L}}^3}+\frac{2}{C_{\mathrm{T}}^3}\right)\omega_{\mathrm{D}}^3 = 9rN. \tag{4.35b}$$

so the specific heat for the Debye model is

$$\begin{aligned} C_{\mathrm{V}}(T) &= \frac{d}{dT}\int_0^{\omega_{\mathrm{D}}} \mathcal{E}(\omega,T)Z(\omega)d\omega \\ &= \frac{1}{2\pi^2}\left(\frac{1}{C_{\mathrm{L}}^3}+\frac{2}{C_{\mathrm{T}}^3}\right)\int_0^{\omega_{\mathrm{D}}} \omega^2 \frac{d}{dT}\mathcal{E}(\omega,T)d\omega \\ &= \frac{9rN}{V}\frac{1}{\omega_{\mathrm{D}}^3}\frac{d}{dT}\int_0^{\omega_{\mathrm{D}}} \hbar\omega^3\left(\frac{1}{2}+\frac{1}{e^{\hbar\omega/k_{\mathrm{B}}T}-1}\right)d\omega. \end{aligned} \tag{4.36}$$

where r is the number of atoms in the unit cell. In the limit $k_{\mathrm{B}}T \gg \hbar\omega_{\mathrm{D}}$, we have

$$\begin{aligned} C_{\mathrm{V}}(T) &= \frac{9rN}{V}\frac{1}{\omega_{\mathrm{D}}^3}\frac{d}{dT}\int_0^{\omega_{\mathrm{D}}} \cancel{\hbar}\omega^3 \frac{k_{\mathrm{B}}T}{\cancel{\hbar\omega}}d\omega \\ &= \frac{9rN}{V}\frac{1}{\omega_{\mathrm{D}}^3}\frac{d}{dT}\frac{1}{3}k_{\mathrm{B}}T\omega_{\mathrm{D}}^3 \end{aligned}$$

number of dynamical degrees of freedom per unit volume (4.37)

$$= \boxed{\frac{3rN}{V}}k_{\mathrm{B}}$$

$= k_{\mathrm{B}}$ per degree of freedom,

so that

$$U \sim k_{\mathrm{B}}T \text{ per degree of freedom.} \tag{4.38}$$

This is called the Dulong-Petit law.

More generally.

$$\begin{aligned} C_{\mathrm{V}}(T) &= \left(\frac{9rN}{V}\frac{1}{\omega_{\mathrm{D}}^3}\right)\frac{d}{dT}\int_0^{\omega_{\mathrm{D}}} \hbar\omega^3\left(\frac{1}{2}+\frac{1}{e^{\hbar\omega/k_{\mathrm{B}}T}-1}\right)d\omega \\ &= \left(\frac{9rN}{V}\frac{1}{\omega_{\mathrm{D}}^3}\right)\int_0^{\omega_{\mathrm{D}}} -\hbar\omega^3\frac{1}{\left(e^{\hbar\omega/k_{\mathrm{B}}T}-1\right)^2}e^{\hbar\omega/k_{\mathrm{B}}T}\left(-\frac{\hbar\omega}{k_{\mathrm{B}}T^2}\right)d\omega. \end{aligned}$$

(4.39)

Make substitutions

$$y = \frac{\hbar\omega}{k_B T} \tag{4.40a}$$

$$d\omega = \frac{k_B T}{\hbar} dy \tag{4.40b}$$

Debye temp

$$k_B\Theta = \hbar\omega_D. \tag{4.40c}$$

The integral limit is

$$y(\omega_D) = \frac{\hbar\omega_D}{k_B T} = \frac{k_B\Theta}{k_B T} = \frac{\Theta}{T}, \tag{4.41}$$

so the specific heat is

$$\begin{aligned} C_V(T) &= \left(\frac{9rN}{V}\frac{1}{\omega_D^3}\right)\int_0^{\Theta/T} \frac{(k_B T y)^3}{\hbar^2}\frac{1}{(e^y-1)^2}e^y \frac{y}{T}\frac{k_B T}{\hbar}dy \\ &= \left(\frac{9rN}{V}\frac{1}{\omega_D^3}\right)\frac{k_B^4 T^3}{\hbar^3}\int_0^{\Theta/T}\frac{y^4 e^y}{(e^y-1)^2}dy. \end{aligned} \tag{4.42}$$

This is an exact result for the Debye model.

In the $T \to 0$ limit where Θ/T is large, and when y is large

$$\frac{y^4 e^y}{(e^y-1)^2} \sim y^4 e^{-y} \to 0. \tag{4.43}$$

Modes are frozen out.

In the $T \ll \hbar\omega_D/k_B$ limit, we have

$$\begin{aligned} C_V(T) &= \frac{9rN}{V}\frac{k_B^4 T^3}{k_B^3\Theta^3}\int_0^\infty \frac{y^4 e^y}{(e^y-1)^2}dy \\ &= \frac{9rN}{V}\frac{k_B^4 T^3}{k_B^3\Theta^3}\frac{4\pi^2}{15} \\ &= \frac{3rN}{V}\frac{4\pi^2 k_B}{5}\frac{T^3}{\Theta^3}. \end{aligned} \tag{4.44}$$

The T^3 dependence here is very important. This comes from

- Boltzman distribution,
- Quantum mechanics
- linear dispersion relation. This provides the number of thermally occupied modes $\propto T^3$

With $\omega \propto q$, the volume of thermally occupied q space $\propto T^3$ and the energy of a thermally occupied mode = T, we have averaged energy of these modes propto

$$\begin{aligned} U(T) &\sim T^4 \\ C(T) &= T^3. \end{aligned} \tag{4.45}$$

4.7 PROBLEMS.

Exercise 4.1 Density of states of a 1D chain. (*2013 ps5 p1*)

Calculate and sketch a plot of the density of states, $Z(\omega)$, for the vibrational modes of a 1-d monatomic chain of length L, with nearest-neighbor spring constant K, atoms of mass M, and lattice constant a. Specifically, start from $\sum_q$ and by transforming this into an integral over ω, obtain $Z(\omega)$. Then draw a sketch of $Z(\omega)$ vs. ω, labeling intercepts and asymptotes.

Answer for Exercise 4.1

For the 2D and 3D ($d = 2, 3$) density of states we'd consider solutions for $Z(\omega)$ of

$$\int Z(\omega) d\omega = \left(\frac{L}{2\pi}\right)^d \int \frac{d\mathbf{f}_\omega}{\left|\boldsymbol{\nabla}_{\mathbf{q}} \omega(q)\right|} d\omega. \tag{4.46}$$

Should we wish to extend this down to $d = 1$ we'd have to figure out how to interpret $d\mathbf{f}_\omega$. In 2D and 3D that was a surface area element, a factor of the differential form $d^d\mathbf{q} = d\mathbf{f}_\omega d\omega_\perp$. In 3D we had $\int d\mathbf{f}_\omega = 4\pi q^2 = d/dq(4\pi q^3/3)$, and for 2D $\int d\mathbf{f}_\omega = 2\pi q = d/dq(\pi q^2)$.

Those 3D and 2D "volumes" (differentiated to obtain the "area" when q of the surface for q held constant) can be obtained by these respective integrals

$$\int_{x^2+y^2+z^2 \le q^2} dx dy dz = \frac{4}{3}\pi q^3 \tag{4.47a}$$

$$\int_{x^2+y^2\leq q^2} dxdy = \pi q^2. \tag{4.47b}$$

We can generalize this down to a single dimension by considering

$$\int_{x^2\leq q^2} dx = 2q. \tag{4.48}$$

for which we could conceivably consider the area of this 1D surface to be the constant 2. However, does this even make sense, since writing $dq = df_\omega dq_\perp$ would split our 1-form into the product of two 1-forms, which isn't a sensible operation? Let's step back and consider the density of states definition from scratch.

Starting from scratch We wish to sum over all the integer values n, subject to a period constraint $2\pi n = qL$, and employ an integral approximation to this sum.

$$\begin{aligned}\sum_n \sim \int dn &= \frac{L}{2\pi}\int dq \\ &= \frac{L}{2\pi}\int \frac{dq}{d\omega}d\omega \\ &\equiv \int Z(\omega)d\omega.\end{aligned} \tag{4.49}$$

From this we find for one dimension

$$Z(\omega) = \frac{L}{2\pi}\frac{dq}{d\omega}. \tag{4.50}$$

Now we are ready to start. For the 1D chain we had

$$\sqrt{\frac{M}{K}}\omega(q) = 2\sin\left(\frac{qa}{2}\right), \tag{4.51}$$

so

$$\sqrt{\frac{M}{K}} = a\cos\left(\frac{qa}{2}\right)\frac{dq}{d\omega}, \tag{4.52}$$

or

$$\begin{aligned} Z(\omega) &= \frac{L}{2\pi}\frac{\sqrt{\frac{M}{K}}}{a\cos\left(\frac{qa}{2}\right)} \\ &= \sqrt{\frac{M}{K}}\frac{L}{2\pi a}\frac{1}{\cos\left(\frac{qa}{2}\right)} \\ &= \sqrt{\frac{M}{K}}\frac{L}{2\pi a}\frac{1}{\cos\sin^{-1}\left(\frac{1}{2}\sqrt{\frac{M}{K}}\omega\right)} \\ &= \frac{1}{2}\sqrt{\frac{M}{K}}\frac{L}{\pi a}\frac{1}{\sqrt{1-\frac{1}{4}\frac{M}{K}\omega^2}}. \end{aligned} \tag{4.53}$$

With $L = Na$, this is

$$\boxed{Z(\omega) = \frac{1}{2}\sqrt{\frac{M}{K}}\frac{N}{\pi}\frac{1}{\sqrt{1-\frac{1}{4}\frac{M}{K}\omega^2}}.} \tag{4.54}$$

This has a minimum at $\omega = 0$, and in that neighborhood is approximately parabolic function

$$\begin{aligned} Z(\omega \approx 0) &= \frac{1}{2}\sqrt{\frac{M}{K}}\frac{N}{\pi}\left(1-\left(-\frac{1}{2}\right)\frac{1}{4}\frac{M}{K}\omega^2\right) \\ &= \frac{1}{2}\sqrt{\frac{M}{K}}\frac{N}{\pi}\left(1+\frac{1}{8}\frac{M}{K}\omega^2\right). \end{aligned} \tag{4.55}$$

As $\omega \to \pm\sqrt{4K/M}$, the density of states approaches vertical asymptotes $Z(\omega) \to \infty$. Observe that these extremes are the edges of the Brillouin zone where $qa/2 = \pm\pi/2$. For $Z(\omega)$ to be useful for probability calculations, we expect that the integral over this first Brillouin zone will be finite, despite these infinite asymptotes. Let's verify this

$$\begin{aligned} \int_{-\sqrt{4K/M}}^{\sqrt{4K/M}} Z(\omega)d\omega &= \frac{1}{2}\sqrt{\frac{M}{K}}\frac{N}{\pi}\int_{-1}^{1}\sqrt{\frac{4K}{M}}dx\frac{1}{\sqrt{1-x^2}} \\ &= \frac{N}{\pi}\pi \\ &= N. \end{aligned} \tag{4.56}$$

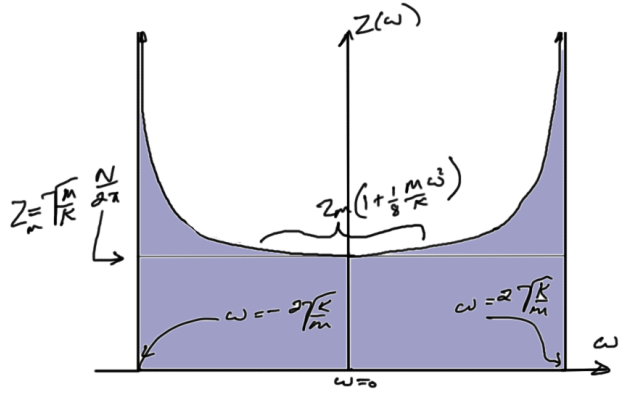

Figure 4.14: 1D density of states for Harmonic chain.

Good, the area under the curve is finite as expected. This curve is sketched in fig. 4.14.

Exercise 4.2 Trends in Debye temperature. (*2013 ps5 p2*)

Table 5.1 on page 120 of Ibach and Luth shows the Debye temperature for various solids. Discuss and explain any trends that you see in the Debye temperature, e.g. as a function of location in the periodic table, bonding type, or atomic mass.

Answer for Exercise 4.2

A plot of Debye temperatures by atomic number can be found in fig. 4.15. This is based on data from [12], and [10]

Some observed trends

- There is a general trend of decreasing Debye temperature with atomic number.
- Lowest Debye temperatures are often at points where we have completely filled or half filled orbitals: H ($1s^1$), Ne ($1s^2 2s^2 1p^6$), Eu($[Xe]4f^7$), Yb ($[Xe]4f^{14}$), Hg ($[Xe]4f^{14}5d^{10}6s^2$).
- We see peak temperatures around elements that are near the middles of their respective orbital filling ranges: C, Si (p block elements), Cr, Ru, Os (d-block elements). Carbon in

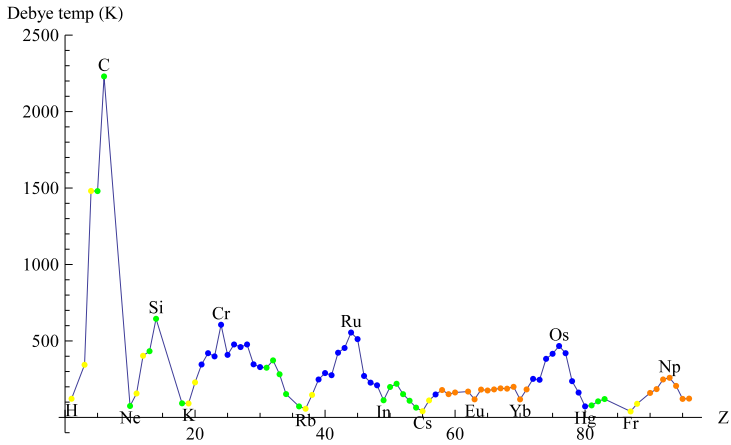

Figure 4.15: Debye temperature vs atomic number.

its diamond form is plotted above (its graphite form comes in much lower at 420K).

Comments The capability of the element for making strong bonds appears to contribute significantly to high Debye temperatures. In particular observe that the diamond form of C, with its strong highly directional covalent bonds, has the highest Debye temperature. Si also in the p block with 4 available p orbital slots has a very high Debye temperature, at least compared to its period table neighbors. The converse is also evident, since we see lack of bonding capability associated with low Debye temperatures for those elements that have completely and half filled orbitals, which have some stability in isolation. This is similar to the previously observed low melting points (a measure of ease of lattice breakup) for elements that have half and completely filled orbitals.

Recall that the Debye frequency (proportional to the Debye temperature) had the form

$$\omega_D \propto \left(\frac{N}{V}\right)^{1/3}. \tag{4.57}$$

Based on this, we expect to see small Debye temperatures when the number density is low, which should occur when the atomic radii is large. That can be observed in fig. 4.16, looking for example at K, Rb, and Cs, that are positioned at local maximums for atomic

radii, in contrast to the local minimums observed for the Debye temperature.

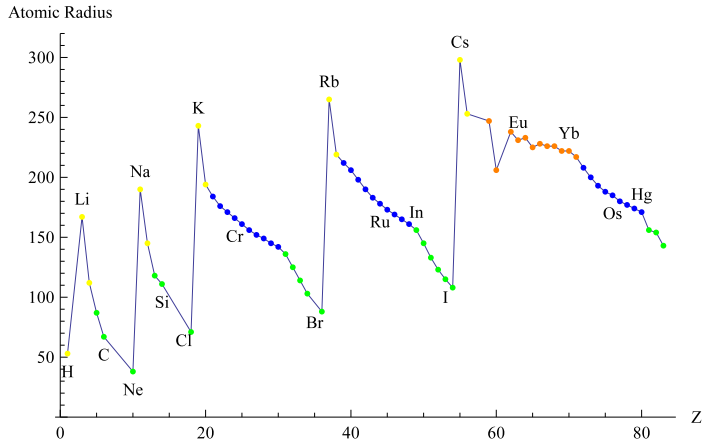

Figure 4.16: Atomic radii.

This plot has some confusing aspects as-is since I didn't label all the elements, just the ones that I wanted to compare to the Debye temperatures (if you look carefully the labels for Cl, Br, I are shifted to the left slightly). It also appears that I didn't explicitly plot those elements for which I didn't have Debye temperature data, which makes it even more misleading if looking at just the radius periodicity.

In fig. 4.17 is a combined plot of both the atomic radius and the Debye temperature. In this second plot we see that, yes, the largest radii are those with the smallest Debye temperatures. As the radius drops from the peak, the Debye temperature increases. However, part way towards the middle of the period, this inverse relationship starts to fail. In fact, they both start trending downwards at these points. Is this where the velocities of the acoustic modes, also variables in the Debye temperatures, start to factor into the mix?

As a final plot, let's look at the inverse of the atomic radius and the Debye temperature together. This is plotted in fig. 4.18.

Exercise 4.3 Debye calculation in 2D. (*2013 ps5 p3*)

Repeat the Debye theory calculation that we did in class, but for a two-dimensional lattice. Assume (quite artificially) that the

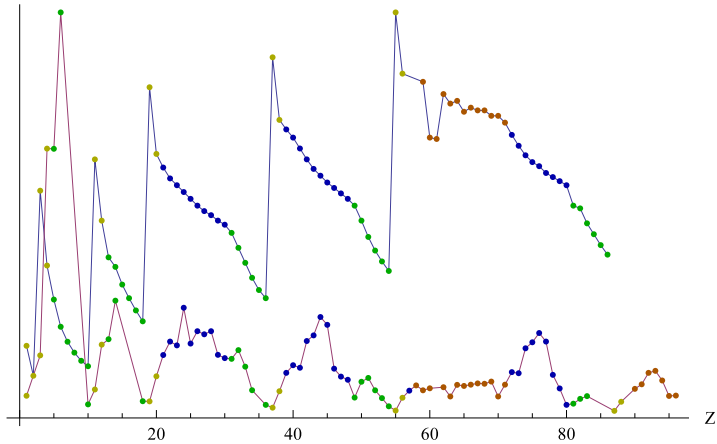

Figure 4.17: Debye and atomic radius.

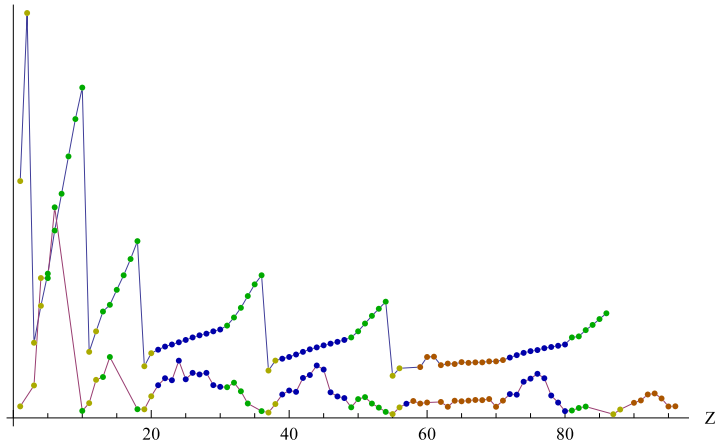

Figure 4.18: Inverse Atomic Radius and Debye temperature.

atoms are free to move only within the plane, so that there are $2rN$ degrees of freedom, and there is only one transverse acoustic phonon mode, instead of two as in the three-dimensional calculation.

Show that the low temperature limit of the specific heat at constant area, per unit area, is:

$$C_A(T) = 7.213\,\frac{4rN}{A}\,k_B\,\frac{T^2}{\Theta^2},$$

where A is the area of the crystal, rN is the number of atoms in the crystal, Θ is defined by $k_B\Theta = \hbar\omega_D$, and

$$\int_0^\infty \frac{y^3 e^y}{(e^y-1)^2}\,dy \simeq 7.213.$$

Answer for Exercise 4.3

We first setup the 2D density of states construction as we did for 3D, also employing the periodic relations

$$\begin{aligned} 2\pi n_x &= L_x q_x \\ 2\pi n_y &= L_y q_y, \end{aligned} \tag{4.58}$$

so that a sum over the quantum numbers $\mathbf{n}$ can be approximated as

$$\begin{aligned} \sum_{\mathbf{n}} &\approx \int dn_x dn_y \\ &= \frac{A}{(2\pi)^2}\int d^2\mathbf{q} \\ &= \frac{A}{(2\pi)^2}\int df_\omega dq_\perp \\ &= \frac{A}{(2\pi)^2}\int \frac{df_\omega}{|\boldsymbol{\nabla}_{\mathbf{q}}\omega(\mathbf{q})|}d\omega \\ &= \int Z(\omega)d\omega. \end{aligned} \tag{4.59}$$

This Debye model we have

$$\omega = \begin{cases} C_L q & \text{longitudinal acoustic} \\ C_T q & \text{transverse acoustic} \end{cases} \tag{4.60}$$

This gives

$$\int Z(\omega)d\omega = \sum_{LA,TA} \frac{A}{(2\pi)^2} \int \frac{df_\omega}{\left|\boldsymbol{\nabla}_{\mathbf{q}}\omega(\mathbf{q})\right|} d\omega$$

$$= \frac{A}{(2\pi)^2} \int \sum_{LA,TA} \frac{df_\omega}{\frac{d\omega}{dq}} d\omega \qquad (q \text{ space surface "area" element})$$

$$= \int df_\omega$$

$$= \int \frac{A}{(2\pi)^2} \left(\frac{1}{C_L} + \frac{1}{C_T}\right) 2\pi q \, d\omega \qquad (4.61)$$

$$= \int \frac{A}{2\pi} \left(\frac{q}{C_L} + \frac{q}{C_T}\right) d\omega$$

$$= \int \frac{A}{2\pi} \left(\frac{1}{C_L^2} + \frac{1}{C_T^2}\right) \omega d\omega,$$

or

$$Z(\omega) = \frac{A}{2\pi} \left(\frac{1}{C_L^2} + \frac{1}{C_T^2}\right) \omega. \qquad (4.62)$$

Define the Debye frequency ω_D by

$$\int_0^{\omega_D} Z(\omega)d\omega = 2rN. \qquad (4.63)$$

$$\begin{aligned} 2rN &= \frac{A}{2\pi} \left(\frac{1}{C_L^2} + \frac{1}{C_T^2}\right) \int_0^{\omega_D} \omega d\omega \\ &= \frac{A}{2\pi} \left(\frac{1}{C_L^2} + \frac{1}{C_T^2}\right) \frac{1}{2}\omega_D^2, \end{aligned} \qquad (4.64)$$

or

$$\frac{A}{2\pi} \left(\frac{1}{C_L^2} + \frac{1}{C_T^2}\right) \omega_D^2 = 4rN. \qquad (4.65)$$

Inserting this Debye frequency into the density of states gives

$$Z(\omega) = \frac{4rN\omega}{\omega_D^2}. \qquad (4.66)$$

We can now start the specific heat calculation

$$\begin{aligned} C_A(T) &= \frac{dU}{dT} \\ &= \frac{d}{dT}\frac{1}{A}\int_0^{\omega_D} \mathcal{E}(\omega,T)Z(\omega)d\omega \\ &= \frac{4rN}{A\omega_D^2}\int_0^{\omega_D} \frac{d}{dT}\mathcal{E}(\omega,T)\omega d\omega \\ &= \frac{4rN}{A\omega_D^2}\frac{d}{dT}\int_0^{\omega_D} \hbar\omega\left(\frac{1}{2}+\frac{1}{e^{\hbar\omega/k_BT}-1}\right)\omega d\omega \\ &= \frac{4rN}{A\omega_D^2}\int_0^{\omega_D} -\hbar\omega^2\frac{1}{\left(e^{\hbar\omega/k_BT}-1\right)^2}e^{\hbar\omega/k_BT}\left(-\frac{\hbar\omega}{k_BT^2}\right)d\omega \\ &= \frac{4rN}{A\omega_D^2}\int_0^{\omega_D} k_B^2T\frac{\hbar^2\omega^3}{k_B^3T^3}\frac{1}{\left(e^{\hbar\omega/k_BT}-1\right)^2}e^{\hbar\omega/k_BT}d\omega. \end{aligned} \tag{4.67}$$

As in class we make substitutions

$$y = \frac{\hbar\omega}{k_BT} \tag{4.68a}$$

$$d\omega = \frac{k_BT}{\hbar}dy \tag{4.68b}$$

$$y(\omega_D) = \frac{\hbar\omega_D}{k_BT} = \frac{k_B\Theta}{k_BT} = \frac{\Theta}{T}. \tag{4.68c}$$

Inserting these we have

$$\begin{aligned} C_A(T) &= \frac{4rN}{A\omega_D^2}\frac{k_B^3T^2}{\hbar^2}\int_0^{\Theta/T}\frac{y^3e^ydy}{\left(e^y-1\right)^2} \\ &= \frac{4rNk_BT^2}{A\Theta^2}\int_0^{\Theta/T}\frac{y^3e^ydy}{\left(e^y-1\right)^2}. \end{aligned} \tag{4.69}$$

In the $k_BT \ll \hbar\omega_D = k_B\Theta$ limit where the integrand is small, the integral limit can be approximated by extension to ∞. This produces the desired result

$$C_A(T) = 7.213\frac{4rN}{A}k_B\frac{T^2}{\Theta^2}. \tag{4.70}$$

Exercise 4.4 Quadratic Debye phonons. (*2013 midterm pr B2*)

Assume a quadratic dispersion relation for the longitudinal and transverse modes

$$\omega = \begin{cases} b_L q^2 \\ b_T q^2 \end{cases} . \tag{4.71}$$

a. Find the density of states.
b. Find the Debye frequency.
c. In terms of $k_B\Theta = \hbar\omega_D$, and

$$\mathcal{I} = \int_0^\infty \frac{y^{5/2} e^y dy}{(e^y - 1)^2}, \tag{4.72}$$

find the specific heat for $k_B T \ll \hbar\omega_D$.
d. Find the specific heat for $k_B T \gg \hbar\omega_D$.

Answer for Exercise 4.4

Part a. Working straight from the definition

$$\begin{aligned} Z(\omega) &= \frac{V}{(2\pi)^3} \sum_{L,T} \int \frac{df_\omega}{|\boldsymbol{\nabla}_{\mathbf{q}}\omega|} \\ &= \frac{V}{(2\pi)^3} \left(\frac{4\pi q^2}{2b_L q}\bigg|_L + \frac{2 \times 4\pi q^2}{2b_T q}\bigg|_T \right) \\ &= \frac{V}{4\pi^2} \left(\frac{q_L}{b_L} + \frac{2q_T}{b_T} \right) . \end{aligned} \tag{4.73}$$

With $q_L = \sqrt{\omega/b_L}$ and $q_T = \sqrt{\omega/b_T}$, this is

$$Z(\omega) = \frac{V}{4\pi^2} \left(\frac{1}{b_L^{3/2}} + \frac{2}{b_T^{3/2}} \right) \sqrt{\omega}. \tag{4.74}$$

Part b. The Debye frequency was given implicitly by

$$\int_0^{\omega_D} Z(\omega) d\omega = 3rN, \tag{4.75}$$

which gives

$$\begin{aligned} 3rN &= \frac{2}{3}\frac{V}{4\pi^2}\left(\frac{1}{b_{\mathrm{L}}^{3/2}}+\frac{2}{b_{\mathrm{T}}^{3/2}}\right)\omega_{\mathrm{D}}^{3/2} \\ &= \frac{V}{6\pi^2}\left(\frac{1}{b_{\mathrm{L}}^{3/2}}+\frac{2}{b_{\mathrm{T}}^{3/2}}\right)\omega_{\mathrm{D}}^{3/2}. \end{aligned} \tag{4.76}$$

Part c. Assuming a Bose distribution and ignoring the zero point energy, which has no temperature dependence, the specific heat, the temperature derivative of the energy density, is

$$\begin{aligned} C_{\mathrm{V}} &= \frac{d}{dT}\frac{1}{V}\int Z(\omega)\frac{\hbar\omega}{e^{\hbar\omega/k_{\mathrm{B}}T}-1}d\omega \\ &= \frac{1}{V}\frac{d}{dT}\int Z(\omega)\frac{\hbar\omega}{\hbar\omega/k_{\mathrm{B}}T+\frac{1}{2}(\hbar\omega/k_{\mathrm{B}}T)^2+\cdots}d\omega \\ &\approx \frac{1}{V}\frac{d}{dT}\int Z(\omega)k_{\mathrm{B}}T d\omega \\ &= \frac{1}{V}k_{\mathrm{B}}3rN. \end{aligned} \tag{4.77}$$

Part d. First note that the density of states can be written

$$Z(\omega) = \frac{9rN}{2\omega_{\mathrm{D}}^{3/2}}\omega^{1/2}, \tag{4.78}$$

for a specific heat of

$$
\begin{aligned}
C_V &= \frac{d}{dT}\frac{1}{V}\int_0^\infty \frac{9rN}{2\omega_D^{3/2}}\omega^{1/2}\frac{\hbar\omega}{e^{\hbar\omega/k_BT}-1}d\omega \\
&= \frac{9rN}{2V\omega_D^{3/2}}\int_0^\infty d\omega\omega^{1/2}\frac{d}{dT}\frac{\hbar\omega}{e^{\hbar\omega/k_BT}-1} \\
&= \frac{9rN}{2V\omega_D^{3/2}}\int_0^\infty d\omega\omega^{1/2}\frac{-\hbar\omega}{\left(e^{\hbar\omega/k_BT}-1\right)^2}e^{\hbar\omega/k_BT}\hbar\omega/k_B\left(-\frac{1}{T^2}\right) \\
&= \frac{9rNk_B}{2V\omega_D^{3/2}}\left(\frac{k_BT}{\hbar}\right)^{3/2} \\
&\qquad \int_0^\infty d\frac{\hbar\omega}{k_BT}\left(\frac{\hbar\omega}{k_BT}\right)^{1/2}\frac{1}{\left(e^{\hbar\omega/k_BT}-1\right)^2}e^{\hbar\omega/k_BT}\left(\frac{\hbar\omega}{k_BT}\right)^2 \\
&= \frac{9rNk_B}{2V\omega_D^{3/2}}\left(\frac{k_BT}{\hbar}\right)^{3/2}\int_0^\infty dy\frac{y^{5/2}e^y}{(e^y-1)^2} \\
&= \frac{9rNk_B}{2V}\left(\frac{T}{\Theta}\right)^{3/2}\mathcal{I}.
\end{aligned}
\tag{4.79}
$$

5 FREE ELECTRON MODEL.

5.1 FREE ELECTRON MODEL OF METALS.

Reading: [10] ch. 6.

We will treat electrons as a gas of free Fermions, a statistical mechanical approach.

Some characteristics of metals that we intuitively understand (i.e. should you ask a 3rd grader)

- Shiny.
- Cold to the touch in cold, or hot if warmed.
- Can bend and hammer it (malleability).
- Can use as a wire (conduct electricity)

Metallic bonding, the sharing of valence electrons with many neighbors, is the fundamental property that we rely on to make our free electron gas model. We can justify this by reflecting on the overlap of the d orbital electrons in a metal. These often have a radial wave function magnitude as illustrated in fig. 5.1.

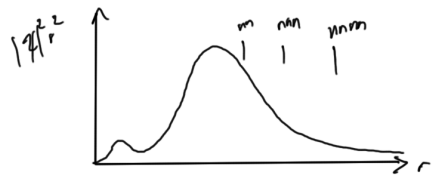

Figure 5.1: Rough sketch of d orbital radial magnitude.

We can justify our treatment of electrons as a gas by noting that we have significant overlap of these orbitals over many sites in the metallic lattice as in fig. 5.2.

- electrons must be treated quantum mechanically

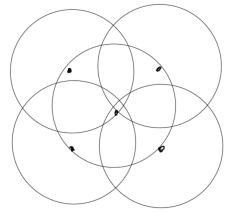

Figure 5.2: Overlapping d orbital wavefunctions.

- periodic lattice complicates things. We'll attempt to ignore that.

We try the simple jellium model, where we "smear" out the positive ions to a uniform background as in the typical 2nd year particle in an infinite potential box problem, as illustrated in fig. 5.3.

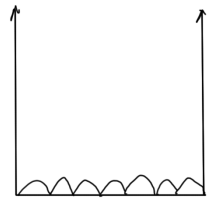

Figure 5.3: One dimensional particle in a box.

where we had solutions like those of fig. 5.4.

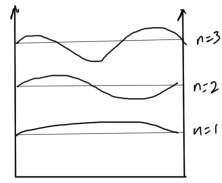

Figure 5.4: First few solutions for particle in a 1D box.

The difference is that we will consider the 3D generalization of this problem, where the potentials are infinite outside of a cubic space as in fig. 5.5.

The free electron in an infinite 3D

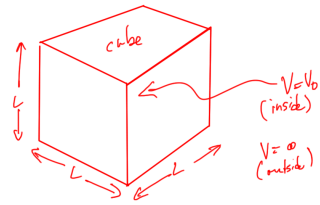

Figure 5.5: 3D particle in a box.

solve for 1 electron

$$-\frac{\hbar^2}{2m}\nabla^2\Psi(\mathbf{r}) + V(\mathbf{r})\Psi(\mathbf{r}) = E\Psi(\mathbf{r}), \tag{5.1}$$

where

$$V(\mathbf{r}) = \begin{cases} V_\circ & \text{inside cube} \\ \infty & \text{outside} \end{cases} \tag{5.2}$$

This implies a boundary condition $\Psi(\mathbf{r}) = 0$ outside of the box. Using separation of variables

$$E = -E' - V_\circ$$

$$-\frac{\hbar^2}{2m}\left(\frac{\partial^2}{\partial x^2} + \frac{\partial^2}{\partial y^2} + \frac{\partial^2}{\partial z^2}\right)\Psi_x(x)\Psi_y(y)\Psi_z(z) = \boxed{E}\Psi_x(x)\Psi_y(y)\Psi_z(z), \tag{5.3}$$

i.e. $\Psi(\mathbf{r})$ is separable.

This is a set of equations of the form

$$-\frac{\hbar^2}{2m}\frac{\partial^2\Psi_x(x)}{\partial x^2} = E_x\Psi_x(x), \tag{5.4}$$

where

$$\Psi_x(0) = \Psi_x(L) = 0. \tag{5.5}$$

Our solution is

$$\Psi(x) = N\sin(k_x x), \tag{5.6}$$

where

$$k_x = \frac{n_x\pi}{L}. \tag{5.7}$$

In 3D this is

$$\Psi(\mathbf{r}) = \left(\frac{2}{L}\right)^{3/2} \sin(k_x x)\sin(k_y y)\sin(k_z z), \tag{5.8}$$

where

$$\begin{aligned} E(\mathbf{k}) &= \frac{\hbar}{2m}\left(k_x^2 + k_y^2 + k_z^2\right) \\ &= \frac{\hbar \mathbf{k}^2}{2m}. \end{aligned} \tag{5.9}$$

This is a parabolic dispersion, sketched in fig. 5.6.

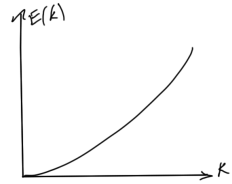

Figure 5.6: Parabolic energy dispersion.

This is

$$\begin{aligned} k_x &= \frac{n_x \pi}{L} \\ k_y &= \frac{n_y \pi}{L} \\ k_z &= \frac{n_z \pi}{L}. \end{aligned} \tag{5.10}$$

We'll one to consider the volume per k point, as roughly sketched in fig. 5.7.

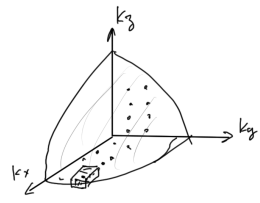

Figure 5.7: Volume per k point.

$$\left(\frac{\pi}{L}\right)^3 = \frac{\pi^3}{V}. \tag{5.11}$$

here we switch notations and use V for volume, and not V as potential.

Density of states As with the phonon, properties are calculated via k space sums using the density of states.

$$\begin{aligned}\sum_{k_x,k_y,k_z,\text{spin}} &\to \sum_{\text{spin}} \int \frac{d^3\mathbf{k}}{(\pi/L)^3} \\ &\quad \text{1 octant} \\ &= \boxed{2}\frac{V}{\pi^3}\int \boxed{\frac{1}{8}} 4\pi k^2 dk \\ &\quad \text{spin, 2 states per k point} \\ &= \frac{V}{\pi^2}\int k^2 dk,\end{aligned} \tag{5.12}$$

where $\to$ represents a quasi continuous approximation. Now turn this into $\int dE$ as with phonons, using

$$E = \frac{\hbar^2 k^2}{2m}, \tag{5.13}$$

so that

$$dE = \frac{\hbar^2 k}{m} dk. \tag{5.14}$$

This gives

$$\begin{aligned}k^2 dk &= \sqrt{\frac{2mE}{\hbar^2}}\frac{m}{\hbar^2}dE \\ &= \frac{1}{2}\left(\frac{2m}{\hbar^2}\right)^{3/2}\sqrt{E}dE,\end{aligned} \tag{5.15}$$

so that

$$\begin{aligned}\sum_{k_x,k_y,k_z,\text{spin}} &\to \frac{V}{2\pi^2}\left(\frac{2m}{\hbar^2}\right)^{3/2}\int \sqrt{E}dE. \\ &\equiv V\int D(E)dE.\end{aligned} \tag{5.16}$$

The density of states per volume

$$D(E) = \frac{1}{2\pi^2}\left(\frac{2m}{\hbar^2}\right)^{3/2}\sqrt{E}. \tag{5.17}$$

This is sketched in fig. 5.8.

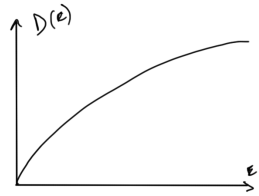

Figure 5.8: 3D density of states.

Reading: §6.2, Fermi gas at $T = 0K$.

This assumes that electrons do not interact. This is the operational definition of an ideal gas.

This may seem more drastic than it actually is. Electrons in plane wave states have constant density. This shifts potential, but is still uniform.

Note that this does break down for some interesting problems. One notable such problem is that of superconductivity, where we must consider the electron electron interactions.

Fermi energy states can only be occupied by one particle with each spin, as illustrated in fig. 5.9.

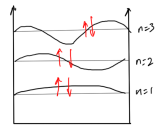

Figure 5.9: Spin packing of energy levels for 1D particle in a box.

Because we can only pack states two per point in k space, we'll consider a Fermi surface in k space as in fig. 5.10, and determine the energy level E_F and momentum k_F associated with that surface, for which no more states can be occupied. This is roughly

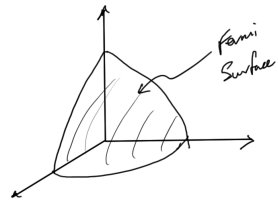

Figure 5.10: Fermi surface in momentum space.

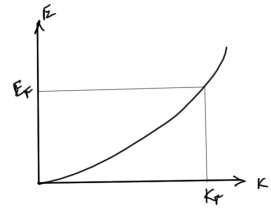

Figure 5.11: Fermi energy and momentum.

illustrated in fig. 5.11. In quasi-continuum, approximately $1/8$ of the occupied state.

k_F is the boundary between occupied and unoccupied states (Fermi wave vector).

The maximum number of these occupied states is then

$$N = 2\frac{\frac{4}{3}\pi k_F^3}{8\left(\frac{\pi}{L}\right)^3} = \frac{V}{3\pi^2}k_F^3. \tag{5.18}$$

so that

$$k_F = \left(3\pi^2 n\right)^{1/3}, \tag{5.19}$$

where

$$n \equiv \frac{N}{V}. \tag{5.20}$$

This is typically of the order $10^{10} m^{-1} = \text{Å}^{-1}$.

For reference, we get for E_F

$$\begin{aligned} E_F &= \frac{\hbar^2 k_F^2}{2m} \\ &= \frac{\hbar^2}{2m}\left(3\pi^2 n\right)^{2/3}. \end{aligned} \tag{5.21}$$

Last time We want to calculate the thermal properties of the free electron gas , characterized by energies of the form fig. 5.12. At $T = 0$, the free electron gas fills up states up to E_F

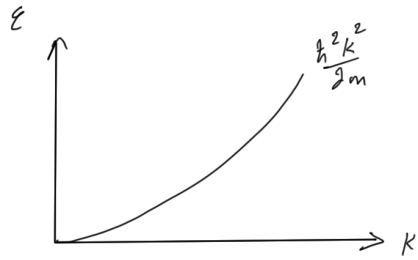

Figure 5.12: Free electron energy distribution.

5.2 FERMI DIRAC DISTRIBUTION FOR $T > 0$.

Note that we are following Einstein here, not the text.

Consider a closed system and reservoir r, as in fig. 5.13, exchanging energy and particles, with a smaller system that has energy ϵ and n particles. The total energy and number of particles are respectively U and N.

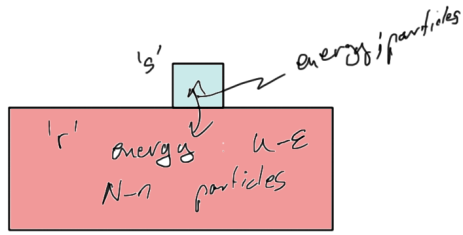

Figure 5.13: Two systems in contact.

The probability of eigenstate ϵ with n particles

$$P(\epsilon, n) \propto g_r(U - \epsilon, N - n), \tag{5.22}$$

where g_r is the number of "microstates of the reservoir when it has energy $U - \epsilon$, and $N - n$ particles. We have

$$\begin{aligned} g_r(U-\epsilon, N-n) &= e^{\ln g_r(U-\epsilon, N-n)} \\ &\approx \exp\left(\ln g_r(U,N) - \epsilon\left(\frac{\partial \ln g_r}{\partial U}\right)_N - n\left(\frac{\partial \ln g_r}{\partial N}\right)_U\right). \end{aligned} \tag{5.23}$$

Introducing the Boltzmann entropy

$$S_r = k_B \ln g_r, \tag{5.24}$$

we have (approximately)

$$P(\epsilon, n) \propto \exp\left(\ln g_r(U,N) - \frac{\epsilon}{k_B}\left(\frac{\partial S_r}{\partial U}\right)_N - \frac{n}{k_B}\left(\frac{\partial S_r}{\partial N}\right)_U\right). \tag{5.25}$$

Recall the thermodynamic relationship, which we simplify immediately, by restricting ourselves volume (and constant pressure) constraint

$$\begin{aligned} dU_r &= TdS_r - \cancel{pdV_r} + \mu dN_r, \\ &= T\left(\frac{\partial S_r}{\partial U_r}dU_r + \frac{\partial S_r}{\partial N_r}dN_r\right) + \mu dN_r. \end{aligned} \tag{5.26}$$

Taking wedge products , and noting that $dx \wedge dx = 0$, we can construct a pair of 2-forms from this

$$\cancel{dU_r \wedge dU_r} = T\left(\frac{\partial S_r}{\partial U_r}\cancel{dU_r \wedge dU_r} + \frac{\partial S_r}{\partial N_r}dN_r \wedge dU_r\right) + \mu dN_r \wedge dU_r \tag{5.27a}$$

$$dU_r \wedge dN_r = T\left(\frac{\partial S_r}{\partial U_r}dU_r \wedge dN_r + \frac{\partial S_r}{\partial N_r}\cancel{dN_r \wedge dN_r}\right) + \cancel{\mu dN_r \wedge dN_r}. \tag{5.27b}$$

Since $dy \wedge dx = -dx \wedge dy$, we can read off the factors of the 2-forms

$$\left(\frac{\partial S_r}{\partial U_r}\right)_{P,V} = \frac{1}{T} \tag{5.28a}$$

$$\left(\frac{\partial S_r}{\partial N}\right)_{P,V} = -\frac{\mu}{T}. \tag{5.28b}$$

Insertion into our probability density gives us

$$P(\epsilon, n) \propto e^{-(\epsilon-\mu n)/k_B T}. \tag{5.29}$$

This is the Boltzmann-Gibbs distribution. Normalizing we have

$$P(\epsilon, n) = \frac{e^{-(\epsilon-\mu n)/k_B T}}{\sum_n \sum_{\epsilon(n)} e^{-(\epsilon-\mu n)/k_B T}}. \tag{5.30}$$

This method is deemed old fashioned because it relies on being able to calculate the eigenstates of the system. Imagine the impossibility of this for, say, a room full of air.

It seems that we are labeling the system as having an energy eigenstate since we imagine that it can be characterized as having a single energy level.

Application to free electrons Select one energy level ($*$), fig. 5.14, as the 'system', and treat all other levels as the 'reservoir'.

Figure 5.14: Selected energy level for system.

Note that $n_i \in \{0, 1\}$ due to the Pauli exclusion principle, and $\epsilon \in \{0, \epsilon_i\}$.

$$P(\epsilon = 0, n = 0) = \frac{1}{1 + e^{-(\epsilon_i - \mu)}} \tag{5.31a}$$

$$P(\epsilon_i, n = 1) = \frac{e^{-(\epsilon_i-\mu)/k_B T}}{1 + e^{-(\epsilon_i - \mu)}}. \tag{5.31b}$$

Average occupancy

$$\langle n_i \rangle = \frac{0 \times 1 + 1 \times e^{-(\epsilon_i - \mu)/k_B T}}{1 + e^{-(\epsilon_i - \mu)/k_B T}}, \tag{5.32}$$

or

$$\boxed{\langle n_i \rangle = \frac{1}{e^{(\epsilon_i - \mu)/k_B T} + 1}.} \tag{5.33}$$

This is the Fermi-Dirac distribution, as sketched roughly in fig. 5.15.

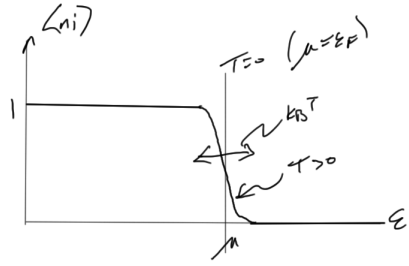

Figure 5.15: Fermi Dirac distribution.

This solved a big mystery, since the equipartition theorem says

$$U = \frac{3}{2} k_B T \times \underbrace{n}_{\text{electron density}}, \tag{5.34}$$

so that

$$C_V = \frac{\partial U}{\partial T} \sim 10^{28} \frac{\text{electrons}}{m^3} \times \frac{3}{2} k_B, \tag{5.35}$$

however the value of C_V that was measured is $1/100$ times too small. Because of the Pauli exclusion principle, most electrons are trapped far below E_F, and can't accept thermal energy.

5.3 HEAT CAPACITY OF FREE ELECTRONS.

Estimate

from F.D. distribution, number of thermally excited electrons

$$U(T) - U(0) \sim \boxed{k_B T \times D(E_F)} \times \boxed{k_B T}. \tag{5.36}$$

thermal energy per thermally excited electron

Plugging in the density of states from eq. (5.17)

$$\begin{aligned} C(T) &= \frac{dU}{dT} \\ &\sim 2k_B^2 D(E_F) T \\ &\sim 2k_B^2 \frac{1}{2\pi^2} \left(\frac{2m}{\hbar^2}\right)^{3/2} \sqrt{E_F}\, T. \end{aligned} \tag{5.37}$$

From eq. (5.21) we have

$$\begin{aligned} \sqrt{E_F} &= \frac{E_F^{3/2}}{E_F} \\ &= \frac{1}{E_F} \left(\frac{\hbar^2}{2m}\right)^{3/2} \left(\left(3\pi^2 n\right)^{2/3}\right)^{3/2} \\ &= \frac{1}{E_F} 3\pi^2 n \left(\frac{\hbar^2}{2m}\right)^{3/2}, \end{aligned} \tag{5.38}$$

so that

$$\begin{aligned} C(T) &\sim \cancel{2} k_B^2 \frac{1}{\cancel{2\pi^2}} \cancel{\left(\frac{2m}{\hbar^2}\right)^{3/2}} \frac{1}{E_F} \cancel{3\pi^2} n \cancel{\left(\frac{\hbar^2}{2m}\right)^{3/2}} T \\ &\sim 3k_B n \boxed{\frac{k_B T}{E_F}}. \end{aligned} \tag{5.39}$$

reduction from classical values

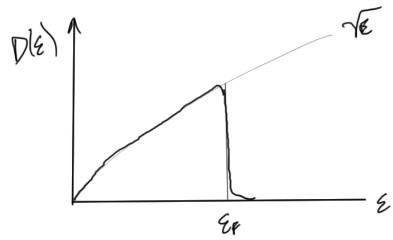

Figure 5.16: Specific heat.

Heat capacity of free electrons (cont.) Last time we found the density of states for Fermions in a period potential

$$D(E) = \frac{1}{2\pi^2}\left(\frac{2m}{\hbar^2}\right)^{3/2}\sqrt{E}. \tag{5.40}$$

Using the Fermi-Dirac distribution fig. 5.17

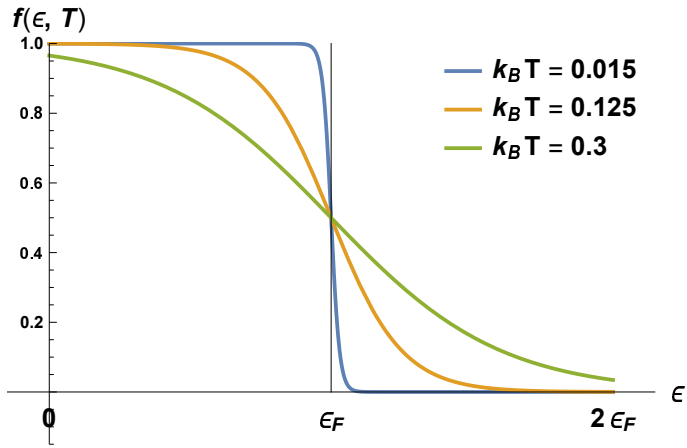

Figure 5.17: Fermi-Dirac distribution.

$$f(E,T) = \frac{1}{e^{(E-\mu)/k_B T}+1}, \tag{5.41}$$

we calculated an approximate value for the specific heat

$$C(T) \sim 2k_B D(E_F)T. \tag{5.42}$$

We will now move on and calculate a more exact expression for the specific heat, defined by

$$U(T) = \int dE D(E) E f(E, T) \tag{5.43a}$$

$$C(T) = \frac{\partial U}{\partial T}, \tag{5.43b}$$

or, in terms of the density of states

$$C(T) = \int dE D(E) E \frac{\partial f(E, T)}{\partial T}. \tag{5.44}$$

In fig. 5.18, are plots of the Fermi-Dirac distribution functions at $T_2 > T_1$ and their difference. Observe that this difference is zero most everywhere

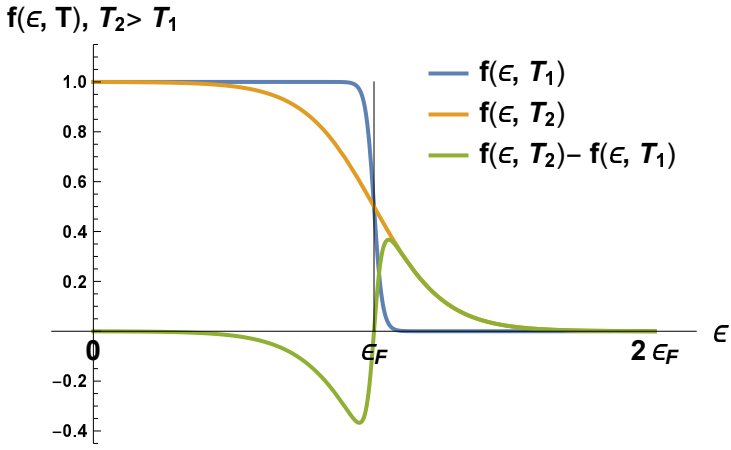

Figure 5.18: Fermi-Dirac curves and their difference.

Calculating that derivative explicitly, we have

$$\begin{aligned} \frac{\partial f(E, T)}{\partial T} &= -\frac{e^{(E-\mu)/k_B T}}{(e^{(E-\mu)/k_B T} + 1)^2} \frac{E - \mu}{k_B} \frac{-1}{T^2} \\ &= \frac{e^{(E-\mu)/k_B T}}{(e^{(E-\mu)/k_B T} + 1)^2} \frac{E - \mu}{k_B T^2}. \end{aligned} \tag{5.45}$$

This is plotted in fig. 5.19.

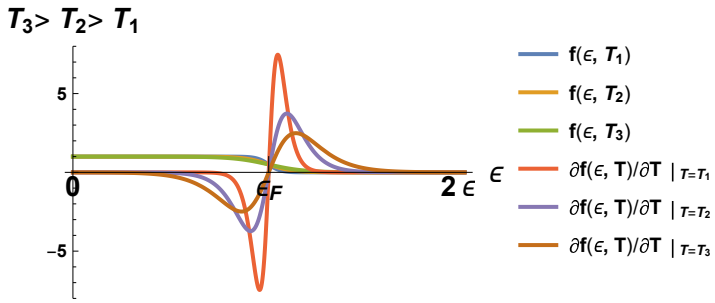

Figure 5.19: Fermi-Dirac distribution and derivatives.

The expected value of the number density is

$$n = \int dE D(E) f(E, T). \tag{5.46}$$

It's derivative with respect to temperature is

$$\frac{\partial n}{\partial T} = \int dE D(E) \frac{\partial f}{\partial T}. \tag{5.47}$$

With a constant constraint on the number of states, this derivative is zero, allowing us to write

$$\begin{aligned} C(T) &= C(T) - E_F \frac{\partial n}{\partial T} \\ &= E_F \int dE D(E)(E - E_F) \frac{\partial f}{\partial T} \\ &\qquad\qquad \text{zero except within a few } k_B T \text{ of } E_F \\ &= \int_0^\infty dE D(E)(E - E_F) \boxed{\frac{E - E_F}{k_B T^2} \frac{e^{(E-\mu)/k_B T}}{(e^{(E-\mu)/k_B T} + 1)^2}} \\ &\approx D(E_F) \int_0^\infty dE (E - E_F) \frac{E - E_F}{k_B T^2} \frac{e^{(E-E_F)/k_B T}}{(e^{(E-E_F)/k_B T} + 1)^2}. \end{aligned} \tag{5.48}$$

Because we have a zero in the integrand, except close to E_F, we have made the approximation $D(E) \to D(E_F)$, with the density function with its value at E_F, perhaps similar to the point sampling sketched in fig. 5.20.

This mostly zero in the integrand also allows us to extend the integration range

$$\int_0^\infty \to \int_{-\infty}^\infty, \tag{5.49}$$

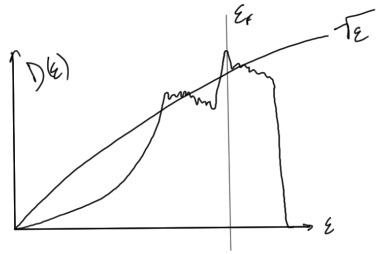

Figure 5.20: Density of states point approximation.

To proceed with the integration, let

$$x = \frac{E - E_F}{k_B T}. \tag{5.50}$$

$$\begin{aligned} C(T) &\approx D(E_F) \int_{-\infty}^{\infty} \overbrace{(dx k_B T)}^{dE} \frac{x^2 \cancel{k_B^2 T^2}}{\cancel{k_B T^2}} \frac{e^x}{e^x + 1)^2} \\ &= D(E_F) k_B^2 T \overbrace{\int_{-\infty}^{\infty} dx \frac{x^2 e^x}{(e^x + 1)^2}}^{\pi^2/3}. \end{aligned} \tag{5.51}$$

We have finally

$$\boxed{C(T) \approx \frac{\pi^2}{3} k_B^2 D(E_F) T.} \tag{5.52}$$

The linear T specific heat is a signature of the Fermi surface (sharp boundary in k-space between occupied and unoccupied states). This doesn't depend on the details form of $D(E)$, but only on $D(E_F)$. This therefore works for all metals.

If you see a $C \sim T^3$ (cubic) relationship you can realize that we are dealing with a Bosonic system with a linear frequency relationship.

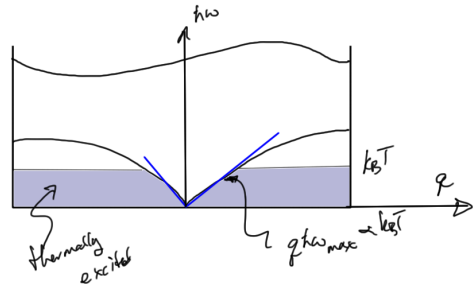

Figure 5.21: Thermally excited region.

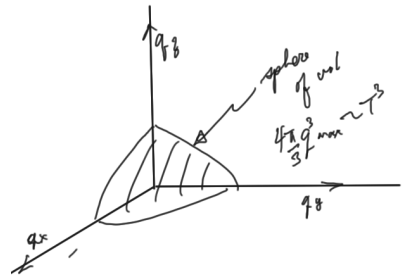

Figure 5.22: Momentum space for linear frequency temperature region.

Electrons Each thermally excited electron has thermal energy k_BT, so

$$U(T) \sim T^2 \implies C(T) \propto T \tag{5.53}$$

If you see a $C \sim T$ (linear) relationship you can realize that we are dealing with a Fermionic system.

At $T > 0$, thin shell of width k_BT thermally excited. Volume is

$$4\pi k_F^2 \delta k \propto 4\pi k_F^2 \delta T. \tag{5.54}$$

5.4 THOMAS-FERMI SCREENING.

Reading: [1] ch. 17, [10] §6.5.

Recall that $\mathbf{E} = 0$ inside a metal in equilibrium as illustrated in fig. 5.25.

Figure 5.23: Free particle energy levels.

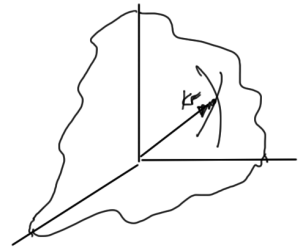

Figure 5.24: Phase space region for Fermi momentum.

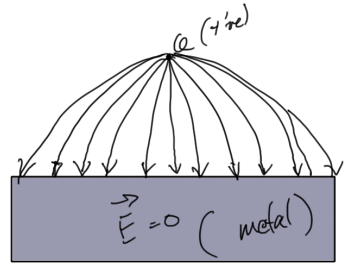

Figure 5.25: Field in conducting metal.

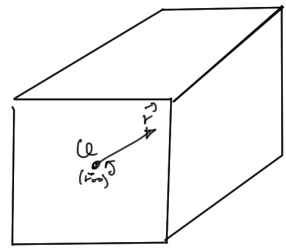

Figure 5.26: Point charge in a box.

Put a fixed point charge Q at $\mathbf{r} = 0$, and an electric potential $\phi(\mathbf{r})$. Our Maxwell equation is

$$\nabla^2\phi(\mathbf{r}) = -\frac{\rho(\mathbf{r})}{\epsilon_\circ}. \tag{5.55}$$

Split the charge density as

$$\rho(\mathbf{r}) = \bar{\rho}_{\text{el}} + \bar{\rho}_{\text{ion}} + \delta\rho_{\text{el}}, \tag{5.56}$$

where $\bar{\rho}_{\text{el}}$ is the average electron density, $\bar{\rho}_{\text{ion}}$ is the positive background, and $\delta\rho_{\text{el}}$ is the perturbation to Q. The first two terms cancel giving

$$\begin{aligned}\rho_{\text{el}} &= -e\int dE D(E)\frac{1}{e^{(E-\mu-e\phi(\mathbf{r}))/k_{\text{B}}T}+1} \\ &\approx -e\int dE D(E)\left(\frac{1}{e^{(E-\mu)/k_{\text{B}}T}+1} - e\phi(\mathbf{r})\frac{\partial f}{\partial E}\bigg|_{E=E-\mu} + \cdots\right).\end{aligned} \tag{5.57}$$

Here $\mu + e\phi(\mathbf{r})$ is the chemical potential shifted at $\mathbf{r}$ by $e\phi(\mathbf{r})$. Note that as $T \to 0$, we have

$$\int_{E_{\text{F}}-\Delta}^{E_{\text{F}}+\Delta} dE\frac{\partial f}{\partial E} = -1, \tag{5.58}$$

where the width of $\partial f/\partial E \to 0$. This is very much like a delta function fig. 5.27 , so we can write

$$\begin{aligned}\rho_{\text{el}} &\approx \bar{\rho}_{\text{el}} - e^2\phi(\mathbf{r})\int dE D(E)\delta(E - E_{\text{F}}) \\ &\approx \bar{\rho}_{\text{el}} - e^2\delta\phi(\mathbf{r})D(E_{\text{F}}).\end{aligned} \tag{5.59}$$

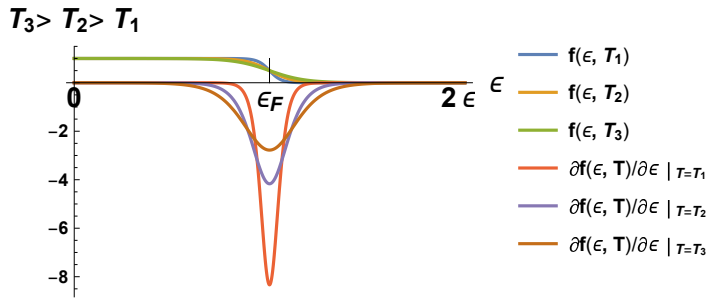

Figure 5.27: Delta function like region.

Recall that the spherical form of the Laplacian of a function with only radial dependence is

$$\nabla^2 f = \frac{\partial^2 f}{\partial r^2} + \frac{2}{r}\frac{\partial f}{\partial r} = \frac{1}{r^2}\frac{\partial}{\partial r}\left(r^2 \frac{\partial f}{\partial r}\right). \tag{5.60}$$

For the potential we have

$$\phi(\mathbf{r}) = \phi_{\text{avg}} + \delta\phi(\mathbf{r}). \tag{5.61}$$

so that the electrostatic equation is

$$\frac{1}{r^2}\frac{\partial}{\partial r}\left(r^2 \frac{\partial \delta\phi(\mathbf{r})}{\partial r}\right) = \frac{e^2 D(E_{\text{F}})}{\epsilon_\circ}\delta\phi(\mathbf{r}). \tag{5.62}$$

This has solution (see: exercise 5.4)

$$\delta\phi(\mathbf{r}) = \frac{\alpha e^{-r/r_{\text{TF}}}}{r}, \tag{5.63}$$

where r_{TF} is the Thomas-Fermi screening length

$$r_{\text{TF}} = \sqrt{\frac{\epsilon_\circ}{e^2 D(E_{\text{F}})}}. \tag{5.64}$$

The functional form of the screened and unscreened potentials are plotted in fig. 5.28.

Example 5.1: Copper.

$$r_{\text{TF}} \sim 0.5\text{Å}. \tag{5.65}$$

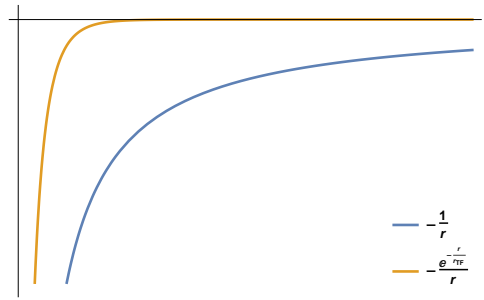

Figure 5.28: Screened vs unscreened Coulomb potential.

Reading: §6.5, especially Mott transition.

5.5 PROBLEMS.

Exercise 5.1 Fermi attributes, free electron model. (*2013 ps6 p1*)

a. Treating potassium as a free electron metal with one conduction electron per potassium, calculate the theoretical value of the Fermi wave-vector k_F, the Fermi energy E_F and the Fermi temperature T_F.

b. Using fig. 5.29 below, determine the experimental value of the Fermi temperature T_F of potassium, and compare it with the theoretical free-electron Fermi temperature. (Ignore the break in the y-axis, that is, only use the numbers at the bottom of the y-axis.)

Potentially useful facts: The density of potassium is 0.862 g/cm^3; the atomic mass of potassium is 39.10; the atomic mass unit is $u = 1.66 \times 10^{-27}$ kg.)

Answer for Exercise 5.1

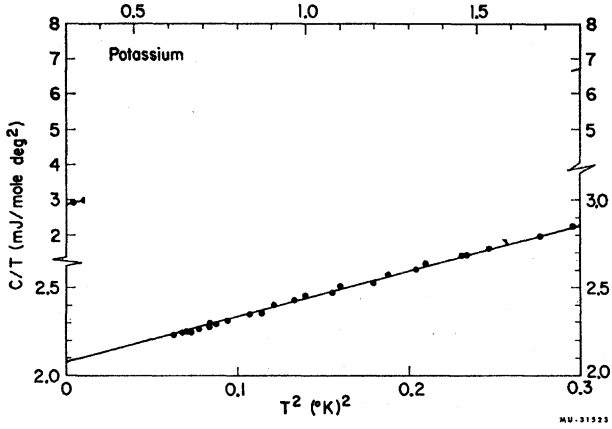

Figure 5.29: Potassium specific heat temperature dependence.

Part a. Using the following values

$$\begin{aligned} 1 \text{ amu} &= 1.66 \times 10^{-24}\,\text{g} \\ \rho_K &= 0.86\,\text{g/cm}^3 \\ \text{Atomic mass of K} &= 39.0983 \\ m_e &= 9.109 \times 10^{-28}\,\text{g} \\ \hbar &= 1.055 \times 10^{-27}\,\text{ergs s} \\ k_B &= 1.381 \times 10^{-16}\,\text{ergs/K}, \end{aligned} \tag{5.66}$$

we find

$$\begin{aligned} m_K &= \text{the mass of 1 Potassium atom} = \text{atomic mass of K} \times 1 \text{ amu} \\ &= 6.49032 \times 10^{-23}\,\text{g}. \end{aligned} \tag{5.67}$$

$$\begin{aligned} n_K &= \rho_K/m_K = n_e(\text{with presumption of one free electron per atom}) \\ &= 1.32505 \times 10^{22}\,/\text{cm}^3. \end{aligned} \tag{5.68}$$

This gives

$$\begin{aligned} k_F &= \left(3\pi^2 n_e\right)^{1/3} &&= 7.32068 \times 10^7\,/\text{cm} \\ E_F &= \hbar^2 k_F^2/(2m_e) &&= 3.27421 \times 10^{-12}\,\text{ergs} \\ T_F &= E_F/k_B &&= 23709\,\text{K} \end{aligned} \tag{5.69}$$

Grading remark: The grader didn't like my use of ergs as a unit, and said I should use either eV or J. Asking Prof Julian, if SI now dominates, he confirms that this was a pretty old school thing to do "Yes, it's a long time since I have seen an erg." We both recall the horror of taking introductory electromagnetism with the CGS Berkeley physics series while our Professors used SI.

Part b. Looking at the graph, we see that the units are different from what we have been using. The dimensions of specific heat $[C_V] = \frac{[U]}{\Theta}$ are those of energy density per unit temperature, or energy per unit volume per unit temperature. The graph provides the specific heat per mole, not per unit volume, so we have to convert by multiplying by the volume per mole N_A/n where N_A is Avogadro's number and n is the number density.

$$\begin{aligned} C &= C_V \frac{N_A}{n} \\ &= \frac{\pi^2}{2} \frac{k_B n T}{T_F} \frac{N_A}{n} \\ &= \frac{\pi^2}{2} \frac{k_B N_A}{T_F} T. \end{aligned} \tag{5.70}$$

Our graphed relation is

$$\begin{aligned} \frac{C}{T} &= \gamma + \beta T^2 \\ &\approx \left(2.08 + \frac{0.85}{0.3} T^2 \right) \text{ mJ/mole deg}^2. \end{aligned} \tag{5.71}$$

With $N_A = 6.022 \times 10^{23}$, plugging in the numbers yields

$$\begin{aligned} T_{F\text{experimental}} &= \frac{\pi^2 k_B N_A}{2 \times 2.08 \,\text{mJ/K}^2} \\ &= \frac{\pi^2 1.381 \times 10^{-23} \,\text{J/K} \times 6.022 \times 10^{23} \times 10^3}{2 \times 2.08 \,\text{J/K}^2} \\ &= 19730.6 \,\text{K}. \end{aligned} \tag{5.72}$$

The ratio of theoretical to experimental is

$$\frac{T_F}{T_{F\text{experimental}}} = 1.20163. \tag{5.73}$$

The numerical calculations for this problem can also be found in problemSet6Problem1.nb

Grading remark: "What do you think is the reason for the discrepancy?". Lost half a mark for that.

Exercise 5.2 Specific heat, 1-2D free electron metals. (*[10] pr 6.1*)

a. Calculate the density of states for a two-dimensional gas of free electrons in a so-called quantum well. The boundary conditions for the electronic wavefunction are:

$$\psi(x, y, z) = 0, \quad \text{for } |x| > a, \tag{5.74}$$

where a is of atomic dimensions.

b. Calculate the density of states for a one-dimensional gas of free electrons in a so-called quantum wire, the boundary conditions:

$$\psi(x, y, z) = 0, \quad \text{for } |x| > a, \text{ and } |y| > b, \tag{5.75}$$

where a and b are of atomic dimensions.

c. Can such electron gases be realized physically?

Clarification The question says something rather obscure about $\psi(x, y, z) = 0$ for $|x| > a$, where a is of atomic dimensions. What they mean is that a two-dimensional electron gas can be thought of as contained in a three-dimensional box, with two of the dimensions being macroscopic, but the third dimension (perpendicular to the plane of the electron gas) being microscopic. As a result, the energy levels are quasi-continuous in two dimensions, but discrete in the third dimension, and we assume that only the ground state of the discrete spectrum is occupied, so there is no summation over that third dimension. Similarly, in the one-dimensional electron gas, only one direction in q space is quasi-continuous.)

Answer for Exercise 5.2

Part a. Consider a pizza box configuration where $L \gg a$ as in fig. 5.30.

Schrödinger's equation for the particle inside the box is

$$-\frac{\hbar^2}{2m}\nabla^2\Psi + V_\circ\Psi = E\Psi. \tag{5.76}$$

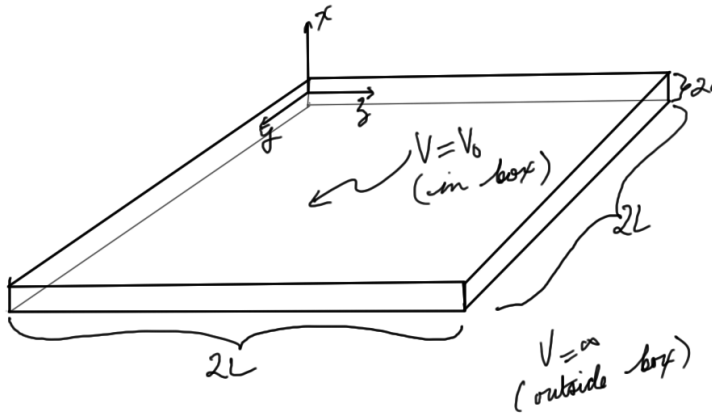

Figure 5.30: Particle in a pizza box.

Solving by separation of variables with $\Psi = XYZ$, we have

$$\frac{X''}{X} + \frac{Y''}{Y} + \frac{Z''}{Z} = -\frac{2m}{\hbar^2}(E - V_\circ). \tag{5.77}$$

Assuming independent solutions

$$\begin{aligned} X'' &= -k_x^2 X \\ Y'' &= -k_y^2 Y \\ Z'' &= -k_z^2 Z, \end{aligned} \tag{5.78}$$

we have

$$k_x^2 + k_y^2 + k_z^2 = \frac{2m}{\hbar^2}(E - V_\circ). \tag{5.79}$$

We could write $E' = E - V_\circ$, but this is equivalent to setting the ground to zero (i.e. $V_\circ = 0$), so let's just do that, dispensing with any primes on the energy.

Our solution is

$$\Psi = A \sin\left(k_x(x-a)\right) \sin\left(k_y y\right) \sin\left(k_z z\right), \tag{5.80}$$

where

$$E(\mathbf{k}) = \frac{\hbar^2 \mathbf{k}^2}{2m}, \tag{5.81}$$

The boundary constraints are

$$\begin{aligned}\Psi(x=a) &= \Psi(x=-a) = 0\\ \Psi(y=2L) &= \Psi(y=0) = 0\\ \Psi(z=2L) &= \Psi(z=0) = 0,\end{aligned} \tag{5.82}$$

so for integers q, r, s, we have

$$\begin{aligned}k_x 2a &= q\pi\\ k_y 2L &= r\pi\\ k_z 2L &= s\pi,\end{aligned} \tag{5.83}$$

Normalizing the wave function gives us

$$\Psi = \frac{1}{\sqrt{aL}} \sin\left(\frac{q\pi(x-a)}{2a}\right) \sin\left(\frac{r\pi y}{2L}\right) \sin\left(\frac{s\pi z}{2L}\right). \tag{5.84}$$

The k-points in momentum space are illustrated in fig. 5.31. However, since we are considering the particle to be in the ground state for the x direction, only the k-space points in the plane, separated by $\pi/2L$ in each direction, will contribute to the density of states.

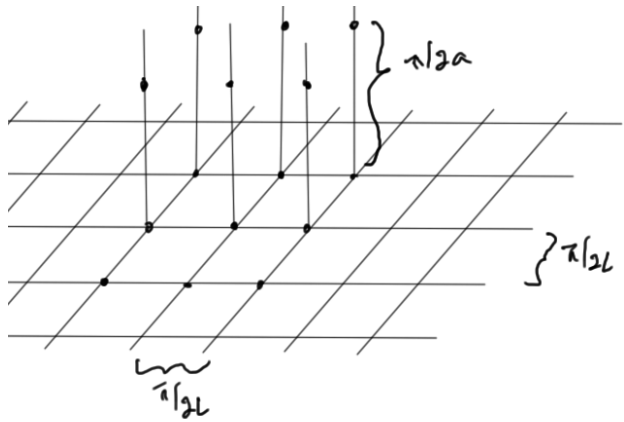

Figure 5.31: K space points for pizza box wavefunction.

We evaluate the density of states in the same fashion as we did in class

$$\sum_{k_y,k_z,\text{spin}} \to \sum_{\text{spin}} \int \frac{d^2\mathbf{k}}{(\pi/2L)^2}$$

$$= \underbrace{2}_{\text{spin, 2 states per k point}} \frac{A}{\pi^2} \int \underbrace{\frac{1}{4}}_{\text{1 quadrant}} 2\pi k dk \tag{5.85}$$

$$= \frac{A}{\pi} \int k dk.$$

To convert to an energy integral, we use

$$dE = \frac{\hbar^2 k}{m} dk, \tag{5.86}$$

or

$$\frac{m}{\hbar^2} dE = k dk. \tag{5.87}$$

The density of states definition is

$$\frac{A}{\pi} \int \frac{m}{\hbar^2} dE \equiv A \int D(E) dE, \tag{5.88}$$

so the density of states is constant in 2D

$$\boxed{D(E) = \frac{m\pi}{\hbar^2}.} \tag{5.89}$$

Part b. We now want to consider a particle in the cigar box configuration of fig. 5.32. The wave function is

$$\Psi = \frac{1}{\sqrt{abL}} \sin\left(\frac{q\pi(x-a)}{2a}\right) \sin\left(\frac{r\pi(y-b)}{2b}\right) \sin\left(\frac{s\pi z}{2L}\right), \tag{5.90}$$

and the k space points of interest are separated by $\pi/2L$ as before. The density of states calculation goes

$$\sum_{k_z,\text{spin}} \to \sum_{\text{spin}} \int \frac{dk_z}{\pi/2L}$$

$$= 2\frac{2L}{\pi} \int dk_z \tag{5.91}$$

$$= \frac{4L}{\pi} \int dk_z.$$

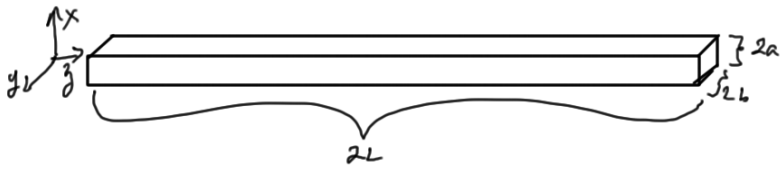

Figure 5.32: Particle in a cigar box.

Converting the differential to energy space, we have

$$\begin{aligned} dk_z &= \frac{m}{\hbar^2}\frac{dE}{k_z} \\ &= \frac{m}{\hbar^2}\frac{dE}{\sqrt{2mE}/\hbar} \\ &= \frac{1}{\hbar}\sqrt{\frac{m}{2E}}dE. \end{aligned} \tag{5.92}$$

Inserting this gives us

$$L\int D(E)dE = \frac{4L}{\pi}\int \frac{1}{\hbar}\sqrt{\frac{m}{2E}}dE, \tag{5.93}$$

or

$$\boxed{D(E) = \frac{2}{\pi}\sqrt{\frac{2m}{\hbar^2}}E^{-1/2}.} \tag{5.94}$$

Part c. In microelectronics the scale of charge carrying conductive pathways are reduced so much that "wires" can exhibit quantum mechanical effects. When the scale of such wires are reduced enough, modeling that conduit as a 1D particle in a box as above is likely possible. A carbon nanotube is likely another possible physical implementation of a 1D particle in a box.

Conducting and semiconducting plane layers of the same sort of microelectronics can likely be reduced to scales that would allow for a 2D particle in a pizza box configuration for which we calculated the density of states above. With planar configuration and electron conduction, graphene is also likely a physical implementation of this potential configuration.

Exercise 5.3 Bulk modulus. ([10] pr 6.3)

The bulk modulus κ is given by the second derivative of the total energy E_{tot} with respect to the volume

$$\kappa = V\frac{\partial^2 E_{\text{tot}}}{\partial V^2}. \tag{5.95}$$

Estimate the bulk moduli of alkali metals by assuming that the total energy is equivalent to the kinetic energy of the Fermi gas. What has been neglected in this estimate?

Answer for Exercise 5.3

We need to start by computing the total energy. At $T = 0$, utilizing the step nature of the Fermi-Dirac distribution, this is approximately

$$\begin{aligned} E_{\text{tot}} &= 2\frac{V}{(2\pi)^3}\int_{|\mathbf{k}|<k_{\text{F}}} d^3\mathbf{k}\frac{\hbar^2\mathbf{k}^2}{2m} \\ &= \frac{V}{4\pi^3}\frac{\hbar^2}{2m}\int_0^{k_{\text{F}}} 4\pi k^4 dk \\ &= \frac{V}{\pi^2}\frac{\hbar^2}{2m}\frac{k_{\text{F}}^5}{5} \\ &= \frac{V\hbar^2}{10m\pi^2}\left(3\pi^2\frac{N}{V}\right)^{5/3} \\ &= \frac{\hbar^2}{10m\pi^2}\left(3\pi^2 N\right)^{5/3} V^{-2/3}. \end{aligned} \tag{5.96}$$

This form is what we want to take derivatives with respect to V. We can however, simplify this total energy expression by expressing it in terms of the Fermi energy

$$\begin{aligned} E_{\text{tot}} &= \frac{V}{5\pi^2}3\pi^2\frac{N}{V}\frac{\hbar^2}{2m}\left(3\pi^2 n\right)^{2/3} \\ &= \frac{3}{5}NE_{\text{F}}. \end{aligned} \tag{5.97}$$

Taking derivatives, we have

$$\begin{aligned} \kappa &= V\frac{\partial^2 E_{\text{tot}}}{\partial V^2} \\ &= V\frac{\hbar^2}{10m\pi^2}\left(3\pi^2 N\right)^{5/3}\frac{d^2}{dV^2}V^{-5/3+1} \\ &= \frac{\hbar^2}{10m\pi^2}\left(3\pi^2 N\right)^{5/3}\left(\frac{-2}{3}\right)\left(\frac{-5}{3}\right)V^{-2/3-2+1}. \end{aligned} \tag{5.98}$$

Factoring out the total energy of the free valence electrons E_{tot}, or equivalently, the Fermi energy, this is

$$\boxed{\kappa = \frac{10}{9}\frac{E_{\text{tot}}}{V} = \frac{2}{3}nE_{\text{F}}.} \tag{5.99}$$

What did we assume and neglect? We have implicitly treated the Alkali metals as a free electron gas, assuming that there was no interaction between the electrons and the nuclei, and no interactions between the electrons themselves (except for Pauli exclusion interaction). We have assumed that only the single outermost (valence) electron of each atom contributes to this energy sum. We have also assumed that the system is big enough that surface effects are irrelevant, and that we can make a continuum approximation for the summation over all the wave-vector states. We have also assumed that there are no differences to the density of the metal (and thus valence electron density n) at absolute zero compared to other temperatures.

Exercise 5.4 Thomas-Fermi screening length.

Find the solution to eq. (5.62), thus finding the Thomas-Fermi screening length expression of eq. (5.64).

Answer for Exercise 5.4

We wish to solve an equation of the form

$$\frac{1}{r^2}\frac{d}{dr}\left(r^2\frac{df}{dr}\right) = af. \tag{5.100}$$

We can make this more tractable with a substitution

$$g = rf, \tag{5.101}$$

for which we have

$$r\frac{dg}{dr} = r\left(f + r\frac{df}{dr}\right), \tag{5.102}$$

or

$$r^2\frac{df}{dr} = r\frac{dg}{dr} - rf = r\frac{dg}{dr} - g. \tag{5.103}$$

This reduces our equation to

$$\begin{aligned} \frac{d}{dr}\left(r\frac{dg}{dr} - g\right) &= arg \\ \cancel{\frac{dg}{dr}} + r\frac{d^2g}{dr^2} - \cancel{\frac{dg}{dr}} &= \end{aligned} \tag{5.104}$$

or just

$$\frac{d^2g}{dr^2} = ag. \tag{5.105}$$

This has the solution

$$g = \sum_{\pm} A_{\pm} e^{\pm\sqrt{a}r}, \tag{5.106}$$

Picking the non-hyperbolic solution, that is

$$f \propto \frac{e^{-\sqrt{a}r}}{r}. \tag{5.107}$$

With $a = e^2 D(E_F)/\epsilon_\circ = 1/r_{TF}^2$, we find eq. (5.64) as desired.

Exercise 5.5 Thomas-Fermi screening. *(2013 ps7 p1)*

a. For $f(E) = 1/(e^{(E-\mu)/k_B T} + 1)$ (i.e. the Fermi-Dirac distribution function), show that in the limit as $T \to 0$ K, $-\partial f/\partial E$ has the following properties expected of the Dirac delta-function:

   - It is zero everywhere, except at $E = \mu$ where it is infinite;
   - $-\int_{-\infty}^{\infty} dE \partial f/\partial E = 1$

   Note : you may know that the Dirac delta function is the derivative of the so-called Heaviside function, so the correspondence between $\partial f/\partial E$ and $\delta(E - \mu)$ is not a surprise.

b. Consider an externally applied periodic charge density wave of the form $\delta\rho_\circ(x) = \delta\rho_\circ \cos(qx)$, inside a metal. In practice this could be a modulation of the ionic charge density due to a static or dynamic charge density wave.

Show, using a result we derived in class

$$\delta\rho_{\text{el}}(\mathbf{r}) = -e^2 D(E_{\text{F}}) U(\mathbf{r}), \tag{5.108}$$

that the induced electron density due to this applied periodic charge density wave is

$$\delta\rho_{\text{el}}(x) = -\frac{e^2 D(E_{\text{F}})}{\epsilon_\circ} \frac{\delta\rho_\circ}{q^2+\kappa^2} \cos(qx), \tag{5.109}$$

where $\kappa^2 = e^2 D(E_{\text{F}})/\epsilon_\circ$.

Answer for Exercise 5.5

Part a. With $\tau = k_{\text{B}}T$, the derivative is

$$\begin{aligned} \frac{\partial f}{\partial E} &= -\frac{1}{\tau} \frac{e^{(E-\mu)/\tau}}{\left(e^{(E-\mu)/\tau}+1\right)^2} \\ &= -\frac{1}{\tau} \frac{1}{\left(e^{(E-\mu)/\tau}+1\right)\left(e^{-(E-\mu)/\tau}+1\right)}. \end{aligned} \tag{5.110}$$

Consider this first for $E > \mu$, where in the limit $\tau \to 0$ we have

$$\begin{aligned} \frac{\partial f}{\partial E} &\approx -\frac{1}{\tau} \frac{1}{\left(e^{(E-\mu)/\tau}+1\right)} \\ &= -\frac{1}{2\tau + (E-\mu) + \frac{1}{2}(E-\mu)^2/\tau + \frac{1}{6}(E-\mu)^3/\tau^2 + \cdots}. \end{aligned} \tag{5.111}$$

As $\tau \to 0$, the denominator is dominated by the ever increasing powers of $1/\tau$, and thus goes to zero.

Similarly for $E < \mu$ and $\tau \to 0$ we have

$$\begin{aligned} \frac{\partial f}{\partial E} &\approx -\frac{1}{\tau} \frac{1}{\left(e^{(\mu-E)/\tau}+1\right)} \\ &= -\frac{1}{2\tau + (\mu-E) + \frac{1}{2}(\mu-E)^2/\tau + \frac{1}{6}(\mu-E)^3/\tau^2 + \cdots}. \end{aligned} \tag{5.112}$$

This has the same form as eq. (5.111), so clearly also approaches zero as $\tau \to 0$.

For the $E = \mu$ condition we have

$$\frac{\partial f}{\partial E} = -\frac{1}{4\tau} \xrightarrow{\tau\to 0} -\infty. \tag{5.113}$$

Now consider the integral of the derivative, taking some care in the neighborhood $|E-\mu|<\epsilon$. We have

$$\begin{aligned}
&-\int_{-\infty}^{\infty} dE \frac{\partial f}{\partial E} \\
&= \int_{-\infty}^{\infty} \frac{dE}{\tau} \frac{e^{(E-\mu)/\tau}}{\left(e^{(E-\mu)/\tau}+1\right)^2} \\
&= \int_{-\infty}^{\mu-\epsilon} \frac{dE}{\tau} \frac{e^{(E-\mu)/\tau}}{\left(e^{(E-\mu)/\tau}+1\right)^2} + \int_{\mu-\epsilon}^{\mu+\epsilon} \frac{dE}{\tau} \frac{e^{(E-\mu)/\tau}}{\left(e^{(E-\mu)/\tau}+1\right)^2} \\
&\quad + \int_{\mu+\epsilon}^{\infty} \frac{dE}{\tau} \frac{e^{(E-\mu)/\tau}}{\left(e^{(E-\mu)/\tau}+1\right)^2}.
\end{aligned} \tag{5.114}$$

With $x=(E-\mu)/\tau$ and $dx=dE/\tau$, we have

$$\begin{aligned}
-\int_{-\infty}^{\infty} dE \frac{\partial f}{\partial E} &= \int_{-\infty}^{-\epsilon/\tau} dx \frac{e^x}{(e^x+1)^2} + \int_{\epsilon/\tau}^{\infty} dx \frac{e^x}{(e^x+1)^2} + \int_{-\epsilon/\tau}^{\epsilon/\tau} dx \frac{e^x}{(e^x+1)^2} \\
&= -\frac{1}{e^x+1}\Big|_{-\infty}^{-\epsilon/\tau} + -\frac{1}{e^x+1}\Big|_{-\epsilon/\tau}^{\epsilon/\tau} + -\frac{1}{e^x+1}\Big|_{\epsilon/\tau}^{\infty} \\
&= \left(\frac{1}{e^{-\infty}+1} - \frac{1}{e^{-\epsilon/\tau}+1}\right) + \left(\frac{1}{e^{-\epsilon/\tau}+1} - \frac{1}{e^{\epsilon/\tau}+1}\right) \\
&\quad + \left(\frac{1}{e^{\epsilon/\tau}+1} - \frac{1}{e^{\infty}+1}\right) \\
&= (1-1)+(1-0)+(0-0)\,.
\end{aligned} \tag{5.115}$$

Here we (rather loosely) consider ϵ fixed, and allow $\tau \to 0$ for that choice of ϵ. This leaves only the integral in the neighborhood of μ, which we find is unity as expected.

Part b. We used the result in class in the Coulomb calculation

$$\boldsymbol{\nabla}^2 U = -\frac{\rho}{\epsilon_\circ}. \tag{5.116}$$

Summing the internal and the external charge densities, we wish to find

$$\rho = \delta\rho_\circ(x) + \delta\rho_{\text{el}} = \delta\rho_\circ \cos(qx) - e^2 D(E_{\text{F}}) U, \tag{5.117}$$

or

$$\boldsymbol{\nabla}^2 U = -\frac{\delta\rho_\circ}{\epsilon_\circ}\cos(qx) + \frac{e^2 D(E_\mathrm{F})}{\epsilon_\circ} U. \tag{5.118}$$

Fourier transforming, assuming the potential has only an x dependence $U = U(x)$, we have

$$\begin{aligned}\int dx e^{ikx}\frac{d^2U(x)}{dx^2} &= -\frac{\delta\rho_\circ}{\epsilon_\circ}\int dx e^{ikx}\cos(qx) + \kappa^2\int dx e^{ikx}U(x) \\ &= -\frac{\delta\rho_\circ}{\epsilon_\circ}\frac{1}{2}\int dx\left(e^{i(k+q)x} + e^{i(k-q)x}\right) + \kappa^2\tilde{U}(k) \\ &= -\frac{\pi\delta\rho_\circ}{\epsilon_\circ}\left(\delta(k+q) + \delta(k-q)\right) + \kappa^2\tilde{U}(k).\end{aligned} \tag{5.119}$$

Integrating the LHS twice by parts, and rearranging, this is

$$\tilde{U}(k) = -\frac{\pi\delta\rho_\circ}{\epsilon_\circ\left(k^2+\kappa^2\right)}\left(\delta(k+q) + \delta(k-q)\right). \tag{5.120}$$

A final inverse transform yields the real space potential

$$\begin{aligned}U(x) &= \frac{1}{2\pi}\int dk e^{-ikx}\tilde{U}(k) \\ &= -\frac{\delta\rho_\circ}{2\epsilon_\circ}\left(\frac{e^{-ikq}}{(q^2+\kappa^2)} + \frac{e^{-ikq}}{((-q)^2+\kappa^2)}\right) \\ &= -\frac{\delta\rho_\circ\cos(qx)}{\epsilon_\circ\left(q^2+\kappa^2\right)}.\end{aligned} \tag{5.121}$$

Referring back to eq. (5.108), the induced electron density is

$$\boxed{\delta\rho_\mathrm{el} = -\epsilon_\circ\kappa^2 U = -\frac{\kappa^2\delta\rho_\circ\cos(qx)}{q^2+\kappa^2},} \tag{5.122}$$

as desired.

6 ELECTRONIC BANDSTRUCTURE.

6.1 ELECTRONS IN A PERIODIC LATTICE.

Reading: [1] ch. 8.

We want to look at the general properties of 1 electron in a periodic potential. We want to solve the Schrödinger equation

$$\left(-\frac{\hbar^2}{2m}\boldsymbol{\nabla}^2 + V(\mathbf{r})\right)\Psi(\mathbf{r}) = E\Psi(\mathbf{r}). \tag{6.1}$$

Here $V(\mathbf{r})$ is periodic $V(\mathbf{r}+\mathbf{r}_n) = V(\mathbf{r})$, with

$$\mathbf{r}_n = n_1\mathbf{a}_1 + n_2\mathbf{a}_2 + n_3\mathbf{a}_3, \tag{6.2}$$

so that

$$V(\mathbf{r}) = \sum_{\mathbf{G}} V_{\mathbf{G}} e^{i\mathbf{G}\cdot\mathbf{r}}, \tag{6.3}$$

where

$$\mathbf{G} = h\mathbf{g}_1 + k\mathbf{g}_2 + l\mathbf{g}_3 \tag{6.4a}$$

$$\mathbf{g}_i \cdot \mathbf{a}_j = \delta_{ij}. \tag{6.4b}$$

Example potential (roughly) sketched in fig. 6.1.

Use a plane wave basis

$$\Psi(\mathbf{r}) = \sum_{\mathbf{k}} C_{\mathbf{k}} e^{i\mathbf{k}\cdot\mathbf{r}}, \tag{6.5}$$

$$\sum_{\mathbf{k}'} \frac{\hbar^2\mathbf{k}'^2}{2m} C'_{\mathbf{k}} e^{i\mathbf{k}'\cdot\mathbf{r}} + \sum_{\mathbf{k}'',\mathbf{G}} V_{\mathbf{G}} C_{\mathbf{k}''} e^{i(\mathbf{k}''+\mathbf{G})\cdot\mathbf{r}} = E\sum_{\mathbf{k}'} e^{i\mathbf{k}'\cdot\mathbf{r}}, \tag{6.6}$$

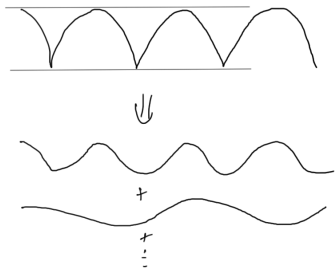

Figure 6.1: Fourier decomposition of 1D periodic potential.

with $\mathbf{k}' = \mathbf{k}'' + \mathbf{G}$, or $\mathbf{k}'' = \mathbf{k}' - \mathbf{G}$, this is

$$0 = \sum_{\mathbf{k}'} \left(\left(\frac{\hbar^2 \mathbf{k}'^2}{2m} - E \right) C'_{\mathbf{k}} + \sum_{\mathbf{G}} V_{\mathbf{G}} C_{\mathbf{k}'-\mathbf{G}} \right) e^{i\mathbf{k}'\cdot\mathbf{r}}. \tag{6.7}$$

Using

$$\int d\mathbf{r} e^{-i(\mathbf{k}'-\mathbf{k})\cdot\mathbf{r}} \propto \delta(\mathbf{k}' - \mathbf{k}), \tag{6.8}$$

and operating with

$$\int d\mathbf{r} e^{-i\mathbf{k}\cdot\mathbf{r}} \times \cdots, \tag{6.9}$$

we decouple the system

$$\boxed{0 = \left(\frac{\hbar^2 \mathbf{k}^2}{2m} - E \right) C_{\mathbf{k}} + \sum_{\mathbf{G}} V_{\mathbf{G}} C_{\mathbf{k}-\mathbf{G}}.} \tag{6.10}$$

Each eigenstate only involves $C_{\mathbf{k}}$'s that differ by reciprocal lattice vectors.

$$\Psi \sim C_k e^{ikx} + C_{k+2\pi/a} e^{i(k+2\pi/a)x} + C_{k-2\pi/a} e^{i(k-2\pi/a)x} + \cdots. \tag{6.11}$$

Label each eigenstate with $\mathbf{k}$

$$\Psi_{\mathbf{k}}(\mathbf{r}) \tag{6.12a}$$

$$E = E_{\mathbf{k}} = E(\mathbf{k}), \tag{6.12b}$$

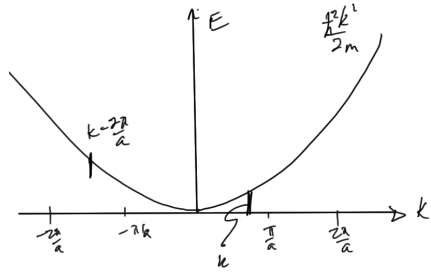

Figure 6.2: Energy vs momentum.

$$\Psi_{\mathbf{k}}(\mathbf{r}) = \sum_{\mathbf{G}} C_{\mathbf{k}-\mathbf{G}} e^{i(\mathbf{k}-\mathbf{G})\cdot\mathbf{r}}$$

$$= \underbrace{\left(\sum_{\mathbf{G}} C_{\mathbf{k}-\mathbf{G}} e^{-i\mathbf{G}\cdot\mathbf{r}}\right)}_{\text{Periodic in } \mathbf{r} \text{ with lattice periodicity}} \underbrace{e^{i\mathbf{k}\cdot\mathbf{r}}}_{\text{plane wave}}. \tag{6.13}$$

$$\boxed{\Psi_{\mathbf{k}}(\mathbf{r}) = U_{\mathbf{k}}(\mathbf{r}) e^{i\mathbf{k}\cdot\mathbf{r}},} \tag{6.14}$$

where $U_{\mathbf{k}}(\mathbf{r})$ is a periodic function. This is Bloch's theorem.

With $\Psi_{\mathbf{k}}(\mathbf{r})$ periodic in $\mathbf{k}$ we have

$$\Psi_{\mathbf{k}+\mathbf{G}}(\mathbf{r}) = \sum_{\mathbf{G}'} C_{\mathbf{k}+\mathbf{G}-\mathbf{G}'} e^{i(\mathbf{k}+\mathbf{G}-\mathbf{G}')\cdot\mathbf{r}}. \tag{6.15}$$

With

$$\mathbf{G}'' = \mathbf{G}' - \mathbf{G}, \tag{6.16}$$

this is

$$\begin{aligned} \Psi_{\mathbf{k}+\mathbf{G}}(\mathbf{r}) &= \sum_{\mathbf{G}''} C_{\mathbf{k}-\mathbf{G}''} e^{i(\mathbf{k}-\mathbf{G}'')\cdot\mathbf{r}} \\ &= \Psi_{\mathbf{k}}(\mathbf{r}). \end{aligned} \tag{6.17}$$

$$\boxed{\begin{aligned} \Psi_{\mathbf{k}+\mathbf{G}}(\mathbf{r}) &= \Psi_{\mathbf{k}}(\mathbf{r}) \\ E(\mathbf{k}+\mathbf{G}) &= E(\mathbf{k}). \end{aligned}} \tag{6.18}$$

We want to examine what this means.

6.2 NEARLY FREE ELECTRON MODEL.

Consider $V(\mathbf{r})$ in the limit $V(\mathbf{r}) \to 0$ in 1D, but still keep periodicity. This leads to

$$\Psi_k(x) = \frac{1}{\sqrt{L}} e^{ikx}$$
$$E(k) = \frac{\hbar^2 k^2}{2m} \tag{6.19}$$

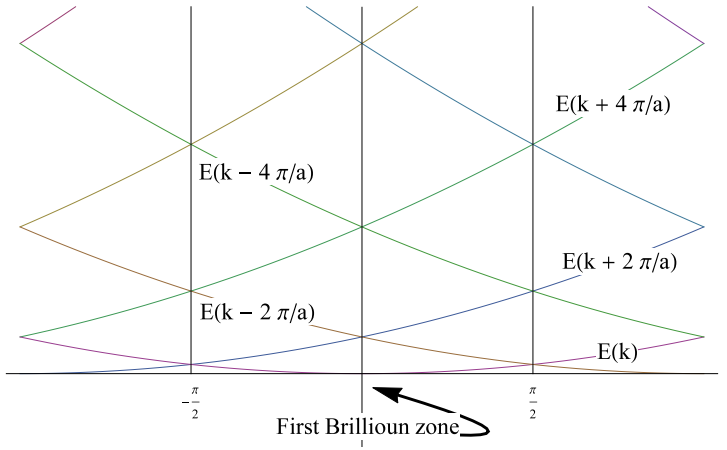

Figure 6.3: Periodic energy solutions.

Solutions outside the first Brillouin zone are redundant. This is called the reduced zone scheme. The periodicity folds the extended solution into the first Brillouin zone as sketched in fig. 6.4.

Bloch's theorem spelled out In **??** 6.1 this is written out explicitly for a couple values.

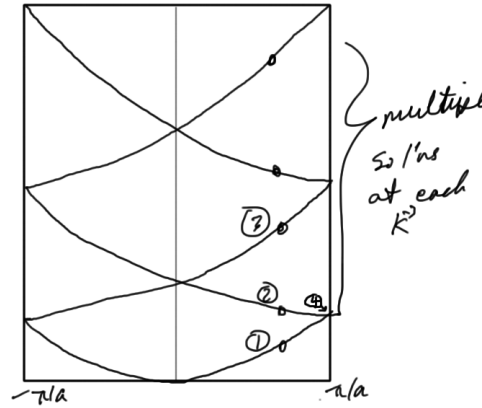

Figure 6.4: First Brillouin zone.

Table 6.1: Bloch's theorem spelled out

	$\Psi_{\mathbf{k}}(x)$	$U_{\mathbf{k}}(x)$	$E(\mathbf{k})$	$C'_{\mathbf{k}}s$
1	$\frac{1}{\sqrt{L}}e^{ikx}$	$\frac{1}{\sqrt{L}}$	$\frac{\hbar^2k^2}{2m}$	$C_k = 1; C_{k-\mathbf{G}} = 0, \mathbf{G} = 0$
2	$\frac{1}{\sqrt{L}}e^{i(k-2\pi/a)kx}$	$\frac{e^{-2\pi x/a}}{\sqrt{L}}$	$\frac{\hbar^2(k-2\pi/a)^2}{2m}$	$C_{k-2\pi/a} = 1$
3	$\frac{1}{\sqrt{L}}e^{i(k+2\pi/a)kx}$	$\frac{e^{2\pi x/a}}{\sqrt{L}}$	$\frac{\hbar^2(k+2\pi/a)^2}{2m}$	$C_{k+2\pi/a} = 1$

Nearly free electron model, periodic potential (cont.)

Reading: [1] ch. 9.

For periodic potential

$$V(\mathbf{r}) = \sum_{\mathbf{G}} V_{\mathbf{G}} e^{i\mathbf{G}\cdot\mathbf{r}}, \tag{6.20}$$

and a trial solution

$$\Psi(\mathbf{r}) = \sum_{\mathbf{k}} C_{\mathbf{k}} e^{i\mathbf{k}\cdot\mathbf{r}}, \tag{6.21}$$

we found that the Schrödinger equation takes the form

$$\left(\frac{\hbar^2\mathbf{k}^2}{2m} - E(\mathbf{k})\right) C_{\mathbf{k}} + \sum_{\mathbf{G}} V_{\mathbf{G}} C_{\mathbf{k}-\mathbf{G}} = 0, \tag{6.22}$$

allowing for a factorization of $\Psi_{\mathbf{k}}$

$$\Psi_{\mathbf{k}}(\mathbf{r}) = \left(\sum_{\mathbf{G}} C_{\mathbf{k}-\mathbf{G}} e^{i\mathbf{G}\cdot\mathbf{r}}\right) e^{i\mathbf{k}\cdot\mathbf{r}} = U_{\mathbf{k}}(\mathbf{r}) e^{i\mathbf{k}\cdot\mathbf{r}}. \tag{6.23}$$

What is $C_{\mathbf{k}-\mathbf{G}}$ on branch $\Psi_{\mathbf{k}}$?

$$\left(\frac{\hbar^2\,(\mathbf{k}-\mathbf{G})^2}{2m} - E(\mathbf{k}-\mathbf{G})\right) C_{\mathbf{k}-\mathbf{G}} + \sum_{\mathbf{G}'} V_{\mathbf{G}'} C_{\mathbf{k}-\mathbf{G}-\mathbf{G}'} = 0. \tag{6.24}$$

Let $\mathbf{G}'' = \mathbf{G} + \mathbf{G}'$, and recall that $E(\mathbf{k}-\mathbf{G}) = E(\mathbf{k})$, giving

$$C_{\mathbf{k}-\mathbf{G}} = \frac{\sum_{\mathbf{G}''} V_{\mathbf{G}''-\mathbf{G}} C_{\mathbf{k}-\mathbf{G}''}}{E(\mathbf{k}) - \frac{\hbar^2(\mathbf{k}-\mathbf{G})^2}{2m}}. \tag{6.25}$$

$C_{\mathbf{k}-\mathbf{G}}$ on a given branch is small unless

$$E(\mathbf{k}) \approx \frac{\hbar^2\,(\mathbf{k}-\mathbf{G})^2}{2m}. \tag{6.26}$$

except at crossing points at $k = (0, \pm\pi/a)$. Only one $C_{\mathbf{k}-\mathbf{G}}$ is large. i.e. at (1) in fig. 6.4

$$E(\mathbf{k}) \approx \frac{\hbar^2\mathbf{k}^2}{2m}. \tag{6.27}$$

so that $C_{\mathbf{k}}$ is large, and all other $C_{\mathbf{k}}$'s are small.

At (2) we have

$$E(\mathbf{k}) \approx \frac{\hbar^2 (k - 2\pi/a)^2}{2m}. \tag{6.28}$$

so that $C_{k-2\pi/a}$ is large, and all other $C_{\mathbf{k}}$'s are small.

However, at $k = (0, \pm\pi/a)$ two or more bands cross (i.e. at (4)). Here

$$\frac{\hbar^2 (k)^2}{2m} = \frac{\hbar^2 (k - 2\pi/a)^2}{2m}, \tag{6.29}$$

so that C_k and $C_{k-2\pi/a}$ are both large.

Generally when

$$C_{\mathbf{k}} = \frac{\sum_{\mathbf{G}''} V_{\mathbf{G}''-\mathbf{G}} C_{\mathbf{k}-\mathbf{G}''}}{E(\mathbf{k}) - \frac{\hbar^2 (\mathbf{k})^2}{2m}} \tag{6.30a}$$

$$C_{\mathbf{k}-\mathbf{G}} = \frac{\sum_{\mathbf{G}''} V_{\mathbf{G}''-\mathbf{G}} C_{\mathbf{k}-\mathbf{G}''}}{E(\mathbf{k}) - \frac{\hbar^2 (\mathbf{k}-\mathbf{G})^2}{2m}}, \tag{6.30b}$$

and $\hbar^2 (\mathbf{k})^2 / 2m = \hbar^2 (\mathbf{k} - \mathbf{G})^2 / 2m$.

Example 6.1: 1D.

Keep 2 C_k's in eq. (6.22), or

$$\begin{aligned} \left(E(k) - \frac{\hbar^2 k^2}{2m} \right) C_k - V_{2\pi/a} C_{k-2\pi/a} &= 0 \\ \left(E(k) - \frac{\hbar^2 (k - 2\pi/a)^2}{2m} \right) C_{k-2\pi/a} - V_{-2\pi/a} C_k &= 0, \end{aligned} \tag{6.31}$$

With solution

$$0 = \begin{vmatrix} \left(\frac{\hbar^2 k^2}{2m} - E(k) \right) & V_{2\pi/a} \\ V_{-2\pi/a} & \left(\frac{\hbar^2 (k-2\pi/a)^2}{2m} - E(k) \right) \end{vmatrix}. \tag{6.32}$$

With $E_k^\circ = \hbar^2 k^2/2m$, and $E_{k-2\pi/a}^\circ = \hbar^2(k-2\pi/a)^2/2m$, we complete the square to find

$$\begin{aligned}
0 &= (E_k^\circ - E)\left(E_{k-2\pi/a}^\circ - E\right) - V_{2\pi/a}V_{-2\pi/a} \\
&= E^2 - E\left(E_k^\circ + E_{k-2\pi/a}^\circ\right) + E_k^\circ E_{k-2\pi/a}^\circ - V_{2\pi/a}V_{-2\pi/a} \\
&= \left(E - \frac{E_k^\circ + E_{k-2\pi/a}^\circ}{2}\right)^2 - \left(\frac{E_k^\circ + E_{k-2\pi/a}^\circ}{2}\right)^2 \\
&\quad + E_k^\circ E_{k-2\pi/a}^\circ - V_{2\pi/a}V_{-2\pi/a} \\
&= \left(E - \frac{E_k^\circ + E_{k-2\pi/a}^\circ}{2}\right)^2 \\
&\quad - \frac{1}{4}\left(E_k^{\circ 2} + {E_{k-2\pi/a}^\circ}^2 + 2E_k^\circ E_{k-2\pi/a}^\circ - 4E_k^\circ E_{k-2\pi/a}^\circ\right) \\
&\quad - V_{2\pi/a}V_{-2\pi/a} \\
&= \left(E - \frac{E_k^\circ + E_{k-2\pi/a}^\circ}{2}\right)^2 - \left(\frac{E_k^\circ - E_{k-2\pi/a}^\circ}{2}\right)^2 - V_{2\pi/a}V_{-2\pi/a},
\end{aligned} \tag{6.33}$$

or

$$E^\pm(k) = \frac{1}{2}\left(E_k^\circ + E_{k-2\pi/a}^\circ\right) \pm \sqrt{\frac{1}{4}\left(E_k^\circ - E_{k-2\pi/a}^\circ\right)^2 + \left|V_{2\pi/a}\right|^2}. \tag{6.34}$$

This is illustrated in fig. 6.5.

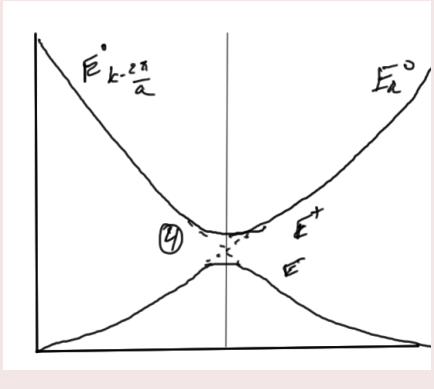

Figure 6.5: Energy solutions for 1D.

A snapshot of a exact Manipulate of this curve is plotted in fig. 6.6.

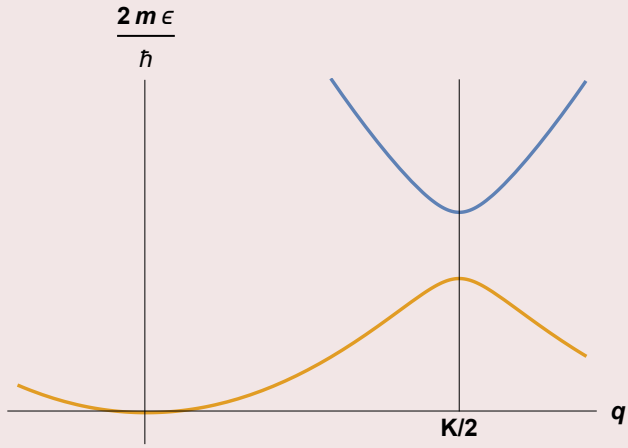

Figure 6.6: Weak binding plot with behavior near Bragg plane.

At the crossing point $k = \pi/a$, and $k - 2\pi/a = -\pi/a$, so that

$$E^{\pm} = \frac{\hbar^2}{2m}\left(\frac{\pi}{a}\right)^2 \pm \left|V_{2\pi/a}\right|, \tag{6.35}$$

or more generally

$$E^{\pm} = \frac{\hbar^2}{2m}\left(\frac{\mathbf{G}}{2}\right)^2 \pm |V_{\mathbf{G}}|. \tag{6.36}$$

This energy gap is sketched in fig. 6.7, with the periodic extension sketched in fig. 6.8.

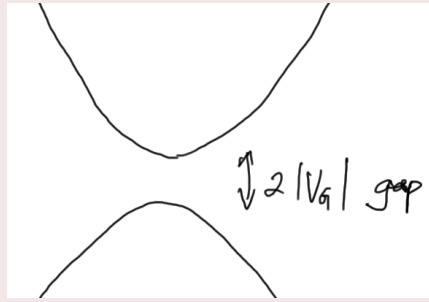

Figure 6.7: Energy gap.

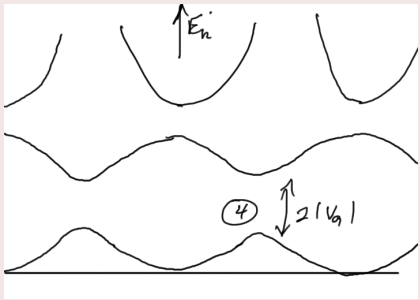

Figure 6.8: Energy gaps and periodic structure.

What does Ψ_k look like at the crossing points (4). Here

$$\Psi_{k=\pi/a} = C_{k=\pi/a} e^{i\frac{\pi}{a}x} + C_{(k=\pi/a)-2\pi/a} e^{i\left(\frac{\pi}{a}-\frac{2\pi}{a}\right)x}. \tag{6.37}$$

Two solutions to $E_k^{\pm}$ correspond to $C_{k=\pi/a} = \pm C_{(k=\pi/a)-2\pi/a}$.

$$\Psi_{k=\pi/a} = \frac{1}{\sqrt{2L}}\left(e^{i\pi x/a} \pm e^{-i\pi x/a}\right), \tag{6.38}$$

Here L is the length of the 1d system. Note that eq. (6.38) is one of

$$\begin{aligned} &\cos\frac{\pi}{a}x \\ &\sin\frac{\pi}{a}x \end{aligned} \tag{6.39}$$

These solutions are sketched along with the potential in fig. 6.9.

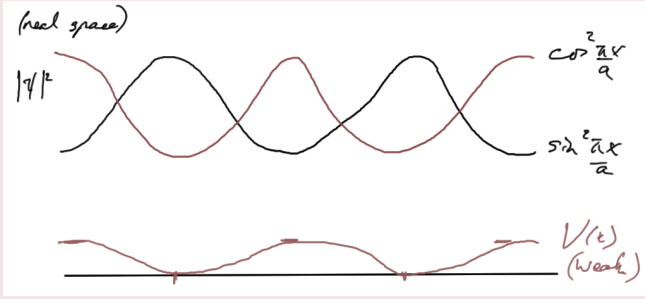

Figure 6.9: Real space 1D solutions and potential.

The cosine is the lower energy branch because electron density is high where $V(x)$ is low. The sine is the higher energy branch because electron density is high when $V(x)$ is high.

6.3 TIGHT BINDING MODEL.

Reading: [10] §7.3, [1] ch. 10.

Assume a periodic lattice with large lattice parameter a, so that atomic potential $V_a(\mathbf{r} - \mathbf{r}_n)$ and wave functions $\phi(\mathbf{r} - \mathbf{r}_n)$ don't overlap much between neighbors, as sketched in fig. 6.10. The potential $\phi_i(\mathbf{r} - \mathbf{r}_n)$ satisfies

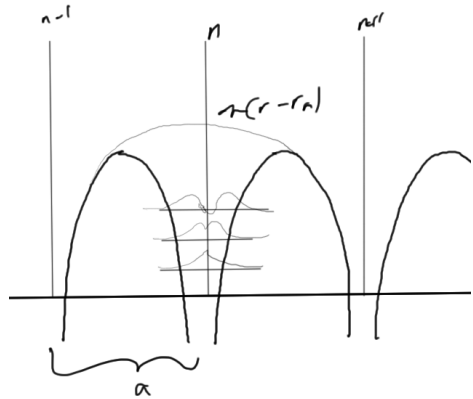

Figure 6.10: Tight binding lattice.

$$\hat{H}_A \phi_i(\mathbf{r} - \mathbf{r}_n) = E_i \phi(\mathbf{r} - \mathbf{r}_n). \tag{6.40}$$

where

$$\hat{H}_A = -\frac{\hbar}{2m}\boldsymbol{\nabla} + V_A(\mathbf{r} - \mathbf{r}_n). \tag{6.41}$$

The one electron Hamiltonian

$$\begin{aligned}\hat{H} &= -\frac{\hbar}{2m}\boldsymbol{\nabla}^2 + \sum_{n'} V_A(\mathbf{r} - \mathbf{r}'_n) \\ &= -\frac{\hbar}{2m}\boldsymbol{\nabla}^2 + V_A(\mathbf{r} - \mathbf{r}_n) + \sum_{n' \neq n} V_A(\mathbf{r} - \mathbf{r}'_n) \\ &= \hat{H}_A(\mathbf{r} - \mathbf{r}_n) + v(\mathbf{r} - \mathbf{r}_n).\end{aligned} \tag{6.42}$$

To get an idea what $v(\mathbf{r}-\mathbf{r}_n)$ might look like, consider $v(x) = -1/|x|$, with $\mathbf{r}_n = 10n\hat{\mathbf{x}}$. The potential looks like fig. 6.11, with the periodic extension in fig. 6.12, and finally, $v(\mathbf{r}-\mathbf{r}_0)$ in fig. 6.13. In the last figure we see the omission of the infinite negative peak at the origin, allowing the trailing contributions from neighboring sites to add up to a value greater than the peak values at the other sites.

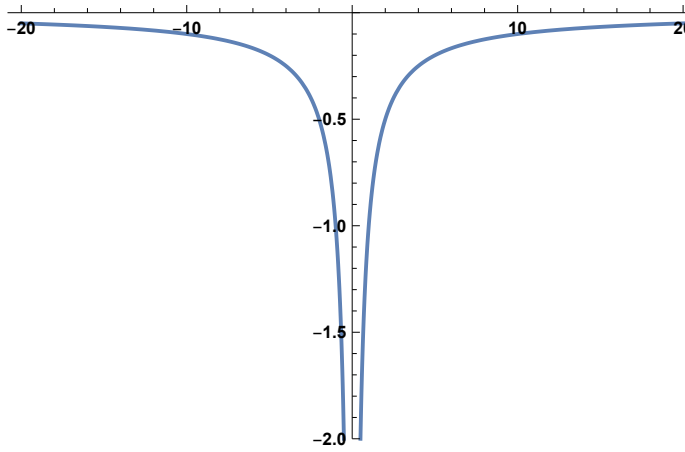

Figure 6.11: Inverse radial potential.

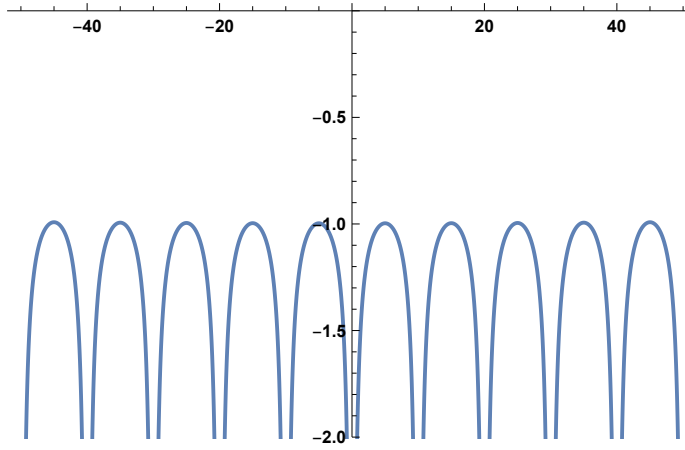

Figure 6.12: Inverse radial periodically extended.

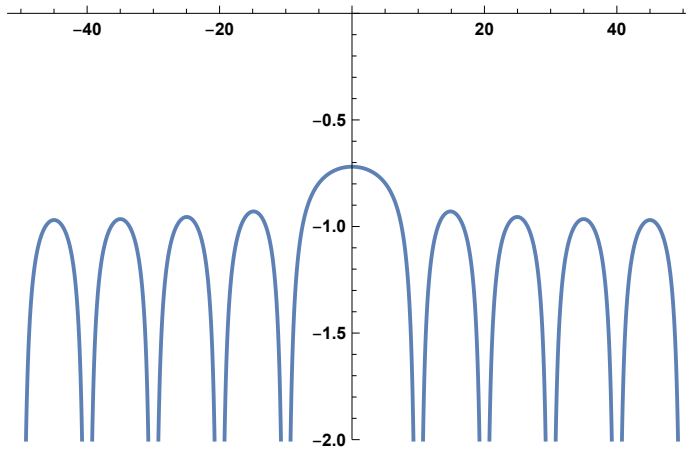

Figure 6.13: Inverse radial, period extension, with one omission.

Look for a solution that is a Linear Combination of Atomic Orbitals (LCAO).

$$\begin{aligned}\Psi_{\mathbf{k}}(\mathbf{r}) \sim \Phi_{\mathbf{k}}(\mathbf{r}) &= \sum_n a_n \phi_i(\mathbf{r} - \mathbf{r}_n) \\ &= \sum_n e^{i\mathbf{k}\cdot\mathbf{r}_n} \phi_i(\mathbf{r} - \mathbf{r}_n),\end{aligned} \tag{6.43}$$

so by Bloch's theorem

$$\Phi_{\mathbf{k}}(\mathbf{r}) = U_{\mathbf{k}} e^{i\mathbf{k}\cdot\mathbf{r}}, \tag{6.44}$$

implies

$$\Phi_{\mathbf{k}}(\mathbf{r} + \mathbf{r}_m) = \Phi_{\mathbf{k}}(\mathbf{r}) e^{i\mathbf{k}\cdot\mathbf{r}_m}, \tag{6.45}$$

$$\begin{aligned}\Phi_{\mathbf{k}}(\mathbf{r} + \mathbf{r}_m) &= \sum_n e^{i\mathbf{k}\cdot\mathbf{r}_n} \phi_i(\mathbf{r} + \mathbf{r}_m - \mathbf{r}_n) \\ &= e^{i\mathbf{k}\cdot\mathbf{r}_m} \sum_n e^{i\mathbf{k}\cdot(\mathbf{r}_n - \mathbf{r}_m)} \phi_i(\mathbf{r} + (\mathbf{r}_n - \mathbf{r}_m)).\end{aligned} \tag{6.46}$$

$$\Phi_{\mathbf{k}+\mathbf{G}} = \sum_n e^{i\mathbf{k}\cdot\mathbf{r}_n} \underbrace{e^{i\mathbf{G}\cdot\mathbf{r}_n}}_{1} \phi_i(\mathbf{r} - \mathbf{r}_n) = \Phi_{\mathbf{k}}(\mathbf{r}). \tag{6.47}$$

Normalization Calculate

$$E(\mathbf{k}) = \frac{\langle \Phi_\mathbf{k} | \hat{H} | \Phi_\mathbf{k} \rangle}{\langle \Phi_\mathbf{k} | \Phi_\mathbf{k} \rangle}. \tag{6.48}$$

With

$$\begin{aligned} \langle \Phi_\mathbf{k} | \Phi_\mathbf{k} \rangle &= \sum_{n,m} e^{i\mathbf{k}\cdot(\mathbf{r}_n - \mathbf{r}_m)} \times \int d\mathbf{r} \phi_i^*(\mathbf{r} - \mathbf{r}_m)\phi_i(\mathbf{r} - \mathbf{r}_n) \\ &= \begin{cases} 1 & \text{if } m = n \\ 0 & \text{otherwise} \end{cases} \\ &\approx N. \end{aligned} \tag{6.49}$$

$E(\mathbf{k})$

$$\begin{aligned} &\approx \frac{1}{N} \sum_{n,m} e^{i\mathbf{k}\cdot(\mathbf{r}_n - \mathbf{r}_m)} \int d\mathbf{r} \phi_i^*(\mathbf{r} - \mathbf{r}_m)(\overbrace{\hat{H}_A(\mathbf{r} - \mathbf{r}_n) + v(\mathbf{r} - \mathbf{r}_n)}^{\text{exact}})\phi_i(\mathbf{r} - \mathbf{r}_n) \\ &\approx \sum_{n,m} e^{i\mathbf{k}\cdot(\mathbf{r}_n - \mathbf{r}_m)} \int d\mathbf{r} \phi_i^*(\mathbf{r} - \mathbf{r}_m) \left(E_i + v(\mathbf{r} - \mathbf{r}_n)\right) \phi_i(\mathbf{r} - \mathbf{r}_n). \end{aligned} \tag{6.50}$$

In the integral we have from $\hat{H}_A$, a value of E_i if $m = n$f, and zero otherwise. For the v contribution to the integral, we have

- $m = n$. Large $\phi_i^*(\mathbf{r} - \mathbf{r}_m)\phi_i(\mathbf{r} - \mathbf{r}_n)$. We've got $v(\mathbf{r} - \mathbf{r}_n)$ small near $\mathbf{r}_n$.
- $m = n \pm 1$. Near $\mathbf{r}_m$, ϕ_i and v are both large, and $\phi_i(\mathbf{r} - \mathbf{r}_n)$ is small.

In short we have to keep both terms. Let

$$\begin{aligned} -A &= \int d\mathbf{r} \phi_i^*(\mathbf{r} - \mathbf{r}_n) v(\mathbf{r} - \mathbf{r}_n) \phi_i(\mathbf{r} - \mathbf{r}_n) \\ -B &= \int d\mathbf{r} \phi_i^*(\mathbf{r} - \mathbf{r}_m) v(\mathbf{r} - \mathbf{r}_n) \phi_i(\mathbf{r} - \mathbf{r}_n) \end{aligned} \tag{6.51}$$

So

$$E(\mathbf{k}) \approx \frac{1}{N} \left(\sum_n E_i - \sum_n A - \sum_{n,m} e^{i\mathbf{k}\cdot(\mathbf{r}_n - \mathbf{r}_m)} B \right), \tag{6.52}$$

or

$$E(\mathbf{k}) \approx E_i - A - B \sum_{m=\text{nn of n}} e^{i\mathbf{k}\cdot(\mathbf{r}_n - \mathbf{r}_m)}. \tag{6.53}$$

In one dimension

Example 6.2: 1D lattice.

For 1D we have

$$\mathbf{r}_n - \mathbf{r}_m = \pm a, \tag{6.54}$$

which implies the nearest neighbor sum is

$$\sum_{nn} \left(e^{ika} + e^{-ika} \right) = 2\cos ka. \tag{6.55}$$

So

The hopping term

$$E(k) \approx E_i - A - \boxed{2B\cos ka}. \tag{6.56}$$

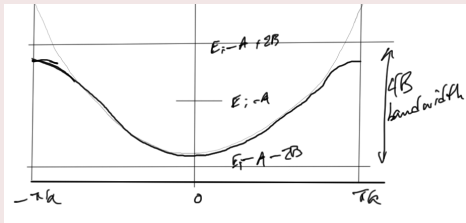

Figure 6.14: Tight binding 1D example.

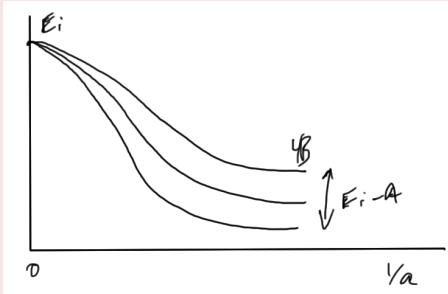

Figure 6.15: Dependence on a.

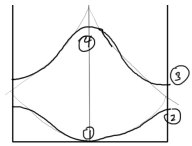

Figure 6.16: NFE comparison points.

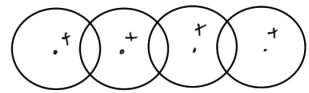

Figure 6.17: (1) bonding s orbitals.

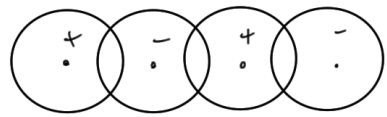

Figure 6.18: (2) antibonding s orbitals.

Correspondence with the Nearly free electron model

6.4 3D BAND STRUCTURES, FERMI SURFACES OF REAL METALS.

Reading: [10] §7.4 Consider a nearly free electron metal, and a hypothetical simple cubic system as in fig. 6.21.

We can ask some questions

- What is the occupancy?
- Where is E_F (the Fermi energy)?

Consider alkali metals, such as Li $1s^2 2s^1$
Is tight-binding-like fully occupied.
$2 \times 1s$ electrons per atom.

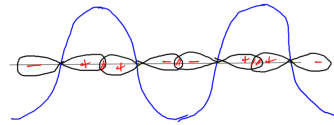

Figure 6.19: (3) bonding p orbitals.

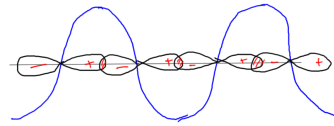

Figure 6.20: (4) antibonding p orbitals.

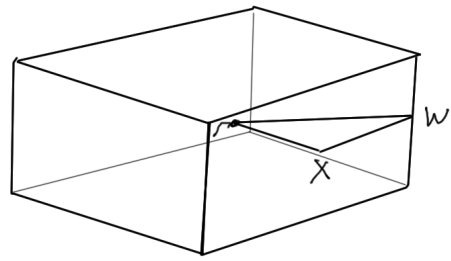

Figure 6.21: Simple cubic Brillouin zone.

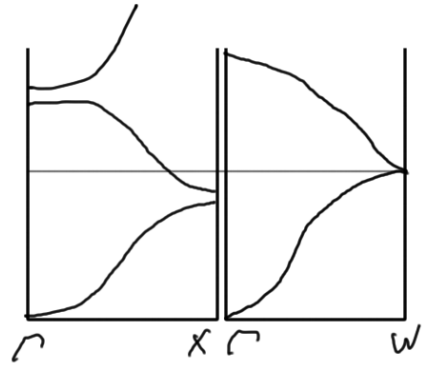

Figure 6.22: Two frequency distributions.

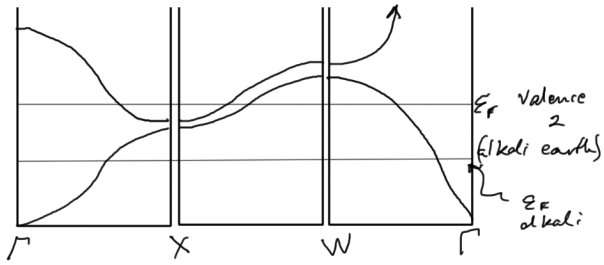

Figure 6.23: Center edge contour distribution.

In 1 band $(2\pi)^3/a^3$ is the volume of k-space, and we have

$$\frac{\cancel{(2\pi)^3}}{a^3} \times \underbrace{2}_{\text{spin}} \overbrace{\frac{V}{\cancel{(2\pi)^3}}}^{\text{density of k points}}, \tag{6.57}$$

for

$$2\frac{V}{a^3} = 2N, \tag{6.58}$$

where N is the number of unit cells.

The 2s orbitals stick out a long way, so this is free electron like. We have half filled orbitals. Where E_F crosses $E(k)$ is a Fermi surface. It never gets close to the Brillouin zone boundary.

This is nearly spherical. See slides for the true Brillouin zone diagram for Li.

Question: In class when discussing Li, K, Na tight binding, and it's relation to the Fermi surface, we were told that the Li and other alkali-metal Fermi surfaces never get close to the BZ boundary, and that they were approximately spherical.

I don't understand how we arrived at the conclusion that for these s-orbital elements "the Fermi surface never gets close to the BZ boundary", nor why those surfaces would necessarily be approximately spherical?

Answer: Unlike the calculation in problem set 8, the band structure of the alkali metals and alkali earths is free-electron-like. This means that the dispersion relation is parabolic, except near the Brillouin zone boundary. So if the Fermi surface never gets close to a Brillouin zone boundary, $E(k_F) \simeq \hbar^2 k_F^2/2m$, independent of direction in k-space, so the Fermi surface is spherical.

You can tell that the Fermi surface doesn't go close to the BZ boundary by calculating the volume of the Fermi sphere, compared with the volume of the Brillouin zone. This doesn't work for the tight-binding band structure, because the dispersion is anisotropic even far from the Brillouin zone.

A very helpful demonstration of exactly that calculation can be found in [13], under section 'Alkali metals'. To understand the details of that calculation (see: bccBasisVectors.nb), it is helpful to note that a BCC basis is

$$\mathbf{a}_i \in \left\{ \frac{a}{2}\begin{bmatrix}1\\1\\1\end{bmatrix}, \frac{a}{2}\begin{bmatrix}1\\1\\-1\end{bmatrix}, a\begin{bmatrix}1\\0\\0\end{bmatrix} \right\}, \tag{6.59}$$

for which the reciprocal basis is

$$\mathbf{g}_i \in \left\{ \frac{2\pi}{a}\begin{bmatrix}0\\1\\1\end{bmatrix}, \frac{2\pi}{a}\begin{bmatrix}0\\1\\-1\end{bmatrix}, \frac{2\pi}{a}\begin{bmatrix}1\\-1\\0\end{bmatrix} \right\}. \tag{6.60}$$

This point is also discussed with typical clarity in [1] ch. 15, "The Alkaki Metals".

Valence 2 For alkali earth's Mg, Ca, $\cdots$, we have $2 \times 2s$ valence electrons. This doesn't fill the band, because of dispersion.

Define a free electron sphere. It extends beyond the first Brillouin zone. This is incorrectly sketched in fig. 6.24 as a simple cubic (actual is perhaps FCC).

Examination hint: For a picture like this, understand what happens at the boundary, and how it reconstructs.

Valence 3 Considering a material such as Al, which is in valance 3. See slide.

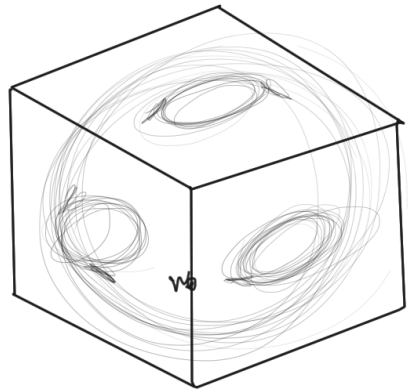

Figure 6.24: Fermi surfaces for Cu like simple cubic.

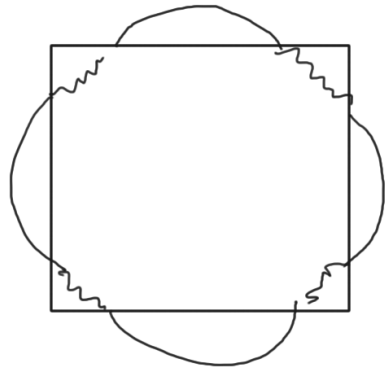

Figure 6.25: Copper Fermi surface side view?.

Examination hint: Valence three won't be examinable

d electron systems We have two kinds of valence electrons.

- s electrons. Free electron like.
- d electrons. compact orbitals that are tight binding like.

Looking with an experienced eye, we see two types of bands. The first are the s-bands that are free electron like and rapidly disburse. This is roughly sketched in fig. 6.26. The others are the d orbital band that disperse a bit, but not very much. What actually happens in here where they cross is also illustrated in the magnified section.

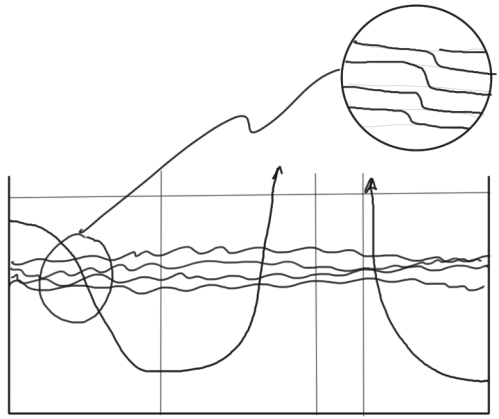

Figure 6.26: d electron distribution.

The occupancy for Cu is $3d^{10}4s^1$. The d orbitals are filled.

E_F intersects 4*s* bands, we have a nearly free electron Fermi surface.

The reason that copper is copper coloured is because there's a high density of states, with absorption in blue, resulting in a brown look.

We have something similar for Ag and Au.

From Sc to Ni, or Y to Pd, or La to Pt, the d orbitals are partially occupied, and E_F is among the d bands. This ends up being a complicated Fermi surface, and there is a high density of states at E_F (see table in slides).

These atoms with $3d$ valence electrons are very prone to magnetism. The atoms with $4d$ valence electrons are very prone to superconductivity.

A high density of states in physics makes for interesting effects.

6.5 PROBLEMS.

Exercise 6.1 Nearly free electron model. (*2013 ps7 p2*)

Figure 6.27 shows the free electron dispersion relation for a one-dimensional metal, in the reduced zone scheme.

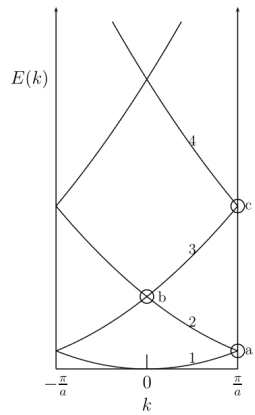

Figure 6.27: dispersion relation for a one-dimensional metal.

a. For each of the branches (1), (2), (3) and (4), state which of the coefficients C_{k-G} are non-zero, and give the corresponding $u_k(x)$ in the electron wave-function

$$\psi_k(x) = \sum_G C_{k-G} e^{-iGx} e^{ikx} = u_k(x) e^{ikx}. \tag{6.61}$$

b. For the circled regions there are two nearly-degenerate energy solutions. If a nearly free electron potential

$$V(x) = V_1 cos(2\pi x/a) + V_2 cos(4\pi x/a). \tag{6.62}$$

is introduced, what is the magnitude of the energy gap that opens up at the band crossings in the circled regions 'a', 'b' and 'c'?

c. What are the gaps at 'a', 'b' and 'c' if instead the lattice potential is described by a periodic array of delta functions:

$$V(x) = \sum_{-\infty}^{\infty} V_\circ \delta(x - na). \tag{6.63}$$

d. Write the form of the wave-function for the two solutions at the level crossing at 'b' on the diagram (i.e. where $k = 0$). Sketch in real space the charge density associated with these solutions relative to the atom positions on the one-dimensional lattice. Also, write these wave functions in the Bloch form, $\psi_k(x) = e^{ikx} u_k(x)$, and thus identify $u_k(x)$ for the two solutions at 'b'.

e. Near point 'a', investigate how the wave-function of the lower-energy branch (branch $G = 0$) evolves as you move away from the Brillouin zone boundary. To do this, calculate $|\psi_k(x)|^2$, and from this sketch the charge density in real space, explaining how it changes as k moves away from π/a. If it helps, you may start far enough away from the Brillouin zone boundary that $E^\circ_{k-2\pi/a} - E^\circ_k \gg \left|V_{2\pi/a}\right|$.

Answer for Exercise 6.1

Part a. Considering each branch in turn:

1. On this branch, the wave function is

$$\psi_k(x) = \frac{1}{\sqrt{a}} e^{ikx}, \tag{6.64}$$

so

$$\begin{aligned} u_k(x) &= \frac{1}{\sqrt{a}} \\ C_k &= \frac{1}{\sqrt{a}} \\ C_{k-2\pi m/a} &= 0, \qquad m \in \{\pm 1, \pm 2, \cdots\}. \end{aligned} \tag{6.65}$$

2. On this branch, the wave function is

$$\begin{aligned}\psi_k(x) &= \frac{1}{\sqrt{a}} e^{i(k-2\pi/a)x} \\ &= \left(\frac{1}{\sqrt{a}} e^{-i\frac{2\pi}{a}x}\right) e^{ikx},\end{aligned} \tag{6.66}$$

so

$$\begin{aligned}u_k(x) &= \frac{1}{\sqrt{a}} e^{-i\frac{2\pi}{a}x} \\ C_{k-2\pi/a} &= \frac{1}{\sqrt{a}} \\ C_{k-2\pi m/a} &= 0, \qquad m \in \{0, -1, \pm 2, \pm 3, \cdots\}.\end{aligned} \tag{6.67}$$

3. On this branch, the wave function is

$$\begin{aligned}\psi_k(x) &= \frac{1}{\sqrt{a}} e^{i(k+2\pi/a)x} \\ &= \left(\frac{1}{\sqrt{a}} e^{-i\frac{-2\pi}{a}x}\right) e^{ikx},\end{aligned} \tag{6.68}$$

so

$$\begin{aligned}u_k(x) &= \frac{1}{\sqrt{a}} e^{i\frac{2\pi}{a}x} \\ C_{k+2\pi/a} &= \frac{1}{\sqrt{a}} \\ C_{k-2\pi m/a} &= 0, \qquad m \in \{0, 1, \pm 2, \pm 3, \cdots\}.\end{aligned} \tag{6.69}$$

4. On this branch, the wave function is

$$\begin{aligned}\psi_k(x) &= \frac{1}{\sqrt{a}} e^{i(k-4\pi/a)x} \\ &= \left(\frac{1}{\sqrt{a}} e^{-i\frac{4\pi}{a}x}\right) e^{ikx},\end{aligned} \tag{6.70}$$

so

$$\begin{aligned}u_k(x) &= \frac{1}{\sqrt{a}} e^{-i\frac{4\pi}{a}x} \\ C_{k-4\pi/a} &= \frac{1}{\sqrt{a}} \\ C_{k-2\pi m/a} &= 0, \qquad m \in \{0, \pm 1, -2, \pm 3, \pm 4, \cdots\}.\end{aligned} \tag{6.71}$$

Part b. With $G = 2\pi/a$, we can write the potential of eq. (6.62) as

$$V(x) = \frac{V_1}{2}\left(e^{iGx} + e^{-iGx}\right) + \frac{V_2}{2}\left(e^{2iGx} + e^{-2iGx}\right). \tag{6.72}$$

That is

$$\begin{aligned} V_{1G} &= V_{-1G} = \frac{V_1}{2} \\ V_{2G} &= V_{-2G} = \frac{V_2}{2}. \end{aligned} \tag{6.73}$$

The coefficients C_k would follow from a solution of

$$\begin{aligned} 0 = &\left(\frac{\hbar^2}{2m}(k - nG)^2 - E\right) C_{k-nG} \\ &+ V_G\left(C_{k-(1+n)G} + C_{k+(1-n)G}\right) + V_{2G}\left(C_{k-(2+n)G} + C_{k+(2-n)G}\right). \end{aligned} \tag{6.74}$$

Written out in full this includes

$$\begin{aligned} 0 &= \left(\frac{\hbar^2}{2m}(k+2G)^2 - E\right) C_{k+2G} + V_G\left(C_{k+G} + C_{k+3G}\right) + V_{2G}\left(C_k + C_{k+4G}\right) \\ 0 &= \left(\frac{\hbar^2}{2m}(k+G)^2 - E\right) C_{k+G} + V_G\left(C_k + C_{k+2G}\right) + V_{2G}\left(C_{k-G} + C_{k+3G}\right) \\ 0 &= \left(\frac{\hbar^2}{2m}k^2 - E\right) C_k + V_G\left(C_{k-G} + C_{k+G}\right) + V_{2G}\left(C_{k-2G} + C_{k+2G}\right) \\ 0 &= \left(\frac{\hbar^2}{2m}(k-G)^2 - E\right) C_{k-G} + V_G\left(C_{k-2G} + C_k\right) + V_{2G}\left(C_{k-3G} + C_{k+G}\right) \\ 0 &= \left(\frac{\hbar^2}{2m}(k-2G)^2 - E\right) C_{k-2G} + V_G\left(C_{k-3G} + C_{k-G}\right) + V_{2G}\left(C_{k-4G} + C_k\right). \end{aligned} \tag{6.75}$$

Dropping $C_{k-4G}, C_{k-3G}, C_{k+3G}, C_{k+4G}$, this is

$$0 = \begin{bmatrix} E^\circ_{k-2G} - E & V_G & V_{2G} & 0 & 0 \\ V_G & E^\circ_{k-G} - E & V_G & V_{2G} & 0 \\ V_{2G} & V_G & E^\circ_k - E & V_G & V_{2G} \\ 0 & V_{2G} & V_G & E^\circ_{k+G} - E & V_G \\ 0 & 0 & V_{2G} & V_G & E^\circ_{k+2G} - E \end{bmatrix} \begin{bmatrix} C_{k-2G} \\ C_{k-G} \\ C_k \\ C_{k+G} \\ C_{k+2G} \end{bmatrix},$$

(6.76)

or

$$0 = \begin{vmatrix} E^\circ_{k-2G} - E & V_G & V_{2G} & 0 & 0 \\ V_G & E^\circ_{k-G} - E & V_G & V_{2G} & 0 \\ V_{2G} & V_G & E^\circ_k - E & V_G & V_{2G} \\ 0 & V_{2G} & V_G & E^\circ_{k+G} - E & V_G \\ 0 & 0 & V_{2G} & V_G & E^\circ_{k+2G} - E \end{vmatrix} \tag{6.77}$$

At point (a) we can get a rough idea of the separation by further dropping $C_{k-G}, C_{k+G}, C_{k+2G}$ terms, so that the system to solve is

$$0 = \begin{bmatrix} E^\circ_{k-G} - E & V_G \\ V_G & E^\circ_k - E \end{bmatrix} \begin{bmatrix} C_{k-G} \\ C_k \end{bmatrix}. \tag{6.78}$$

At the boundary where $E^\circ_k = E^\circ_{k-G}$, this is

$$0 = \begin{vmatrix} E^\circ_k - E & V_G \\ V_G & E^\circ_k - E \end{vmatrix}, \tag{6.79}$$

or

$$E_\pm = E^\circ_k \pm V_G = E \pm \frac{V_1}{2}. \tag{6.80}$$

The (approximate) separation between the energy curves at that point is

$$\boxed{\Delta E = E_+ - E_- = V_1.} \tag{6.81}$$

At point (b) dropping all but the C_{k-G}, C_{k+G} terms gives us

$$0 = \begin{bmatrix} E^\circ_{k-G} - E & V_{2G} \\ V_{2G} & E^\circ_{k+G} - E \end{bmatrix} \begin{bmatrix} C_{k-G} \\ C_{k+G} \end{bmatrix}. \tag{6.82}$$

Taking the determinant and noting that at the intersection $E^\circ_{k-G} = E^\circ_{k+G}$, this has solution

$$E_\pm = E^\circ_{k-G} \pm V_{2G} = E \pm \frac{V_2}{2}. \tag{6.83}$$

This time the approximate separation between the energy curves at that point is

$$\boxed{\Delta E = E_+ - E_- = V_2.} \tag{6.84}$$

Finally, at point (c) we have $E^\circ_{k-2G} = E^\circ_{k+G}$. Our system eq. (6.76) can be approximated by

$$0 = \begin{bmatrix} E^\circ_{k-2G} - E & 0 \\ 0 & E^\circ_{k+G} - E \end{bmatrix} \begin{bmatrix} C_{k-2G} \\ C_{k+G} \end{bmatrix}, \tag{6.85}$$

with approximate solution

$$E_\pm = E^\circ_{k+G}. \tag{6.86}$$

We find that the approximate separation at this point is zero. Should we require a better estimate, we must retain of more of the coefficients C_{k-hG}.

Part c. Let's start by assuming the periodic delta function potential has a Fourier representation, and computing the associated Fourier components

$$V(x) = V_\circ \sum_n \delta(x - na) = \sum_h C_{G_h} e^{-iG_h x}, \tag{6.87}$$

where

$$G_h = Gh = \frac{2\pi}{a} h, \tag{6.88}$$

and h is an integer. The Fourier coefficient follows directly from the Fourier integral

$$\begin{aligned} \int_{-1/2}^{1/2} du V(ua) e^{ih'Gau} &= \sum_h C_{G_h} \int_{-1/2}^{1/2} du e^{ih'Gau} e^{-iGhau} \\ &= \sum_h C_{G_h} \int_{-1/2}^{1/2} du e^{2\pi i(h'-h)u} \\ &= \sum_h C_{G_h} \delta_{h,h'} \\ &= C_{G_{h'}}. \end{aligned} \tag{6.89}$$

Integrating the LHS gives us

$$\begin{aligned} C_{G_h} &= \int_{-1/2}^{1/2} du V(ua) e^{ihGau} \\ &= V_\circ \int_{-1/2}^{1/2} du \sum_n \delta((u-n)a) e^{2\pi i h u}. \end{aligned} \tag{6.90}$$

Only one of the delta functions in the $\sum_n$ falls in $[-1/2, 1/2]$, so this integral is just $V_\circ/a$, leaving

$$V(x) = \frac{V_\circ}{a} \sum_h e^{iG_h x}. \tag{6.91}$$

Schrödinger's equation for this potential is

$$0 = \sum_{k'} \left(\frac{\hbar^2 (k')^2}{2m} - E \right) C_{k'} e^{ik'x} + \frac{V_\circ}{a} \sum_G e^{iGx} C_{k'} e^{ik'x}, \tag{6.92}$$

Operating with $\int dx e^{-ikx}$ gives

$$0 = \left(\frac{\hbar^2 k^2}{2m} - E \right) C_k + \frac{V_\circ}{a} \sum_G C_{k-G}. \tag{6.93}$$

Noting that

$$0 = \left(\frac{V_\circ}{a} + \frac{\hbar^2 k^2}{2m} - E \right) C_k + \frac{V_\circ}{a} \sum_{G \neq k} C_{k-G}, \tag{6.94}$$

we could put this in matrix form, but that's not too helpful since the matrix is infinite dimensional. It's possible to find an implicit relation for $E(k)$ by summing C_k, since

$$C_k = \frac{V_\circ}{a} \sum_G C_{k-G} \frac{1}{E - \frac{\hbar^2 k^2}{2m}}, \tag{6.95}$$

and

$$\cancel{\sum_k C_k} = \frac{V_\circ}{a} \cancel{\sum_G C_{k-G}} \sum_k \frac{1}{E - \frac{\hbar^2 k^2}{2m}}, \tag{6.96}$$

or

$$\frac{a}{V_\circ} = \sum_k \frac{1}{E - \frac{\hbar^2 k^2}{2m}}. \tag{6.97}$$

While I'd guess that this can be summed using the Euler-MacLaren theorem, Mathematica says this is

$$\sqrt{E} = \frac{V_\circ}{a} \frac{2\pi m}{\hbar^2} \cot\left(2\pi m \frac{\sqrt{E}}{\hbar^2} \right). \tag{6.98}$$

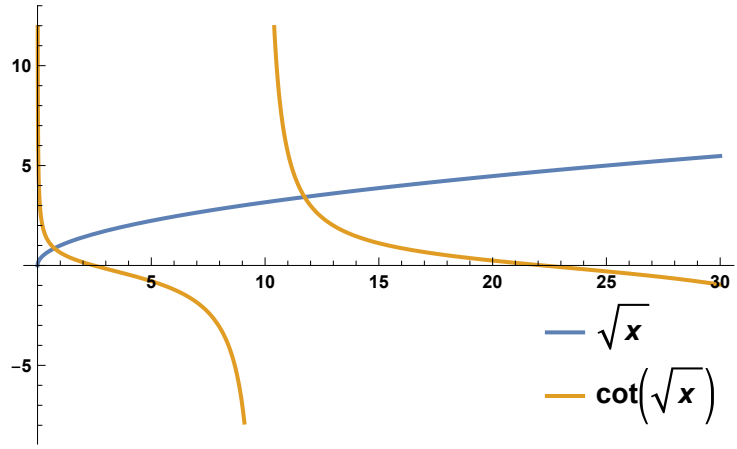

Figure 6.28: Implicit function curves for delta-function-potential energy.

This implicit function has two discrete solutions, as illustrated by representative plots in fig. 6.28. This could clearly be solved numerically. None of this helps with an estimate of the gap at the crossing points. Considering point (a) as representative, let's make a crude approximation of eq. (6.94) as

$$0 \approx \begin{bmatrix} \frac{V_\circ}{a} + \frac{\hbar^2(k-G)^2}{2m} - E & \frac{V_\circ}{a} \\ \frac{V_\circ}{a} & \frac{V_\circ}{a} + \frac{\hbar^2 k^2}{2m} - E \end{bmatrix} \begin{bmatrix} C_{k-G} \\ C_k \end{bmatrix}. \tag{6.99}$$

At the crossing (a) where $E_k^\circ = E_{k-G}^\circ$ we have

$$0 \approx \begin{vmatrix} \frac{V_\circ}{a} + E_k^\circ - E & \frac{V_\circ}{a} \\ \frac{V_\circ}{a} & \frac{V_\circ}{a} + E_k^\circ - E \end{vmatrix}, \tag{6.100}$$

or

$$E_\pm \approx E_k^\circ - \frac{V_\circ}{a} \pm \left|\frac{V_\circ}{a}\right|. \tag{6.101}$$

The gap distance at this point (or the others) is thus approximately

$$\boxed{\Delta E \approx 2\frac{V_\circ}{a}.} \tag{6.102}$$

Part d. From eq. (6.82) we see that the coefficients are related by

$$C_{k-G} = -C_{k+G}\frac{V_{2G}}{E_{k-G}^\circ - E}, \tag{6.103}$$

so our wave functions $\psi = \sum_k C_k e^{ikx}$ are

$$\psi_\pm \propto \left(E^\circ_{k-G} - E_\pm\right) e^{i(k+G)x} - V_{2G} e^{i(k-G)x}. \tag{6.104}$$

However, $V_{2G} = V_2/2$, and $E^\circ_{k-G} - E_\pm = \pm V_2/2$, so we have

$$\psi_\pm \propto e^{i(k+G)x} \mp e^{i(k-G)x}. \tag{6.105}$$

Normalizing and putting in Bloch form, these are

$$\begin{aligned} \psi_+ &= \sqrt{\frac{2}{a}} e^{ikx} \sin(Gx) \\ \psi_+ &= \sqrt{\frac{2}{a}} e^{ikx} \cos(Gx). \end{aligned} \tag{6.106}$$

or

$$\begin{aligned} u_{k+}(x) &= \sqrt{\frac{2}{a}} \sin(Gx) \\ u_{k-}(x) &= \sqrt{\frac{2}{a}} \cos(Gx). \end{aligned} \tag{6.107}$$

These have respective charge densities

$$\begin{aligned} \rho_+ &= \frac{2e}{a} \sin^2(Gx) \\ \rho_- &= \frac{2e}{a} \cos^2(Gx). \end{aligned} \tag{6.108}$$

These are sketched in fig. 6.29.

Part e. We start with eq. (6.78), for which we find

$$E_\pm = \frac{1}{2}\left(E^\circ_{k-G} + E^\circ_k \pm \sqrt{\left(E^\circ_k - E^\circ_{k-G}\right)^2 + V_1^2}\right), \tag{6.109}$$

so that the wave function coefficients are given by

$$C_{k-G}\frac{1}{2}\left(E^\circ_{k-G} - E^\circ_k \mp \sqrt{\left(E^\circ_k - E^\circ_{k-G}\right)^2 + V_1^2}\right) = -C_k \frac{V_1}{2}. \tag{6.110}$$

This gives

$$\psi_{k,\pm}(x) \propto -V_1 e^{i(k-G)x} + \left(E^\circ_{k-G} - E^\circ_k \mp \sqrt{\left(E^\circ_k - E^\circ_{k-G}\right)^2 + V_1^2}\right) e^{ikx}.$$

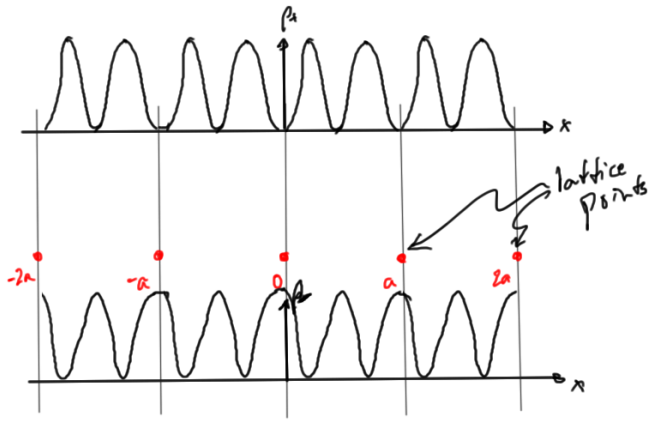

Figure 6.29: Density plots.

(6.111)

The kinetic energy difference is

$$\begin{aligned} E^{\circ}_{k-G} - E^{\circ}_{k} &= \frac{\hbar^2 (k-G)^2}{2m} - \frac{\hbar^2 k^2}{2m} \\ &= \frac{\hbar^2 \left(G^2 - 2kG\right)}{2m}, \end{aligned} \tag{6.112}$$

so we have

$$\begin{aligned} \psi_{k,\pm}(x) \propto -V_1 e^{i(k-G)x} + \Bigg(& \frac{\hbar^2 \left(G^2 - 2kG\right)}{2m} \\ & \mp \sqrt{\left(\frac{\hbar^2 \left(G^2 - 2kG\right)}{2m} \right)^2 + V_1^2} \Bigg) e^{ikx} \end{aligned} \tag{6.113}$$

To make this less cumbersome, let's write

$$\epsilon_{\pm}(k) = \left(\frac{\hbar^2 G \left(G - 2k\right)}{2m} \mp \sqrt{\left(\frac{\hbar^2 G \left(G - 2k\right)}{2m} \right)^2 + V_1^2} \right). \tag{6.114}$$

Writing out $G = 2\pi/a$ explicitly, the (still unnormalized) wave functions are

$$\psi_{k,\pm}(x) = \left(-V_1 e^{-i\pi x/a} + \epsilon_{\pm}(k) e^{i\pi x/a} \right) e^{-i\pi x/a} e^{ikx}, \tag{6.115}$$

and the densities are proportional to

$$\rho_{k,\pm}(x) = \left| -V_1 e^{-i\pi x/a} + \epsilon_{\pm}(k) e^{i\pi x/a} \right|^2. \tag{6.116}$$

We are interested in the lower energy branch $\rho_{k,-}$ where

$$\begin{aligned} \epsilon_-(k) &= \left(\frac{\hbar^2 G\,(G-2k)}{2m} + \sqrt{\left(\frac{\hbar^2 G\,(G-2k)}{2m} \right)^2 + V_1^2} \right) \\ &= \left(\frac{h^2 \left(1 - \frac{ka}{\pi}\right)}{2ma^2} + \sqrt{\left(\frac{h^2 \left(1 - \frac{ka}{\pi}\right)}{2ma^2} \right)^2 + V_1^2} \right). \end{aligned} \tag{6.117}$$

Observe that the kinetic energy difference terms are zero at the Brillouin boundary ($k = \pi/a$). At a distance approaching that boundary, say

$$k = \frac{\pi}{a}(1-\alpha), \tag{6.118}$$

we have

$$\begin{aligned} \epsilon_-(k) &= \frac{h^2\alpha}{2ma^2} + \sqrt{\left(\frac{h^2\alpha}{2ma^2} \right)^2 + V_1^2} \approx \frac{h^2\alpha}{2ma^2} + V_1 + \frac{1}{2}\left(\frac{h^2\alpha}{2ma^2} \right)^2 \\ &= V_1 + O(\alpha). \end{aligned} \tag{6.119}$$

Thus near the boundary we have a (without normalization) nearly sine density

$$\begin{aligned} \rho_{k,-}(x) &= \left| 2iV_1 \sin(\pi x/a) + O(\alpha) e^{i\pi x/a} \right|^2 \\ &\approx V_1^2 \sin^2(\pi x/a). \end{aligned} \tag{6.120}$$

This approaches zero in real space near the atomic lattice positions.

On the other extreme, far enough from the boundary that

$$\frac{h^2 \left(1 - \frac{ka}{\pi}\right)}{2ma^2} \gg V_1^2, \tag{6.121}$$

we have

$$\epsilon_-(k) \approx \frac{h^2\left(1-\frac{ka}{2}\right)}{ma^2}, \tag{6.122}$$

and our (unnormalized) density is nearly constant

$$\begin{aligned}\rho_{k,\pm}(x) &\approx \left| -V_1 e^{-i\pi x/a} + \frac{h^2\left(1-\frac{ka}{2}\right)}{ma^2} e^{i\pi x/a} \right|^2 \\ &\approx \frac{h^2\left(1-\frac{ka}{2}\right)}{ma^2}.\end{aligned} \tag{6.123}$$

Some of these curves are plotted in fig. 6.30 for various relative values of $E^\circ_{k-2\pi/2} - E^\circ_k, V_1$, where the most peaked is near the $k = \pi/a$ boundary, and the flattest, near the origin.

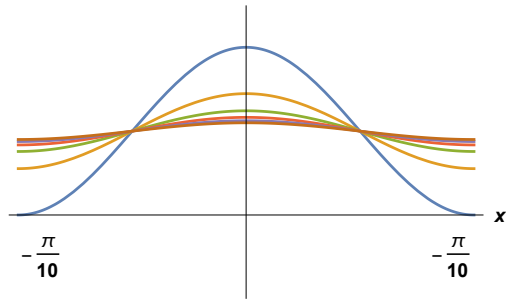

Figure 6.30: Real space variation with k in the Brillouin zone.

Exercise 6.2 Tight binding, square lattice. *(2013 ps8 p1)*

Consider a two-dimensional square lattice with lattice parameter a, and thus basis vectors $(a, 0)$ and $(0, a)$. We will construct a tight binding band from an s-orbital ϕ_s that is a solution of the Schrodinger equation for the isolated atom, with eigenvalue E_s: $\hat{\mathcal{H}}_A(\mathbf{r}-\mathbf{r}_n)\phi_s(\mathbf{r}-\mathbf{r}_n) = E_s\phi_s(\mathbf{r}-\mathbf{r}_n)$, where $\mathbf{r}_n$ is a lattice vector.

a. If the tight binding integrals (defined in class) are

$$\begin{aligned} A &\equiv -\int d\mathbf{r}\, \phi_s^*(\mathbf{r}-\mathbf{r}_n) v(\mathbf{r}-\mathbf{r}_n)\phi_s(\mathbf{r}-\mathbf{r}_n) \quad \text{and} \\ B &\equiv -\int d\mathbf{r}\, \phi_s^*(\mathbf{r}-\mathbf{r}_n \pm (a,0)) v(\mathbf{r}-\mathbf{r}_n)\phi_s(\mathbf{r}-\mathbf{r}_n) = B_x \\ &= -\int d\mathbf{r}\, \phi_s^*(\mathbf{r}-\mathbf{r}_n \pm (0,a)) v(\mathbf{r}-\mathbf{r}_n)\phi_s(\mathbf{r}-\mathbf{r}_n) = B_y, \end{aligned}$$

show that

$$E(\mathbf{k}) \simeq E_s - A - 2B(\cos(k_x a) + \cos(k_y a)).$$

b. Plot $E(\mathbf{k})$ along the following lines in k-space: (i) from $\mathbf{k} = (0,0)$ to $(2\pi/a, 0)$; (ii) from $\mathbf{k} = (0,0)$ to $(0, 2\pi/a)$; (iii) from $\mathbf{k} = (0,0)$ to $(2\pi/a, 2\pi/a)$.

c. What is the bandwidth of this tight-binding band, as a multiple of B?

d. Plot contours of constant energy in the first Brillouin zone (i.e. the (k_x, k_y) plane, using only the first Brillouin zone), for the following energies: (i) $E = E_s - A - 2B$; (ii) $E = E_s - A - B$; (iii) $E = E_s - A$; (iv) $E = E_s - A + 2B$. You may use a plotting package, or plot by hand by calculating k_x and k_y along a few directions in k-space and then interpolating. Use these plots to identify which constant energy contour represents the "half-filled state" (the state where, if all of the levels up to $E = E_F$ are filled then there is one electron per site, or N electrons in total, where N is the number of atoms in the lattice).

e. By considering how the A and B integrals would be affected, discuss in qualitative terms how the $E(k)$ relation changes if, instead of atomic s-orbitals, the basis functions for this band are p_x-orbitals. Sketch contours of constant energy as the 'filling' of the band changes from E_F near the bottom of the band, to E_F near the top of the band. [9 marks]

Notes and Hints: Note that the p_x orbitals break the 90 degree rotational symmetry, so now $B_y \neq B_x$. If the lattice parameter is large, so that there is weak overlap as is assumed in tight-binding calculations, then you will have $|B_y| \ll |B_x|$. Explain why. Note too that the p_x-orbitals have odd-parity, compared with the even-parity of the s-orbitals. You may find it helpful, in discussing the B orbitals, to sketch the p_x orbitals on neighboring atoms, to visualize how they overlap.

Answer for Exercise 6.2

Part a. In class (or [10] (eq. 7.37)) we found for the tight binding energy at the lattice point at $\mathbf{r}_n$

$$E(\mathbf{k}) \approx E_i - A - B \sum_{m=\text{nn of n}} e^{i\mathbf{k}\cdot(\mathbf{r}_n - \mathbf{r}_m)}. \tag{6.124}$$

The nearest neighbor differences are illustrated in fig. 6.31, which we see are

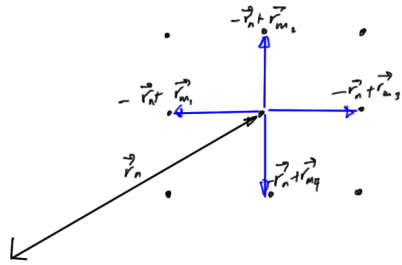

Figure 6.31: Cubic nearest neighbor differences.

$$\mathbf{r}_m - \mathbf{r} \in \{(0, a), (0, -a), (a, 0), (-a, 0)\}. \tag{6.125}$$

The sum of exponentials is just

$$\begin{aligned}\sum_m e^{i\mathbf{k}\cdot(\mathbf{r}_n - \mathbf{r}_m)} &= e^{i(k_x,k_y)\cdot(0,-a)} + e^{i(k_x,k_y)\cdot(0,a)} + e^{i(k_x,k_y)\cdot(a,0)} + e^{i(k_x,k_y)\cdot(-a,0)} \\ &= e^{-iak_y} + e^{iak_y} + e^{-iak_x} + e^{iak_x} \\ &= 2\cos ak_x + 2\cos ak_y.\end{aligned} \tag{6.126}$$

Equation (6.124) takes the form

$$E(\mathbf{k}) \approx E_i - A - 2B\left(\cos ak_x + \cos ak_y\right), \tag{6.127}$$

as desired.

Part b.

(i) Parameterize this trajectory with

$$\mathbf{k}(u) = \frac{2\pi}{a} u(1, 0), \tag{6.128}$$

so the energy on this trajectory is

$$\begin{aligned} E(\mathbf{k}(u)) &= E_s - A - 2B\,(\cos 2\pi u + 1) \\ &= E_s - A - 2B - 2B\cos 2\pi u. \end{aligned} \tag{6.129}$$

This is plotted in fig. 6.32.

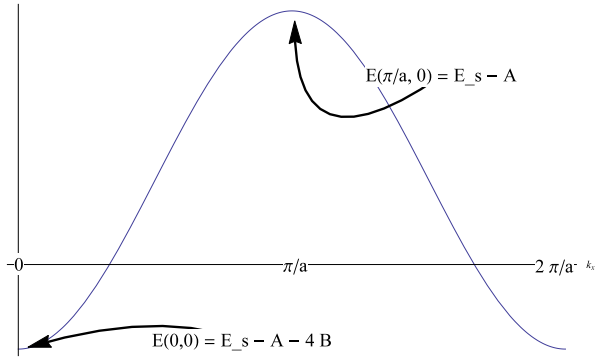

Figure 6.32: $E(k)$ on $k \in [(0,0), 2\pi(1,0)/a]$.

(ii) Parameterize this trajectory with

$$\mathbf{k}(v) = \frac{2\pi}{a} v(0,1), \tag{6.130}$$

so the energy on this trajectory is

$$\begin{aligned} E(\mathbf{k}(v)) &= E_s - A - 2B\,(1 + \cos 2\pi v) \\ &= E_s - A - 2B - 2B\cos 2\pi v. \end{aligned} \tag{6.131}$$

This, identical to (i) in form, is plotted in fig. 6.33.

(iii) Parameterize this trajectory with

$$\mathbf{k}(w) = \frac{2\pi}{a} w(1,1), \tag{6.132}$$

so the energy on this trajectory is

$$\begin{aligned} E(\mathbf{k}(w)) &= E_s - A - 2B\,(2\cos 2\pi w) \\ &= E_s - A - 4B\cos 2\pi w. \end{aligned} \tag{6.133}$$

This, identical to (i) and (ii) in form, but with different extremums, is plotted in fig. 6.34.

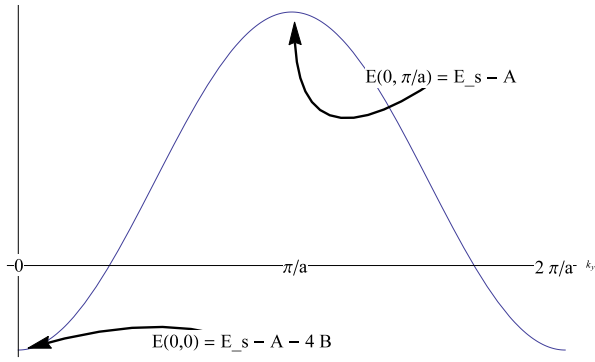

Figure 6.33: $E(k)$ on $k \in [(0,0), 2\pi(0,1)/a]$.

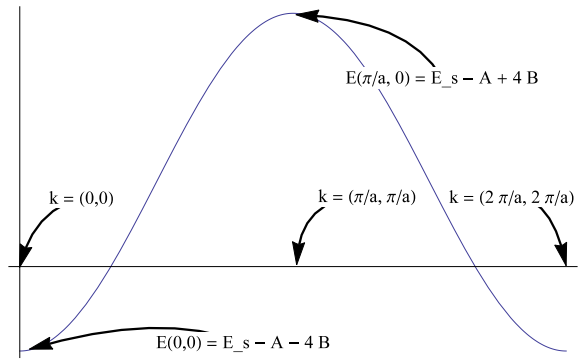

Figure 6.34: $E(k)$ on $k \in [(0,0), 2\pi(1,1)/a]$.

Part c. $E(\mathbf{k})$ ranges from $E_s - A - 2B(1+1)$ to $E_s - A - 2B(-1-1)$. That maximum difference is

$$4B - (-4B) = 8B. \tag{6.134}$$

Part d.

(i) $E = E_s - A - 2B$ The first contour is that defined by

$$E = E_s - A - 2B\left(\cos k_x a + \cos k_y a\right) = E_s - A - 2B, \tag{6.135}$$

or

$$\cos k_x a + \cos k_y a = 1. \tag{6.136}$$

(ii) $E = E_s - A - B$ Next we have the contour defined by

$$\cos k_x a + \cos k_y a = \frac{1}{2}. \tag{6.137}$$

(iii) $E = E_s - A$ This contour is defined by

$$\cos k_x a + \cos k_y a = 0. \tag{6.138}$$

(iv) $E = E_s - A + 2B$ And the last contour defined by

$$\cos k_x a + \cos k_y a = -1. \tag{6.139}$$

These are plotted as functions of $u = k_x a$ and $v = k_y a$ in fig. 6.35. These are level curves of the surface plotted in fig. 6.36.

In class when discussing the tight binding characteristics of s-orbital alkali metals (Li, K, Na, ...), it was noted that their Fermi surfaces never get close to the Brillouin boundary, and that they were approximately spherical. All of the surfaces constrained to the bucket ($E < E_s - A$) are far from the Brillouin boundary, but at $E = E_s - A - 2B$ we are just starting to loose the "spherical" (aka. circular for this lattice) character of these surfaces. We expect that the Fermi energy E_F has an upper bound of $E_F = E_s - A - 2B$, a position in the bucket where the contours are still nearly circular.

Grading remark: "? half filled?". Two marks lost. My attempt to BS this above clearly failed. Prof Julian provided some helpful comments on this:

"Unlike the calculation in problem set 8, the band structure of the alkali metals and alkali earths is free-electron-like. This means that the dispersion relation is parabolic, except near the Brillouin zone boundary. So if the Fermi surface never gets close to a Brillouin zone boundary, $E(k_F) \simeq \hbar^2 k_F^2/2m$, independent of direction in k-space, so the Fermi surface is spherical.

You can tell that the Fermi surface doesn't go close to the BZ boundary by calculating the volume of the Fermi sphere, compared with the volume of the Brillouin zone. This doesn't work for the tight-binding band structure, because the dispersion is anisotropic even far from the Brillouin zone."

As a followup it would be good to:

1. Try this calculation of E_F for the alkali metals, then compare to the BZ volume to verify.

2. Figure out how to calculate the density of states (and thus E_F...).

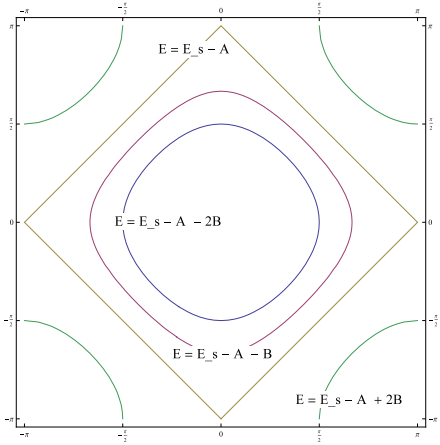

Figure 6.35: 2D Contour plots of selected tight binding energy levels.

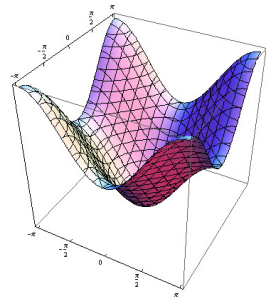

Figure 6.36: Energy level curves.

Part e. The $2p_x$ orbital function in Cartesian coordinates are

$$\phi_{2p_x} = \frac{1}{\sqrt{\pi}} \left(\frac{Z}{2a_\circ} \right)^{5/2} e^{-Zr/a_\circ} x, \tag{6.140}$$

where $r = \sqrt{x^2 + y^2 + z^2}$. The overlap of these orbitals in the lattice could look something like fig. 6.37.

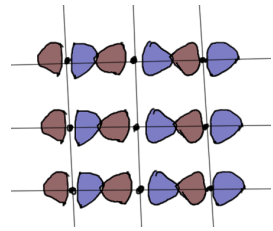

Figure 6.37: $2p_x$ overlap.

Grading remarks: $x \pm a$ is circled "be careful with this. Need to presume parity of orbital", and "B_x is negative". Putting the origin at $\mathbf{r}_n$, writing $\alpha = Z/a_\circ$, and $c^2 = (Z/2a_\circ)^5/\pi$, the A and B integrals for this basis are

$$\begin{aligned}
A &= -c^2 \int dxdydz e^{-2\alpha\sqrt{x^2+y^2+z^2}} v(x,y,z) x^2 \\
B_x &= -c^2 \int dxdydz e^{-\alpha\sqrt{(x\pm a)^2+y^2+z^2}} \left(x \pm a\right) v(x,y,z) e^{-\alpha\sqrt{x^2+y^2+z^2}} x \\
B_y &= -c^2 \int dxdydz e^{-\alpha\sqrt{x^2+(y\pm a)^2+z^2}} x^2 v(x,y,z) e^{-\alpha\sqrt{x^2+y^2+z^2}}
\end{aligned} \tag{6.141}$$

We can rewrite these as

$$\begin{aligned} A &= -c^2 \int d^3\mathbf{r} v(\mathbf{r}) e^{-2\alpha r} x^2 \\ B_x &= -c^2 \int d^3\mathbf{r} v(\mathbf{r}) e^{-\alpha\left(r+\sqrt{r^2 \pm 2xa+a^2}\right)} \left(x^2 \pm ax\right) \\ B_y &= -c^2 \int d^3\mathbf{r} v(\mathbf{r}) e^{-\alpha\left(r+\sqrt{r^2 \pm 2ya+a^2}\right)} x^2 \end{aligned} \tag{6.142}$$

The energy then becomes

$$\begin{aligned} E(\mathbf{k}) &= E_s - A - B_{x_+} e^{i(-a,0)\cdot(k_x,k_y)} - B_{x_-} e^{i(a,0)\cdot(k_x,k_y)} \\ &\quad - B_{y_+} e^{i(0,-a)\cdot(k_x,k_y)} - B_{y_-} e^{i(0,a)\cdot(k_x,k_y)} \\ &= E_s - A - B_{x_+} e^{-iak_x} - B_{x_-} e^{iak_x} \\ &\quad - B_{y_+} e^{-iak_y} - B_{y_-} e^{iak_y} \\ &= E_s + c^2 \int d^3\mathbf{r} v(\mathbf{r}) e^{-2\alpha r} x^2 \\ &\quad + c^2 \int d^3\mathbf{r} v(\mathbf{r}) e^{-\alpha\left(r+\sqrt{r^2-2xa+a^2}\right)} \left(x^2 - ax\right) e^{iak_x} \\ &\quad + c^2 \int d^3\mathbf{r} v(\mathbf{r}) e^{-\alpha\left(r+\sqrt{r^2+2xa+a^2}\right)} \left(x^2 + ax\right) e^{-iak_x} \\ &\quad + c^2 \int d^3\mathbf{r} v(\mathbf{r}) e^{-\alpha\left(r+\sqrt{r^2-2ya+a^2}\right)} x^2 e^{iak_y} \\ &\quad + c^2 \int d^3\mathbf{r} v(\mathbf{r}) e^{-\alpha\left(r+\sqrt{r^2+2ya+a^2}\right)} x^2 e^{-iak_y} \end{aligned} \tag{6.143}$$

Zeroth order approximation In the limiting case where $v(\mathbf{r}) \approx 0$ unless $|\mathbf{r}| \ll a$, this gives us

$$E(\mathbf{k}) \approx E_s - \beta(2) - 2\beta(1) e^{-Za/a_\circ} \left(\cos k_x a + \cos k_y a\right), \tag{6.144}$$

where

$$\beta(n) = -c^2 \int d^3\mathbf{r} v(\mathbf{r}) e^{-nZr/a_\circ} x^2. \tag{6.145}$$

In this limit we have the same "bucket" constant energy contours as found above, however for a constant surface

$$E = E_s - E_s - \beta(2) - 2\beta(1)\mu. \tag{6.146}$$

the contours are defined by

$$\cos k_x a + \cos k_y a = \mu e^{Za/a_\circ}. \tag{6.147}$$

This flattens the surface as Z increases.

First order approximation Allowing for an additional order of r/a in the square root expansions above, so that, for instance

$$\begin{aligned} e^{-\alpha\left(r+\sqrt{r^2-2xa+a^2}\right)} &\approx \exp\left(-\alpha\left(r + a\left(1 + \frac{1}{2}\frac{r^2-2xa}{a^2}\right)\right)\right) \\ &= e^{-\alpha(r-x)}e^{-a\alpha}e^{-\alpha r^2/2a^2}. \end{aligned} \tag{6.148}$$

Now we see the parity effects of the p_x orbital start to manifest. The energy to this order of approximation is

$$\begin{aligned} E(\mathbf{k}) = E_s &+ c^2 \int d^3\mathbf{r} v(\mathbf{r}) e^{-2\alpha r} x^2 \\ &+ c^2 e^{-a\alpha} \int d^3\mathbf{r} v(\mathbf{r}) e^{-\alpha(r-x)-\alpha r^2/a^2} \left(x^2 - ax\right) e^{iak_x} \\ &+ c^2 e^{-a\alpha} \int d^3\mathbf{r} v(\mathbf{r}) e^{-\alpha(r+x)-\alpha r^2/a^2} \left(x^2 + ax\right) e^{-iak_x} \\ &+ c^2 e^{-a\alpha} \int d^3\mathbf{r} v(\mathbf{r}) e^{-\alpha(r-y)-\alpha r^2/a^2} x^2 e^{iak_y} \\ &+ c^2 e^{-a\alpha} \int d^3\mathbf{r} v(\mathbf{r}) e^{-\alpha(r+y)-\alpha r^2/a^2} x^2 e^{-iak_y} \end{aligned} \tag{6.149}$$

In the B_x integrals we have integrands including factors of the form $(x^2 - ax)e^{\alpha x}$ or $(x^2 + ax)e^{-ax}$ both of which have $x^2 e^{a|x|}$ contributions for portions of the integral. In the B_y integrals we have $x^2 e^{a|y|}$ factors in the integrands, which will have less total contribution to the integral. That justifies the $|B_x| \gg |B_y|$ condition for weak overlap.

Given this difference in magnitude, we can roughly expect that the energy can be written as approximately

$$E(\mathbf{k}) = E_s - A + |B_x| \cos k_x a - |B_y| \cos k_y a. \tag{6.150}$$

Grading remark: Originally had $-|B_x|$, which resulted in a squished plot instead of the one below that has a saddle. The comment was "negative B_x makes $(0,0)$ a saddle point". Consider constant energy contours

$$E(\mathbf{k}) = E_s - A - 2\mu\sqrt{B_x^2 + B_y^2}, \tag{6.151}$$

so that the constant surfaces are given by

$$-\cos k_x a + \left|\frac{B_y}{B_x}\right| \cos k_y a = 2\mu\sqrt{1 + \frac{B_y^2}{B_x^2}}. \tag{6.152}$$

This is plotted for $\mu \in [-1, 1]$, and $\left|B_y/B_x\right| = 0.41$ in fig. 6.38 and fig. 6.39.

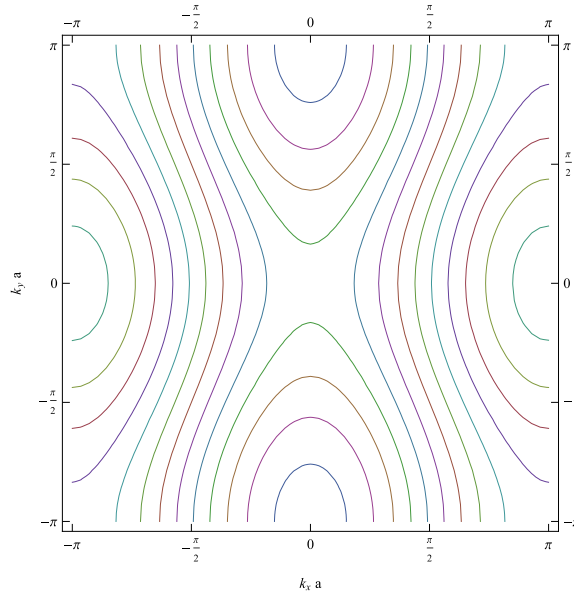

Figure 6.38: Sample energy contours for p_x orbital basis.

Exercise 6.3 2-3D band structure, Fermi surface. (*2013 ps9 p1*)

Consider a two-dimensional square lattice with one atom per unit cell, where each atom contributes two electrons to the conduction band. Assume that the band structure is free-electron-like.

a. Show that the free-electron Fermi surface extends beyond the boundary of the first Brillouin zone, and state by how much the free-electron Fermi wave-vector, k_F, extends beyond the boundary.
b. Sketch how the circular free-electron Fermi surface reconstructs due to the lattice potential, assuming that the lattice potential introduces only small energy gaps at the Brillouin zone boundary. State whether the reconstructed Fermi surfaces enclose filled states (so-called "electron pockets") or empty states (so-called "hole pockets").

Answer for Exercise 6.3

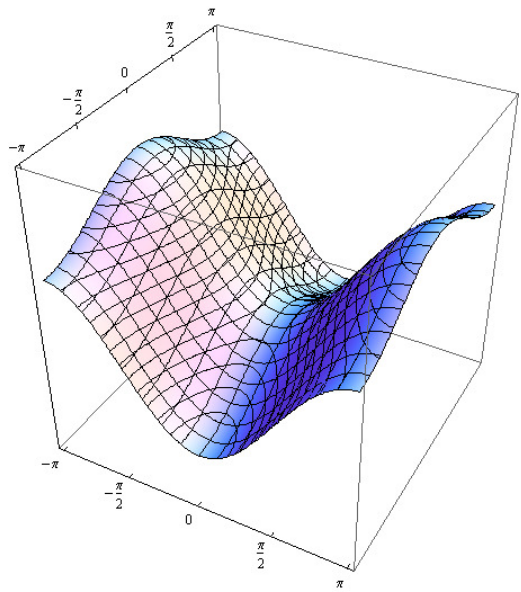

Figure 6.39: 3D plot for p_x orbital basis.

Part a. Our geometry is sketched in fig. 6.40.

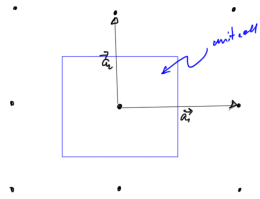

Figure 6.40: 2D cubic lattice.

With just a single atom in the primitive unit cell, the number density of the electrons is just

$$n = \frac{N}{V} = \frac{2}{a^2}. \tag{6.153}$$

The 2D Fermi wave-vector is given implicitly by this area number density, considering the unit circle of radius k_{F} that can contain that number of electrons

$$N = 2 \times \pi k_{\mathrm{F}}^2 \times \frac{A}{(2\pi)^2} = \frac{A k_{\mathrm{F}}^2}{2\pi}, \tag{6.154}$$

or

$$k_F = \sqrt{2\pi n}. \tag{6.155}$$

For this bivalent lattice we have

$$k_F = \sqrt{2\pi \frac{2}{a^2}} = \frac{2\sqrt{\pi}}{a} \approx \frac{3.54}{a}. \tag{6.156}$$

The first Brillouin zone is sketched in fig. 6.41.

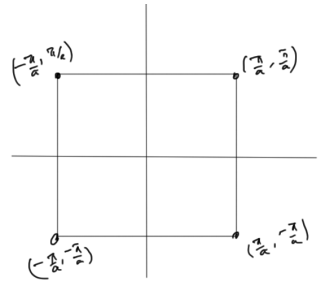

Figure 6.41: First BZ for cubic 2D lattice.

From the center of the BZ to the nearest point on the boundary we have a distance of

$$\frac{\pi}{a} \approx \frac{3.14}{a} < k_F. \tag{6.157}$$

So k_F extends beyond the BZ boundary by

$$\boxed{k_F - \frac{\pi}{a} = \frac{2\sqrt{\pi} - \pi}{a} \approx \frac{0.40}{a}.} \tag{6.158}$$

Part b. The BZ and the Fermi circle has been plotted to scale, with the reconstruction surfaces sketched over top of the plot in fig. 6.42.

Sketching the repeated zone scheme rather roughly (no longer to scale) in fig. 6.43, it's easier to visualize the disconnected pockets of (blue) enclosing unfilled states (hole pockets).

Grading remark: my comment "hole pockets" was marked wrong. This was, in truth, a guess, and I didn't understand this business

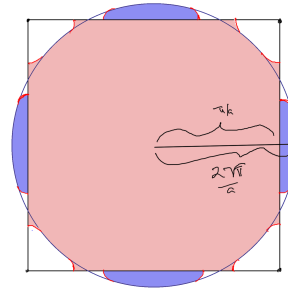

Figure 6.42: Fermi surface for 2D cubic lattice.

of hole pocket vs. electron pocket and didn't find the text particularly helpful to explain it. A corrected sketch was drawn (somewhat like fig. 6.43). Prof Julian responded about this: "If you go back to the free electron sphere, then the ellipsoids that are along the edges of the Brillouin zone have occupied states between the Fermi surface and the Brillouin zone boundary. So when you close the pocket on the other size of the Brillouin zone, occupied states are enclosed.

On the other hand, the corner pockets come from sections of the free electron sphere that have unoccupied states between the Fermi surface and the Brillouin zone corner. Thus when you enclose the BZ corner by closing the Fermi surface in the repeated zone scheme, you are enclosing empty states."

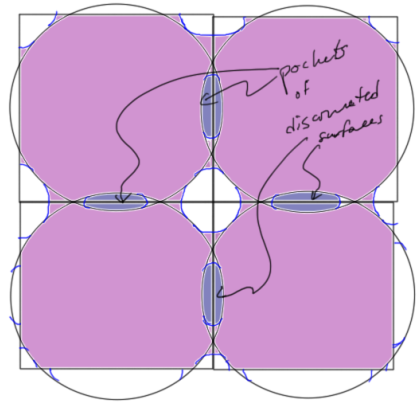

Figure 6.43: Repeated zone scheme for cubic lattice.

Exercise 6.4 Density of states and effective mass. (*2013 ps9 p2*)

The dispersion relation of a two-dimensional square lattice with lattice parameter a, with nearest-neighbor tight-binding integrals A and B, is

$$E(\mathbf{k}) \simeq E_s - A - 2B(\cos(k_x a) + \cos(k_y a)).$$

a. Expanding $E(k)$ around the bottom and the top of the band to second order in $\mathbf{k}$ (i.e. approximating the bands as parabolic) show that the density of states per unit area jumps from zero when E is outside the band, to a finite value as E passes the bottom or top of the band. What is the finite value?

b. Consider now the analogous three-dimensional simple cubic system, such that

$$E(\mathbf{k}) \simeq E_s - A - 2B(\cos(k_x a) + \cos(k_y a) + \cos(k_z a)).$$

Show that the density of states now grows continuously from zero, and is proportional to $\sqrt{(E - E_b)}$, and $\sqrt{(E_t - E)}$, as the bottom (E_b) and top (E_t) of the band are crossed. Find the constants of proportionality.

c. For the three-dimensional cubic system of part b, find the group velocity $\mathbf{v}_g$ along the k_x direction, as a function of k_x, and sketch its behavior from $k_x = 0$ to π/a.

d. Using our definition of group velocity from class, and defining the velocity effective mass m^* by $v_g = \hbar k/m^*$, plot m^* vs k_x from o to π/a.

Answer for Exercise 6.4

Part a. It's helpful to recall the geometry of the energy distribution in k-space. This was plotted in fig. 6.36. At the bottom of the distribution, to second order, we have

$$\begin{aligned} E(\mathbf{k}) &\approx E_s - A - 2B\left(1 - \frac{1}{2}(k_x a)^2 + 1 - \frac{1}{2}(k_y a)^2\right) \\ &= E_s - A - 4B + Ba^2\left(k_x^2 + k_y^2\right). \end{aligned} \tag{6.159}$$

For the gradient we have

$$\begin{aligned}\boldsymbol{\nabla}_{\mathbf{k}} E(\mathbf{k}) &= Ba^2 \boldsymbol{\nabla} \left(k_x^2 + k_y^2\right) \\ &= Ba^2 \left(2k_x, 2k_y\right) \\ &= 2Ba^2 \mathbf{k}.\end{aligned} \tag{6.160}$$

With cylindrical coordinates, we have

$$\begin{aligned}d\mathbf{k} &= k d\phi_k dk \\ &= k d\phi_k \frac{dE}{|\boldsymbol{\nabla}_{\mathbf{k}} E|},\end{aligned} \tag{6.161}$$

So that the density of states is given by

$$\begin{aligned}D(E)dE = 2 \times \frac{1}{A} \frac{A}{(2\pi)^2} \times \\ \int_{\phi_k=0}^{2\pi} \cancel{k} d\phi_k \frac{dE}{2Ba^2 \cancel{k}},\end{aligned} \tag{6.162}$$

or

$$\boxed{D(E) = \frac{1}{2\pi Ba^2}.} \tag{6.163}$$

For the top of the energy levels, we can also expand to second order in k_x, k_y, at the points $k_x, k_y = \pm\pi/a$. With k for one of k_x, or k_y we have at the corner $k = \pm\pi/a$

$$\begin{aligned}\cos ka &= \frac{1}{0!} \cos ka|_{k=\pm\pi/a} + \frac{1}{1!} \cos' ka\big|_{k=\pm\pi/a} (k \mp \pi/a) \\ &\quad + \frac{1}{2!} \cos' ka\big|_{k=\pm\pi/a} (k \mp \pi/a)^2 + \cdots \\ &\approx \cos(\pm\pi) - a \sin(\pm\pi)(k \mp \pi/a) - a^2 \cos(\pm\pi)(k \mp \pi/a)^2 \\ &= -1 + \frac{1}{2}(ka \mp \pi)^2.\end{aligned} \tag{6.164}$$

So, at the corner $\mathbf{k} = \pm(1,1)\pi/a$ the energy is approximately

$$E(\mathbf{k}) = E_s - A + 4B - B\left((k_x a \mp \pi)^2 + \left(k_y a \mp \pi\right)^2\right), \tag{6.165}$$

with gradient

$$\begin{aligned}\boldsymbol{\nabla}_{\mathbf{k}} E(\mathbf{k}) &= -2Ba\left(k_x a \mp \pi, +k_y a \mp \pi\right) \\ &= -2Ba^2\left(k_x \mp \pi/a, +k_y \mp \pi/a\right).\end{aligned} \tag{6.166}$$

At the corners $\mathbf{k} = \pm(1,-1)\pi/a$ we have approximately

$$E(\mathbf{k}) = E_s - A + 4B - B\left(\left(k_x a \mp \pi\right)^2 + \left(k_y a \pm \pi\right)^2\right), \tag{6.167}$$

which have gradients

$$\boldsymbol{\nabla}_{\mathbf{k}} E(\mathbf{k}) = -2Ba^2\left(k_x \mp \pi/a, +k_y \pm \pi/a\right). \tag{6.168}$$

Consider the $\mathbf{k} = -(1,1)\pi/a$ corner, and make the change of variables

$$\begin{aligned}k_x + \pi/a &= k\cos\phi_k \\ k_y + \pi/a &= k\sin\phi_k.\end{aligned} \tag{6.169}$$

We see that we have to only consider this portion of the k-space area, quadrupling the integral, so that the density of states is

$$D(E)dE = 2\times 4\frac{1}{(2\pi)^2}\int_{\phi_k=0}^{\pi/2} k d\phi_k \frac{dE}{|-2Ba^2 k|}. \tag{6.170}$$

This is identical to eq. (6.163), the constant value for the density of states found for the bottom of the band, provided we expand the energy only to second order in k_x, k_y.

Part b. At the bottom of the band, again approximating the energy to second order in k_x, k_y, k_z, we have

$$\begin{aligned}E(\mathbf{k}) &\approx E_s - A - 2B\left(3 - \frac{1}{2}k_x^2 a^2 - \frac{1}{2}k_y^2 a^2 - \frac{1}{2}k_z^2 a^2\right) \\ &= E_s - A - 6B + Ba^2\left(k_x^2 + k_y^2 + k_z^2\right).\end{aligned} \tag{6.171}$$

The energy gradient is

$$\boldsymbol{\nabla}_{\mathbf{k}} E = Ba^2 \boldsymbol{\nabla}_{\mathbf{k}} \mathbf{k}^2 = 2Ba^2\mathbf{k}. \tag{6.172}$$

Our density of states at the bottom of the band is thus

$$\begin{aligned} D(E) &= 2 \times \frac{1}{8\pi^3} \frac{4\pi k^2}{2Ba^2 k}\bigg|_{k=k(E)} \\ &= \frac{1}{2\pi^2 Ba^2} \left(\frac{E - E_s + A + 6B}{Ba^2} \right)^{1/2} \\ &= \frac{1}{2\pi^2 B^{3/2} a^3} \sqrt{E - E_s + A + 6B}. \end{aligned} \tag{6.173}$$

$$\boxed{D(E) = \frac{1}{2\pi^2 B^{3/2} a^3} \sqrt{E - E_b},} \tag{6.174}$$

where $E_b = E_s - A - 6B$.

For the calculation at the top of the band, we can expand the cosines around the corner coordinates. Considering just the $\mathbf{k} = -(1,1,1)\pi/a$ octet, and multiplying by 8 for the total density of states we have

$$\begin{aligned} &E(\mathbf{k}) \\ &\approx E_s - A - 2B \left(-3 + \frac{1}{2}(k_x a + \pi)^2 + \frac{1}{2}(k_y a + \pi)^2 + \frac{1}{2}(k_z a + \pi)^2 \right) \\ &= E_s - A + 6B - B \left((k_x a + \pi)^2 + (k_y a + \pi)^2 + (k_z a + \pi)^2 \right). \end{aligned} \tag{6.175}$$

The gradient at this point is

$$\begin{aligned} \boldsymbol{\nabla}_{\mathbf{k}} E(\mathbf{k}) &= -Ba^2 \boldsymbol{\nabla}_{\mathbf{k}} \left((k_x + \pi/a)^2 + (k_y + \pi/a)^2 + (k_z + \pi/a)^2 \right) \\ &= -2Ba^2 \left(k_x + \pi/a, k_y + \pi/a, k_z + \pi/a \right). \end{aligned} \tag{6.176}$$

Now introduce spherical coordinates with the origin at this point

$$\begin{aligned} k_x + \pi/a &= k \sin\theta_k \cos\phi_k \\ k_y + \pi/a &= k \sin\theta_k \sin\phi_k \\ k_z + \pi/a &= k \cos\theta_k, \end{aligned} \tag{6.177}$$

So that the density of states is

$$\begin{aligned} D(E) &= 2 \times 8 \times \frac{1}{(2\pi)^3} \int_0^{\pi/2} \sin\theta_k d\theta_k \times \\ &\qquad \int_0^{\pi/2} d\phi_k \frac{k^2}{2Ba^2 k}\bigg|_{k=k(E)} \\ &= \frac{1}{\pi^3 Ba^2} \frac{\pi}{2} \left(\frac{E - E_s + A - 6B}{-Ba^2} \right)^{1/2}. \end{aligned} \tag{6.178}$$

This is

$$\boxed{D(E) = \frac{1}{2\pi^2 B^{3/2} a^3} \sqrt{E_t - E},} \tag{6.179}$$

where $E_t = E_s - A + 6B$. The constant of proportionality is the same we found for the bottom of the band in eq. (6.174).

Part c. The expectation value of the velocity operator is given by

$$\begin{aligned} \mathbf{v}_g &= \frac{1}{\hbar} \boldsymbol{\nabla}_{\mathbf{k}} E \\ &= \frac{-2B}{\hbar} \boldsymbol{\nabla}_{\mathbf{k}} \left(\cos k_x a + \cos k_y a + \cos k_z a \right) \\ &= \frac{2Ba}{\hbar} \left(\sin k_x a, \sin k_y a, \sin k_z a \right). \end{aligned} \tag{6.180}$$

Along the k_x direction we have

$$\mathbf{v}_g \cdot (1,0,0) = \frac{2Ba}{\hbar} \sin k_x a. \tag{6.181}$$

This is plotted for the $k_x = [0, \pi/a]$ region in fig. 6.44.

Part d. From eq. (6.180) and our definition, we have

$$v_g = \frac{2Ba}{\hbar} \left(\sin^2 k_x a + \sin^2 k_y a + \sin^2 k_z a \right)^{1/2} = \frac{\hbar k}{m^*}, \tag{6.182}$$

or

$$m^* = \frac{\hbar^2}{2Ba} \sqrt{\frac{k_x^2 + k_y^2 + k_z^2}{\sin^2 k_x a + \sin^2 k_y a + \sin^2 k_z a}}. \tag{6.183}$$

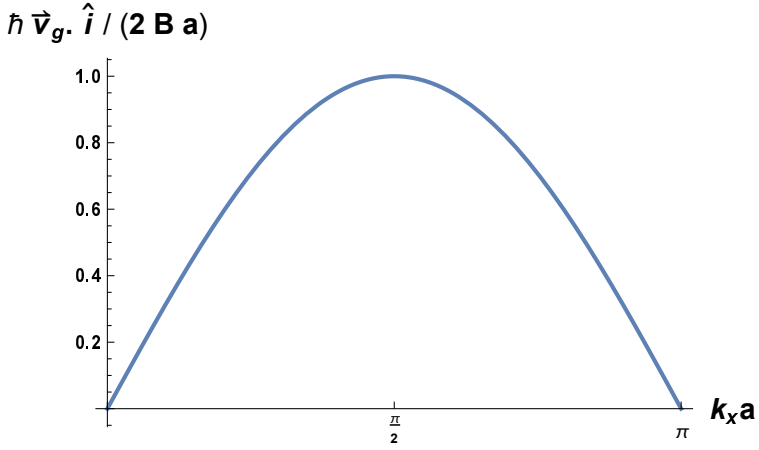

Figure 6.44: k_x component of $\mathbf{v}_g$.

Along the k_x axis we have

$$m^*(k_x, 0, 0) = \frac{\hbar^2}{2Ba^2}\left|\frac{k_x a}{\sin k_x a}\right|. \tag{6.184}$$

This is plotted in fig. 6.45.

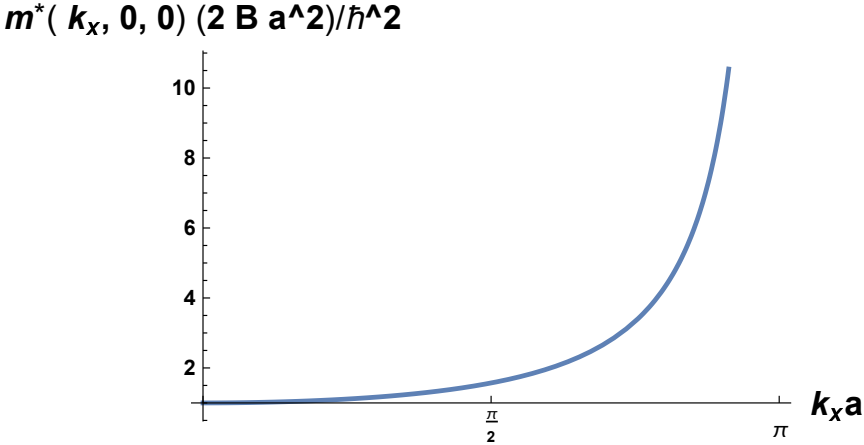

Figure 6.45: Effective mass for 3D cubic system.

7 ELECTRICAL CONDUCTIVITY.

7.1 SEMICONDUCTORS.

We continue with examination of the band structures of real materials. In particular, start looking at semiconductors

- diamond
- Si
- Ge
- GaAs
- InP
- InAs

Example 7.1: Diamond bandstructure.

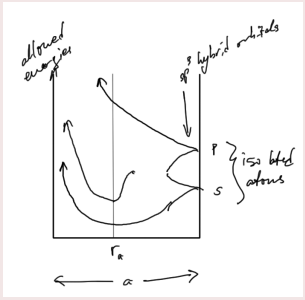

Figure 7.1: Diamond bandstructure.

The two branches are because we have two atoms per unit cell. Those are due to antibonding and bonding conditions as in fig. 7.2.

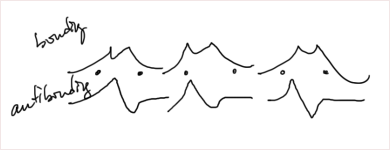

Figure 7.2: Bonding and antibonding functions in unit cells.

Example 7.2: Band structure of Ge and Si.

Also see slides and [10] §7.13.

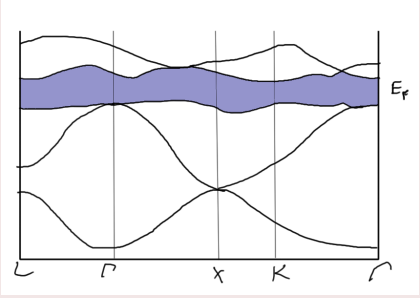

Figure 7.3: Ge, Si band structure.

E_F falls in a full gap, where there is no Fermi surface. The gap is small. Carriers can be thermally excited at room temperature.

The lower energy curves correspond to bonding orbitals. In general in materials the bonding orbitals will always be occupied, because they are energy favourable.

Example 7.3: Insulators: large gap semiconductors.

[10] fig 7.10.

For KCl as in fig. 7.4

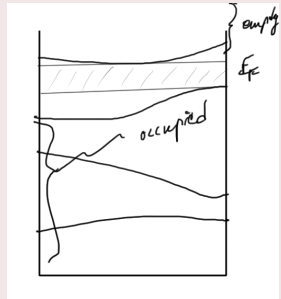

Figure 7.4: KCl band structure.

all bands near E_F are tight binding like. There's a large gap at E_F.

7.2 DENSITY OF STATES.

Reading: [1] ch. 8. Recall

$$\sum_{k,\sigma=\pm 1/2} \to \overset{\text{spin}}{\boxed{2}} \frac{1}{(2\pi/L)^3} \int d\mathbf{k} \to V \int D(E) dE. \tag{7.1}$$

For the free electron model we found

$$\begin{aligned} D(E) &= \text{density of states per unit volume} \\ &= \frac{1}{2\pi^2} \left(\frac{2m}{\hbar} \right)^{3/2} \sqrt{E}, \end{aligned} \tag{7.2}$$

and in general

$$D(E)dE = \frac{2}{(2\pi)^3} \int \frac{df_E}{|\boldsymbol{\nabla}_{\mathbf{k}} E(\mathbf{k})|} dE. \tag{7.3}$$

Referring to fig. 7.5.

$$\begin{aligned} d\mathbf{k} &= df_E dk_\perp \\ &= df_E \frac{dE}{|\boldsymbol{\nabla}_{\mathbf{k}} E(\mathbf{k})|}. \end{aligned} \tag{7.4}$$

Some observations:

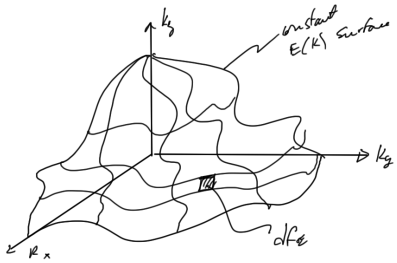

Figure 7.5: Fermi surface for constant energy.

- Flat bands due to $1/|\nabla_{\mathbf{k}} E(\mathbf{k})|$ will have a high density of states.
- At local extremums of $E(\mathbf{k})$ you get a peak in $D(E)$. This is called a van Hove singularity. See slides and [1] fig. 8.3.

d-metals High density of states in the d-orbitals, and small elsewhere. Recall

$$C(T) = \overbrace{\gamma T}^{\text{electrons}} + \overbrace{\beta T^3}^{\text{phonons}}. \tag{7.5}$$

$$\begin{aligned} \gamma_{\text{Cu}} &\sim 0.69\,\text{mJ/mole K}^2 \\ \gamma_{\text{Fe}} &\sim 4.98\,\text{mJ/mole K}^2 \end{aligned} \tag{7.6}$$

Germanium Here we have Van Hove singularities. Max/min at Γ does not produce a Van Hove singularity, because df_{E} is vanishingly small.

7.3 ELECTRICAL TRANSPORT.

Reading: [10] §9.1,[1] ch. 12.

We want to talk about how to make an electrical current flow. Imagine that we are considering a block of material with leads on it, as in fig. 7.6.

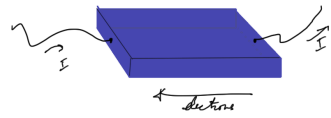

Figure 7.6: Conducting block of metal.

How do we use our Bloch description for such a volume? A pure Bloch wave

$$\Psi_{\mathbf{k}} = U_{\mathbf{k}}(\mathbf{r})e^{i\mathbf{k}\cdot\mathbf{r}}, \tag{7.7}$$

is uniformly spread out over the sample

$$\left|\frac{1}{\sqrt{V}}e^{i\mathbf{k}\cdot\mathbf{r}}\right|^2 = \frac{1}{V}. \tag{7.8}$$

Such a plane wave cannot transport charge. Introduce a wave packet

example: a Gaussian, centered on $\mathbf{k}$

$$\Psi_{\mathbf{k}}(\mathbf{r},t) \sim \int_{|\mathbf{k}'|<\Delta} a_{\mathbf{k}'} U_{\mathbf{k}}(\mathbf{r})e^{i(\mathbf{k}\cdot\mathbf{r}-\omega t)}d\mathbf{k}'. \tag{7.9}$$

This will spread as plotted in fig. 7.7.

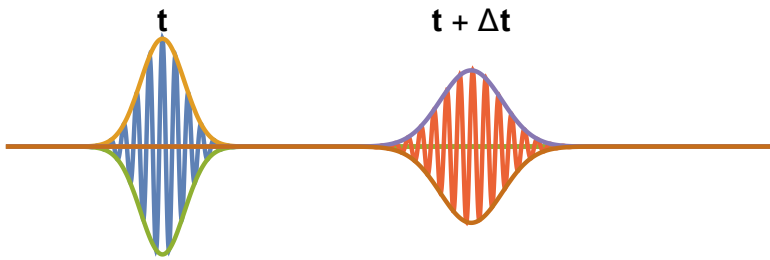

Figure 7.7: Packet spreading with time.

Moves with group velocity

$$\mathbf{v}_{\mathbf{k}} = \frac{d\omega(\mathbf{k})}{d\mathbf{k}} = \frac{1}{\hbar}\nabla_{\mathbf{k}}E(\mathbf{k}). \tag{7.10}$$

Electrical transport (cont.) Last time we noted that we can't use plain Bloch waves to model this, but must introduce a wave packet centered on some $\mathbf{k}$, such as the Gaussian of fig. 7.8, moving with group velocity

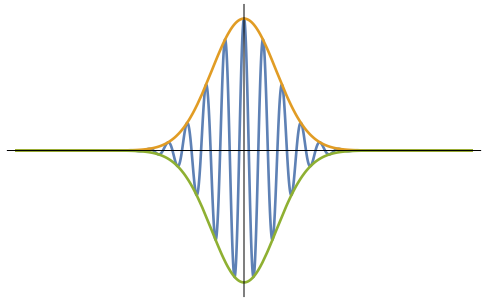

Figure 7.8: Gaussian wave packet.

$$\mathbf{v} = \frac{1}{\hbar}\boldsymbol{\nabla}_{\mathbf{k}} E(\mathbf{k}). \tag{7.11}$$

For nearly free electrons where $E(\mathbf{k}) = \hbar^2\mathbf{k}^2/2m$ this gives the intuitively appealing

$$\mathbf{v} = \frac{\hbar\mathbf{k}}{m} = \frac{\mathbf{p}}{m}, \tag{7.12}$$

where we have velocity as momentum over mass.

For tight binding

$$E(k) = E_i - A - 2B\cos ka. \tag{7.13}$$

so that

$$v = \frac{2Ba}{\hbar}\sin ka. \tag{7.14}$$

An important quantity is the Fermi velocity

$$\mathbf{v}_{\mathrm{F}} = \mathbf{v}(\mathbf{k} = \mathbf{k}_{\mathrm{F}}). \tag{7.15}$$

Linearizing $E(\mathbf{k})$ around $\mathbf{k}_{\mathrm{F}}$

$$\begin{aligned} E(\mathbf{k}) &= E(\mathbf{k}_{\mathrm{F}}) + \delta k_{\perp}\left(\frac{dE}{dk_{\perp}}\right). \\ &\qquad\qquad \mathbf{p}_{\mathrm{F}} \\ &\equiv E(\mathbf{k}_{\mathrm{F}}) + \delta k_{\perp}\boxed{\frac{\hbar\mathbf{k}_{\mathrm{F}}}{m^*}}. \end{aligned} \tag{7.16}$$

Here m^* is the effective mass. Keep in mind that the Fermi surface is often not spherical as in fig. 7.9, and fig. 7.10.

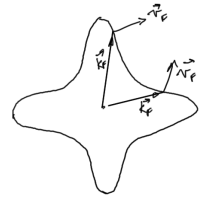

Figure 7.9: Non-spherical Fermi surface.

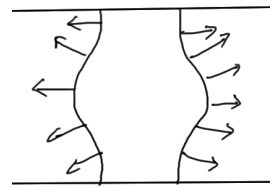

Figure 7.10: Second non-spherical Fermi surface.

$$\mathbf{v}_{\mathrm{F}}(\mathbf{k}) = \frac{1}{\hbar}\boldsymbol{\nabla}_{\mathbf{k}} E(\mathbf{k})\Big|_{\mathbf{k}_{\mathrm{F}}} = \frac{\hbar \mathbf{k}_{\mathrm{F}}}{m^*}. \tag{7.17}$$

response to applied electric field $\boldsymbol{\mathcal{E}}$ Our $\mathbf{F} = m\mathbf{a}$ equivalent for a wave packet is

$$\dot{\mathbf{p}} = \hbar \dot{\mathbf{k}} = -e\boldsymbol{\mathcal{E}}. \tag{7.18}$$

Wave vector of wave package advances steadily, as in fig. 7.11, provided we ignore scattering (for now).

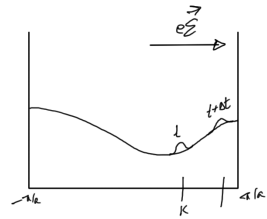

Figure 7.11: Wave packet along distribution curve.

The time rate of change of the velocity is

$$\begin{aligned}\dot{v}_i &= \frac{1}{\hbar}\frac{d}{dt}\left(\boldsymbol{\nabla}_{\mathbf{k}} E(\mathbf{k})\right)_i \\ &= \frac{1}{\hbar}\sum_j \frac{\partial^2 E}{\partial k_i \partial k_j}\dot{k}_j \\ &= \sum_j \left(\frac{1}{m^*}\right)_{ij} \left(-e\mathcal{E}_j\right).\end{aligned} \tag{7.19}$$

This time we call

$$\left(\frac{1}{m^*}\right)_{ij} = \frac{1}{\hbar^2}\frac{\partial^2 E}{\partial k_i \partial k_j}. \tag{7.20}$$

the effective mass tensor, which represents "resistance" to applied force. For example in fig. 7.12.

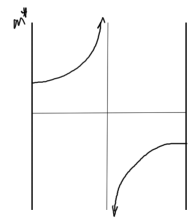

Figure 7.12: Effective mass tensor.

Some interesting conditions for the effective mass tensor are

- For $m^* > 0$, then $\dot{\mathbf{v}}$ is parallel to the force.
- For $|m^*| = \infty$, then $\dot{\mathbf{v}} = 0$.
- For $m^* < 0$, the wave packet slows down under a force parallel to $\mathbf{v}$.

7.4 ELECTRIC CURRENT.

Reading: [10] §9.2, [1] ch. 12.

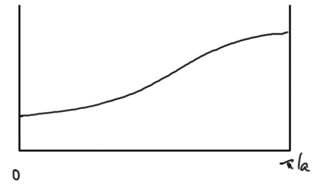

Figure 7.13: Illustration for points above.

We've been considering a single electron. What about a metal?

$$\begin{aligned}\mathbf{j} &= -\frac{e}{V}\sum_{\mathbf{k}}\mathbf{v}(\mathbf{k}) \\ &= -e\frac{2}{(2\pi)^3}\int d\mathbf{k} v(\mathbf{k}) \\ &= -e\frac{2}{8\pi^3}\int d\mathbf{k} f(E(\mathbf{k}), \boldsymbol{\mathcal{E}})\boldsymbol{\nabla}_{\mathbf{k}} E(\mathbf{k}).\end{aligned} \tag{7.21}$$

Here $f(E(\mathbf{k}, \boldsymbol{\mathcal{E}})$ is the electron distribution in presence of field $\boldsymbol{\mathcal{E}}$.

In equilibrium $\boldsymbol{\mathcal{E}} = 0$ In 1D for every occupied $+\mathbf{v}(\mathbf{k})$ state there exists a $\mathbf{v}(-\mathbf{k})$ state is occupied so that $\mathbf{v}(-\mathbf{k}) = -\mathbf{v}(\mathbf{k})$, so

$$\sum \mathbf{v}(\mathbf{k}) = 0. \tag{7.22}$$

Electric current (cont.) $\boldsymbol{\mathcal{E}} \neq 0$ shifts the Fermi distribution so that so that $+\mathbf{v}_1 - \mathbf{v}$ no longer cancel.

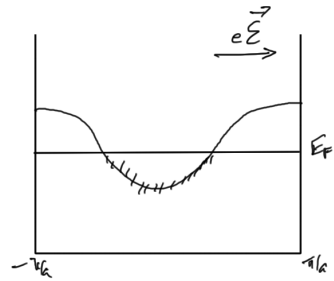

Figure 7.14: Fermi filling for a metal.

Current flows, unless the band is completely full, or empty as sketched in fig. 7.15.

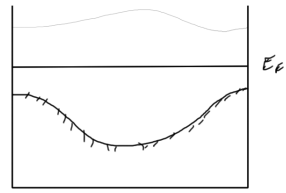

Figure 7.15: Fermi filling of an insulator.

Full band has $f(E, \mathbf{E}) = F(E, 0)$, so that there is no current

An "insulator" has all bands either completely full or completely empty.

A "metal" is a solid with a Fermi surface (partly filled band(s)).

The $\mathcal{E}$ field displaces the Fermi surface, but scattering restores equilibrium, limiting $\mathbf{j}$.

Note that a periodic lattice does not cause scattering, it causes band structure.

Scattering is due to departures from periodicity, and is due to impurities and/or vacancies and lattice vibrations (phonons), as sketched in fig. 7.16.

Figure 7.16: Vacancy.

A metric for this is called the resistivity, a temperature dependent effect as sketched in fig. 7.17.

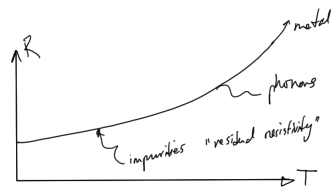

Figure 7.17: Resistivity.

Non-equilibrium $f(E, \mathcal{E})$ With imposition of a field the Fermi filling is shifted as sketched in fig. 7.18.

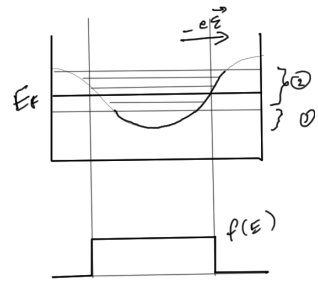

Figure 7.18: Fermi filling shift due to imposed field.

Electrons in the range (1) cannot scatter due to the Pauli exclusion principle, whereas those in the energy range (2) can scatter from $+k$ to $-k$. The net scattering is from $+\mathbf{v}$ to $-\mathbf{v}$.

For 3D see [10] fig. 9.5, roughly as in fig. 7.19.

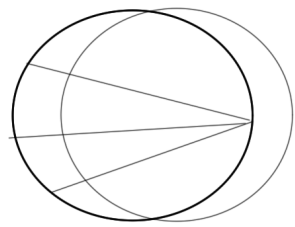

Figure 7.19: A displaced Fermi sphere.

Steady state rate of scattering from $+\mathbf{v}$ to $-\mathbf{v}$ is the rate at which new $+\mathbf{v}$ carriers appear, where

$$\hbar\dot{\mathbf{k}} = -e\boldsymbol{\mathcal{E}}. \tag{7.23}$$

Introduce τ as the mean scattering time, and let

$$\Delta k = \dot{k}\tau = -\frac{e\mathcal{E}}{\hbar}\tau, \tag{7.24}$$

the amount by which the Fermi surface is displaced.

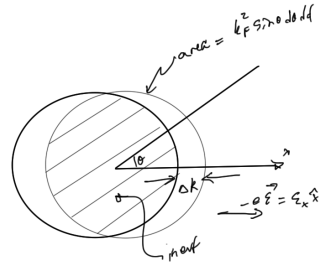

Figure 7.20: Integration region, difference between displaced Fermi sphere.

In the shaded region, the electrons are inert, because the $-\mathbf{v}$ and $\mathbf{v}$ contributions cancel. It's only the non-shaded portions of the overlapping spheres that we have to consider.

$$j_x = -\frac{e}{V}\sum_{k,\sigma} v_x(k,\sigma)$$

$$= -\frac{e}{\cancel{V}}\frac{2\cancel{V}}{(2\pi)^3}\int \underbrace{k_F^2 \sin\theta d\theta d\phi}_{\text{area element at } \theta,\phi}\underbrace{\left(-\frac{e\mathcal{E}}{\hbar}\tau\cos\theta\right)}_{\Delta k \text{ at } \theta,\phi}\times \underbrace{v_F\cos\theta}_{v_x} \tag{7.25}$$

$$\approx \frac{e^2}{4\pi^3}\tau k_F^2\frac{v_F}{\hbar}\underbrace{\int_0^\pi \sin\theta\cos^2\theta d\theta}_{-\int_0^\pi \cos^2\theta d(\cos\theta) = -\int_1^{-1} u^2 du = 2/3}\underbrace{2\pi}_{\int d\phi}\mathcal{E}_x.$$

With

$$v_F = \frac{\hbar k_F}{m^*}, \tag{7.26}$$

this is

$$j_x \approx \frac{e^2\tau}{m^*}\frac{k_F^3}{3\pi^2}\mathcal{E}_x. \tag{7.27}$$

$$j_x = \frac{ne^2\tau}{m^*}\mathcal{E}_x. \tag{7.28}$$

or

$$\boxed{\sigma = \frac{ne^2\tau}{m^*}.} \tag{7.29}$$

This is the Drude formula for conductivity.

On Drude's derivation Note that Drude's derivation, see [1] ch. 1, predated quantum mechanics. He treated the electrons classically introducing a drift velocity fig. 7.21.

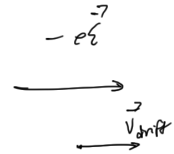

Figure 7.21: Drude drift velocity in an electric field.

where

$$v_{\text{drift}} = (\text{acceleration})\,\tau = -\frac{e\mathcal{E}}{m}\tau, \tag{7.30}$$

so that

$$\mathbf{j} = -env_{\text{drift}}\boldsymbol{\mathcal{E}} = \frac{ne^2\tau}{m}\boldsymbol{\mathcal{E}}. \tag{7.31}$$

7.5 PROBLEMS.

Exercise 7.1 Drude conductivity formula. (*2013 ps10 p1*)

The density of point-like impurities in a metal can be characterized by a 'mean free path,' $l_\circ$, of the conduction electrons, this being the distance between scattering centers that randomize the velocity.

a. Assuming that electrons travel at the Fermi velocity between scattering centers in a free electron metal, show that

the Drude formula for the conductivity can be rewritten as:

$$\sigma = \frac{k_F^2 e^2 l_\circ}{3\hbar\pi^2}. \tag{7.32}$$

b. A sample of copper has a residual resistivity below 1 K of $10^{-8}\Omega\,\mathrm{m}$. (Note: resistivity $\rho = 1/\sigma$.) Treating copper as a free electron metal with a spherical Fermi surface accommodating one charge carrier per copper atom, estimate $l_\circ$ below 1 K for this sample of copper. (Free-electron parameters of copper are given in [10] Table 6.1)
c. Calculate the mean scattering time τ for this sample of copper below 1 K.

Answer for Exercise 7.1

Part a. The Fermi velocity is

$$v_F = \frac{p_F}{m} = \frac{\hbar k_F}{m^*}, \tag{7.33}$$

so that the 'mean free path' is

$$l_\circ = v_F \tau = \frac{\hbar k_F \tau}{m^*}. \tag{7.34}$$

Putting these all together, the conductivity as given by eq. (7.32) is

$$\begin{aligned}\sigma &= \frac{k_F^2 e^2}{3\cancel{\hbar}\pi^2}\frac{\cancel{\hbar} k_F \tau}{m^*} \\ &= \frac{k_F^3}{3\pi^2}\frac{e^2\tau}{m^*} \\ &= n\frac{e^2\tau}{m^*},\end{aligned} \tag{7.35}$$

which recovers the form we derived in class.

Part b. Using the tabulated info

$$l_\circ = \frac{3\pi^2\hbar}{k_F^2 e^2 \rho} = \frac{3\pi^2\left(1.05\times10^{-34}\,\mathrm{Js}\right)}{\left(1.36\times\frac{10^8}{10^{-2}\,\mathrm{m}}\right)^2\left(1.6\times10^{-19}\,\mathrm{C}\right)^2\left(10^{-8}\,\mathrm{Js/C^2\,m}\right)}.$$

(7.36)

This is

$$\boxed{l_\circ = 6.57 \times 10^{-6}\,\text{cm}.} \tag{7.37}$$

With copper having an FCC lattice constant of ~ 3.6Å, the number of atoms that an electron moves past before a collision is on the order of 10^2.

Part c. The mean scattering time is

$$\begin{aligned} \tau &= \frac{l_\circ}{v_\text{F}} \\ &= \frac{6.57 \times 10^{-6}\,\text{cm}}{1.57 \times 10^{8}\,\text{cm/s}}. \end{aligned} \tag{7.38}$$

This is

$$\boxed{\tau = 4.18 \times 10^{-14}\,\text{s},} \tag{7.39}$$

a surprisingly fast seeming time until the magnitude of $v_\text{F} \approx 0.005c$ is considered.

8 ELECTRON SCATTERING.

8.1 ELECTRON-PHONON SCATTERING.

Reading: [10] ch. 9 (pp 258-259).

Last time

$$\mathbf{j} = \sigma \boldsymbol{\mathcal{E}} \tag{8.1a}$$

$$\sigma = \frac{ne^2\tau}{m^*}. \tag{8.1b}$$

Here τ is the "mean scattering time", which is the time to randomize $\mathbf{v}$.

We now continue to discuss scattering, a phenomena due to departure from periodicity. For phonons, this is proportional to $\langle n_q \rangle_{th}$, where $E_q = (n_q + 1/2)\hbar\omega_q$.

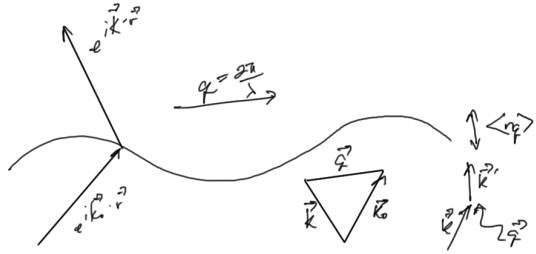

Figure 8.1: k-space scattering.

Small q (long λ) phonons are not very effective at randomizing $\mathbf{v}$. The effectiveness of the scattering is $\propto q^2$.

We'd found

$$\frac{1}{\tau_{\text{ph}}(q)} \propto q^2 \langle n_q \rangle \tag{8.2a}$$

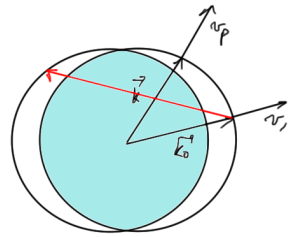

Figure 8.2: Scattering confinement to small range of k-space.

$$\langle n_q \rangle = \frac{1}{e^{\hbar\omega_q/k_B T} - 1}. \tag{8.2b}$$

Combining these, we have

$$\frac{1}{\tau_{ph}} \propto (\cdots) \int 4\pi q^2 dq q^2 \frac{1}{e^{\hbar\omega_q/k_B T} - 1}. \tag{8.3}$$

In the high temperature limit, all modes have $\langle n_q \rangle \propto T$, for

$$\frac{1}{\tau_{ph}} \propto T \tag{8.4a}$$

$$\sigma \propto \frac{1}{T} \tag{8.4b}$$

$$\rho = \frac{1}{\sigma} \alpha T. \tag{8.4c}$$

In the low temperature limit. As in the Debye theory, let

$$x = \frac{\hbar\omega}{k_B T} = \frac{\hbar c q}{k_B T}, \tag{8.5}$$

for

$$\frac{1}{\tau_{ph}} \propto (\cdots) (k_B T)^5 \boxed{\int_0^{\Theta/T} \frac{x^5 dx}{e^x - 1}}. \tag{8.6}$$

some number

This gives

$$\rho = \rho_0 + AT^5. \tag{8.7}$$

At high T, the T^1 behavior is very general. At low T, T^5 is less universal.

The full range of resistivity is sketched in fig. 8.3.

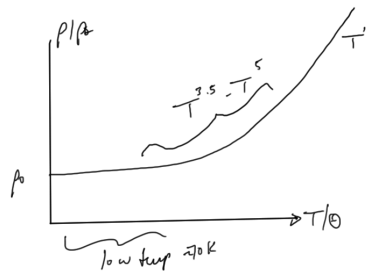

Figure 8.3: Resistivity temperature dependence.

8.2 ELECTRON-ELECTRON SCATTERING.

Reading: May not be in the text?

Electrons can scatter from other electrons, but they must conserve energy and (crystal) momentum.

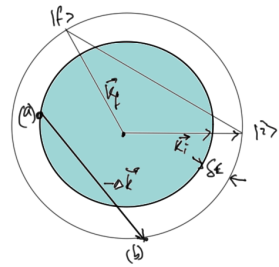

Figure 8.4: Filled Fermi sphere.

$T = 0$ Consider 1 electron outside a Fermi sphere. The transition $|i\rangle \to |f\rangle$ can only go to an empty state, within δE of E_F.

Must scatter off an electron that starts inside E_F, ends outside E_F, and it's $\Delta E \simeq \delta E$. eg. (a) to (b).

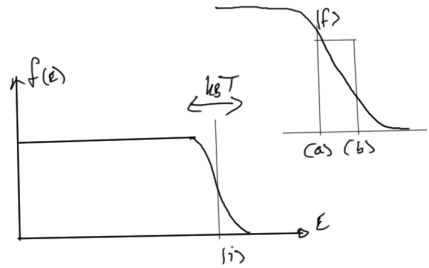

Figure 8.5: With temperature dependence state transitions still effectively confined to range of energies.

So both scattering events are restricted by δE, or

$$\boxed{\frac{1}{\tau} \propto (\delta E)^2.} \tag{8.8}$$

A state at E_F has infinite lifetime.

At $T > 0$, the argument is similar.

F6

$|i\rangle$ has a choice of states from within $k_B T$ of E_F to scatter to. States within $k_B T$ of E_F to scatter from.

$$\frac{1}{\tau} \propto T^2, \qquad \max(T^2, (\delta E)^2), \tag{8.9}$$

or

$$\boxed{\rho(T) = \rho_\circ + AT^2.} \tag{8.10}$$

This is universal. This is a famous result, from "Fermi liquid theory", developed by Landau and Fermi.

9 SEMICONDUCTOR PHYSICS.

9.1 CONDUCTION AND VALENCE BANDS.

Reading: [10] §12.1 Si, Ge, C, GaAs

All of these have a small gap at the Fermi energy E_F. The interesting physics all happens at the top of the valence band and at the bottom of the conduction band as sketched in fig. 9.1.

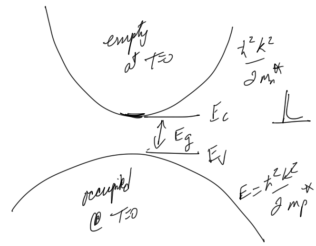

Figure 9.1: Conduction and valence bands.

Elements and compounds that have four valence electrons have a chance at being semi-conductors because they can form sp^3 hybrid orbitals. Note that there are also pressure dependencies here since putting enough pressure on a semiconductor will force it to metalize. That pressure changes the interatomic spacing and the associated energy distribution.

What we really want to figure out is how to calculate the density of the electrons in the conduction band, and the density of the holes that are left behind.

In ps9 we calculated the density of states at a band edge, which is what we have here. We found for $E > E_C$

$$D_C(E) = \frac{(2m_n^*)^{3/2}}{2\pi^2\hbar^3}\sqrt{E - E_C}, \tag{9.1}$$

and for $E < E_V$

$$D_V(E) = \frac{\left(2m_p^*\right)^{3/2}}{2\pi^2\hbar^3}\sqrt{E_V - E}. \tag{9.2}$$

This gives us

$$\begin{aligned} n &= \int_{E_C} D_C(E) f(E,T) dE \\ p &= \int^{E_V} D_V(E)(1 - f(E,T)) dE, \end{aligned} \tag{9.3}$$

for which the density of states and contributing regions are sketched in fig. 9.2.

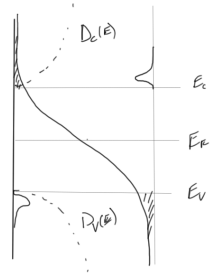

Figure 9.2: Conduction and valence density of states.

The "intrinsic" number of electrons in the conduction band equals the number of holes in the valence band, so that $n = p$: E_F adjusts accordingly.

So, for $E > E_C$ we have approximately the Boltzmann factor for the distribution

$$\frac{1}{e^{(E-E_F)/k_BT} + 1} \approx e^{-(E-E_F)/k_BT}, \tag{9.4}$$

and the electron density is

$$n = \frac{(2m_n^*)^{3/2}}{2\pi^2\hbar^3} e^{E_F/k_BT} \int_{E_C}^{\infty} \sqrt{E - E_C} e^{-E/k_BT} dE. \tag{9.5}$$

Since

$$\int_a^{\infty} \sqrt{E-a} e^{-E/\tau} dE = \frac{1}{2}\sqrt{\pi}\tau^{3/2} e^{-a/\tau}, \tag{9.6}$$

we have

$$n = 2\left(\frac{2\pi m_n^* k_B T}{h^2}\right)^{3/2} e^{-(E_C - E_F)/k_B T}. \tag{9.7}$$

This is written as

$$n = N_{\text{eff}}^C e^{-(E_C - E_F)/k_B T}, \tag{9.8}$$

where we note that N_{eff}^C is temperature dependent.

Similarly

$$p = 2\left(\frac{2\pi m_p^* k_B T}{h^2}\right)^{3/2} e^{-(E_F - E_V)/k_B T}, \tag{9.9}$$

or

$$p = N_{\text{eff}}^P e^{-(E_F - E_V)/k_B T}. \tag{9.10}$$

$$n_i = p_i = \sqrt{N_{\text{eff}}^C N_{\text{eff}}^V} e^{-(E_V - E_C)/k_B T} = \sqrt{N_{\text{eff}}^C N_{\text{eff}}^V} e^{-E_S/k_B T}. \tag{9.11}$$

9.2 DOPED SEMICONDUCTORS.

Reading: §12.3 pp 428-430.

We introduce a "donor", such as P in Si, as sketched in fig. 9.3. Four electrons make sp^3 hybrid orbitals with one electron left over.

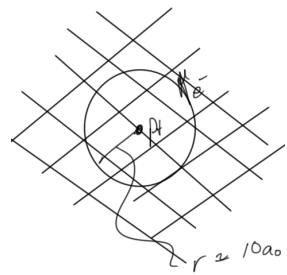

Figure 9.3: P donor, $T = 0$ (cf. hydrogen atom).

$$E_{\text{binding}} = \frac{m^* e^4}{2\left(4\pi\epsilon_\circ \epsilon_r \hbar\right)^2} \frac{1}{n^2} \approx 6\,\text{meV}. \tag{9.12}$$

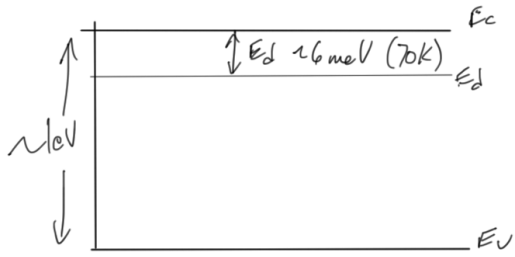

Figure 9.4: Donors are ionized at low T.

Here m^* is the conduction electron effective mass $\approx 0.2m_e$, and $\epsilon_r \approx 10$ in Si.

For "acceptors", e.g. B^- in Si, we need one electron to form four sp^3 hybrid orbitals. One is taken from the valence band. The density distribution is sketched in fig. 9.5.

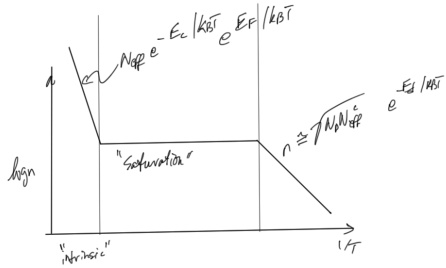

Figure 9.5: N-type (donor) temperature dependence.

For "intrinsic", $k_B T \gg E_g$, $n_i \gg N_D$. For "saturation", $n_i \ll N_D$, $n \approx N_D$. Donors are ionized, intrinsic carriers are frozen out. For "freeze out" $k_B T < E_d$

Details to follow... Two ways to write n

$$\begin{aligned} n &= N_D \left(1 - \frac{1}{1 + e^{(E_D - E_F)/k_B T}}\right) \\ &= N_D \left(1 - \frac{1}{1 + e^{E_d/k_B T}}\right), \end{aligned} \tag{9.13}$$

Also

...

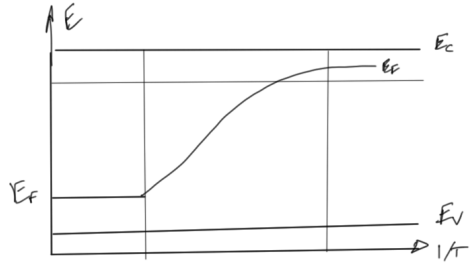

Figure 9.6: Acceptor energy distribution with temperature.

9.3 PROBLEMS.

Exercise 9.1 Doped carrier density. (*2013 ps10 p2*)

Germanium has an energy gap of $E_C - E_V = 0.67\,\text{eV}$, and an intrinsic carrier density $n_i = 2.5 \times 10^{19}\,\text{m}^{-3}$ at room temperature. A sample of germanium is doped with arsenic, which has a donor level located at $E_d = 0.0127\,\text{eV}$ below E_C. The concentration of arsenic atoms is $N_D = 1.0 \times 10^{22}\,\text{m}^{-3}$.

Show the temperature dependence of the carrier density in this sample by drawing a plot of $\ln(n)$ vs. $1/T$, between 1 K and 293 K (room temperature), and a second plot covering the temperature range from 100 K to 1000 K. Explain the main features of the plots.

Answer for Exercise 9.1

In class we didn't carry the doping discussion far enough for this problem, but our text treats the n-type semiconductor, arriving eventually at

$$n \approx 2N_D \left(1 + \sqrt{1 + 4\frac{N_D}{N_{\text{eff}}^C} e^{E_d/k_B T}}\right)^{-1}, \tag{9.14}$$

For this problem, noting that $k_B \sim 0.086\,^{\text{eV}}/_{\text{K}}$, we have

$$\frac{E_d}{k_B} \sim 147\,\text{K}, \tag{9.15}$$

so the exponential is large for small temperatures. How about the ratio N_D/N_{eff}^C? For Ge, §12.3 says we have $m_n^* \sim 0.13 m_e$, so

$$N_{eff}^C \sim 2\left(\frac{2\pi \times 0.13 m_e \times k_B T}{h^2}\right)^{3/2} \sim 4 \times 10^3 T^{3/2}\,\mathrm{m}^{-3}. \tag{9.16}$$

FIXME: Grading remark: Review the ps10plots.nb numerical calculation (stated above). Correct answer is supposed to be $\sim 4 \times 10^{20}$. The failure of UnitSimplify is likely related to that large difference.

This is plotted in fig. 9.7.

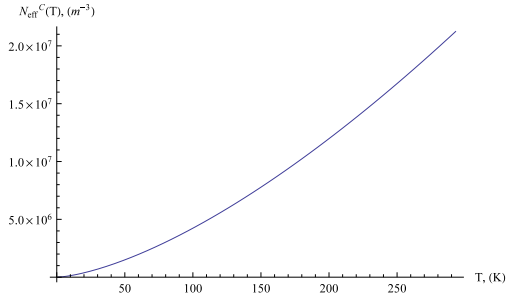

Figure 9.7: N_{eff}^C for Ge.

Combining the exponential and power dependent terms, using non-dimensionalized temperature $t = t/(1\,\mathrm{K})$, we have

$$4\frac{N_D}{N_{eff}^C} e^{E_d/k_B T} \sim \frac{9 \times 10^{18}}{t^{3/2}} e^{147/t}\,\mathrm{m}^{-3}. \tag{9.17}$$

In the $T \in [1, 293]$ interval, this ranges from 10^{83} down to 10^{15} as plotted in fig. 9.8.

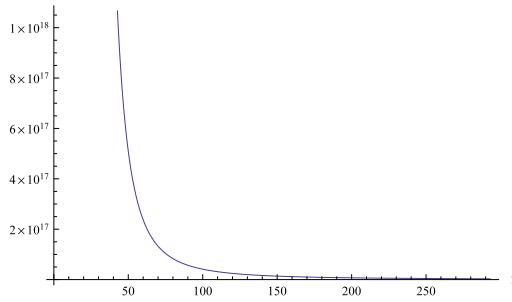

Figure 9.8: Illustrating scale of term in square root.

Grading remark: "Don't forget the intrinsic carriers!" This justifies a $4\frac{N_D}{N_{eff}^C}e^{E_d/k_BT} \gg 1$ approximation of eq. (9.14)

$$\begin{aligned} n &\approx 2N_D\left(1+\sqrt{4\frac{N_D}{N_{eff}^C}e^{E_d/k_BT}}\right)^{-1} \\ &\approx \frac{2N_D}{2\sqrt{N_DN_{eff}^C}e^{E_d/2k_BT}} \\ &= \sqrt{\frac{N_D}{N_{eff}^C}}e^{-E_d/2k_BT}. \end{aligned} \tag{9.18}$$

Taking logarithms we have

$$\begin{aligned} \ln n &\sim \frac{1}{2}\ln N_D + \frac{1}{2}\ln N_{eff}^C - \frac{E_d}{2k_BT}. \\ &\sim 11\ln 10 + \frac{1}{2}\ln 4 + \frac{3}{2}\ln 10 - \frac{3}{4}\ln\frac{1}{T} - 73\frac{1}{T} \\ &\approx 29 - \frac{3}{4}\ln\frac{1}{T} - 73\frac{1}{T}. \end{aligned} \tag{9.19}$$

This is plotted for $T^{-1} \in [1/293, 1]$ in fig. 9.9, along the nearly linear asymptote (with slope $-E_d/2k_B$). The lowest temperature range in this plot is the "freeze out" range where a large number of the donors still retain their electrons.

Zooming in on the high temperature domain by plotting $T^{-1} \in [1/1000, 1/100]$ in fig. 9.10. In this range we have $4\frac{N_D}{N_{eff}^C}e^{E_d/k_BT}$ taking values in the range $[10^{14}, 10^{16}]$, with $n \in [10^{14}, 10^{15}]\,\mathrm{m}^{-3}$. That is probably close enough to flat that we can still describe this as approaching the saturation range of [10] (eq. 12.28), at which point

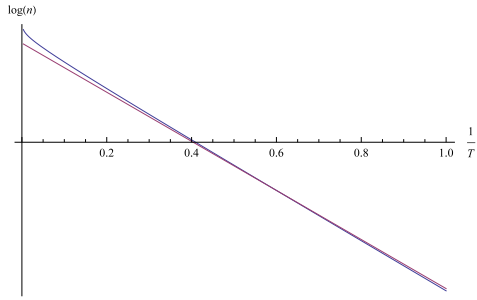

Figure 9.9: Concentration log vs inverse temperature.

"the concentration of donor electrons in the condition band has reached the maximum possible value".

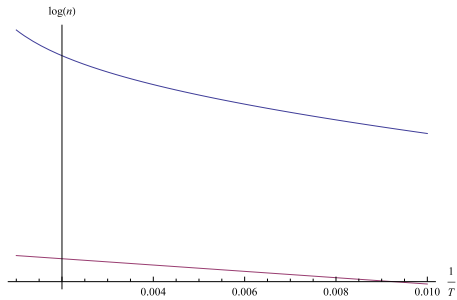

Figure 9.10: Concentration log vs inverse temperature for higher temperatures.

FIXME: Grading remark: Spike for the intrinsic carriers added to my plot with comment "intrinsic carriers appear ~ 0.002".

10 SUPERCONDUCTIVITY.

10.1 SUPERCONDUCTIVITY OVERVIEW.

Reading: [10] §10.1

The effect is actually not as rare as one would imagine (see [10] fig. 10.2 for a chart shown of many superconductive elements). Even O and S are superconductive, with fairly high transition temperatures, if pressurized enough to metalize it.

Some of the non-superconductive elements are those with very spherical Fermi surfaces.

The basic phenomena, that of resistivity drop at a critical temperature, is sketched in fig. 10.1. We also have a corresponding difference in the specific heat for these materials, as sketched in fig. 10.2.

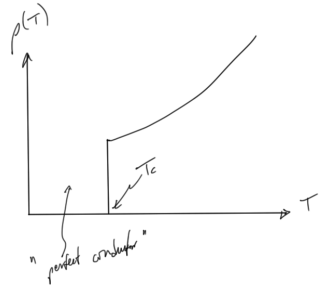

Figure 10.1: Electrical resistivity.

The exponential indicates that there's a gap to the first excited state (cf exponentials from the semiconductor theory?)

The essential feature of superconductivity is not that they are "perfect conductors", but that they are perfect dimagnets as illustrated in [10] fig. 10.4, and more roughly in fig. 10.3.

We have a circulating current that screens the field. This costs energy. There are two types of superconductors

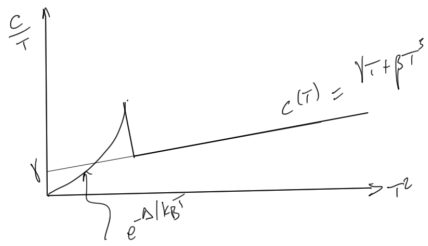

Figure 10.2: Specific heat of superconductor.

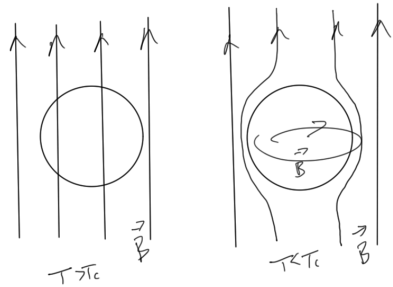

Figure 10.3: Diamagnetic phenomena.

- Type I, superconductivity collapses above H_c, sketched in fig. 10.4.
- Type II, particle flux expulsion above H_c, sketched in fig. 10.5.

10.2 LONDON EQUATIONS, AND PERFECT CONDUCTORS.

Reading: [10] §10.2

With resistivity $\rho = 0$, we have

$$m\dot{\mathbf{v}} = -e\boldsymbol{\mathcal{E}}, \tag{10.1}$$

and current density

$$\mathbf{j} = -n_s e\mathbf{v}, \tag{10.2}$$

for

$$\frac{\partial \mathbf{j}}{\partial t} = \frac{n_s e^2}{m}\boldsymbol{\mathcal{E}}, \tag{10.3}$$

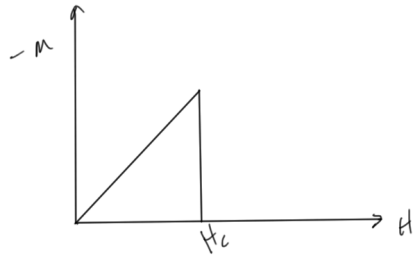

Figure 10.4: Type I.

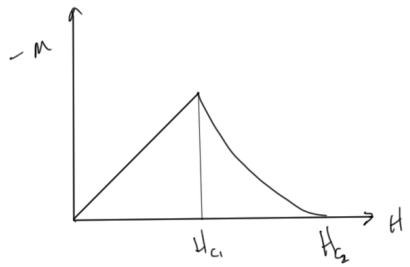

Figure 10.5: Type II.

With Maxwell's third

$$\boldsymbol{\nabla} \times \boldsymbol{\mathcal{E}} = -\frac{\partial \mathbf{B}}{\partial t}, \tag{10.4}$$

we have

$$\frac{\partial}{\partial t}\left(\frac{m}{n_s e^2}\boldsymbol{\nabla} \times \mathbf{j} + \mathbf{B}\right) = 0, \tag{10.5}$$

so that the equation for a perfect diamagnet satisfies

$$\boxed{\frac{m}{n_s e^2}\boldsymbol{\nabla} \times \mathbf{j} = -\mathbf{B}} \tag{10.6}$$

$$\boldsymbol{\nabla} \times \mathbf{j} = -\frac{n_s e^2}{m}\mathbf{B} = -\frac{1}{\lambda_L}\mathbf{B}. \tag{10.7}$$

Example 10.1: Solution for constant magnetic field.

Consider a unidirectional magnetic field

$$\mathbf{B} = (B_x, 0, 0), \tag{10.8}$$

as sketched in fig. 10.6.

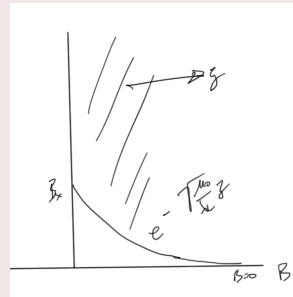

Figure 10.6: Magnetic Field.

With no time dependence of the electric field (no displacement term $\mu_\circ \epsilon_\circ \partial \mathbf{E}/\partial t$) Ampere's Maxwell's equations is

$$\boldsymbol{\nabla} \times \mathbf{B} = \mu_\circ \mathbf{j}. \tag{10.9}$$

Taking cross products of both sides of eq. (10.7), we have

$$\boldsymbol{\nabla} \times (\boldsymbol{\nabla} \times \mathbf{j}) = \boldsymbol{\nabla} \times \left(-\frac{\mathbf{B}}{\lambda_L} \right) = -\frac{\mu_\circ}{\lambda_L} \mathbf{j}. \tag{10.10}$$

By taking dot products of eq. (10.9), and noting that $\boldsymbol{\nabla} \cdot (\boldsymbol{\nabla} \times \mathbf{X}) = 0$, for sufficiently continuous fields $\mathbf{X}$, we must have $\boldsymbol{\nabla} \cdot \mathbf{j} = 0$, and thus

$$\begin{aligned} \boldsymbol{\nabla} \times (\boldsymbol{\nabla} \times \mathbf{j}) &= -\boldsymbol{\nabla}^2 \mathbf{j} + \boldsymbol{\nabla}(\boldsymbol{\nabla} \cdot \mathbf{j}) \\ &= -\boldsymbol{\nabla}^2 \mathbf{j}. \end{aligned} \tag{10.11}$$

Equation (10.10) is now decoupled

$$-\boldsymbol{\nabla}^2 \mathbf{j} = -\frac{\mu_\circ}{\lambda_L} \mathbf{j}. \tag{10.12}$$

This has solution

$$\mathbf{j} = \mathbf{j}_\circ e^{-\sqrt{\mu_\circ/\lambda_L} z}, \tag{10.13}$$

and

$$\mathbf{B} = \hat{\mathbf{x}} B_x^\circ e^{-\sqrt{\mu_\circ/\lambda_L} z}. \tag{10.14}$$

10.3 COOPER PAIRING.

Reading: [10] §10.2

There's an effective attraction between the electrons in a metal that is mediated by phonons, as sketched in fig. 10.7.

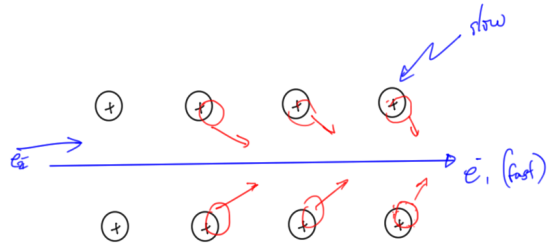

Figure 10.7: Lattice distorts after the electron passes.

The second electron can lower it's energy by travelling in the "wake" of the first. Note that this is actually an incorrect picture, since what really goes on is that the second electron passes in the opposite direction from the first to take advantage of the wake.

It is important that the lattice reaction is retarded in time.

electron-phonon interaction The Cooper calculation considered a filled Fermi surface (such as a sphere) at $T = 0$. He considered what happens if you add two electrons above E_F as sketched in fig. 10.8.

The electron phonon interaction looks like

$$\rho_{el}(x,t)\rho_{ph}(x,t). \tag{10.15}$$

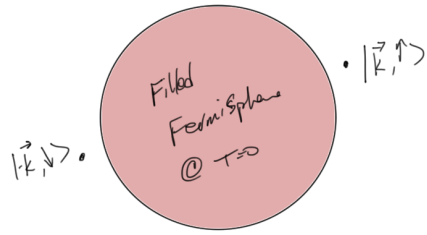

Figure 10.8: Filled Fermi sphere at $T = 0$.

$$|\mathbf{k},\uparrow\rangle \to |\mathbf{k},\uparrow,\ \text{o phonons}\ \rangle + \sum_{\mathbf{q}} \alpha_q |\mathbf{k}-\mathbf{q}_i\,|\mathbf{q}\rangle\,. \tag{10.16}$$

Here the state has a Bloch form

$$|\mathbf{k},\uparrow\rangle = \frac{1}{\sqrt{L^3}} e^{i\mathbf{k}\cdot\mathbf{r}}\,|\sigma\rangle\,. \tag{10.17}$$

electron density

$$\begin{aligned}\langle\psi|\psi\rangle &= \frac{1}{L^3}\left(e^{-i\mathbf{k}\cdot\mathbf{r}}\langle 0_q| + \alpha_q e^{-i(\mathbf{k}-\mathbf{q})\cdot\mathbf{r}}\langle 1_q|\right)\left(e^{i\mathbf{k}\cdot\mathbf{r}}|0_q\rangle + e^{i(\mathbf{k}-\mathbf{q})\cdot\mathbf{r}}|1_q\rangle\right)\\ &= \frac{1}{L^3}1 + \alpha_q^2 + \alpha_q\left(e^{i\mathbf{q}\cdot\mathbf{r}} + e^{-i\mathbf{q}\cdot\mathbf{r}}\right)\\ &= \frac{1}{L^3}1 + \alpha_q^2 + \alpha_q\cos\left(\mathbf{q}\cdot\mathbf{r}\right)\end{aligned} \tag{10.18}$$

Here the cosine is the modulated charge density. This transition is sketched in fig. 10.9.

Cooper pairing (cont.)

Reading: [10] §10.2

Electron-phonon interaction

$$|\mathbf{k},\uparrow\rangle \to |\mathbf{k},\uparrow,0_q\rangle + \alpha_q\,|\mathbf{k},\uparrow,1_q\rangle\,. \tag{10.19}$$

$$|\mathbf{k}',\downarrow\rangle \to |\mathbf{k}'-\mathbf{q},\downarrow,0_q\rangle + \alpha_{-q}\,|\mathbf{k}-\mathbf{q},\downarrow,1_q\rangle\,. \tag{10.20}$$

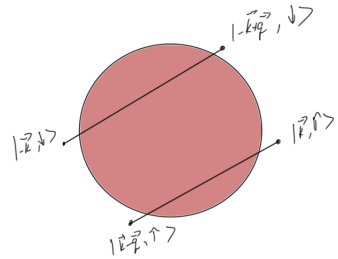

Figure 10.9: Pair state transitions outside of Fermi sphere.

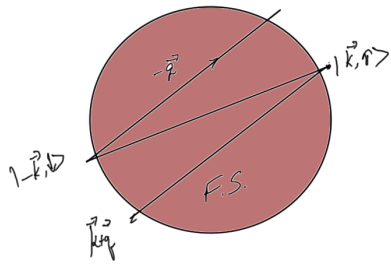

Figure 10.10: Electron-phonon interaction.

Using perturbation theory, you set an effective interaction

$$V_{\text{eff}} = \frac{\left|V_{\text{e,ph}}\right|^2}{\left(\mathcal{E}_{\mathbf{k}+\mathbf{q}} - \mathcal{E}_{\mathbf{k}}\right)^2 - \hbar^2\omega_{\mathbf{q}}^2}. \tag{10.21}$$

$$|\Psi\rangle = \sum_k g(\mathbf{k}) e^{i\mathbf{k}\cdot(\mathbf{r}_1 - \mathbf{r}_2)}. \tag{10.22}$$

$$\begin{aligned} &\left(-\frac{\hbar^2}{2m}\left(\boldsymbol{\nabla}_1^2 + \boldsymbol{\nabla}_2^2\right) + V(\mathbf{r}_1, \mathbf{r}_2)\right) \sum_k g(\mathbf{k}) e^{i\mathbf{k}\cdot(\mathbf{r}_1 - \mathbf{r}_2)} \\ &\qquad E\,|\Psi\rangle \\ &= \boxed{(2E_{\text{F}} + \mathcal{E})} \sum_k g(\mathbf{k}) e^{i\mathbf{k}\cdot(\mathbf{r}_1 - \mathbf{r}_2)}. \end{aligned} \tag{10.23}$$

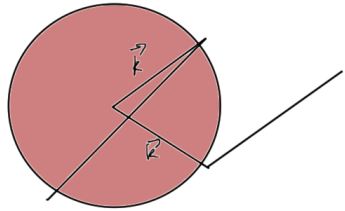

Figure 10.11: Limited options for paired states available.

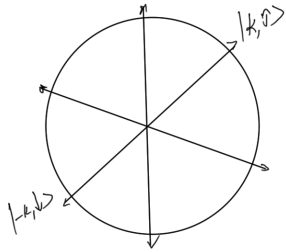

Figure 10.12: Cooper filled Fermi sphere plus two electrons.

Operating with $\int d\mathbf{r}_1 d\mathbf{r}_2 e^{-i\mathbf{k}'\cdot(\mathbf{r}_1-\mathbf{r}_2)}$, we have

$$\begin{aligned}\int d\mathbf{r}_1 d\mathbf{r}_2 e^{-i\mathbf{k}'\cdot(\mathbf{r}_1-\mathbf{r}_2)} \left(\boldsymbol{\mathcal{E}}_{\mathbf{k}} + \boldsymbol{\mathcal{E}}_{-\mathbf{k}} + V\right) \sum_k g(\mathbf{k}) e^{i\mathbf{k}\cdot(\mathbf{r}_1-\mathbf{r}_2)} \\ = \int d\mathbf{r}_1 d\mathbf{r}_2 e^{-i\mathbf{k}'\cdot(\mathbf{r}_1-\mathbf{r}_2)} (2E_{\mathrm{F}} + \mathcal{E}) \sum_k g(\mathbf{k}) e^{i\mathbf{k}\cdot(\mathbf{r}_1-\mathbf{r}_2)}.\end{aligned} \tag{10.24}$$

This is

$$2\boldsymbol{\mathcal{E}}_{\mathbf{k}'} g(\mathbf{k}') + \sum_{\mathbf{k}} V_{\mathbf{k}'\mathbf{k}} g(\mathbf{k}) = (2E_{\mathrm{F}} + \mathcal{E})\, g(\mathbf{k}'), \tag{10.25}$$

where

$$V_{\mathbf{k},\mathbf{k}'} = \int d\mathbf{r}_1 d\mathbf{r}_2 e^{-i\mathbf{k}'\cdot(\mathbf{r}_1-\mathbf{r}_2)} V(\mathbf{r}_1, \mathbf{r}_2) e^{i\mathbf{k}\cdot(\mathbf{r}_1-\mathbf{r}_2)}. \tag{10.26}$$

Make the approximation

$$V_{\mathbf{k},\mathbf{k}'} = \begin{cases} V_\circ & \text{if } \mathcal{E}_{\mathbf{k}}, \mathcal{E}_{\mathbf{k}'} \text{ between } E_{\mathrm{F}} \text{ and } E_{\mathrm{F}} + \hbar\Omega_D \\ 0 & \text{otherwise} \end{cases} \tag{10.27}$$

This has solution

$$g(\mathbf{k}') = \frac{1}{2E_F + \mathcal{E} - 2\mathcal{E}_{\mathbf{k}'}} \sum_{\mathbf{k}} V_{\mathbf{k}',\mathbf{k}} g(\mathbf{k}). \tag{10.28}$$

Sum this over $\mathbf{k}'$

$$\sum_{\mathbf{k}'} g(\mathbf{k}') = \sum_{\mathbf{k}'} \frac{V_\circ}{2E_F + \mathcal{E} - 2\mathcal{E}_{\mathbf{k}'}} \sum_{\mathbf{k}} g(\mathbf{k}). \tag{10.29}$$

$$\begin{aligned} 1 &= V_\circ \int_{E_F}^{E_F + \hbar\omega_D} \frac{D(E)dE}{2E_F + \mathcal{E} - 2E} \\ &\approx V_\circ D(E_F) \frac{1}{2} \ln\left(2E_F + \mathcal{E} - 2E\right)\Big|_{E_F}^{E_F + \hbar\omega_D} \\ &\approx \frac{V_\circ D(E_F)}{2} \ln \frac{2E_F + \mathcal{E} - 2E_F}{2E_F + \mathcal{E} - 2(E_F + \hbar\omega_D)}. \end{aligned} \tag{10.30}$$

Giving

$$e^{2/V_\circ D(E_F)} = \frac{\mathcal{E} - 2\hbar\omega_D}{\mathcal{E}}. \tag{10.31}$$

or

$$\mathcal{E} = \frac{-2\hbar\omega_D}{e^{2/V_\circ D(E_F)} - 1}. \tag{10.32}$$

$$\boxed{\mathcal{E} \approx -2\hbar\omega_D e^{-2/V_\circ D(E_F)}} \tag{10.33}$$

Bound state Fermi surface $(2E_F + \mathcal{E}) < 2E_F$.

A filled Fermi sphere at $T = 0$ is unstable against Fermiation of Cooper pairs.

10.4 BCS THEORY.

Reading: [10] §10.4

Difficult to make a multiple Cooper pair state.

BCS guess was:

$$|0_{BCS}\rangle = \Pi_{\mathbf{k}} \left(u_{\mathbf{k}} \left|0_{\mathbf{k}\uparrow}, 0_{-\mathbf{k}\downarrow}\right\rangle + v_{\mathbf{k}} \left|1_{\mathbf{k}\uparrow}, 1_{-\mathbf{k}\downarrow}\right\rangle\right). \tag{10.34}$$

At every: states are either empty (prob $u_{\mathbf{k}}^2$) or filled (prob $v_{\mathbf{k}}^2$) in pairs.

The energy

Need a superposition of occupied and unoccupied

$$W = \sum_{\mathbf{k}} 2\mathcal{E}_{\mathbf{k}} v_{\mathbf{k}}^2 + \sum_{\mathbf{k},\mathbf{k}'} V_{\mathbf{k},\mathbf{k}'} u_{\mathbf{k}'} v_{\mathbf{k}'} u_{\mathbf{k}} v_{\mathbf{k}} . \tag{10.35}$$

A

HUYGENS DIFFRACTION.

We were presented with a diffraction result, that the intensity can be expressed as the Fourier transform of the aperture. Let's review a derivation of that based on the Huygens principle. Consider the aperture of fig. A.1.

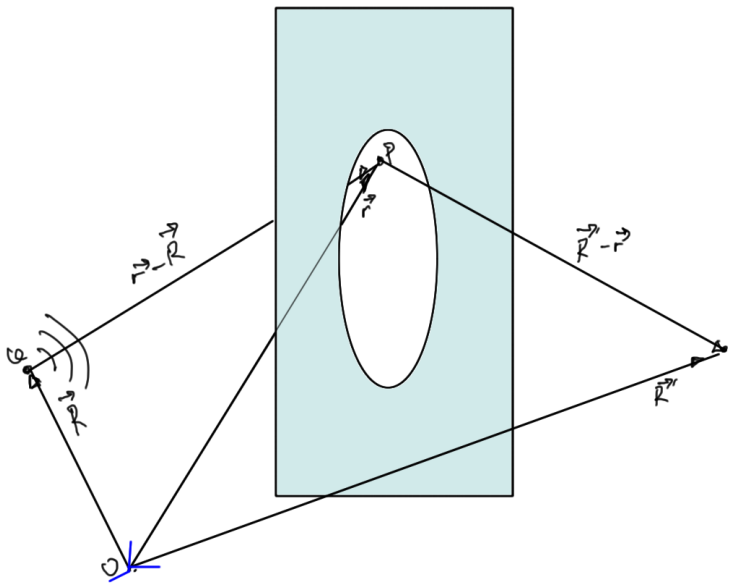

Figure A.1: Diffraction aperture.

The Huygens principle expresses the amplitude of a wave $U(\mathbf{r})$ in terms of it's amplitude $U_\circ$ at $\mathbf{r} = 0$ as

$$U(\mathbf{r}) \propto \frac{U_\circ e^{ik|\mathbf{r}|}}{|\mathbf{r}|}. \tag{A.1}$$

For multiple point diffraction, the diffracted wave is a superposition of such contributions from all points in the aperture. For example, two exponentials are summed when considering a two

slit diffraction apparatus. For a more general aperture as above, we'd form

$$U(\mathbf{R}') \propto U_\circ \int_A d^2\mathbf{r} \frac{e^{ik|\mathbf{r}-\mathbf{R}|}}{|\mathbf{r}-\mathbf{R}|} \frac{e^{ik|\mathbf{R}'-\mathbf{r}|}}{|\mathbf{R}'-\mathbf{r}|}. \tag{A.2}$$

Note that this the Huygens result is an approximation in many ways. Fresnel later fixed up the proportionality factor and considered the angular dependence of the between the source and diffracted rays (the obliquity factor). That corrected result is known as the Huygens-Fresnel principle. Kirchhoff later considered solutions to the scalar wave equations for the electromagnetic field components **E** and **B**, ignoring the Maxwell coupling of these fields. See §8.3.1 [2], §A.2 §10.4 of [9], or §5.2 of [5] for details. See §9.8 [11] for a vector diffraction treatment.

Let's proceed with using eq. (A.2) to obtain our result from class. For simplicity, first position the origin in the aperture itself as in fig. A.2.

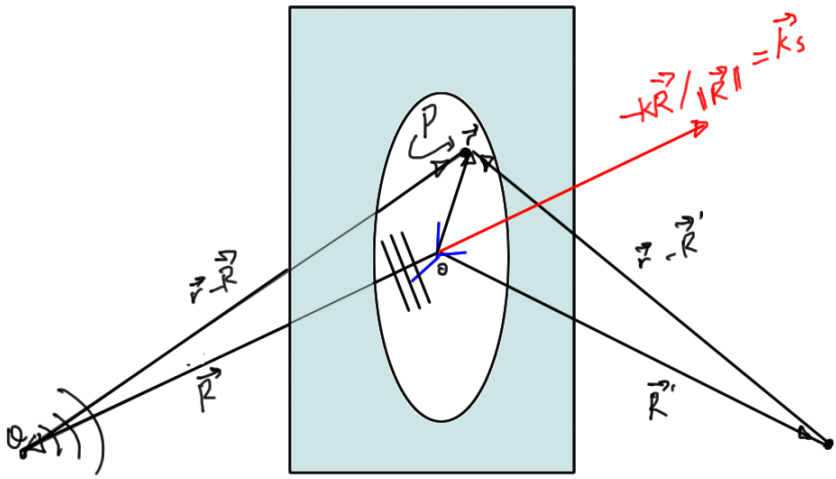

Figure A.2: Diffraction aperture with origin in aperture.

Now we are set to perform a first order expansion of the vector lengths $|\mathbf{r} - \mathbf{R}|$ and $|\mathbf{r} - \mathbf{R}'|$. It's sufficient to consider just one of these, expanding to first order

$$\begin{aligned}
|\mathbf{r} - \mathbf{R}| &= \sqrt{(\mathbf{r} - \mathbf{R})^2} \\
&= \sqrt{\mathbf{R}^2 + \mathbf{r}^2 - 2\mathbf{r} \cdot \mathbf{R}} \\
&= R\sqrt{1 + \frac{\mathbf{r}^2}{\mathbf{R}^2} - 2\mathbf{r} \cdot \frac{\mathbf{R}}{\mathbf{R}^2}} \\
&\approx R\left(1 + \frac{1}{2}\frac{\mathbf{r}^2}{\mathbf{R}^2} - \mathbf{r} \cdot \frac{\mathbf{R}}{\mathbf{R}^2}\right) \\
&= R + \frac{1}{2}\frac{\mathbf{r}^2}{R} - \mathbf{r} \cdot \frac{\mathbf{R}}{R}.
\end{aligned} \tag{A.3}$$

Assume that both $\mathbf{R}$ and $\mathbf{R}'$ to be far enough from the aperture that we can approximate the $|\mathbf{R} - \mathbf{r}|$ and $|\mathbf{R}' - \mathbf{r}|$ terms downstairs as $R = |\mathbf{R}|$ and $R' = |\mathbf{R}'|$ respectively. Additionally, ignore the second order term above, significant for Fresnel diffraction where the diffraction pattern close to the aperture is examined, but not in the far field. This gives

$$\begin{aligned}
U(\mathbf{R}') &\sim \frac{U_\circ}{RR'} \int_{\mathrm{A}} d^2\mathbf{r} e^{ik\left(R - \mathbf{r}\cdot\hat{\mathbf{R}}\right)} e^{ik\left(R' - \mathbf{r}\cdot\hat{\mathbf{R}}'\right)} \\
&= \frac{U_\circ}{RR'} e^{ik(R+R')} \int_{\mathrm{A}} d^2\mathbf{r} e^{-ik\mathbf{r}\cdot\hat{\mathbf{R}}} e^{-ik\mathbf{r}\cdot\hat{\mathbf{R}}'}.
\end{aligned} \tag{A.4}$$

Finally write

$$\begin{aligned}
\mathbf{k}_s &= -k\hat{\mathbf{R}} \\
\mathbf{k} &= k\hat{\mathbf{R}}',
\end{aligned} \tag{A.5}$$

for

$$U(\mathbf{R}') \sim \frac{U_\circ}{RR'} e^{ik(R+R')} \int_{\mathrm{A}} d^2\mathbf{r} e^{-i\mathbf{r}\cdot(\mathbf{k} - \mathbf{k}_s)}. \tag{A.6}$$

Finally, write

$$\mathbf{K} = \mathbf{k} - \mathbf{k}_s, \tag{A.7}$$

and introduce an aperture function $\rho(\mathbf{r})$ (we called this the scattering density). This aperture function is unity for any regions of the aperture that light is allowed through, and zero when light

is blocked, and some value in $[0, 1]$ for translucent regions of the aperture. We can now expand the integral over the surface containing the aperture

$$\boxed{U(\mathbf{R}') \sim \frac{U_\circ}{RR'} e^{ik(R+R')} \int \rho(\mathbf{r}) e^{-i\mathbf{r}\cdot\mathbf{K}}.} \tag{A.8}$$

B

DISCRETE FOURIER TRANSFORM.

For decoupling trial solutions of lattice vibrations we have what appears to be a need for the use of a discrete Fourier transform. This is described briefly in [8], but there's no proof of the inversion formula. Let's work through that detail.

Let's start given a periodic signal of the following form

$$a_n = \sum_{k=0}^{N-1} A_k e^{-2\pi i k n/N}, \tag{B.1}$$

and assume that there's an inversion formula of the form

$$A'_k \propto \sum_{n=0}^{N-1} a_n e^{2\pi i k' n/N}. \tag{B.2}$$

Direct substitution should show if such a transform pair is valid, and determine the proportionality constant. Let's try this

$$\begin{aligned}\sum_{n=0}^{N-1} a_n e^{2\pi i k' n/N} &= \sum_{n=0}^{N-1} e^{2\pi i k' n/N} \sum_{k=0}^{N-1} A_k e^{-2\pi i k n/N} \\ &= \sum_{k=0}^{N-1} A_k \sum_{n=0}^{N-1} e^{2\pi i (k'-k) n/N}.\end{aligned} \tag{B.3}$$

Observe that the interior sum is just N when $k' = k$. Let's sum this for the values $k \neq k'$, writing

$$S_N(k' - k) = \sum_{n=0}^{N-1} e^{2\pi i (k'-k) n/N}. \tag{B.4}$$

With $a = \exp(2\pi i(k' - k)/N)$ we have

$$\begin{aligned} S_N(k' - k) &= \sum_{n=0}^{N-1} a^n \\ &= \frac{a^N - 1}{a - 1} \\ &= \frac{a^{N/2}}{a^{1/2}} \frac{a^{N/2} - a^{-N/2}}{a^{1/2} - a^{-1/2}} \\ &= e^{\pi i(k'-k)(1-1/N)} \frac{\sin \pi(k' - k)}{\sin \pi(k' - k)/N}. \end{aligned} \tag{B.5}$$

Observe that $k' - k \in [-N+1, N-1]$, and necessarily takes on just integer values. We have terms of the form $\sin \pi m$, for integer m in the numerator, always zero. In the denominator, the sine argument is in the range

$$[\pi \left(-1 + \frac{1}{N}\right), \pi \left(1 - \frac{1}{N}\right)], \tag{B.6}$$

We can visualize that range as all the points on a sine curve with the integer multiples of π omitted, as in fig. B.1.

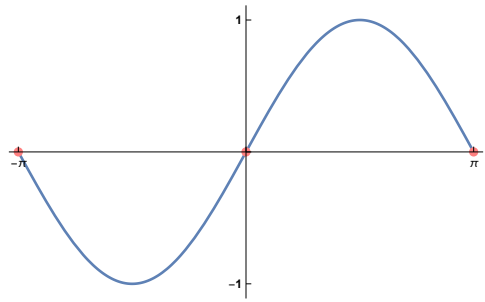

Figure B.1: Sine with integer multiples of π omitted.

Clearly the denominator is always non-zero when $k \neq k'$. This provides us with the desired inverse transformation relationship

$$\begin{aligned} \sum_{n=0}^{N-1} a_n e^{2\pi i k' n/N} &= N \sum_{k'=0}^{N-1} A'_k \delta_{k,k'} \\ &= N A'_k. \end{aligned} \tag{B.7}$$

Summary. Now that we know the relationship between the discrete set of values a_n and this discrete transformation of those values, let's write the transform pair in a form that explicitly expresses this relationship.

$$\begin{aligned} a_n &= \sum_{k=0}^{N-1} \tilde{a}_k e^{-2\pi i k n/N} \\ \tilde{a}_k &= \frac{1}{N} \sum_{n=0}^{N-1} a_n e^{2\pi i k n/N}. \end{aligned} \tag{B.8}$$

We have also shown that our discrete sum of exponentials has an delta function operator nature, a fact that will likely be handy in various manipulations.

$$\sum_{n=0}^{N-1} e^{2\pi i (k'-k) n/N} = N\delta_{k,k'}. \tag{B.9}$$

C

SECOND ORDER SYSTEMS.

C.1 MOTIVATION.

We're discussing specific forms to systems of coupled linear differential equations, such as a loop of "spring" connected masses (i.e. atoms interacting with harmonic oscillator potentials) as sketched in fig. C.1.

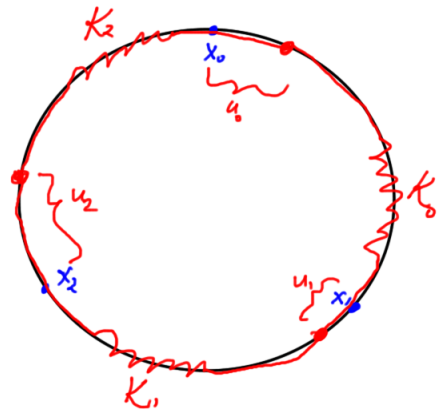

Figure C.1: Three springs loop.

Instead of assuming a solution, let's see how far we can get attacking this problem systematically.

C.2 MATRIX METHODS.

Suppose that we have a set of N masses constrained to a circle interacting with harmonic potentials. The Lagrangian for such a system (using modulo N indexing) is

$$\mathcal{L} = \frac{1}{2}\sum_{k=0}^{2} m_k \dot{u}_k^2 - \frac{1}{2}\sum_{k=0}^{2} \kappa_k \left(u_{k+1} - u_k\right)^2 . \tag{C.1}$$

The force equations follow directly from the Euler-Lagrange equations

$$0 = \frac{d}{dt}\frac{\partial \mathcal{L}}{\partial \dot{u}_{n,\alpha}} - \frac{\partial \mathcal{L}}{\partial u_{n,\alpha}}. \tag{C.2}$$

For the simple three particle system depicted above, this is

$$\begin{aligned}\mathcal{L} = &\frac{1}{2}m_0\dot{u}_0^2 + \frac{1}{2}m_1\dot{u}_1^2 + \frac{1}{2}m_2\dot{u}_2^2 \\ &- \frac{1}{2}\kappa_0\left(u_1 - u_0\right)^2 - \frac{1}{2}\kappa_1\left(u_2 - u_1\right)^2 - \frac{1}{2}\kappa_2\left(u_0 - u_2\right)^2,\end{aligned} \tag{C.3}$$

with equations of motion

$$\begin{aligned}0 &= m_0\ddot{u}_0 + \kappa_0\left(u_0 - u_1\right) + \kappa_2\left(u_0 - u_2\right) \\ 0 &= m_1\ddot{u}_1 + \kappa_1\left(u_1 - u_2\right) + \kappa_0\left(u_1 - u_0\right) \\ 0 &= m_2\ddot{u}_2 + \kappa_2\left(u_2 - u_0\right) + \kappa_1\left(u_2 - u_1\right),\end{aligned} \tag{C.4}$$

Let's partially non-dimensionalize this. First introduce average mass $\bar{m}$ and spring constants $\bar{\kappa}$, and rearrange slightly

$$\begin{aligned}\frac{\bar{m}}{\bar{k}}\ddot{u}_0 &= -\frac{\kappa_0\bar{m}}{\bar{k}m_0}\left(u_0 - u_1\right) - \frac{\kappa_2\bar{m}}{\bar{k}m_0}\left(u_0 - u_2\right) \\ \frac{\bar{m}}{\bar{k}}\ddot{u}_1 &= -\frac{\kappa_1\bar{m}}{\bar{k}m_1}\left(u_1 - u_2\right) - \frac{\kappa_0\bar{m}}{\bar{k}m_1}\left(u_1 - u_0\right) \\ \frac{\bar{m}}{\bar{k}}\ddot{u}_2 &= -\frac{\kappa_2\bar{m}}{\bar{k}m_2}\left(u_2 - u_0\right) - \frac{\kappa_1\bar{m}}{\bar{k}m_2}\left(u_2 - u_1\right).\end{aligned} \tag{C.5}$$

With

$$\tau = \sqrt{\frac{\bar{k}}{\bar{m}}}t = \Omega t \tag{C.6a}$$

$$\mathbf{u} = \begin{bmatrix} u_0 \\ u_1 \\ u_2 \end{bmatrix} \tag{C.6b}$$

$$B = \begin{bmatrix} -\frac{\kappa_0\bar{m}}{\bar{k}m_0} - \frac{\kappa_2\bar{m}}{\bar{k}m_0} & \frac{\kappa_0\bar{m}}{\bar{k}m_0} & \frac{\kappa_2\bar{m}}{\bar{k}m_0} \\ \frac{\kappa_0\bar{m}}{\bar{k}m_1} & -\frac{\kappa_1\bar{m}}{\bar{k}m_1} - \frac{\kappa_0\bar{m}}{\bar{k}m_1} & \frac{\kappa_1\bar{m}}{\bar{k}m_1} \\ \frac{\kappa_2\bar{m}}{\bar{k}m_2} & \frac{\kappa_1\bar{m}}{\bar{k}m_2} & -\frac{\kappa_2\bar{m}}{\bar{k}m_2} - \frac{\kappa_1\bar{m}}{\bar{k}m_2} \end{bmatrix}. \tag{C.6c}$$

Our system takes the form

$$\frac{d^2\mathbf{u}}{d\tau^2} = B\mathbf{u}. \tag{C.7}$$

We can at least theoretically solve this in a simple fashion if we first convert it to a first order system. We can do that by augmenting our vector of displacements with their first derivatives

$$\mathbf{w} = \begin{bmatrix} \mathbf{u} \\ \frac{d\mathbf{u}}{d\tau} \end{bmatrix}, \tag{C.8}$$

So that

$$\frac{d\mathbf{w}}{d\tau} = \begin{bmatrix} 0 & I \\ B & 0 \end{bmatrix} \mathbf{w} = A\mathbf{w}. \tag{C.9}$$

Now the solution is conceptually trivial

$$\mathbf{w} = e^{A\tau}\mathbf{w}_\circ. \tag{C.10}$$

We are however, faced with the task of exponentiating the matrix A. All the powers of this matrix A will be required, but they turn out to be easy to calculate

$$\begin{bmatrix} 0 & I \\ B & 0 \end{bmatrix}^2 = \begin{bmatrix} 0 & I \\ B & 0 \end{bmatrix} \begin{bmatrix} 0 & I \\ B & 0 \end{bmatrix} = \begin{bmatrix} B & 0 \\ 0 & B \end{bmatrix} \tag{C.11a}$$

$$\begin{bmatrix} 0 & I \\ B & 0 \end{bmatrix}^3 = \begin{bmatrix} B & 0 \\ 0 & B \end{bmatrix} \begin{bmatrix} 0 & I \\ B & 0 \end{bmatrix} = \begin{bmatrix} 0 & B \\ B^2 & 0 \end{bmatrix} \tag{C.11b}$$

$$\begin{bmatrix} 0 & I \\ B & 0 \end{bmatrix}^4 = \begin{bmatrix} 0 & B \\ B^2 & 0 \end{bmatrix} \begin{bmatrix} 0 & I \\ B & 0 \end{bmatrix} = \begin{bmatrix} B^2 & 0 \\ 0 & B^2 \end{bmatrix}, \tag{C.11c}$$

allowing us to write out the matrix exponential

$$e^{A\tau} = \sum_{k=0}^{\infty} \frac{\tau^{2k}}{(2k)!} \begin{bmatrix} B^k & 0 \\ 0 & B^k \end{bmatrix} + \sum_{k=0}^{\infty} \frac{\tau^{2k+1}}{(2k+1)!} \begin{bmatrix} 0 & B^k \\ B^{k+1} & 0 \end{bmatrix}. \tag{C.12}$$

Case I: No zero eigenvalues Provided that B has no zero eigenvalues, we could factor this as

$$\begin{bmatrix} 0 & B^k \\ B^{k+1} & 0 \end{bmatrix} = \begin{bmatrix} 0 & B^{-1/2} \\ B^{1/2} & 0 \end{bmatrix} \begin{bmatrix} B^{k+1/2} & 0 \\ 0 & B^{k+1/2} \end{bmatrix}, \tag{C.13}$$

This initially leads us to believe the following, but we'll find out that the three springs interaction matrix B does have a zero eigenvalue, and we'll have to be more careful. If there were any such interaction matrices that did not have such a zero we could simply write

$$\begin{aligned} e^{A\tau} &= \sum_{k=0}^{\infty} \frac{\tau^{2k}}{(2k)!} \begin{bmatrix} \sqrt{B}^{2k} & 0 \\ 0 & \sqrt{B}^{2k} \end{bmatrix} \\ &\quad + \begin{bmatrix} 0 & B^{-1/2} \\ B^{1/2} & 0 \end{bmatrix} \sum_{k=0}^{\infty} \frac{\tau^{2k+1}}{(2k+1)!} \begin{bmatrix} \sqrt{B}^{2k+1} & 0 \\ 0 & \sqrt{B}^{2k+1} \end{bmatrix} \\ &= \cosh \begin{bmatrix} \sqrt{B}\tau & 0 \\ 0 & \sqrt{B}\tau \end{bmatrix} + \begin{bmatrix} 0 & 1/\sqrt{B}\tau \\ \sqrt{B}\tau & 0 \end{bmatrix} \sinh \begin{bmatrix} \sqrt{B}\tau & 0 \\ 0 & \sqrt{B}\tau \end{bmatrix}. \end{aligned} \tag{C.14}$$

This is

$$e^{A\tau} = \begin{bmatrix} \cosh \sqrt{B}\tau & (1/\sqrt{B}) \sinh \sqrt{B}\tau \\ \sqrt{B} \sinh \sqrt{B}\tau & \cosh \sqrt{B}\tau \end{bmatrix}. \tag{C.15}$$

The solution, written out is

$$\begin{bmatrix} \mathbf{u} \\ \mathbf{u}' \end{bmatrix} = \begin{bmatrix} \cosh \sqrt{B}\tau & (1/\sqrt{B}) \sinh \sqrt{B}\tau \\ \sqrt{B} \sinh \sqrt{B}\tau & \cosh \sqrt{B}\tau \end{bmatrix} \begin{bmatrix} \mathbf{u}_\circ \\ \mathbf{u}'_\circ \end{bmatrix}, \tag{C.16}$$

so that

$$\boxed{\mathbf{u} = \cosh \sqrt{B}\tau \mathbf{u}_\circ + \frac{1}{\sqrt{B}} \sinh \sqrt{B}\tau \mathbf{u}'_\circ.} \tag{C.17}$$

As a check differentiation twice shows that this is in fact the general solution, since we have

$$\mathbf{u}' = \sqrt{B} \sinh \sqrt{B}\tau \mathbf{u}_\circ + \cosh \sqrt{B}\tau \mathbf{u}'_\circ, \tag{C.18}$$

and

$$\begin{aligned}\mathbf{u}'' &= B\cosh\sqrt{B}\tau\mathbf{u}_\circ + \sqrt{B}\sinh\sqrt{B}\tau\mathbf{u}'_\circ \\ &= B\left(\cosh\sqrt{B}\tau\mathbf{u}_\circ + \frac{1}{\sqrt{B}}\sinh\sqrt{B}\tau\mathbf{u}'_\circ\right) \\ &= B\mathbf{u}.\end{aligned} \tag{C.19}$$

Observe that this solution is a general solution to second order constant coefficient linear systems of the form we have in eq. (C.5). However, to make it meaningful we do have the additional computational task of performing an eigensystem decomposition of the matrix B. We expect negative eigenvalues that will give us oscillatory solutions (ie: the matrix square roots will have imaginary eigenvalues).

Example C.1: An example diagonalization to try things out.

Let's do that diagonalization for the simplest of the three springs system as an example, with $\kappa_j = \bar{k}$ and $m_j = \bar{m}$, so that we have

$$B = \begin{bmatrix} -2 & 1 & 1 \\ 1 & -2 & 1 \\ 1 & 1 & -2 \end{bmatrix}. \tag{C.20}$$

A orthonormal eigensystem for B is

$$\{\mathbf{e}_{-3,1}, \mathbf{e}_{-3,2}, \mathbf{e}_{0,1}\} = \left\{ \frac{1}{\sqrt{6}}\begin{bmatrix} -1 \\ -1 \\ 2 \end{bmatrix}, \frac{1}{\sqrt{2}}\begin{bmatrix} -1 \\ 1 \\ 0 \end{bmatrix}, \frac{1}{\sqrt{3}}\begin{bmatrix} 1 \\ 1 \\ 1 \end{bmatrix} \right\}. \tag{C.21}$$

With

$$U = \frac{1}{\sqrt{6}} \begin{bmatrix} -\sqrt{3} & -1 & \sqrt{2} \\ 0 & 2 & \sqrt{2} \\ \sqrt{3} & -1 & \sqrt{2} \end{bmatrix}$$
$$D = \begin{bmatrix} -3 & 0 & 0 \\ 0 & -3 & 0 \\ 0 & 0 & 0 \end{bmatrix} \tag{C.22}$$

We have

$$B = UDU^{\mathrm{T}}, \tag{C.23}$$

We also find that B and its root are intimately related in a surprising way

$$\begin{aligned} \sqrt{B} &= \sqrt{3}iU \begin{bmatrix} 1 & 0 & 0 \\ 0 & 1 & 0 \\ 0 & 0 & 0 \end{bmatrix} U^{\mathrm{T}} \\ &= \frac{1}{\sqrt{3}i} B. \end{aligned} \tag{C.24}$$

We also see, unfortunately that B has a zero eigenvalue, so we can't compute $1/\sqrt{B}$. We'll have to back and up and start again differently.

Case II: allowing for zero eigenvalues Now that we realize we have to deal with zero eigenvalues, a different approach suggests itself. Instead of reducing our system using a Hamiltonian transformation to a first order system, let's utilize that diagonalization directly. Our system is

$$\mathbf{u}'' = B\mathbf{u} = UDU^{-1}\mathbf{u}, \tag{C.25}$$

where $D = [\lambda_i \delta_{ij}]$ and

$$\left(U^{-1}\mathbf{u}\right)'' = D\left(U^{-1}\mathbf{u}\right). \tag{C.26}$$

Let

$$\mathbf{z} = U^{-1}\mathbf{u}, \tag{C.27}$$

so that our system is just

$$\mathbf{z}'' = D\mathbf{z}, \tag{C.28}$$

or

$$z_i'' = \lambda_i z_i. \tag{C.29}$$

This is N equations, each decoupled and solvable by inspection. Suppose we group the eigenvalues into sets $\{\lambda_n < 0, \lambda_p > 0, \lambda_z = 0\}$. Our solution is then

$$\begin{aligned}\mathbf{z} = &\sum_{\lambda_n<0,\lambda_p>0,\lambda_z=0} \left(a_n \cos\sqrt{-\lambda_n}\tau + b_n \sin\sqrt{-\lambda_n}\tau\right)\mathbf{e}_n \\ &+ \sum_{\lambda_n<0,\lambda_p>0,\lambda_z=0} \left(a_p \cosh\sqrt{\lambda_p}\tau + b_p \sinh\sqrt{\lambda_p}\tau\right)\mathbf{e}_p + (a_z + b_z\tau)\,\mathbf{e}_z.\end{aligned} \tag{C.30}$$

Transforming back to lattice coordinates using $\mathbf{u} = U\mathbf{z}$, we have

$$\begin{aligned}\mathbf{u} = &\sum_{\lambda_n<0,\lambda_p>0,\lambda_z=0} \left(a_n \cos\sqrt{-\lambda_n}\tau + b_n \sin\sqrt{-\lambda_n}\tau\right)U\mathbf{e}_n \\ &+ \sum_{\lambda_n<0,\lambda_p>0,\lambda_z=0} \left(a_p \cosh\sqrt{\lambda_p}\tau + b_p \sinh\sqrt{\lambda_p}\tau\right)U\mathbf{e}_p + (a_z + b_z\tau)\,U\mathbf{e}_z.\end{aligned} \tag{C.31}$$

We see that the zero eigenvalues integration terms have no contribution to the lattice coordinates, since $U\mathbf{e}_z = \lambda_z\mathbf{e}_z = 0$, for all $\lambda_z = 0$.

If $U = [\mathbf{e}_i]$ are a set of not necessarily orthonormal eigenvectors for B, then the vectors $\mathbf{f}_i$, where $\mathbf{e}_i \cdot \mathbf{f}_j = \delta_{ij}$ are the reciprocal frame vectors. These can be extracted from $U^{-1} = [\mathbf{f}_i]^{\mathrm{T}}$ (i.e., the rows of U^{-1}). Taking dot products between $\mathbf{f}_i$ with $\mathbf{u}(0) = \mathbf{u}_\circ$ and $\mathbf{u}'(0) = \mathbf{u}'_\circ$, provides us with the unknown coefficients a_n, b_n

$$\begin{aligned}\mathbf{u}(\tau) = &\sum_{\lambda_n<0,\lambda_p>0} \left((\mathbf{u}_\circ \cdot \mathbf{f}_n)\cos\sqrt{-\lambda_n}\tau + \frac{\mathbf{u}'_\circ \cdot \mathbf{f}_n}{\sqrt{-\lambda_n}}\sin\sqrt{-\lambda_n}\tau\right)\mathbf{e}_n \\ &+ \sum_{\lambda_n<0,\lambda_p>0} \left((\mathbf{u}_\circ \cdot \mathbf{f}_p)\cosh\sqrt{\lambda_p}\tau + \frac{\mathbf{u}'_\circ \cdot \mathbf{f}_p}{\sqrt{-\lambda_p}}\sinh\sqrt{\lambda_p}\tau\right)\mathbf{e}_p.\end{aligned}$$

(C.32)

Supposing that we constrain ourself to looking at just the oscillatory solutions (i.e. the lattice does not shake itself to pieces), then we have

$$\mathbf{u}(\tau) = \sum_{\lambda_n < 0} \left(\sum_j \mathbf{e}_{n,j} \mathbf{f}_{n,j}^{\mathrm{T}} \right) \left(\mathbf{u}_\circ \cos \sqrt{-\lambda_n}\tau + \frac{\mathbf{u}'_\circ}{\sqrt{-\lambda_n}} \sin \sqrt{-\lambda_n}\tau \right).$$

(C.33)

Eigenvectors for eigenvalues that were degenerate have been explicitly enumerated here, something previously implied. Observe that the dot products of the form $(\mathbf{a} \cdot \mathbf{f}_i)\mathbf{e}_i$ have been put into projector operator form to group terms more nicely. The solution can be thought of as a weighted projector operator working as a time evolution operator from the initial state.

Example C.2: Our example interaction revisited.

Recall that we had an orthonormal basis for the $\lambda = -3$ eigensubspace for the interaction example of eq. (C.20) again, so $\mathbf{e}_{-3,i} = \mathbf{f}_{-3,i}$. We can sum $\mathbf{e}_{-3,1}\mathbf{e}_{-3,1}^{\mathrm{T}} + \mathbf{e}_{-3,2}\mathbf{e}_{-3,2}^{\mathrm{T}}$ to find

$$\mathbf{u}(\tau) = \frac{1}{3} \begin{bmatrix} 2 & -1 & -1 \\ -1 & 2 & -1 \\ -1 & -1 & 2 \end{bmatrix} \left(\mathbf{u}_\circ \cos \sqrt{3}\tau + \frac{\mathbf{u}'_\circ}{\sqrt{3}} \sin \sqrt{3}\tau \right).$$

(C.34)

The leading matrix is an orthonormal projector of the initial conditions onto the eigen subspace for $\lambda_n = -3$. Observe that this is proportional to B itself, scaled by the square of the non-zero eigenvalue of $\sqrt{B}$. From this we can confirm by inspection that this is a solution to $\mathbf{u}'' = B\mathbf{u}$, as desired.

C.3 FOURIER TRANSFORM METHODS.

Let's now try another item from our usual toolbox on these sorts of second order systems, the Fourier transform. For a one variable function of time let's write the transform pair as

$$x(t) = \int_{-\infty}^{\infty} \tilde{x}(\omega) e^{-i\omega t} d\omega \tag{C.35a}$$

$$\tilde{x}(\omega) = \frac{1}{2\pi} \int_{-\infty}^{\infty} x(t) e^{i\omega t} dt. \tag{C.35b}$$

One mass harmonic oscillator The simplest second order system is that of the harmonic oscillator

$$0 = \ddot{x}(t) + \omega_\circ^2 x. \tag{C.36}$$

Application of the transform gives

$$\begin{aligned} 0 &= \left(\frac{d^2}{dt^2} + \omega_\circ^2 \right) \int_{-\infty}^{\infty} \tilde{x}(\omega) e^{-i\omega t} d\omega \\ &= \int_{-\infty}^{\infty} \left(-\omega^2 + \omega_\circ^2 \right) \tilde{x}(\omega) e^{-i\omega t} d\omega. \end{aligned} \tag{C.37}$$

We clearly have a constraint that is a function of frequency, but one that has to hold for all time. Let's transform this constraint to the frequency domain to consider that constraint independent of time.

$$\begin{aligned} 0 &= \frac{1}{2\pi} \int_{-\infty}^{\infty} dt e^{i\omega t} \int_{-\infty}^{\infty} \left(-\omega'^2 + \omega_\circ^2 \right) \tilde{x}(\omega') e^{-i\omega' t} d\omega' \\ &= \int_{-\infty}^{\infty} d\omega' \left(-\omega'^2 + \omega_\circ^2 \right) \tilde{x}(\omega') \frac{1}{2\pi} \int_{-\infty}^{\infty} dt e^{i(\omega - \omega')t} \\ &= \int_{-\infty}^{\infty} d\omega' \left(-\omega'^2 + \omega_\circ^2 \right) \tilde{x}(\omega') \delta(\omega - \omega') \\ &= \left(-\omega^2 + \omega_\circ^2 \right) \tilde{x}(\omega). \end{aligned} \tag{C.38}$$

How do we make sense of this? Since ω is an integration variable, we can't just mandate that it equals the constant driving frequency $\pm\omega_\circ$. It's clear that we require a constraint on the transform $\tilde{x}(\omega)$ as well. As a trial solution, imagine that

$$\tilde{x}(\omega) = \begin{cases} \tilde{x}_\circ & \text{if } |\omega - \pm\omega_\circ| < \omega_{\text{cutoff}} \\ 0 & \text{otherwise} \end{cases} \tag{C.39}$$

This gives us

$$0 = \tilde{x}_\circ \int_{\pm\omega_\circ - \omega_{\text{cutoff}}}^{\pm\omega_\circ + \omega_{\text{cutoff}}} \left(\omega^2 - \omega_\circ^2\right) e^{-i\omega t} d\omega. \tag{C.40}$$

Now it is clear that we can satisfy our constraint only if the interval $[\pm\omega_\circ - \omega_{\text{cutoff}}, \pm\omega_\circ + \omega_{\text{cutoff}}]$ is made infinitesimal. Specifically, we require both a $\omega^2 = \omega_\circ^2$ constraint and that the transform $\tilde{x}(\omega)$ have a delta function nature. That is

$$\tilde{x}(\omega) = A\delta(\omega - \omega_\circ) + B\delta(\omega + \omega_\circ). \tag{C.41}$$

Substitution back into our transform gives

$$x(t) = Ae^{-i\omega_\circ t} + Be^{i\omega_\circ t}. \tag{C.42}$$

We can verify quickly that this satisfies our harmonic equation $\ddot{x} = -\omega_\circ x$.

Two mass harmonic oscillator Having applied the transform technique to the very simplest second order system, we can now consider the next more complex system, that of two harmonically interacting masses (i.e. two masses on a frictionless spring).

Our system is described by

$$\mathcal{L} = \frac{1}{2} m_1 \dot{u}_1^2 + \frac{1}{2} m_2 \dot{u}_2^2 - \frac{1}{2} \kappa \left(u_2 - u_1\right)^2, \tag{C.43}$$

and the pair of Euler-Lagrange equations

$$0 = \frac{d}{dt} \frac{\partial \mathcal{L}}{\partial \dot{u}_i} - \frac{\partial \mathcal{L}}{\partial u_i}. \tag{C.44}$$

The equations of motion are

$$\begin{aligned} 0 &= m_1 \ddot{u}_1 + \kappa \left(u_1 - u_2\right) \\ 0 &= m_2 \ddot{u}_2 + \kappa \left(u_2 - u_1\right). \end{aligned} \tag{C.45}$$

Let

$$\begin{aligned} u_1(t) &= \int_{-\infty}^{\infty} \tilde{u}_1(\omega) e^{-i\omega t} d\omega \\ u_2(t) &= \int_{-\infty}^{\infty} \tilde{u}_2(\omega) e^{-i\omega t} d\omega. \end{aligned} \tag{C.46}$$

Insertion of these transform pairs into our equations of motion produces a pair of simultaneous integral equations to solve

$$\begin{aligned} 0 &= \int_{-\infty}^{\infty} \left(\left(-m_1\omega^2 + \kappa \right) \tilde{u}_1(\omega) - \kappa \tilde{u}_2(\omega) \right) e^{-i\omega t} d\omega \\ 0 &= \int_{-\infty}^{\infty} \left(\left(-m_2\omega^2 + \kappa \right) \tilde{u}_2(\omega) - \kappa \tilde{u}_1(\omega) \right) e^{-i\omega t} d\omega. \end{aligned} \tag{C.47}$$

As with the single spring case, we can decouple these equations with an inverse transformation operation $\int e^{i\omega' t}/2\pi$, which gives us (after dropping primes)

$$0 = \begin{bmatrix} \left(-m_1\omega^2 + \kappa \right) & -\kappa \\ -\kappa & \left(-m_2\omega^2 + \kappa \right) \end{bmatrix} \begin{bmatrix} \tilde{u}_1(\omega) \\ \tilde{u}_2(\omega) \end{bmatrix}. \tag{C.48}$$

Taking determinants gives us the constraint on the frequency

$$\begin{aligned} 0 &= \left(-m_1\omega^2 + \kappa \right) \left(-m_2\omega^2 + \kappa \right) - \kappa^2 \\ &= m_1 m_2 \omega^4 - (m_1 + m_2)\omega^2 \\ &= \omega^2 \left(m_1 m_2 \omega^2 - \kappa(m_1 + m_2) \right). \end{aligned} \tag{C.49}$$

Introducing a reduced mass

$$\frac{1}{\mu} = \frac{1}{m_1} + \frac{1}{m_2}, \tag{C.50}$$

the pair of solutions are

$$\begin{aligned} \omega^2 &= 0 \\ \omega^2 &= \frac{\kappa}{\mu} \equiv \omega_\circ^2. \end{aligned} \tag{C.51}$$

As with the single mass oscillator, we require the functions $\tilde{u}\omega$ to also be expressed as delta functions. The frequency constraint and that delta function requirement together can be expressed, for $j \in \{0, 1\}$ as

$$\tilde{u}_j(\omega) = A_{j+}\delta(\omega - \omega_\circ) + A_{j0}\delta(\omega) + A_{j-}\delta(\omega + \omega_\circ). \tag{C.52}$$

With a transformation back to time domain, we have functions of the form

$$\begin{aligned} u_1(t) &= A_{j+}e^{-i\omega_\circ t} + A_{j0} + A_{j-}e^{i\omega_\circ t} \\ u_2(t) &= B_{j+}e^{-i\omega_\circ t} + B_{j0} + B_{j-}e^{i\omega_\circ t}. \end{aligned} \tag{C.53}$$

Back insertion of these into the equations of motion, we have

$$\begin{aligned}
0 &= -m_1\omega_\circ^2\left(A_{j+}e^{-i\omega_\circ t} + A_{j-}e^{i\omega_\circ t}\right) \\
&\quad + \kappa\left(\left(A_{j+} - B_{j+}\right)e^{-i\omega_\circ t} + \left(A_{j-} - B_{j-}\right)e^{i\omega_\circ t} + A_{j0} - B_{j0}\right) \\
0 &= -m_2\omega_\circ^2\left(B_{j+}e^{-i\omega_\circ t} + B_{j-}e^{i\omega_\circ t}\right) \\
&\quad + \kappa\left(\left(B_{j+} - A_{j+}\right)e^{-i\omega_\circ t} + \left(B_{j-} - A_{j-}\right)e^{i\omega_\circ t} + B_{j0} - A_{j0}\right)
\end{aligned} \tag{C.54}$$

Equality requires identity for all powers of $e^{i\omega_\circ t}$, or

$$\begin{aligned}
0 &= B_{j0} - A_{j0} \\
0 &= -m_1\omega_\circ^2 A_{j+} + \kappa\left(A_{j+} - B_{j+}\right) \\
0 &= -m_1\omega_\circ^2 A_{j-} + \kappa\left(A_{j-} - B_{j-}\right) \\
0 &= -m_2\omega_\circ^2 B_{j+} + \kappa\left(B_{j+} - A_{j+}\right) \\
0 &= -m_2\omega_\circ^2 B_{j-} + \kappa\left(B_{j-} - A_{j-}\right),
\end{aligned} \tag{C.55}$$

or $B_{j0} = A_{j0}$ and

$$0 = \begin{bmatrix} \kappa - m_1\omega_\circ^2 & 0 & -\kappa & 0 \\ 0 & \kappa - m_1\omega_\circ^2 & 0 & -\kappa \\ -\kappa & 0 & \kappa - m_2\omega_\circ^2 & 0 \\ 0 & -\kappa & 0 & \kappa - m_2\omega_\circ^2 \end{bmatrix} \begin{bmatrix} A_{j+} \\ A_{j-} \\ B_{j+} \\ B_{j-} \end{bmatrix}. \tag{C.56}$$

Observe that

$$\begin{aligned}
\kappa - m_1\omega_\circ^2 &= \kappa - m_1\kappa\left(\frac{1}{m_1} + \frac{1}{m_2}\right) \\
&= \kappa\left(1 - 1 - \frac{m_1}{m_2}\right) \\
&= -\kappa\frac{m_1}{m_2},
\end{aligned} \tag{C.57}$$

(with a similar alternate result). We can rewrite eq. (C.56) as

$$0 = -\kappa\begin{bmatrix} m_1/m_2 & 0 & 1 & 0 \\ 0 & m_1/m_2 & 0 & 1 \\ 1 & 0 & m_2/m_1 & 0 \\ 0 & 1 & 0 & m_2/m_1 \end{bmatrix} \begin{bmatrix} A_{j+} \\ A_{j-} \\ B_{j+} \\ B_{j-} \end{bmatrix}. \tag{C.58}$$

It's clear that there's two pairs of linear dependencies here, so the determinant is zero as expected. We can read off the remaining relations. Our undetermined coefficients are given by

$$\begin{aligned} B_{j0} &= A_{j0} \\ m_1 A_{j+} &= -m_2 B_{j+} \\ m_1 A_{j-} &= -m_2 B_{j-} \end{aligned} \tag{C.59}$$

$$\boxed{\begin{aligned} u_1(t) &= a + m_2 b e^{-i\omega_\circ t} + m_2 c e^{i\omega_\circ t} \\ u_2(t) &= a - m_1 b e^{-i\omega_\circ t} - m_1 c e^{i\omega_\circ t}. \end{aligned}} \tag{C.60}$$

Observe that the constant term is not really of interest, since it represents a constant displacement of both atoms (just a change of coordinates).

Check:

$$u_1(t) - u_2(t) = +(m_1 + m_2) b e^{-i\omega_\circ t} + (m_1 + m_2) c e^{i\omega_\circ t}, \tag{C.61}$$

$$\begin{aligned} & m_1 \ddot{u}_1(t) + \kappa(u_1(t) - u_2(t)) \\ &= -m_1 m_2 \omega_\circ^2 \left(b e^{-i\omega_\circ t} + c e^{i\omega_\circ t} \right) + (m_1 + m_2)\kappa \left(b e^{-i\omega_\circ t} + c e^{i\omega_\circ t} \right) \\ &= \left(-m_1 m_2 \omega_\circ^2 + (m_1 + m_2)\kappa \right) \left(b e^{-i\omega_\circ t} + c e^{i\omega_\circ t} \right) \\ &= \left(-m_1 m_2 \kappa \frac{m_1 + m_2}{m_1 m_2} + (m_1 + m_2)\kappa \right) \left(b e^{-i\omega_\circ t} + c e^{i\omega_\circ t} \right) \\ &= 0. \end{aligned} \tag{C.62}$$

C.4 REFLECTION.

We've seen that we can solve any of these constant coefficient systems exactly using matrix methods, however, these will not be practical for large systems unless we have methods to solve for all the non-zero eigenvalues and their corresponding eigenvectors. With the Fourier transform methods we find that our solutions in the frequency domain is of the form

$$\tilde{u}_j(\omega) = \sum a_{kj} \delta(\omega - \omega_{kj}), \tag{C.63}$$

or in the time domain

$$u(t) = \sum a_{kj} e^{-i\omega_{kj} t}. \tag{C.64}$$

We assumed exactly this form of solution in class. The trial solution that we used in class factored out a phase shift from a_{kj} of the form of e^{iqx_n}, but that doesn't change the underling form of that assumed solution. We have however found a good justification for the trial solution we utilized.

D

PERIODIC FOURIER COEFFICIENTS.

We've been using the fact that a periodic function

$$V(\mathbf{r}) = V(\mathbf{r} + \mathbf{r}_n), \tag{D.1}$$

where

$$\mathbf{r}_n = a_1\mathbf{a}_1 + a_2\mathbf{a}_2 + a_3\mathbf{a}_3, \tag{D.2}$$

has a Fourier representation

$$V(\mathbf{r}) = \sum_{\mathbf{G}} V_{\mathbf{G}} e^{i\mathbf{G}\cdot\mathbf{r}}. \tag{D.3}$$

Here $\mathbf{G}$ is a vector in reciprocal space, say

$$\mathbf{G}_{rst} = r\mathbf{g}_1 + s\mathbf{g}_2 + t\mathbf{g}_3, \tag{D.4}$$

where

$$\mathbf{g}_i \cdot \mathbf{a}_j = 2\pi\delta_{ij}. \tag{D.5}$$

Now let's express the explicit form for the Fourier coefficient $V_{\mathbf{G}}$ so that we can compute the Fourier representation for some periodic potentials for some numerical experimentation. In particular, let's think about what it meant to integrate over a unit cell. Suppose we have a parameterization of the points in the unit cell

$$\mathbf{r} = u\mathbf{a}_1 + v\mathbf{a}_2 + w\mathbf{a}_3, \tag{D.6}$$

as sketched in fig. D.1. Here $u, v, w \in [0, 1]$. We can compute the values of u, v, w for any vector $\mathbf{r}$ in the cell by reciprocal projection

$$\mathbf{r} = \frac{1}{2\pi}\left((\mathbf{r}\cdot\mathbf{g}_1)\,\mathbf{a}_1 + (\mathbf{r}\cdot\mathbf{g}_2)\,\mathbf{a}_2 + (\mathbf{r}\cdot\mathbf{g}_3)\,\mathbf{a}_3\right), \tag{D.7}$$

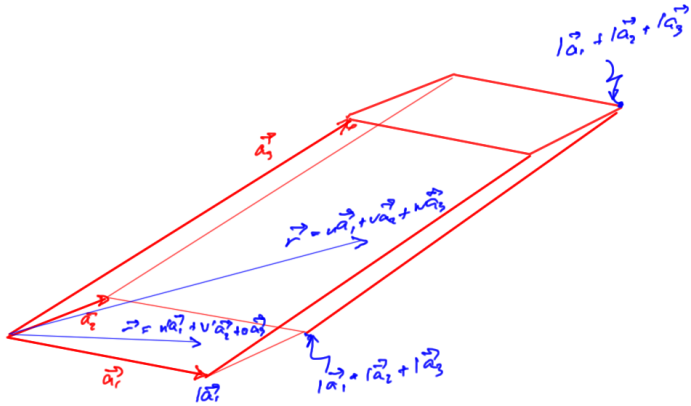

Figure D.1: Unit cell.

or

$$\begin{aligned} u(\mathbf{r}) &= \frac{1}{2\pi}\mathbf{r}\cdot\mathbf{g}_1 \\ v(\mathbf{r}) &= \frac{1}{2\pi}\mathbf{r}\cdot\mathbf{g}_2 \\ w(\mathbf{r}) &= \frac{1}{2\pi}\mathbf{r}\cdot\mathbf{g}_3. \end{aligned} \tag{D.8}$$

Let's suppose that $\mathbf{V}(\mathbf{r})$ is period in the unit cell spanned by $\mathbf{r} = u\mathbf{a}_1 + v\mathbf{a}_2 + w\mathbf{a}_3$ with $u, v, w \in [0,1]$, and integrate over the unit cube for that parameterization to compute $V_{\mathbf{G}}$

$$\begin{aligned} &\int_0^1 du \int_0^1 dv \int_0^1 dw V(u\mathbf{a}_1 + v\mathbf{a}_2 + w\mathbf{a}_3) e^{-i\mathbf{G}'\cdot\mathbf{r}} \\ &\quad = \sum_{rst} V_{\mathbf{G}_{rst}} \int_0^1 du \int_0^1 dv \int_0^1 dw e^{-i\mathbf{G}'\cdot\mathbf{r}} e^{i\mathbf{G}\cdot\mathbf{r}}. \end{aligned} \tag{D.9}$$

Let's write

$$\begin{aligned} \mathbf{G} &= r\mathbf{g}_1 + s\mathbf{g}_2 + t\mathbf{g}_3 \\ \mathbf{G} &= r'\mathbf{g}_1 + s'\mathbf{g}_2 + t'\mathbf{g}_3, \end{aligned} \tag{D.10}$$

so that

$$e^{-i\mathbf{G}'\cdot\mathbf{r}} e^{i\mathbf{G}\cdot\mathbf{r}} = e^{2\pi i(r-r')u} e^{2\pi i(s-s')u} e^{2\pi i(t-t')u}. \tag{D.11}$$

Picking the u integral of this integrand as representative, we have when $r = r'$

$$\begin{aligned}\int_0^1 du e^{2\pi i(r-r')u} &= \int_0^1 du \\ &= 1,\end{aligned} \tag{D.12}$$

and when $r \neq r'$

$$\begin{aligned}\int_0^1 du e^{2\pi i(r-r')u} &= \left.\frac{e^{2\pi i(r-r')u}}{2\pi i(r-r')}\right|_{u=0}^1 \\ &= \frac{1}{2\pi i(r-r')}\left(e^{2\pi i(r-r')} - 1\right).\end{aligned} \tag{D.13}$$

This is just zero since $r - r'$ is an integer, so we have

$$\int_0^1 du e^{2\pi i(r-r')u} = \delta_{r,r'}. \tag{D.14}$$

This gives us

$$\begin{aligned}&\int_0^1 du \int_0^1 dv \int_0^1 dw V(u\mathbf{a}_1 + v\mathbf{a}_2 + w\mathbf{a}_3) e^{-2\pi i r' u} e^{-2\pi i s' v} e^{-2\pi i t' w} \\ &= \sum_{rst} V_{\mathbf{G}_{rst}} \delta_{rst,r's't'} \\ &= V_{\mathbf{G}_{r's't'}}.\end{aligned} \tag{D.15}$$

This is our Fourier coefficient. The Fourier series written out in gory but explicit detail is

$$\begin{aligned}&V(u\mathbf{a}_1 + v\mathbf{a}_2 + w\mathbf{a}_3) \\ &= \sum_{rst}\left(\int_0^1 du' \int_0^1 dv' \int_0^1 dw' V(u'\mathbf{a}_1 + v'\mathbf{a}_2 + w'\mathbf{a}_3) e^{-2\pi i(ru' + sv' + tw')}\right) \times \\ &\quad e^{2\pi i(ru+sv+tw)}.\end{aligned} \tag{D.16}$$

Also observe the unfortunate detail that we require integrability of the potential in the unit cell for the Fourier integrals to converge. This prohibits the use of the most obvious potential for numerical experimentation, the inverse radial $V(\mathbf{r}) = -1/|\mathbf{r}|$.

It was temporarily useful to expand this in terms of $\mathbf{r} = u\mathbf{a}_1 + v\mathbf{a}_2 + w\mathbf{a}_3$, but with the Fourier coefficients computed, let's put things back into vector form noting that

$$\begin{aligned} 2\pi\,(ru + sv + tw) &= 2\pi\left(\frac{1}{2\pi}(\mathbf{r}\cdot\mathbf{g}_1)r + \frac{1}{2\pi}(\mathbf{r}\cdot\mathbf{g}_1)s + \frac{1}{2\pi}(\mathbf{r}\cdot\mathbf{g}_1)t\right) \\ &= \mathbf{G}_{rst}\cdot\mathbf{r}. \end{aligned} \tag{D.17}$$

So, to summarize

$$\boxed{\begin{aligned} V_{rst} &= \int_0^1 du' \int_0^1 dv' \int_0^1 dw' V(u'\mathbf{a}_1 + v'\mathbf{a}_2 + w'\mathbf{a}_3) e^{-2\pi i(ru' + sv' + tw')} \\ V(\mathbf{r}) &= \sum_{rst} V_{rst} e^{\mathbf{G}_{rst}\cdot\mathbf{r}}. \end{aligned}} \tag{D.18}$$

E

MATHEMATICA NOTEBOOKS.

These Mathematica notebooks, some just trivial ones used to generate figures, others more elaborate, and perhaps some even polished, can be found in

https://github.com/peeterjoot/mathematica/tree/master/phy487/.

The free Wolfram CDF player, is capable of read-only viewing these notebooks to some extent.

Files saved explicitly as CDF have interactive content that can be explored with the CDF player.

- Sep 11, 2013 legengreCompare.nb

  This was an attempt to decode the notation used in Desai for the Legendre functions used for Hydrogenic atoms. He defines the orbital functions in terms of Legendre functions, but does not precisely define his Legendre functions.

- Sept 19, 2013 qmSolidsPs1P2.nb

  Hybrid orbital plots

- Sept 19, 2013 qmSolidsPs1P3b.nb

  Madelung constant calculations for NaCl

- Sept 24, 2013 problemSet2Problem3Visualization.nb

  Visualize the Bravais lattice given

- Sept 25, 2013 meltingPointVsZplots.nb

  Plots of melting points in Kelvin vs Z

- Sept 29, 2013 qmSolidsPs3P1.nb

  Reciprocal vector calculation from measurements

- Oct 7, 2013 periodicComplexExponentialPV.nb

  Plot of infinite sum of exponentials showing periodic sinc form. Also diagonalization of the interaction matrix for three harmonically coupled particles in a loop

- Oct 9, 2013 qmSolidsPs4P2dGenerated.nb

  Labeled plots of 1D two spring constant lattice frequency distributions. This is a generated notebook.

- Oct 10, 2013 IbachAndLuth4_15_verify.nb

  Verify equation 4.15 of the text, for the frequencies of the diatomic linear chain

- Oct 10, 2013 qmSolidsPs4P2d.nb

  Plots of 1D two spring constant lattice frequency distributions

- Oct 10, 2013 qmSolidsPs4P2cAnimation.nb

  Dynamic animation of two atom harmonic oscillation

- Oct 11, 2013 discreteFourierRangeFig1.nb

  Plot of sine with omitted points at integer multiples of pi.

- Oct 15, 2013 ps5p1Plot.nb

  Plot calculated density of states function

- Oct 17, 2013 deybeTemperatureTable.nb

  Debye temperature plot for a number of elements, and atomic radius plot. Using hash like function mappings, and ElementData. Also used colors in these plots to visually distinguish each of the s, p, d, f orbital regions. For a less selective atomic radii plotting function, I used Cases and pattern matching to filter out the ElementData values that were missing or unavailable. In a final version of the plotting function, overlapped atomic radii and Debye plots were made. A static image of that plot is saved into the notes for discussion, but the live notebook version has cool ToolTip's on all the points showing the atomic symbols and the values in question.

- Oct 20, 2013 anharmonicOscillator.nb

  Plot of anharmonic oscillator solution for problem 5.5 of the text

- Oct 29, 2013 fermiDiracPlot.nb

  Plots of the Fermi-Dirac distribution and its derivatives. Includes one Manipulate for exploring the effect of temperature dynamically

- Nov 3, 2013 problemSet6Problem1.nb

  Numeric calculation of Fermi temperature and related values. Various wolfram queries were done here to look up the values and units. Also used Column and Row to make tables of the physical constants and the associated calculations.

- Nov 4, 2013 problemSet6Problem2CheckNormalization.nb

  Minor normalization check for particle in a box calculations.

- Nov 4, 2013 tightBindingPotentials.nb

  Plots of periodic extension of inverse radial potential, with and without omission of one such potential

- Nov 7, 2013 latticePotential.nb

  Attempt at a 2D lattice fitting.

- Nov 7, 2013 piecewiseInverseRadialCapCircular.nb

  A radial cap for an inverse radial function. This may have been for a stackexchange post, since I was seeing a discontinuity in the plot that should not have existed. Looks like I found a post that explained things.

- Nov 8, 2013 cubicFittingForInverseRadial.nb

  1D inverse radial lattice Fourier fitting, with cubic rounding part way down the infinite hole.

- Nov 10, 2013 cubicFittingForInverseRadial2D.nb

  Attempt at 2D Fourier fitting of capped radial.

  The reason for some of these inverse radial Fourier fitting attempts was because I wanted to compute the Fourier coefficients for some sample periodic potentials for some numerical experimentation. Naturally, the first one that I tried was an inverse radial potential, however, it turns out that this

isn't re presentable by Fourier series since it is not square integrable.

It is possible to artificially alter the Coulomb potential so that some neighborhood of the origin is omitted, setting the potential to some constant value after that, but that doesn't seem like a physically reasonable model. Asking Prof Julian about this he said:

"There are two effects, one is that the potential doesn't go to -infty at the origin, due to Pauli exclusion. As you suggest, putting a flat bottom on the potential probably works okay. But also, due to screening (in a metal at least) the potential isn't 1/r, but rather it cuts off more quickly.

A commonly used compromise is the "muffin tin potential, which has a flat bottom in a sphere around the atomic position, then a step up to another flat region between the atoms. In solving this one puts a linear combination of spherical harmonics inside the muffin tin, and plane waves in the interstitial region, and match them at the boundary.

But putting a flat bottom on a screened Coulomb potential is probably a reasonable first thing to try."

I appear to have hit convergence issues attempting the Fourier fittings for such a cap in a more interesting 2D lattice.

- Nov 12, 2013 nearlyFreeFig1.nb

  Parabolic Brillouin zone plots

- Nov 12, 2013 nearlyFreeFig1GeneratedLabelled.nb

  Generated notebook with saved label definitions

- Nov 13, 2013 problemSet7problem2c.nb

  Summation that lead to the cotangent result and intersection plot

- Nov 13, 2013 problemset7problem2dNormalization.nb

  Cos squared normalization

- Nov 13, 2013 ps7p2dPlots.nb

  Sine and Cos plots. Ended up sketching instead

- Nov 13, 2013 ps7p2ePlot.nb

  A manipulate to explore the variation with k at point a in the problem. Also some representative plots for the submission

- Nov 16, 2013 hcpLatticeDataBugReport.nb

  Report a bug for Mathematica HCP LatticeData function

- Nov 17, 2013 2dFourierColorizationBugReport.nb

  FourierSeries Mathematica colorizing front end UI bug report

- Nov 17, 2013 inverseRadial2Dtry2.nb

  Second attempt to get the computation of 2D FourierSeries computed for cubic capped inverse radial function. Mathematica gives up the computation after a long delay

- Nov 18, 2013 guassianPlotsL18L19.nb

  Minor plots of Gaussians for L18 and L19

- Nov 18, 2013 qmSolidsPs8bPlots.nb

  Plot generator for ps8 b

- Nov 18, 2013 qmSolidsPs8biFig1Generated.nb

  Ps8 i Plot with labels, generated

- Nov 18, 2013 qmSolidsPs8biiFig2Generated.nb

  Ps8 ii Plot with labels, generated

- Nov 18, 2013 qmSolidsPs8biiiFig3Generated.nb

  Ps8 iii Plot with labels, generated

- Nov 19, 2013 qmSolidsPs8dContourPlot.nb

  Contour plot of tight binding energy level curves. Used the really handy getTheGraphics function from stackexchange for combining the plot with the legend in one graphics object

- Nov 19, 2013 qmSolidsPs8dFig1Generated.nb

  Manually labeled the level curves instead, with the energies. This generated notebook has the labeling data.

- Nov 20, 2013 ps8e.nb

  Scratch notes and plots for ps8.e

- Nov 25, 2013 ps9p2deFigures.nb

  Ps9 figures for q2

- Nov 26, 2013 bccBasisVectors.nb

  Look for BCC basis vectors. First try was wrong, but found suitable vectors with small correction. This verifies that the new ones work, and also finds the reciprocal basis. Also used this notebook to experiment with the Report stylesheet, mixing text, inline math, and math cells in one doc. End result looks much nicer than a plain styled notebook.

- Nov 26, 2013 ps9p1bFigures.nb

  Simple plot of the cubic lattice BZ overlaid with Fermi wavevector radial surface.

- Nov 30, 2013 bccTwoBases.nb

  Aborted attempt to write up a nicely formatted Report for the verification of an Ashcroft and Mermin suggested exercise.

- Dec 1, 2013 fermiInfoForElementOrig.nb

  This notebook generalizes the notebook for problem set 6, problem 1, which had a Fermi energy/temperature calculation. This splits out the generic physical constants, and splits out the ElementData and ChemicalData lookup. The subsequent calculation and formatting of the data was split somewhat. It would be worthwhile to experiment with reworking this to use Rule lists, like perl hashes, to tag the various fields with names, which would make the parameter passing more flexible.

- Dec 1, 2013 lecture22SemiconductorIntegrals.nb

  Sqrt exponential integral ... probably a gamma function.

- Dec 2, 2013 fermiInfoForElement.nb

Rework fermiInfoForElementOrig.nb passing parameters by hashes, ie. Rule Lists. As expected, this was a much cleaner result, as the huge lists of Module local variables are not required passing along the previous phases of the computations. In the end, the descriptive Rule List can be used directly as a ReplaceAll on the values List, with all the grunt work of the display done by a single Rule to List, and TableFormat operation.

- Dec 4, 2013 ps1oplots.nb

  Log concentration vs. inverse temperature and some physical constant lookup and order of magnitude calculations.

- Dec 9, 2013 weakBindingPotentialNearBraggPlane.nb

  A Dynamic visualization of the Bragg plane behavior of a weak periodic potential. Sliders provided for K, and U as a fraction of K, are provided

- Dec 13, 2013 rasterizeAntialiasInset.nb

  Experimentation with rasterizing only the 3D plot part of a 3D plot, and not the axes. This was to attempt to produce a small Mathematica plot of stuff that ends up huge when plotted as eps

- Dec 13, 2013 rasterizeAntialiasInsetExperiment.nb

  Like rasterizeAntialiasInset.nb, but with a plotopts function. Should have noted the stackexchange post I was attempting to use.

- Dec 18, 2013 coupledHarmonicUsingDisplacements.nb

  Verified a hand calculated solution for a non-homogeneous form of the single variable harmonic oscillator. Realized after this that a more sensible approach would have been to just make a change of variables.

- Dec 20, 2013 harmonicOscillatorTwoMasses.cdf

  An animation of a two particle harmonic oscillator, considered as the most simple lattice problem. This highlighted a problem, where the masses passed through each other,

since I did not include a rest length of the spring in the Lagrangian.

- Dec 31, 2013 determinantOfLambdaIminusAfor3Dmatrix.nb

  A check if the determinant and trace expansion for the characteristic equation of A - lambda I holds in 3D. It does not. This shows the structure, but not the underlying mechanism for a general expansion.

- Jan 12, 2014 oneAtomBasisPhononSquareLatticeEigensystem.nb

  Here's a bit of a laborious symbolic calculation that I messed up by hand with, phy487/oneAtomBasisPhonon.tex

- Feb 17, 2014 PhononModesFor2DLatticeVibrationsV4.nb

  N atom basis diamond lattice calculations. Allows up to 5 mass locators in the grid and a vector parameterized parallelepiped lattice cell. This uses TabView and Nasser's tricks to avoid evaluation where undesirable. This also includes the distribution relation. This is my most sophisticated sample of Mathematica programming so far.

INDEX

BIBLIOGRAPHY

[1] Neil W Ashcroft and N David Mermin. *Solid State Physics*. Holt, Rinehart and Winston, New York, 1976. (Cited on pages xi, 1, 9, 35, 36, 41, 45, 51, 52, 75, 102, 122, 127, 129, 163, 181, 186, 191, 199, 235, 236, 240, and 245.)

[2] M. Born and E. Wolf. *Principles of optics: electromagnetic theory of propagation, interference and diffraction of light*. Cambridge university press, 1980. (Cited on page 272.)

[3] Raymond Chang. *Chemistry*. McGraw-Hill, 1991. (Cited on pages 1 and 3.)

[4] C. Doran and A.N. Lasenby. *Geometric algebra for physicists*. Cambridge University Press New York, Cambridge, UK, 1st edition, 2003. (Cited on page 70.)

[5] G.R. Fowles. *Introduction to modern optics*. Dover Pubns, 1989. (Cited on page 272.)

[6] David Jeffrey Griffiths and Reed College. *Introduction to electrodynamics*. Prentice hall Upper Saddle River, NJ, 3rd edition, 1999. (Cited on page 15.)

[7] Ibach Harald and Hans Lèuth. *Solid-state Physics: An Introduction to Principles of Materials Science; with 100 Problems*. Springer, 2003. (Cited on page 93.)

[8] S.S. Haykin. *Communication systems*. Wiley, 1994. (Cited on page 275.)

[9] E. Hecht. *Optics*. 1998. (Cited on page 272.)

[10] Harald Ibach and Hans Lüth. *Solid-state physics: An introduction to Principles of Material Science*. Springer, Berlin, 2009. (Cited on pages xi, 1, 3, 6, 11, 14, 15, 31, 33, 34, 38, 45, 48, 52, 55, 79, 82, 102, 122, 136, 147, 163, 170, 175, 191, 196, 215, 234, 236, 240, 243, 246, 249, 253, 259, 261, 262, 265, 266, and 269.)

[11] JD Jackson. *Classical Electrodynamics*. John Wiley and Sons, 2nd edition, 1975. (Cited on pages 15 and 272.)

[12] KnowledgeDoor LLC. *Debye temperatures*, 2013. URL http://www.knowledgedoor.com/2/elements_handbook/debye_temperature.html. [Online; accessed 22-May-2014]. (Cited on page 136.)

[13] Oxford. *The nearly-free electron model*, 2005. URL http://www2.physics.ox.ac.uk/sites/default/files/BandMT_03.pdf. [Online; accessed 22-May-2014]. (Cited on page 199.)

[14] Raymond Tung. *Solid State Physics 745, Bravais Lattice*, 2013. URL https://web.archive.org/web/20140630014416/http://academic.brooklyn.cuny.edu/physics/tung/GC745S12/vg4-7.pdf. [Online; accessed 22-May-2014]. (Cited on page 31.)

[15] Wikipedia. Brillouin zone — wikipedia, the free encyclopedia, 2013. URL https://en.wikipedia.org/w/index.php?title=Brillouin_zone&oldid=554772892. [Online; accessed 30-September-2013]. (Cited on page 55.)

[16] Wikipedia. Allotropes of boron — wikipedia, the free encyclopedia, 2013. URL https://en.wikipedia.org/w/index.php?title=Allotropes_of_boron&oldid=570995646. [Online; accessed 26-September-2013]. (Cited on page 27.)

[17] Wikipedia. Bravais lattice — wikipedia, the free encyclopedia, 2013. URL https://en.wikipedia.org/w/index.php?title=Bravais_lattice&oldid=566779959. [Online; accessed 21-September-2013]. (Cited on page 33.)

[18] Wikipedia. Poisoning of alexander litvinenko — wikipedia, the free encyclopedia, 2013. URL https://en.wikipedia.org/w/index.php?title=Poisoning_of_Alexander_Litvinenko&oldid=574237492. [Online; accessed 24-September-2013]. (Cited on page 35.)